

The copyright of this thesis vests in the author. No quotation from it or information derived from it is to be published without full acknowledgement of the source. The thesis is to be used for private study or non-commercial research purposes only.

Published by the University of Cape Town (UCT) in terms of the non-exclusive license granted to UCT by the author.

Design of Power System Stabilizers using Evolutionary Algorithms

PREPARED BY:
SEVERUS PANDULENI NAPANDULWE SHEETEKELA



This thesis is submitted to the University of Cape Town in full fulfilment of the academic requirements for the Master of Science degree in Electrical Engineering

SUPERVISOR:
PROF. K.A FOLLY



UNIVERSITY OF CAPE TOWN
IDYUNIVESITHI YASEKAPA • UNIVERSITEIT VAN KAAPSTAD

DEPARTMENT OF ELECTRICAL ENGINEERING
UNIVERSITY OF CAPE TOWN
CAPE TOWN

Date: May 2010

Declaration

I hereby declare that this is my own work. All alternative sources used have been identified and referenced. This thesis has not been submitted before for any degree at this or any other institution for any degree or examination.

University of Cape Town

Signature:

Mr. Severus P.N Sheetekela

Signed at the University of Cape Town

25 May 2010.

Acknowledgements

First and foremost, my gratitude goes to the almighty for giving me the strength and the courage towards finishing my dissertation, and for keeping me safe and clear of any difficulties that could have hindered me from finishing my research.

Secondly I would like to express my special appreciation to my supervisor Prof K. Folly. You have been an inspiration, a person that I have always relied on for help when things were not going well. Thank you for keeping the trust in me by allowing me to do my dissertation under your supervision.

Thirdly I would like to thank my parents Olivia Sheetekela and Simon Sheetekela, my grandmother Teopolina Ndeshitiwa, my brothers (Setson and Shetu) Sheetekela and sisters (Selma, Shangelao, Sanette and Sarty) Sheetekela for allowing me to travel that long distance and be able to finish my degree. I know it has been hard seeing me away for the best part of six years, but you have remained patient and I gladly appreciate it. I don't want to forget Mrs Penehafo Angula and Mr Jacob Angula and the family for the support you have given me. I am very much grateful for that.

I don't want to forget my fellow colloquies from the Power Engineering Research Group as well as my friends both at UCT and home; you have been supportive, and helpful in whatever difficulties that I faced. Special appreciation must go to Magnaem Simon for all the prayers, courage, mental support and the love that you have shown me. Least, but not last I want to thank Dr Zechariah Mushaandja and Mrs Robyn Newton for the good feedback and support you offered during the compilation of this thesis and Prof O P Malik, University of Calgary for the help in allowing me to use your laboratory, during my visit to Calgary in 2008.

Finally I have to thank my sponsors Petrofund, for giving me this opportunity to be able to realize my dream of finishing my Msc Engineering degree. Thank you very much for your financial support.

Synopsis

Over the past decades, the issue of low frequency oscillations has been of major concern to power system engineers. These oscillations range from 0.1 to 3Hz and tend to be poorly damped especially in systems equipped with high gain fast acting AVRs and highly interconnected networks. If these oscillations are not adequately damped, they may sustain and grow, which may lead to system separation and loss of power transfer. As a means to alleviate such problems of low damping in power systems, Power System Stabilizer (PSS) has been proposed. PSS produces a component of the electrical torque in phase with the rotor speed deviations, thus adding damping to the generators rotor oscillation. The PSS is comprised of various blocks, including the gain K and the lead/lag blocks made of time constants T_1 , T_2 , T_3 and T_4 . The gain and lead/lag blocks require some tuning to give the best possible combination so that adequate damping can be provided to the system.

Conventional methods have been applied to the design of the PSS over the years and they have been employed by utility engineers due to their simplicity. Other reasons include the ease of online tuning of the CPSS as well as the lack of assurance of the system's relative stability related to some adaptive or variable structure techniques. In designing the CPSS, the system is linearized around the nominal operating condition and phase compensation method is applied to provide the phase lead required in the system designed around a single operating condition. But due to the dynamic nature of the system, the CPSS tends to operate optimally only around the nominal operating condition, but poorly as the system power transfer and loading increases, leading to the need for optimal tuning of Power System Stabilizers.

This thesis deals with the damping of electromechanical oscillations using Power System Stabilizers (PSS). Evolutionary Algorithm (EA) techniques are used to optimally tune the parameters of PSSs to stabilize the system over a set of operating conditions instead of a single operating condition. Evolutionary algorithm techniques use iterative methods in order to obtain the best possible parameters (solutions) to solve the problem at hand. The

problem of tuning the PSSs was converted into a mathematical problem and solved by the use of EAs. The designed PSSs are required to stabilize the system over wide range of operating conditions.

Three EA techniques were considered in determining the optimal parameters for the PSSs. These methods include the: standard Genetic Algorithm (referred to as GA), Breeder Genetic Algorithm (BGA) and Population Based Incremental Learning (PBIL). The genetic algorithm is a biological inspired search algorithm pioneered by Holland around the 1970s and it's based on Darwin's survival of the fittest. It is as a directed search based upon the ideas of biological evolution. GA is robust, conceptually simple to problems where there is little knowledge on the problem being solved. GA has the ability to solve very complex, non-linear and non-differentiable problems that are hard to solve by conventional methods. However GA tends to have a problem of premature convergence, where the search converges to local optima, instead of a global one. Furthermore GA has many parameters (e.g. crossover, mutation, selection) that have to be selected by the user.

Breeder Genetic Algorithm (BGA) applies almost the same ideas as in GA, except that it is based on artificial selection as practised in animal breeding rather than natural selection (Darwinian evolution). Artificial selection (selective breeding) refers to the intentional breeding for certain qualities or a combination of qualities (e.g. breeding a rose plant to produce large flowers or chicken to lay more eggs). This has been recently applied to cattle to produce more milk and beef. This is in contrast with natural selection in which the differential reproduction of organisms with certain qualities is attributed to the improved survival or reproductive ability (Darwinian fitness). Usually in BGA the individuals are represented as real numbers instead of binary or integers that are used in GA. However, recently real value representation has been used in GA. This thesis uses real value representation for the chromosomes in GA. BGA turns out to be an extremely versatile and effective function optimiser, with very few parameters which have to be chosen by the user. It is expected that artificial selection be much more efficient than natural selection as it works by mating two parents with better characteristics as compared to

natural selection which is determined by the probability of mating two parents with good characteristics.

PBIL on the other hand combines the idea of genetics and competitive learning, but the role of the population in PBIL is redefined and replaced by the probability vector (PV). The PV controls the bit strings generated by the PBIL which is used to create other individuals through learning. The main features of PBIL are: (a) few parameters are needed, as there is no crossover operator and selection in PBIL, (b) less memory is required, as there is no need to store all solutions in the population only two solutions are stored in PBIL (the current best solution and the solution being evaluated) and the probability vector. PBIL is faster, effective and therefore better for online tuning

An eigenvalue objective function was used to test the fitness of each possible solution within the problem domain. The objective function used was to maximize the lowest damping ratio of the electromechanical modes in the system. This was specifically done to improve the small signal stability of the system and to allow comparison between the three optimization techniques.

To demonstrate the ability of the three EA techniques, two power system models are used, namely, a single machine connected to an infinity bus system (SMIB) and the Two-Area Multi-machine system. For comparison purposes, a Conventional PSS was also designed and its performance compared with the EA-PSSs.

In the SMIB system, a restriction was imposed on the maximum damping ratio that the electromechanical modes can attain. The maximum damping ratio was limited to 0.5. This was applied to all the optimization techniques, the reason being that high damping in electromechanical modes may reduce the frequency of oscillations of the electromechanical modes, which may negatively affect the response of the system during transient disturbances. Also high damping of electromechanical modes reduces the damping of other oscillatory modes in the system. Following the simulations, it was observed that optimizing the PSS parameters over a range of operating conditions result in a very effective and robust controller that effectively damp out the oscillations in both small and large disturbances. As expected, the CPSS provides adequate damping during

the nominal operating condition, but less effective as the loading conditions change. Furthermore, simulations show that the BGA and PBIL work slightly better than GA. Optimized PSS parameters work well than Conventional Power System Stabilizers.

Having designed the PSS using simulations, the results were validated using the experimental setup. The experimental (SMIB) system was set up at the department of electrical engineering at the University of Calgary. Only the PSS designed using BGA and PBIL were tested due to the time constraints. The two EA- PSSs were compared to the CPSS; it was found that the PBIL and BGA performed better than CPSS across all the operating conditions considered. The different operating conditions were obtained by varying the voltage on the terminal of the generator as well as the power transmitted.

The task of designing an effective and robust PSS that effectively stabilizes the system during both small and large disturbances was achieved. All the PSSs obtained from the three EA techniques provide an adequate damping for the electromechanical modes across all the operating conditions considered. The optimal PSSs perform better than CPSS as expected, except during the nominal operating condition. The BGA and PBIL PSS provided a slightly better damping than the GA; furthermore it was found that the PBIL, BGA and GA are effective in maximizing or minimizing an objective function. All the simulations were carried out using the Matlab/ Simulink software packages.

Results obtained in this thesis could be improved by carefully tuning the PSSs by including small and large disturbances conditions, within the objective function. It was found that a high gain value of the PSS slightly negatively affected the initial oscillations after the fault application. The initial oscillations have higher amplitudes due to the high gains. It is also suggested that the optimal locations of the PSS be considered within the optimization, especially for a Multi-machine systems.

Table of Contents

Declaration	i
Acknowledgements	ii
Synopsis	iii
Table of Contents	vii
List of Figures	xi
List of Tables	xvii
Nomenclature	xviii
Chapter 1	1
1 Introduction	1
1.1 Stability Phenomena, Basic concepts and Definitions.....	3
1.2 Electromechanical Oscillations.....	5
1.3 Evolution of stability problems.....	6
1.4 Functions of PSS and PSS Design Methods.....	8
1.4.1 Conventional PSS design methods	11
1.4.2 New PSS Design Methods.....	12
1.5 Objectives of the Research.....	14
1.6 Limitations and scope of investigation	15
1.7 Software packages used for the Simulations	15
1.8 Outline of the Thesis.....	16
Chapter 2	17
2 System Linearization and State Space Representation	17
2.1 Introduction.....	17
2.2 State Space Representation	17
2.3 Linearization	18
2.4 Eigenproperties of the state matrix	20
2.4.1 Eigenvalues	20
2.4.2 Eigenvectors.....	22
2.4.3 Eigenvalue sensitivity	22

2.4.4	Participation factors	23
2.5	Summary	24
Chapter 3		25
3 Background Theory to Evolutionary Algorithms		25
3.1	Introduction	25
3.2	Genetic Algorithm (GA)	25
3.2.1	Evaluation and objective function	26
3.2.2	Selection	27
3.2.3	Crossover or Recombination	28
3.2.4	Mutation	31
3.2.5	Chromosome Representations	32
3.2.6	Termination	33
3.3	Breeder Genetic Algorithm (BGA)	34
3.3.1	Selection	35
3.3.2	Recombination	35
3.3.3	Adaptive Mutation	37
3.4	Population Based Incremental Learning (PBIL)	37
3.4.1	Competitive Learning	38
3.4.2	Population in PBIL	38
3.4.3	Mutation	39
3.4.4	Learning rate	39
3.4.5	Termination	40
3.5	Summary	40
Chapter 4		41
4 Application of Evolutionary Algorithms to Power System Stabilizer Design ...		41
4.1	Introduction	41
4.2	Structure of the PSS	41
4.3	Objective function and PSS tuning	42
4.4	PSS Design based on Evolutionary Algorithms (EAs)	44
4.5	Design Case Studies	49
4.5.1	Single Machine to Infinite Bus system	49
4.5.2	Two Area Multi-machine System	51

4.6	Summary	55
Chapter 5		56
5 Simulation Results for the Single Machine Infinite Bus System (SMIB)		56
5.1	Introduction.....	56
5.2	Fitness Values and PSS parameters	56
5.3	Small Signal Stability	59
5.3.1	Eigenvalue Analysis.....	60
5.3.2	Time Domain Simulation.....	62
5.3.3	PSS Robustness Evaluation	73
5.4	Transient Stability.....	76
5.4.1	Case 1: nominal operating condition	77
5.4.2	Case 2: System condition, $P_e=0.5\text{pu}$; $Q_e=0.2184\text{pu}$; $X_e=0.3\text{pu}$	80
5.4.3	Case 3: System condition, $P_e=0.8\text{pu}$; $Q_e=0.2933\text{pu}$; $X_e=0.7\text{pu}$	83
5.4.4	Case 4: System condition, $P_e=1.1\text{pu}$; $Q_e=0.4070\text{pu}$; $X_e=0.7\text{pu}$	86
5.4.5	Case 5: System condition, $P_e=0.5\text{pu}$; $Q_e=1839\text{pu}$; $X_e=1.1\text{pu}$	89
5.5	Summary	92
Chapter 6		93
6 Simulation Results for the Multi-machine system		93
6.1	Introduction.....	93
6.2	Fitness Values and PSS parameters	93
6.3	Small Signal Stability	96
6.3.1	Eigenvalue Analysis.....	96
6.3.2	Time domain Simulations	101
6.3.3	PSS Robustness.....	109
6.4	Transient Stability.....	114
6.4.1	Case 1: Nominal operating condition	114
6.4.2	Case 2: Middle loading operating condition.....	117
6.4.3	Case 3: Heavy loading operating condition	119
6.5	Summary	122
Chapter 7		123
7 Real Time Implementation of Power System Stabilizers		123
7.1	Introduction.....	123

7.2	The Experimental System Description	123
7.3	Power System Stabilizer Implementation	126
7.4	Real Time Simulation Results	127
7.5	Simulations results for the real time system	131
7.5.1	Step responses	132
7.5.2	Large disturbance	137
7.6	Summary	145
Chapter 8	146
8	Conclusions and Recommendations	146
	References	151
	Research Publications	158
	Appendix	A

University of Cape Town

List of Figures

Figure 1.1: Lead- Lag PSS structure.....	9
Figure 3.1: Roulette wheel selection.....	27
Figure 3.2: Single point crossover	29
Figure 3.3: Six point multiple point crossover.....	29
Figure 3.4: An example of Arithmetic crossover.....	30
Figure 3.5: Mutation	31
Figure 3.6: Flowchart of the Genetic Algorithm	33
Figure 3.7: Volume recombination	36
Figure 3.8: Line recombination.....	36
Figure 4.1: GA, BGA and PBIL parameters used in the simulations	45
Figure 4.2: Flow chart for the PSS design using Genetic Algorithm	46
Figure 4.3: Flow chart for the PSS design using Breeder Genetic Algorithm.....	47
Figure 4.4: Flow chart for the PSS design using PBIL.....	48
Figure 4.5: Single machine to infinite bus system.....	49
Figure 4.6: Two Area multi-machine system line diagram	52
Figure 5.1: Fitness value from GA objective function	58
Figure 5.2: Fitness value from the BGA objective function.....	58
Figure 5.3: Fitness value from the PBIL objective function.....	59
Figure 5.4: System response (speed) for Case 1	63
Figure 5.5: System response (active power) for Case 1.....	64
Figure 5.6: System response (speed) for Case 2	65
Figure 5.7: System response (active power) for Case 2.....	65
Figure 5.8: System response (speed) for Case 3	66
Figure 5.9: System response (active power) for Case 3.....	67
Figure 5.10: System response (speed) for Case 4.....	68
Figure 5.11: System response (active power) for Case 4.....	68
Figure 5.12: System response for Case 5.....	69
Figure 5.13: System response (active power) for Case 5.....	70

Figure 5.14: System response (speed) for Case 6	71
Figure 5.15: System response (active power) for Case 6.....	71
Figure 5.16: System response (speed) for Case 7	72
Figure 5.17: System response (active power) for Case 7.....	73
Figure 5.18: System response (speed) for Case 8	74
Figure 5.19: System response (active power) for Case 8.....	74
Figure 5.20: System response (speed) for Case 9	75
Figure 5.21: System response (active power) for Case 9.....	76
Figure 5.22: Voltage terminal response of Case 1 under three phase fault	78
Figure 5.23: Power response of Case 1 under three phase fault	78
Figure 5.24: Speed response of the generator under three phase fault	79
Figure 5.25: Rotor angle response of the system under three phase fault	79
Figure 5.26: Electric field voltage response of the system under a three phase fault of Case 1	80
Figure 5.27: Voltage terminal response of the system under three phase fault of Case 2	81
Figure 5.28: Power output response of the system under three phase fault of Case 2.....	81
Figure 5.29: Speed response of the generator under three phase fault of Case 2	82
Figure 5.30: Rotor angle response of the system under three phase fault of Case 2	82
Figure 5.31: Electric field voltage response of the system under three phase fault of Case 2.....	83
Figure 5.32: Voltage terminal response of the system under three phase fault of Case 3	84
Figure 5.33: Active Power response of the generator under three phase fault of Case 3 .	84
Figure 5.34: Generator speed response under three phase fault of Case 3	85
Figure 5.35: Rotor angle response of the system under three phase fault for Case 3.....	85
Figure 5.36: Electric field voltage response of the system under three phase fault of Case 3.....	86
Figure 5.37: Voltage terminal response of the system to a three phase fault of Case 4 ...	87
Figure 5.38: Active power response of the generator to a three phase fault at Case 4	87
Figure 5.39: Generator speed response under three phase fault of Case 4	88
Figure 5.40: Rotor angle response of the generator under three phase fault at Case 4.....	88
Figure 5.41: Electric field voltage response of the generator under three phase fault at Case 4.....	89

Figure 5.42: Voltage terminal response under three phase fault at Case 5..... 90

Figure 5.43: Active power response of the generator under three phase fault at Case 5.. 90

Figure 5.44: Generator speed response under three phase fault at Case 5..... 91

Figure 5.45: Rotor angle response of the generator under three phase fault at Case 5..... 91

Figure 5.46: Electric field voltage response of the system under three phase fault at Case 5..... 92

Figure 6.1: Fitness value curve from the GA optimization 94

Figure 6.2: Fitness value curve from the BGA optimization..... 94

Figure 6.3: Fitness value curve from the PBIL optimization..... 95

Figure 6.4: Spread of the eigenvalues across all three operating conditions 99

Figure 6.5: Case 1: Step response of G1 under the 10% step change in Vref of G2 102

Figure 6.6: Case 2: Step response of G2 to the 10% step change in Vref of G2 102

Figure 6.7: Case 3: Step response of G2 to the 10% step change in Vref of G2 103

Figure 6.8: Case 1: Step response of G2 under the 10% step change in Vref of G2 104

Figure 6.9: Case 2: Step response of G2 under the 10% step change in Vref of G2 104

Figure 6.10: Case 3: Step response of G2 under the 10% step change in Vref of G2 105

Figure 6.11: Case 1: Step response of G3 under the 10% step change in Vref of G2 106

Figure 6.12: Case 2: Step response of G3 under the 10% step change in Vref of G2 106

Figure 6.13: Case 3: Step response of G3 under the 10% step change in Vref of G2 107

Figure 6.14: Case 1: Step response of G4 under the 10% step change in Vref of G2 108

Figure 6.15: Case 2: Step response of G4 under the 10% step change in Vref of G2 108

Figure 6.16: Case 3: Step response of G4 under the 10% step change in Vref of G2 109

Figure 6.17: Case 4: Step response of G1 under the 10% step change in Vref of G2 110

Figure 6.18: Case 4: Step response of G2 under the 10% step change in Vref of G2 110

Figure 6.19: Case 4: Step response of G3 under the 10% step change in Vref of G2 111

Figure 6.20: Case 4: Step response of G4 under the 10% step change in Vref of G2 111

Figure 6.21: Case 5: Step response of G1 under the 10% step change in Vref of G2 112

Figure 6.22: Case 5: Step response of G2 under the 10% step change in Vref of G2 112

Figure 6.23: Case 5: Step response of G3 under the 10% step change in Vref of G2 113

Figure 6.24: Case 5: Step response of G4 under the 10% step change in Vref of G2 113

Figure 6.25: Voltage on Bus 3 following a three phase fault on bus 3 for Case 1 115

Figure 6.26: Active power response of generator 2 to a three phase fault on bus 1 for Case 1.....	115
Figure 6.27: Speed response for generator 2 after the 3 phase fault on bus 3 for Case 1	116
Figure 6.28: Electric field voltage of generator 2 following a 3 phase fault on Bus 3 for Case 1.....	116
Figure 6.29: Voltage on Bus 3 following a three phase fault on Bus 3 for Case 2.....	117
Figure 6.30: Active power response of generator 2 to a three phase fault at bus 3 for Case 2.....	118
Figure 6.31: Speed response of generator 2 to a three phase fault at bus 3 for Case 2...	118
Figure 6.32: Electric field voltage response of generator 2 to a 3 phase fault on Bus 3 for Case 2.....	119
Figure 6.33: Voltage on Bus 3 following a 3 phase fault on bus 3 for Case 3	120
Figure 6.34: Active power response of generator 2 to the 3 phase fault on bus 3 for Case 3	120
Figure 6.35: Speed response of generator 2 to a 3 phase fault on Bus 3 for Case 3.....	121
Figure 6.36: Electric field voltage response of generator 2 to a three phase fault on Bus 3 for Case 3	121
Figure 7.1: Experimental System physical model	125
Figure 7.2: Simulink implementation model	126
Figure 7.3: System response to a single phase fault at $P=0.83pu$; $V=1.0pu$ at 0.94 leading power factor	128
Figure 7.4: System response to a single phase fault at $P=0.83pu$; $V=1.1pu$ at 0.96 lagging power factor	128
Figure 7.5: System response to a single phase fault at $P=0.33pu$; $V=1.03pu$ at 0.98 leading power factor	129
Figure 7.6: System response to a single phase fault at $P=0.50pu$; $V=1.07pu$ at 0.88 lagging power factor	129
Figure 7.7: System response to a single phase fault at $P=0.90pu$; $V=1.05pu$ at 0.98 lagging power factor	130
Figure 7.8: System response to a single phase fault at $P=1.0pu$; $V=1.01pu$ at 0.98 leading power factor	130

Figure 7.9: Step response of the system to a 10% change in reference voltage at $P=0.33$ and $V_t=1.03$ 133

Figure 7.10: Step response of the system to a 10% change in reference voltage at $P=0.5$ and $V_t=1.07$ 134

Figure 7.11: Step response of the system to a 10% change in reference voltage at $P=0.83$ and $V_t=1.0$ 135

Figure 7.12: Step response of the system to a 10% change in reference voltage at $P=0.83$ and $V_t=1.1$ 135

Figure 7.13: Step response of the system to a 10% change in reference voltage at $P=0.9$ and $V_t=1.05$ 136

Figure 7.14: Step response of the system to a 10% change in reference voltage at $P=1.0$ and $V_t=1.01$ 137

Figure 7.15: Bus 2 voltage response to a single phase fault on Bus 2 at $P=0.33$ and $V_t=1.03$ 138

Figure 7.16: Generator active power response to a single phase fault on Bus 2 at $P=0.33$ and $V_t=1.03$ 138

Figure 7.17: Bus 2 voltage response to a single phase fault on Bus 2 at $P=0.5$ and $V_t=1.07$ 139

Figure 7.18: Generator active power response to a single phase fault on Bus 2 at $P=0.5$ and $V_t=1.07$ 140

Figure 7.19: Bus 2 voltage response to a single phase fault on Bus 2 at $P=0.83$ and $V_t=1.0$ 141

Figure 7.20: Generator active power response to a single phase fault on Bus 2 at $P=0.83$ and $V_t=1.0$ 141

Figure 7.21: Bus 2 voltage response to a single phase fault on Bus 2 at $P=0.9$ and $V_t=1.05$ 142

Figure 7.22: generator active power response to a single phase fault on Bus 2 at $P=0.9$ and $V_t=1.05$ 143

Figure 7.23: Bus 2 voltage response to a single phase fault on Bus 2 at $P=0.83$ and $V_t=1.1$ 144

Figure 7.24: Generator active power response to a single phase fault on Bus 2 at $P=0.83$ and $V_t=1.1$ 144

Figure A.1: Diagram for the system used in the simulations for Chapter 6	B
Figure B.1: AVR block diagram used in the SMIB system.....	D
Figure B.2: Power system stabilizer structure used in the SMIB system.....	F
Figure C.1: Fitness value for the GA optimization.....	H
Figure C.2: Fitness value for the BGA optimization.....	I
Figure C.3: Fitness value for the PBIL optimization.....	I
Figure C.4: Active power deviation for Case 1 under small disturbance.....	K
Figure C.5: Active power deviation for Case 2 under small disturbance.....	L
Figure C.6: Active power deviation for Case 3 under small disturbance.....	L
Figure C.7: Active power deviation for Case 4 under small disturbance.....	M
Figure C.8: Active power deviation for Case 5 under small disturbance.....	M
Figure C.9: Active power deviation for Case 6 under small disturbance.....	N
Figure C.10: Active power deviation for Case 7 under small disturbance.....	N
Figure C.11: Active power deviation for Case 8 under small disturbance.....	O
Figure C.12: Active power deviation for Case 9 under small disturbance.....	O
Figure D.1: Speed governor block diagram used in the simulations for multi-machine...	Q
Figure D.2: Block diagram for the PSS used in the Multi-machine system.....	R

List of Tables

Table 4.1: Open Loop operating conditions used in the PSS design	51
Table 4.2: Case 1 generator's Output Values	52
Table 4.3: Case 2 generator Output Values	53
Table 4.4: Case 3 generators Output Values.....	53
Table 4.5: Open loop poles for the selected design operating conditions	54
Table 4.6: Open loop electromechanical modes for Case 4 and Case 5	54
Table 5.1: Power System Stabilizer parameters for different optimization programs.....	59
Table 5.2: Electromechanical modes of the system with different PSSs Designs	62
Table 6.1: PSS parameters for the BGA-PSS	95
Table 6.2: PSS parameters for the GA-PSS	95
Table 6.3: PSS parameters for the PBIL-PSS	96
Table 6.4: PSS parameters for the CPSS	96
Table 6.5: Inter-area modes for Two-Area Multi-machine system and the respective damping ratios.....	97
Table 6.6: Local Area mode 1.....	98
Table 6.7: Local Area mode 2.....	98
Table 6.8: Inter-area modes for the closed loop system	100
Table 6.9: Local area mode 1.....	100
Table 6.10: Local area mode 2.....	100
Table B.1: High frequency oscillatory modes for the SMIB system.....	G
Table C.1: Electromechanical modes and their damping ratios.....	J
Table C.2: High frequency oscillatory modes for the SMIB system.....	J

Nomenclature

A	State matrix
P_e	Electrical power
P_m	Mechanical power
T_e	Electrical torque
T_m	Mechanical torque
Δ	Small perturbation
T'_{do}, T'_{qo}	d-axis, q-axis transient open circuit time constants
T''_{do}, T''_{qo}	d-axis, q-axis sub-transient open circuit time constants
e_d, e_q	d-axis, q-axis terminal voltage component
i_d, i_q	d-axis, q-axis terminal current component
H	Inertia constant
K_D	Damping torque coefficient
L_{fd}	Field winding leakage inductance
L_l	Stator leakage inductance
L_{ad}, L_{aq}	d-axis, q-axis stator to rotor mutual inductance
L_d, L_q	d-axis, q axis synchronous inductance
L'_d, L'_q	d-axis, q axis transient inductance
L''_d, L''_q	d-axis, q axis subtransient inductance
R_{fd}	Field resistance
λ	Eigenvalue
ζ	Damping ratio
δ	Rotor angle
ω	Rotor angular velocity
ω_0	Base angular velocity
Ψ_d, Ψ_q	d-axis, q axis stator flux linkage
Ψ_{fd}	Field flux linkage
pu	per unit
AVR	Automatic Voltage Regulator

SMIB	Single machine infinite bus
PSS	Power System Stabilizer
CPSS	Conventional Power System Stabilizer
GA-PSS	Genetic Algorithm Power System Stabilizer
BGA -PSS	Breeder Genetic Algorithm Power System Stabilizer
PBIL-PSS	Population Based Incremental Learning Power System Stabilizer
CL	Competitive Learning
PV	Probability Vector
EA	Evolutionary Algorithm
AI	Artificial Intelligence
SVC	Static Var Compensator
STATCOM	Static Compensators
FACTS	Flexible Alternating Current Transmission Systems

Remarks:

- *when any of the abbreviations is used in plural, then an (s) is added at the end of the listed abbreviations. Also pu and per unit have been used interchangeably within the thesis, but they are the same.*
- *The notation for the complex numbers used in this thesis is i and not j .*
- *Case and Case study have been used interchangeably in the document, but they all refer to the same thing.*

Chapter 1

Introduction

This chapter introduces the concept of power system stability, the cause of power system instability as well as ways of limiting and mitigating the instability in power systems. It also gives background history to the stability problems. The chapter ends with the objectives of the research as well as the limitations and restrictions that were observed.

Stability of electromechanical oscillations is of major importance to power systems operation and is a major requirement for maximum power transfer and power system security [1], [2]. Importance of robust centralised power system control becomes even more apparent with the introduction of the deregulation of power systems, the recent exponential increase in power demand as well as the open access transmission line. Power subsystems operate under highly constrained, uncertain and stressful operating conditions, increasing the possibility of the inherent low frequency electromechanical oscillations. Also the introduction of automatic controls, specifically the Automatic Voltage Regulator (AVR) tends to produce negative damping for modes in the low power system frequency oscillation range [1]. The AVR, especially those with high gain, fast acting low time constants tend have large effects on the damping of the system's low frequency modes. If the low frequency oscillations persist, the oscillations may sustain and grow, resulting in the danger of system separation and thus loss of power transfer. If no adequate damping is provided to dampen the electromechanical modes, synchronism may be lost which would lead to system failure [1]. As a result of this shortcoming in power systems, various controllers have been implemented, particularly a Power System Stabilizer (PSS) controller has been used to provide supplementary damping to the electromechanical oscillations in the system. The PSS is the most cost effective controller in improving the damping of oscillatory modes and thus enhancing the stability of the system. But since the system's operating conditions change, designing a PSS to provide adequate damping across all operating conditions of the system is not an easy task [1], [3]. Conventional Power System Stabilizers (CPSS) designed around a single point have

been used in the past. They tend to only operate optimally around the nominal operating condition and perform dismally as the operating conditions change [4]-[8] and therefore their influence becomes limited and ineffective. As a result modern control theory and techniques have been proposed and are being used to help with the design of PSS. Some of the methods include: optimal control [9], adaptive control [10], variable structure control [11] as well as H_{∞} control [4], [6], [12], [13]. In the last few years the development of intelligence techniques has received increased attention and has been deployed in the tuning of power system stabilizer parameters. This helps in maintaining a robust system across all possible operating scenarios.

Genetic Algorithm (GA) has been the front runner in the field of artificial intelligence due to its simplicity in basic operations and its ability to solve many difficult optimization problems. Despite its ability to provide a robust and simple adaptive search tool, it also has some drawbacks. The performance of the GA is readily dependant on the optimal selection of the genetic operators, and optimizing the genetic parameters at the same time is no easy task. There is a loss of diversity within the population as the search progresses due to the problem of “*genetic drift*”. This results in a high probability of premature convergence within the optimization, a scenario where the search converges onto local optima rather than a global optimal [14]. This is especially common in binary representation GAs. As a result of these drawbacks, recent research has led to a proposal of more efficient and better optimization techniques like Breeder Genetic Algorithm (BGA) [15], [16] and Population Based Incremental Learning (PBIL) [14] that yield better results than genetic algorithm and have been used in this thesis. BGA uses a similar concept of survival of the fittest as employed in GA, but use breeding similar to the one practised in artificial animal breeding, resulting in an offspring with the best qualities and characteristics of the parents. In other words GA can be referred to as a model based on natural selection, while BGA is based on artificial selection and it’s expected that artificial selection be more efficient in optimization than natural selection. This has been shown in [16] that BGA outperforms standard GA approaches in many optimization problems including the commonly used benchmark problems. In order to minimise the likelihood of premature convergence in BGA, there is a need to preserve diversity by means of a small additional injection of randomness, or ‘mutation’. Before each “child” trial solution is inserted into the population, a vector of small normal – distributed zero mean random number

with standard deviation R is added. The initial value of R is critical [15], as a small value may lead to premature convergence, while a bigger value may disrupt the search and impair its ability to converge. The value of R is determined by a rule of thumb, which may not work optimally as the initial value is problem dependent. To alleviate such a problem a simple feed-back is used in this thesis called adaptive mutation [15], whereby the mutation rate is adjusted depending on the convergence of the population. Due to the adaptive mutation employed in this BGA, the initial value of R becomes uncritical, since the mutation rate gets optimized as the search progresses. As has been mentioned before, another proposed method that performs slightly better than GA is PBIL. PBIL combines the mechanism of genetic algorithm and simple competitive learning. It is an extension to the genetic algorithm through the re-examination of the performance of the GA in terms of competitive learning. PBIL results in a much simpler and faster optimization technique, with fewer parameters to be chosen by the user. In PBIL the probability vector is updated using the best individual, thereby enhancing the possibility of producing solutions that are similar to the current best individual [14], [17]. In the past, the application of optimization methods to PSS design was applied mostly in simulations. As part of the investigation carried out in this thesis, the simulations were extended to testing the optimized PSSs on an experimental system and observing their performance in damping out the simulations.

1.1 Stability Phenomena, Basic concepts and Definitions

Power system stability is defined as the ability of the system to remain in a state of equilibrium during normal operation and to attain a certain acceptable state of equilibrium after being subjected to certain disturbances [1], [3]. Instability in power systems depends on the system dynamic configuration as well as the operation condition. Stability has been known as a problem of maintaining synchronism. But since power systems are dependent on the synchronous machines for electrical power generation, conventionally for satisfactory system operation, the requirement is that all synchronous generators should remain in synchronism or “*step*” [1], [3]. The stability of the synchronous generators is influenced by the generator rotor angle dynamics and power angle relationships. Another form of instability may also arise without any loss of synchronism. An example is when a system’s synchronous generator is feeding an

induction motor load through a transmission line resulting in instability due to collapse of load voltage [1], [3]. In this regard, maintenance of synchronism is not an issue, but instead the concern is the stability and control of voltage. This form of instability can also occur from load covering an extensive area supplied by a large system [1], [3].

In defining power system disturbance, the focus is given to two types, namely; transient (large disturbances) stability and small signal (small disturbances) stability. Large disturbances occur as a result of severe disturbance which can arise from the following scenarios; short circuits, loss of transmission, loss of a big load or a big generator. Small disturbances arise as a result of continuous and small load or generation changes or self adjustment of the system due to changing operating conditions [1]. If the system is unstable under large and small disturbances, the system should be able to recover to its pre-disturbance or another steady state operating condition and be able to supply the load efficiently [1],[3].

Small signal stability is classified in two categories namely:

- ❖ Rotor angle stability
- ❖ Voltage stability

Rotor angle stability in the small signal is the ability of the system to remain in synchronism following a small disturbance. In the event of instability, two forms exist:

- ❖ Steady increase in rotor angle as a result of insufficient synchronizing torque
- ❖ Rotor oscillations of increasing amplitude as a result of insufficient damping torque.

Voltage stability in the small signal domain is defined as the ability of the system to maintain acceptable voltage at all the buses in the system during and after a small disturbance. Voltage instability occurs in two different forms:

- ❖ Inability of the system to meet reactive power demands and
- ❖ Deep voltage drops that occur as a result of active and reactive power flow through inductive reactance associated with the network [1], [3].

There are a number of factors that contribute prominently to the response and behaviour of the system to small signal disturbances and these include the initial operating point, grid strength and the type of secondary control being used (i.e. excitation control). For

systems without Automatic voltage Regulators (AVR), inadequate synchronising torque contributes to instability which results in a non oscillatory behaviour [1], [3].

For a system with AVR on the generators, AVR tends to improve the transient stability behaviour of the power system, but negatively affect the small signal stability of the system. The damping of the electromechanical modes tends to be reduced, especially if the gain of the AVR is very large or the regulator time constant is very small, usually referred to as a fast acting AVR. The AVR introduces a phase lag between the exciter input and the generator electrical torque, resulting in sustained constant or increasing amplitude oscillations which if allowed to grow further, may result in reduced power supply and eventually system failure [1], [3], [18]-[20]. Angle and voltage stability are related and often contributes to each other interchangeably.

The study of small signal stability is classified in different categories of electromechanical oscillations and this includes: local-area oscillations, inter-area oscillations and inter plant oscillations. Electromechanical or low frequency oscillations as commonly known are in the range of 0.1Hz to 3.0Hz, and these are due to power interchange between different components in the system. Electromechanical oscillations are discussed in detail in the next section.

1.2 Electromechanical Oscillations

The power demand on power systems is increasing daily, resulting in an increase in power systems interconnections so that generated power can be transferred to the necessary consumers. As a result of these interconnections, electromechanical oscillations tend to develop. Different low frequency oscillations exist in different parts of the network, the categories are stated in the previous section and a detailed definition is given here.

Inter-area oscillations occur as a result of a group of generators in one area interconnected via weak tie lines to a group of generators in another area, oscillating against each other. The frequency range of inter-area oscillations is 0.1Hz to 0.8Hz. Inter-area oscillations are much more prominent in an interconnected network with many groups of generators [1], [21].

Local area oscillations are associated with a single generator oscillating against the rest of the network. The frequency range of local mode oscillations is 0.8Hz to 2.0Hz. Local area oscillations are much more prominent when a single generator is connected to a very large network. This is referred to as the single machine to infinite bus system (SMIB) [22].

Inter-plant oscillations occur as a result of the exchange of power between electrical components which are closer to each other and they are usually in the frequency range of 2.0Hz to 3.0Hz [22].

There are other forms of oscillations that may present some difficulties to the stability of the system. These include: control modes and torsional modes.

Control modes are associated with the generators and their control units, often as a result of poorly tuned exciters, speed governors, HVDC converters as well as static compensators [22].

Torsional modes are associated with the turbine-generator shafts systems rotational components. Instability of torsional modes is likely to be caused by interaction with excitation controls, speed governors, HVDC controls and series-capacitor-compensated lines [22].

1.3 Evolution of stability problems

Power system stability is a complex phenomenon, which has attracted much attention over the past few decades. Early stability problems were associated with remote hydroelectric generating power stations feeding into metropolitan load centres over long distance transmission [1], [3]. Such systems were operated close to their steady-state stability limits due to various economic reasons. Occasionally, instability occurred during steady state conditions, but in most instances it occurred during large disturbances which included short circuits and loss of major generators or big loads. The strength of the

transmission lines was highly influential in stability problems, with insufficient synchronizing and damping torque contributing greatly to instability [1], [3].

The methods of analysis used were dictated by developments in the art of computation and the stability of vector theory of dynamic systems [1]. But as the evolution of power systems started and the interconnections between independent systems became economically attractive, the stability problems increased [1]. In 1930, a significant step toward the improvement of stability problems was developed using the network analyser. *“A network analyser is a scaled model of an ac power system with adjustable resistors, reactors and capacitor to represent transmission networks and loads, voltage sources whose magnitude and angle can be adjusted to represent generators and meters to measure voltage, currents and power anywhere in the network”* [1].

The theoretical work carried out in the 1920's and 1930's, helped with the basic understanding of the power system stability phenomena [1]. The principal developments and knowledge of power systems stability came as a result of the study of long distance transmission, rather than as an extension of synchronous machine theory. More attention was given to the network, while generators were seen as simple voltage sources behind fixed reactance, and loads considered as constant impedances [1]. This was deemed as a necessity due to the restrictive ability of the computers available at the time. They were more equipped to solve algebraic problems, than differential and dynamic equations.

Around 1950's, the complexity of computational methods started improving and the detailed analysis of stability increased, taking into account the synchronous generator modelling, excitation systems and speed-governor was easily done. First it was electronic analogue computers that were used before the middle of 1950s, but later the development of digital computers allowed the improvement over network analysers, enabling researchers to model detailed generator models and be able to simulate large systems [1]. Interconnections of large systems started growing as a result of the digital computers. This was more common and prominent in Canada and the United States [1].

By the early 1960's, most digital simulation programs were developed to simulate and analyse the transient stability problems in power systems. Most of the generating units were equipped with exciters (AVRs). Exciters were perceived to help in improving transient stability performance of the system, and since much industry effort was concentrated in transient stability problems, AVRs were perceived as the solution [1]. Although AVRs provided a solution to transient stability problems, they tend to make the system exhibit oscillatory instability. This is attributed to the fast-response exciters with high exciter gains and low regulator time constants [1], [3], [7]-[8], [18]-[20], [22].

Other factors include the reduction in the strength of the transmission lines as compared to the size of the generation units. Instability in power systems also occurs as a result of the increase in the interconnection of power generators connected via weak tie lines, with heavy power transfers likely to exhibit inter-area oscillatory modes, making it a major concern for power system engineers. Research has allowed the control of these low frequency oscillatory modes since the early 1970's when power system stabilisers have been proposed to provide supplementary damping to the low frequency modes to counter the negative damping introduced by the fast and high gain exciters. The PSS can use the generator electric power deviations as an input or other signals such as speed variations, frequency, etc to damp rotor oscillations. Other controllers that have been used in damping electromechanical oscillatory modes include SVCs, STATCOM [1], [23] and FACTS controllers [24].

Even though PSS has been perceived as the best way of damping the low frequency modes, the tuning of its parameters is also very important, especially when dealing with dynamic system. In the past engineers used the conventional methods to tune the parameters, but recently modern control methods and computational intelligence techniques have been used in the design of PSS to provide adequate damping as the system operating condition changes [4] – [6].

1.4 Functions of PSS and PSS Design Methods

The function of the power system stabilizer is to add extra damping to the generator rotor oscillations by controlling its excitation using auxiliary stabilizing signals

[1],[18],[22],[25]. In so doing, the stabiliser must produce an electric torque component in phase with the rotor speed oscillations, thus adding damping to the generator rotor oscillations [26]. In many instances the preferred signal used to control excitation or input to the PSS is the generator speed deviation (delta-omega), although electrical power deviation (delta-power) is frequently used as well [1], [22]. Apart from speed deviation (delta-omega) and power deviation stabilizers, different types of stabilizers can be used like frequency based, terminal voltage and digital stabilizers [1], [26]

The equation for a speed input PSS is given in (1.1) and the block diagram is given in Figure 1.1.

$$U_{pss}(s) = K \frac{sT_W}{1+sT_W} \frac{1+sT_1}{1+sT_2} \frac{1+sT_3}{1+sT_4} \Delta\omega(s) \quad (1.1)$$

where

K denotes the PSS gain

T_1, T_2, T_3 and T_4 denote the PSS lead-lag time constants

T_W denotes the washout time constant

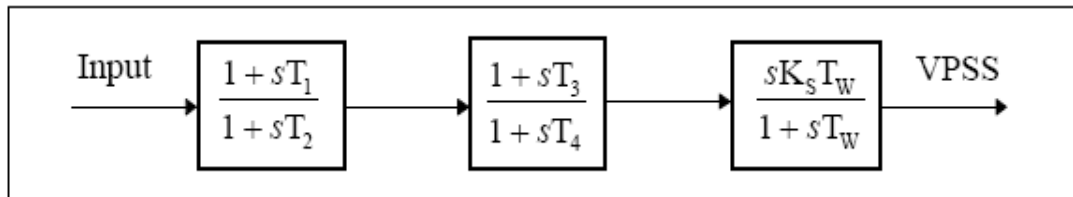


Figure 1.1: Lead- Lag PSS structure

The structure of the PSS is shown in Figure 1.1, consists of the washout block, the PSS gain and the stabilizer lead-lag blocks. The gain (K) of the PSS helps in improving the damping ratio of the low frequency oscillatory modes. It determines the amount of damping introduced, which ideally should be set to the maximum damping corresponding value, however certain limitations, such as high gain might impact the performance of the PSS under severe transient disturbances, and therefore this value might not be optimal enough. The lead-lag blocks or phase compensation blocks as it is commonly known, provide enough phase lead to compensate for the phase lag introduced by the exciter,

between the exciter input and the generator electrical torque [1]. Care must be taken when tuning the lead-lag parameters, such that the PSS does not provide excessive compensation to the phase lag. Conventionally the PSS can provide slightly under compensation to the phase lag. In addition the PSS is required to provide adequate damping over a certain range of frequencies, usually the low frequencies in the range of 0.1Hz to 3.0Hz than just a single frequency. Concurrently the PSS should be able to adequately provide damping to the system as the operating conditions change. Generally one or two lead-lag blocks are used, but more blocks than two can be used if the situation requires it. This is dependent on the magnitude of the network phase lag at the operating condition.

The last block is the washout block, which serves as a high pass filter, with a time constant (T_w) high enough to allow the speed signal to go through unchanged. Without the washout filter, steady state changes in speed might alter the terminal voltage. It should only allow the PSS to respond to speed changes. The value of the time constant is not really critical even though certain preferences are given depending on the type of system and oscillations in question. For local area oscillation modes, which usually occur in a single machine connected to an infinity bus system, a value between 1 to 5 seconds is recommended, while in multi-machine interconnected systems where inter-area and inter-plant oscillations exist, a value between 5 to 20 seconds is desired [1], [3], [18]-[20]. The only requirement is that it must be long enough not to alter the steady state variables. When using the PSS, the overall stability of the system should be enhanced and not only small signal stability. There is also a limiter block that is used to prevent the output of the PSS from driving the excitation into heavy saturation. It prevents or limits the output of the PSS from countering the effect of the AVR. The negative limiter is of outmost importance during the back swing of the rotor after initial acceleration of the generator is over [26]. In the past, PSS designs were solely based on single machine to infinite bus systems (SMIBs), considering that researchers used the concepts of damping and synchronising torques. The design was aimed at stabilizing the local oscillation modes only that exists in SMIB. The simultaneous coordination of multi-machine PSSs was not really entertained. But recently computers have allowed for the design of multiple PSSs for multi-machine systems [27].

The method of PSS design in recent years has gained importance due to the research methods being implemented and the performances associated with it. PSS design can be classified into two methods which are linear and non-linear. Linear methods require the system to be linearized around a certain equilibrium point (operating point). Linear methods have been used over the years and it is the method considered in this thesis. Within linear methods, design can be performed using classical or conventional methods and modern control methods. Non-linear methods work by first approximation to determine the small signal stability of the system. Some of the methods that have been applied are differential geometric approach [28], Hamiltonian structure control [29], [30] and adaptive backstabbing control [31]. These methods are outside the scope of this thesis.

1.4.1 Conventional PSS design methods

Conventional methods have been applied to the design of the PSS over the years and they have been employed by utility engineers due to their simplicity. Other reasons include the ease of online tuning of the CPSS as well as the lack of assurance of the system's relative stability related to some adaptive or variable structure techniques. In using conventional methods, the system is linearized around the nominal operating condition and the phase compensation method is applied to provide the phase lead required in the system. This method works by initially identifying the phase lag that exists in the open loop, with voltage reference being the input while the output is the electrical torque. Once this is obtained, the time constants of the PSS are adjusted to match the ideal phase lead, whereby the phase lead is the negative value of the phase lag. The gain is usually obtained by trial and error or root locus design [32], [33]. This method is much more prominent in single machine to infinite bus systems, where local area oscillations are much more common, usually in the range of 0.8Hz to 2.0Hz.

In multi-machine systems, inter-area modes are much more prominent and therefore together with local mode oscillations need to be taken into consideration when a PSS is being designed. Other methods that are used to design conventional PSS include root-

locus, eigenvalue and frequency response techniques. PSS designed using conventional methods improve the stability of the system around the operating condition, but does not maintain the same level of stability in the system as the operating condition changes. Therefore the PSS might not be able to maintain the same level of performance across all the operating conditions or in the event of severe system faults. In light of this, researchers have proposed new methods such as artificial intelligence, H_∞ control and adaptive techniques to help in the design of power system stabilisers that are more flexible and robust.

1.4.2 New PSS Design Methods

An important design criterion in PSS is the robustness of the PSS, whereby robustness is defined as the ability of the PSS to maintain the same level of performance and the stability of the closed loop for the entire range of operating conditions. Most of the conventional methods tend to have problems in providing a robust PSS. The controllers designed using conventional methods are only able to provide effective damping for conditions around the nominal operating point, but adequate damping is not guaranteed across all operating conditions as the system dynamics change. As a result, researchers have been focusing on new control theories and techniques to help with the design and tuning of a robust PSS. This following section only covers a few selected ones, but there are many more.

Pole placement method works in conjunction with the root locus; it makes use of modern computational programs to decide where to place the closed-loop poles in the complex s -plane. It allows for the shaping of the dynamic response of the system [34]-[36]. This method works properly, but tends to have some problems, especially as the state matrix of the system grows. It makes the process complex and computationally intensive. This method gets even more complex if there are certain states in the system that are uncontrollable or unobservable [3].

Adaptive control is based on the idea of continuously updating the controller parameters according to recent measurements. Adaptive stabilizers are much more flexible in terms

of their parameter tuning as compared to conventional methods. Parameters in conventional PSS are fixed, while in adaptive PSS they are dynamic. They change as the operating conditions change. These parameters are usually tuned online, as the dynamics of the generators and loads change. This makes the adaptive controllers much more robust across all the operating conditions. Also in adaptive PSS, the real physical system is considered as opposed to the computer simulations that assume a much more ideal system, while in essence the physical system is not ideal and there is noise and saturation of the elements that exist as well as unexpected disturbances [5], [37], [38]. However there are factors that may affect the robustness of the adaptive PSS. These include the complexity of the system model and the speed of the controller, as a slow PSS might have a devastating effect on the system [3]. Furthermore there are some disadvantages associated with the complexity of the controller design and its cost as well as their poor performance during the learning phase, especially if they are not properly initialised [39]. In most cases the adaptive PSSs are designed using neural and fuzzy logic networks [5], [37], [38].

Robust control: H_∞ techniques have also been applied to the problem of the PSS design [5], [13], [40]. However there are some difficulties in selecting the weighing functions of the optimization. At the same time the multiplicative and/or additive uncertainty representations are not suitable for situations where the nominal stable system becomes unstable after being perturbed. In addition, the mixed sensitivity approach produces closed loop poles whose damping is directly dependent on the open loop system. This effect is caused by the pole-zero cancellation phenomena associated with such an approach. Moreover the H_∞ based PSS tend to have the same order as the plant, therefore resulting in highly complex stabilizers [6], [13], [40]-[42].

Evolutionary Algorithm (EA): the application of **Evolutionary Algorithm** has recently attracted the attention of researchers in the area of power system control. This is specifically true for Genetic Algorithms (GAs) which have gained momentum over the past few decades. GA based PSS allows for the design and tuning of PSS parameters to simultaneously stabilize the system over a wide range of operating conditions [32], [43], [44]. It allows for the conversion of the problem of selecting PSS parameters into a

simple optimization problem that is solved iteratively. The result is a controller that is able to effectively stabilize the system over a certain range of operating conditions. Although GA allows for the design of such a controller, the main drawback of GA is the issue of premature convergence, which sometimes may result in non-optimal parameters for the PSS. In order to counter such problems, highly EA such as BGA and PBIL techniques have been proposed. This thesis compares the performance of the PSS designed using three EA methods (GA, BGA and PBIL). PSS designed using EA offers the following advantages:

- ❖ EA allows the design of a robust PSS, where several operating conditions and dynamic configurations have been considered in the design process.
- ❖ It is independent of the non-linearity, continuity or complexity of the problems and systems to be considered.
- ❖ EA is population based; it searches a solution from a population of points, instead of a single point. This helps the algorithm in locating the global best instead of the local best.
- ❖ It relies on random sampling, which makes it a nondeterministic method.

There are other PSS design methods such as Fuzzy logic [45]-[47], Adaptive Neural Networks, [48], Particle Swarm Optimization (PSO) [49], and Simulated Annealing (SA) [50] that have been applied over the years, but have not been discussed in this thesis.

1.5 Objectives of the Research

The objectives of this thesis are therefore to:

- ❖ Compare the performance of three optimization techniques based on Evolutionary Algorithms, paying particular attention to their application in tuning PSS parameters.
- ❖ Simultaneously optimize the power system stabilizers parameters using Evolutionary Algorithm techniques (Genetic algorithm, Breeder Genetic Algorithm and Population Based Incremental Learning).
- ❖ Tune power system stabilizers parameters to stabilize the system robustly, over a wide range of operating conditions.

- ❖ Compare the performance of the power system stabilizers designed with the above mentioned evolutionary algorithms and make some recommendations using the single machine to infinite bus system as well as a Two-Area Multi-Machine system
- ❖ To test and validate the PSS designed using EAs on a real time system (experimental system).

1.6 Limitations and scope of investigation

The scope of the investigation was to design a Power System Stabilizers using three methods of evolutionary algorithm (GA, BGA and PBIL), and compare their performances in damping out electromechanical modes in the system. The investigation done was mainly based on the small signal stability of the system (SMIB and Two-Area Multi-machine system), with focus on local and inter-area oscillation modes. However transient disturbances were also considered to investigate whether the designed PSS also improves the transient stability and check whether the system is robust enough. The investigation carried out and the results presented and conclusions made in this thesis are based on the systems that were used in the simulations. Also the results obtained are based on the objective function presented in section 4.3.

1.7 Software packages used for the Simulations

The Power System Toolbox (PST) developed by Graham Rogers [51] has been used in modelling and simulating the behaviour of the system. This includes the load flow/power flow analysis, systems dynamics and linear system analysis. All the eigenvalues, small signal analysis and transient simulations for both single machine and multi-machine systems were modelled in PST. PST generates the system linear state space matrices which represents the linearized mathematical model of the power system. The PST software uses different *m-files* developed in the Matlab environment. A genetic algorithm toolbox developed by Houck, Joines and Kay in [52] called “*A Genetic Algorithm for Function Optimization (GAOT)*” was used in optimizing the PSS parameters for the GA-PSS. The GA toolbox also use different m-files developed in Matlab. The BGA program used in this thesis was developed by John Greene [15] and was used to run the BGA PSS optimization.

1.8 Outline of the Thesis

The thesis is summarized as follows:

- Chapter 1** Gives a background on the stability concept, basic concept definitions and the evolution of stability problems.
- Chapter 2** Deals with the review on system linearization and state space representation.
- Chapter 3** Introduces the idea of evolutionary algorithm, specifically focusing on the theory behind Genetic Algorithm (GA), Breeder Genetic Algorithm (BGA) and Population Based Incremental Learning (PBIL).
- Chapter 4** Presents an overview on the application of Evolutionary Algorithm and the procedures used to design the evolutionary algorithm based power system stabilizers. Also included are the optimization parameters used.
- Chapter 5** Presents the optimized power System Stabilizers parameters, eigenvalues analysis and the time domain simulations for the Single Machine to Infinite Bus system (SMIB) and the discussion thereof.
- Chapter 6** Presents the optimized power System Stabilizers parameters, eigenvalues analysis and the time domain simulations for the Two-Area Multi-machine system and the discussion thereof.
- Chapter 7** Summarise the real time simulation as well as the implementation of the PSS that was carried out at the University of Calgary, Alberta.
- Chapter 8** Concludes the thesis and give recommendations as well as giving suggestions for future work.
- References** The references used in the thesis are presented in this section.
- Appendix** The Appendix chapter gives the different data of the systems used in the simulation as well the mathematical modelling of the generators. The Appendix is divided into four sections, from A to D.

Chapter 2

System Linearization and State Space Representation

2.1 Introduction

Eigenproperties are widely often used in small-signal stability studies. Eigenproperties of the system include eigenvalues, eigenvectors, and sensitivity analysis as well as participation factors. In this chapter, an analytical technique is studied and the linearization of the system differential equations is reviewed. The construction of the state matrices is represented and the analysis of the eigenproperties is also reviewed.

2.2 State Space Representation

The dynamic behaviour of electrical system can be represented by first order non-linear differential equations of the form:

$$\dot{x} = f_i(x_1, x_2, \dots, x_n; u_1, u_2, \dots, u_r; t) \quad (2.1)$$

where: $i = 1, 2, 3, 4 \dots n$

That can be written in vector representation form:

$$\dot{x} = f(x; u; t) \quad (2.2)$$

where:

x : the state vector of an (nx1) order

\dot{x} : the derivative vector of the state variables

f : the vector of the non-linear functions

u : the vector of the inputs

t : the time

n : the order of the system

r : the number of inputs

Sometimes derivatives of the states variables are time invariant and this is referred to as autonomous systems of the form:

$$\dot{\mathbf{x}} = \mathbf{f}(\mathbf{x}, \mathbf{u}) \quad (2.3)$$

The order n , of the system depends on the complexity of the generator models, from the simple classical model of order two to much more complex models of order, six, seven and eight which include windings on both the d and q axis. The choice of the generator model is dependent on the accuracy of the study required and its complexity. Often output variables which are observed on the system are also expressed in terms of the state variables and the input variables [1], [19].

$$\mathbf{y} = \mathbf{g}(\mathbf{x}, \mathbf{u}) \quad (2.4)$$

\mathbf{y} is the output vector

\mathbf{g} is the vector of non-linear equations that relates the output variables to the state and input variables

2.3 Linearization

Under small disturbances, the differential equations that describe the response of the system disturbance may be linearized to simplify the analysis. The state equations are linearized around a certain operating point denoted by the state-variables \mathbf{x}_0 and \mathbf{u}_0 . Since the system is at equilibrium, the following equation should be true for certain \mathbf{x}_0 and \mathbf{u}_0 [1], [18]-[20], [53], [54].

$$\dot{\mathbf{x}}_0 = \mathbf{f}(\mathbf{x}_0, \mathbf{u}_0) \quad (2.5)$$

Upon a small perturbation in the system, the state and input variables are perturbed and deviate from the operating point by small variations $\Delta\mathbf{x}$ and $\Delta\mathbf{u}$ respectively, with the new system equation changing as in [1] to:

$$\dot{\mathbf{x}} = \dot{\mathbf{x}}_0 + \Delta\dot{\mathbf{x}} = \mathbf{f}(\mathbf{x}_0 + \Delta\mathbf{x}, \mathbf{u}_0 + \Delta\mathbf{u}) \quad (2.6)$$

Assuming that the perturbations in the system are so small, the system equations $\mathbf{f}(\mathbf{x}, \mathbf{u})$ can be expressed in Taylor's series expansion terms and neglecting the second and higher order partial derivatives, results in the following approximations [1], [19].

$$f_i[(x_0 + \Delta x), (u_0 + \Delta u)] = f_i(x_0, u_0) + \frac{\partial f_i}{\partial x_1} \Delta x_1 + \dots + \frac{\partial f_i}{\partial x_n} \Delta x_n + \frac{\partial f_i}{\partial u_1} \Delta u_1 + \dots + \frac{\partial f_i}{\partial u_r} \Delta u_r \quad (2.7)$$

Since $\dot{\mathbf{x}}_0 = \mathbf{f}_i(x_0, u_0)$, the above expression gets simplified to:

$$\Delta\dot{x}_i = \frac{\partial f_i}{\partial x_1} \Delta x_1 + \dots + \frac{\partial f_i}{\partial x_n} \Delta x_n + \frac{\partial f_i}{\partial u_1} \Delta u_1 + \dots + \frac{\partial f_i}{\partial u_r} \Delta u_r \quad (2.8)$$

Likewise, the output equation is reduced to:

$$\Delta y_j = \frac{\partial g_j}{\partial x_1} \Delta x_1 + \dots + \frac{\partial g_j}{\partial x_n} \Delta x_n + \frac{\partial g_j}{\partial u_1} \Delta u_1 + \dots + \frac{\partial g_j}{\partial u_r} \Delta u_r \quad (2.9)$$

where $j = 1, 2, 3 \dots m$

After applying the Taylor's series expansion to all the state system equations and output equations and linearizing, the system equations are given in the form [1]:

$$\Delta\dot{\mathbf{x}} = \mathbf{A}\Delta\mathbf{x} + \mathbf{B}\Delta\mathbf{u} \quad (2.10)$$

$$\Delta\mathbf{y} = \mathbf{C}\Delta\mathbf{x} + \mathbf{D}\Delta\mathbf{u}$$

where:

$$\mathbf{A} = \begin{pmatrix} \frac{\partial f_1}{\partial x_1} & \dots & \dots & \dots & \frac{\partial f_1}{\partial x_n} \\ \vdots & & & & \vdots \\ \vdots & & & & \vdots \\ \vdots & & & & \vdots \\ \vdots & & & & \vdots \\ \frac{\partial f_n}{\partial x_1} & \dots & \dots & \dots & \frac{\partial f_n}{\partial x_n} \end{pmatrix} \quad \mathbf{B} = \begin{pmatrix} \frac{\partial f_1}{\partial u_1} & \dots & \dots & \dots & \frac{\partial f_1}{\partial u_r} \\ \vdots & & & & \vdots \\ \vdots & & & & \vdots \\ \vdots & & & & \vdots \\ \vdots & & & & \vdots \\ \frac{\partial f_n}{\partial u_1} & \dots & \dots & \dots & \frac{\partial f_n}{\partial u_r} \end{pmatrix}$$

$$\mathbf{C} = \begin{pmatrix} \frac{\partial g_1}{\partial x_1} & \dots & \frac{\partial g_1}{\partial x_n} \\ \cdot & & \cdot \\ \cdot & & \cdot \\ \cdot & & \cdot \\ \frac{\partial g_m}{\partial x_1} & \dots & \frac{\partial g_m}{\partial x_n} \end{pmatrix} \quad \mathbf{D} = \begin{pmatrix} \frac{\partial g_1}{\partial u_1} & \dots & \frac{\partial g_1}{\partial u_r} \\ \cdot & & \cdot \\ \cdot & & \cdot \\ \cdot & & \cdot \\ \frac{\partial g_m}{\partial u_1} & \dots & \frac{\partial g_m}{\partial u_r} \end{pmatrix}$$

$\Delta \mathbf{x}$ is the linearised state vector of dimension n

$\Delta \mathbf{y}$ is the linearized output vector of dimension m

$\Delta \mathbf{u}$ is the linearized input vector of dimension r

\mathbf{A} is the state matrix of size (nxn)

\mathbf{B} is the input matrix, size (nxr)

\mathbf{C} is the output matrix, size (mxn)

\mathbf{D} is the feed forward matrix, size (mxr)

Once the system has been linearized, the system stability can be analysed using the eigenproperties.

2.4 Eigenproperties of the state matrix

For small signal stability studies, eigenproperties of the state matrix play a major role and should be computed and analysed.

2.4.1 Eigenvalues

Sometimes referred to as the roots of the state matrix, eigenvalues of the matrix \mathbf{A} are computed by solving the equation

$$\mathbf{A}\mathbf{u} = \lambda\mathbf{u}; \quad \mathbf{u} \neq 0 \tag{2.11}$$

where:

λ is a scalar parameter for which there exist a non-trivial solution to the above equation

\mathbf{u} is an nxn vector

\mathbf{A} is the state matrix

For a certain λ value, the following equation should be true

$$\det(\mathbf{A} - \lambda \mathbf{I}) = 0 \quad (2.12)$$

where:

\det denotes the determinant

\mathbf{I} is the identity matrix

The equation above is called the characteristics equation and its solutions, the eigenvalues $\lambda_1, \lambda_2, \lambda_3, \dots, \lambda_n$.

The eigenvalues can be real or complex. For a real \mathbf{A} matrix, the complex eigenvalues occurs in conjugate pairs. A real eigenvalue corresponds to a non-oscillatory mode, while a complex eigenvalue corresponds to an oscillatory mode. Complex modes are usually denoted by, $\lambda = \sigma \pm j\omega$, whereby σ is the real component, while ω denoting the imaginary component gives the frequency of oscillations in rad/s. This frequency can be expressed in [1] in Hz as follows:

$$f = \frac{\omega}{2\pi} \quad (2.13)$$

The damping ratio ζ , determines the rate of decay of the amplitude of the oscillations and is given by the following equation:

$$\zeta = \frac{-\sigma}{\sqrt{\sigma^2 + \omega^2}} \quad (2.14)$$

For power systems, a damping ratio of 5% and above is considered adequate, but a damping ratio of 20% and above is often preferred, especially for electromechanical oscillations [3]. The system is considered stable if the real part of the modes is negative. A positive real mode gives an aperiodic instability. If a complex mode has a positive real part, then the amplitude of the oscillations grow with time. For larger systems, methods like QR algorithm methods are used to compute the eigenvalues instead of using the characteristics equation.

2.4.2 Eigenvectors

For every eigenvalue λ_i , there exists a n column vector \mathbf{u}_i called the right eigenvector, such that;

$$A\mathbf{u}_i = \lambda_i\mathbf{u}_i; \quad i = 1,2,3 \dots n; \quad \mathbf{u}_i \neq 0 \quad (2.15)$$

Right eigenvectors have a dimension equal to the number of state variables. Eigenvectors are not unique and each remains a valid eigenvector when multiplied by a scalar and they describe the activity of the states variable in a specific mode.

There also exist a left eigenvector \mathbf{v}_i such that;

$$\mathbf{v}_i A = \lambda_i \mathbf{v}_i; \quad i = 1,2,3, \dots n \quad \mathbf{v}_i \neq 0 \quad (2.16)$$

The left eigenvector describes the contribution of the activity of a state variable in a mode.

2.4.3 Eigenvalue sensitivity

Eigenvalue sensitivity allows for the examination of the sensitivity of the eigenvalues to the parameters of the state matrix. It helps determine whether the system is sensitive to a certain change in the system's elements. It also represents a very important design tool in control and measurement of many engineering problems. To evaluate the sensitivity analysis, consider a system defined by the following equation [1]:

$$A\mathbf{u}_i = \lambda_i\mathbf{u}_i \quad (2.17)$$

Differentiating the above equation with respect to the A-matrix element a_{kj} , chosen randomly gives [1];

$$\frac{\partial A}{\partial a_{kj}} \mathbf{u}_i + A \frac{\partial \mathbf{u}_i}{\partial a_{kj}} = \frac{\partial \lambda_i}{\partial a_{kj}} \mathbf{u}_i + \lambda_i \frac{\partial \mathbf{u}_i}{\partial a_{kj}} \quad (2.18)$$

Multiplying both sides with the i^{th} left eigenvector, we get

$$v_i \frac{\partial A}{\partial a_{kj}} u_i + v_i A \frac{\partial u_i}{\partial a_{kj}} = v_i \frac{\partial \lambda_i}{\partial a_{kj}} u_i + v_i \lambda_i \frac{\partial u_i}{\partial a_{kj}} \quad (2.19)$$

Using the definition of left eigenvector above, the terms involving $v_i A$ and $v_i \lambda_i$ in (2.19) are cancelled, therefore we have:

$$v_i \frac{\partial A}{\partial a_{kj}} u_i = v_i \frac{\partial \lambda_i}{\partial a_{kj}} u_i \quad (2.20)$$

Finally sensitivity is obtained by altering the above equation to give;

$$\frac{\partial \lambda_i}{\partial a_{kj}} = \frac{v_i \frac{\partial A}{\partial a_{kj}} u_i}{v_i u_i} \quad (2.21)$$

where u_i is the right eigenvector of A, corresponding to the eigenvalue λ_i , while v_i is the left eigenvector.

2.4.4 Participation factors

Considering a certain element p_{ki} called the participation factor, it is defined as the measure of the relative participation of the k_{th} state variable in the i_{th} mode and vice versa. The participation factor tells how much a certain state contributes to a certain mode. As given in [1], the participation factor p_{ki} is given by:

$$p_{ki} = \frac{\partial \lambda_i}{\partial a_{kk}} \quad (2.22)$$

Participation factors are an important aspect of control design and especially in design of power system stabilizers [22]. In the event of speed participation factors being used, they indicate the sensitivity of a mode to the addition of mechanical damping at the generator shaft. If the corresponding speed participation factor of a generator in a mode is zero, then that particular generator does not contribute to the damping of the mode. The participation factors indicate possible locations where a stabilizer may effectively control

the mode of concern and therefore helping in the placement of the power system stabilizers in multi-generators systems [21].

2.5 Summary

This Chapter explored the mathematical modelling of the system for small signal stability studies. Particular attention was paid to the eigenproperties of the system. These include Eigenvalues, eigenvectors, and eigenvalue sensitivity and participation factors.

University of Cape Town

Chapter 3

Background Theory to Evolutionary Algorithms

3.1 Introduction

Evolutionary algorithm is a search algorithm gleaned from organic evolution. It combines the biological ideas of genetics and natural selection. Initiated and formulated in the 1960's by Charles Darwin, which later led to the "*Darwinian theory of evolution*" [55], EA kick started the era of computer science, when researchers tried to solve complex problems by emulating the intelligence capacity of a human mind [55]. During that time, intensive research led to ideas such as artificial neural networks and artificial intelligence. In other words, EA is defined as "*a direct, probabilistic search and optimization algorithm gleaned from the model of organic evolution*" [55]. Artificial Intelligence (AI) uses the properties exhibited by human species via the extreme diversity that results as a mixture of the genetic materials from different individuals of the population. Evolutionary algorithms use some of the genetic operators employed in the evolution of human nature, such as recombination and mutation [55]-[56]. EAs work by copying the principle of "*natural selection*", such that individuals who are better and fitter may survive to form the next generation, while unfit individuals are cut from entering the next generation. As a result of this process, new population tend to produce better and fitter offsprings (solutions) that are fully equipped to solve highly nonlinear complex problems. This thesis employs three different types of EAs, namely; Genetic Algorithms, Breeder Genetic Algorithms and Population Based Incremental Learning. Evolutionary algorithm techniques use iterative methods to obtain a set of parameters (possible solutions) that will be able to solve the problem at hand.

3.2 Genetic Algorithm (GA)

The genetic algorithm is a directed search based on the idea of biological evolution. It is a biologically motivated adaptive system based upon the principles of natural selection and

genetic recombination. It was first developed by John Holland in the 1970s at the University of Michigan. It was a design with two main objectives [55]-[56].

- ❖ To understand the adaptive process of natural systems and to design artificial systems software that retains the robustness of natural systems.
- ❖ To understand it as a tool that provides efficient and effective methods for optimization and machine learning applications.

Generally genetic algorithms use binary codes to represent their chromosomes, even though other representations exist, such as integer and floating point [55]-[58]. There are certain terms that are used in genetic algorithms, which are worth a definition. These are *phenotypes* which are the variables in the problem domain that constitute an individual. *Chromosome* is the real or binary string formed from the individual. A *gene* is an individual position in a chromosome, while an *allele* is the respective values that a gene can take. Genetic algorithms use the principal of survival of the fittest, by manipulating a set of potential solutions in order to generate hopefully better and fitter solutions [58]. The fittest individuals survive and help in the formation of the next population. There are certain operators that govern the optimization in genetic algorithms, such as selection, crossover, mutation and fitness or evaluation [57], [58].

3.2.1 Evaluation and objective function

The core aspect of each genetic algorithm is its evaluation commonly known as fitness and objective functions. The objective function gives a measure of the individuals' brilliance in the problem domain [58]. It is transferred to the fitness function that assigns a fitness value to the individual. The fitness value gives a measurement of the individuals' strength in the problem domain as compared to other individuals. Individuals that give higher fitness values (in the case of maximization) are deemed better and fitter in achieving the objective. Both fitness and objective functions are problem dependent and therefore it is required that the binary chromosomes are converted to their equivalent real value representations for evaluation in the event where binary representation is being used. Once the fitness of an individual has been tested, the individual goes through selection, crossover and mutation [58].

3.2.2 Selection

Selection is defined as a “*process determining the number of times, or trials a particular individual are chosen for reproduction and thus the number of offsprings that an individual will reproduce*” [51]. Selection is naturally a stochastic and cumbersome process in its operation, especially the way it translates a certain individual’s relative fitness into the probability of being selected for the next generation. In most cases the performance of a selection process is determined by its biasness, spread and efficiency, whereby bias is defined as the absolute difference between an individual’s actual and expected selection probability [58].

The most commonly used selection type is the roulette wheel, whereby each individual is allocated a space on the wheel according to the magnitude of their fitness. The fittest individuals tend to have a larger allocation on the wheel as compared to weaker individuals and therefore stand a better chance of being selected for the next generation. An example is shown in Figure 3.1 for six individuals from one to six.

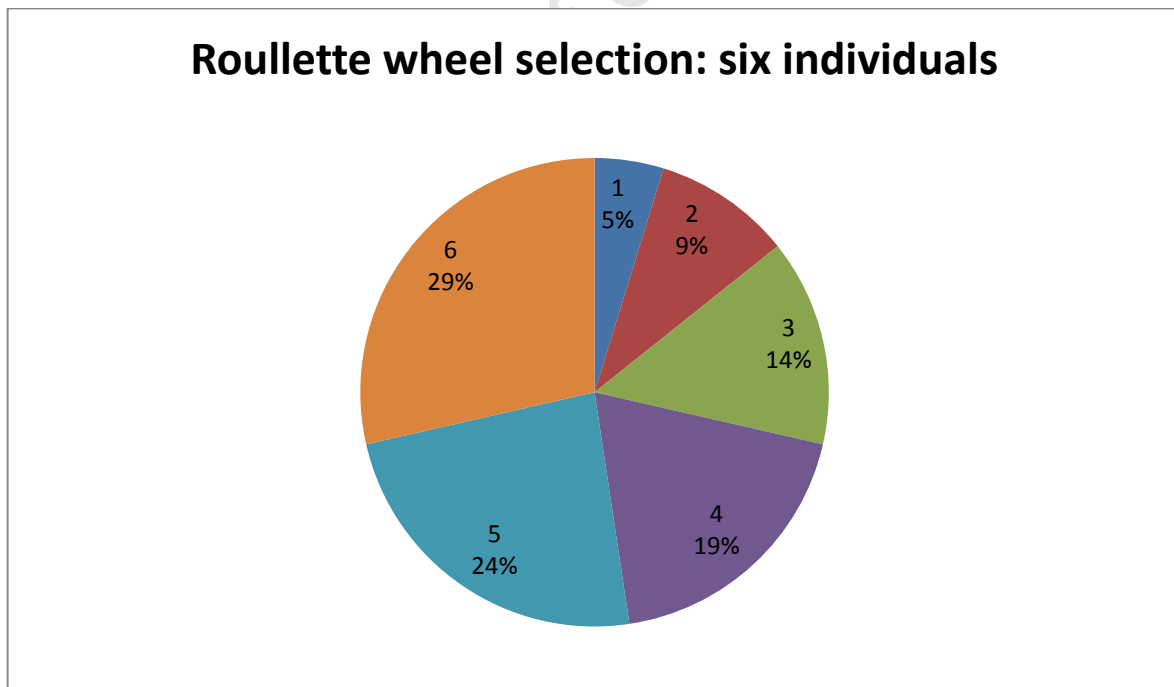


Figure 3.1: Roulette wheel selection

The six individuals (represented by numbers from one to six) are shown in the roulette wheel above in Figure 3.1 according to their fitness values. A random number is

generated and the wheel is spun around a few times and the individual whose segment spans the random number is selected. This process is done repeatedly until all the parents for the next generation are obtained.

This thesis uses a different type of selection method from the roulette wheel, called the normal geometric selection method, whereby the probability of selecting an individual is calculated by the following expression [52], [59]-[60].

$$P_i(\text{probability of selecting the } i^{\text{th}} \text{ individual}) = q'(1 - q)^{r-1} \quad (3.1)$$

where:

$$q' = \frac{q}{1 - (1 - q)^n}$$

q is the probability of selecting the best individual

r is the rank of the individual, 1 being the best

n is the population size

It can be seen from equation 3.1, that the probability of selecting a certain individual is not only dependent on the rank of the individual within the problem domain, but also on the population size as well as the probability of selecting the best individual. Choosing the probability of selecting the best individual is based on trial and error and thus may not be the best value.

Apart from the types of selection methods discussed, there are many others that can be used, and these include: proportionate selection, tournament selection [61], truncation selection, [15], [61] stochastic universal sampling [58], [61], as well as linear and geometric selection [52], [61].

3.2.3 Crossover or Recombination

Crossover is an equivalent of recombination in binary number representation. Crossover produces offsprings which resemble the genetic mixture of the two parents. There are a handful of crossover methods available in the literature [15], [52], [58], but only a few will be discussed in this thesis. Single point crossover or simple crossover as commonly

known is discussed with an example shown in Figure 3.2. Two offsprings are produced from the respective two parents A and B [58].

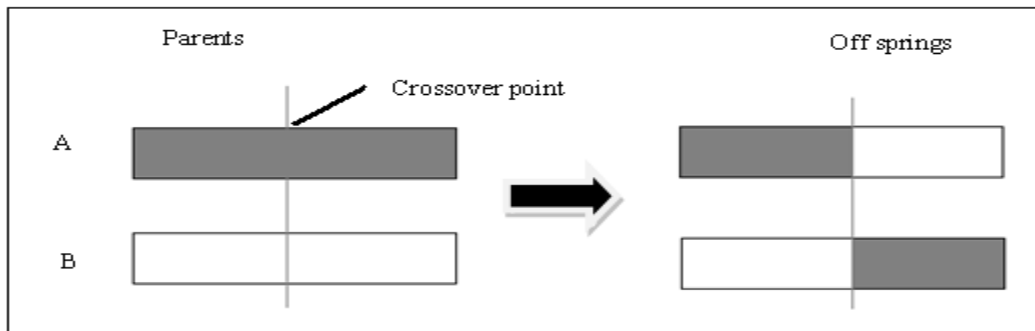


Figure 3.2: Single point crossover

A single point crossover is applied in the middle of the two parents, such that the offsprings take half of each of their parent's characteristics.

The same analogy used in simple crossover is repeated in multi point crossover. Multi point is obtained by repeatedly applying single point crossover to the parents. In the event of six point crossover being used, the parents get sampled at six different points and the offspring produced interchange the genetic materials of the parents. Usually this type of crossover is used in a binary coded representation genetic algorithm. Recombination is an equivalent of crossover in real valued representation and is discussed under the Breeder Genetic Algorithm technique. There are two other common types of crossover method which are usually employed in floating point representation or real-coded representation; referred to as uniform and arithmetic crossovers.

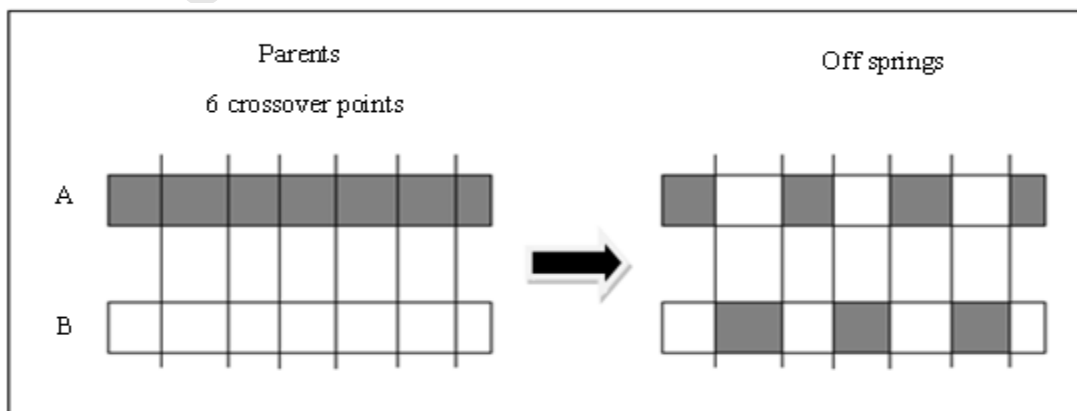


Figure 3.3: Six point multiple point crossover

In simple crossover, a certain random number r is generated from a uniform distribution from 1 to m ; m being the dimension of the row vector denoting the parents from the population and creates two individuals using the following expressions [52], [55]-[56], [58]:

$$x'_i = \begin{cases} x_i & \text{if } i < r \\ y_i & \text{otherwise} \end{cases} \quad (3.2)$$

$$y'_i = \begin{cases} y_i & \text{if } i > r \\ x_i & \text{otherwise} \end{cases}$$

where, x_i and y_i denote the two parents respectively, while

x'_i and y'_i denote the two (produced) offspring

Arithmetic crossover takes two parents and performs an interpolation along the line formed by the two parents. It is constructed by borrowing the concept of linear combination of vectors from the area of convex sets [62]. Arithmetic crossover produces two complimentary linear combinations of the parents:

$$X' = rX + (1 - r)Y \quad (3.3)$$

$$Y' = rY + (1 - r)X$$

Where r is a uniform random number between 0 and 1

X and Y denote the parents

X' and Y' denote the offsprings

An example of Arithmetic crossover is illustrated in Figure 3.4. The two parents are X and Y , while the offsprings are \bar{X}' and \bar{Y}' . The value of r used in the Arithmetic is 0.5.

	Parents X and Y											offsprings \bar{X}' and \bar{Y}'										
X	0.1	0.2	0.3	0.4	0.5	0.6	0.7	0.8	0.9		0.2	0.2	0.3	0.3	0.4	0.4	0.5	0.5	0.6	0.6	\bar{X}'	
Y	0.3	0.2	0.3	0.2	0.3	0.2	0.3	0.2	0.3	→	0.2	0.2	0.3	0.3	0.4	0.4	0.5	0.5	0.6	0.6	\bar{Y}'	

Figure 3.4: An example of Arithmetic crossover

Arithmetic crossover has been used in this thesis in running the Genetic Algorithm.

3.2.4 Mutation

In natural evolution, mutation is a random process where an allele of a gene gets replaced by a new allele to produce a new chromosome. In GAs, a small probability is randomly applied to the chromosomes to perform mutation. The random probability is usually in the region of 0.001 to 0.01 [58]. Mutation provides a degree of diversity in the next population. It also helps with the recovery of the good genetic material that might have been lost in the selection and crossover processes. An example of the effect of mutation in a binary string is given in Figure 3.5.

	Binary	Real	Gray
Original string	0001100010	0.9659	0.6634
Mutated string	0011100010	2.2146	1.8439

Figure 3.5: Mutation

In the example shown in Figure 3.5, the third bit in the original binary string has been changed from a zero to a one. This has resulted in a completely different bit string and therefore a completely different number as shown by their respective real gray code values. The type of mutation that has been used in this thesis is the non-uniform mutation. Non-uniform mutation changes one of the parameters of the parent based on a non-uniform probability distribution. The Gaussian distribution starts out wide and narrows to a point distribution as the current generation approaches the maximum generation [62].

In non-uniform mutation, the change that a gene undergoes is dependent on the value of the current generation. This property of the non-uniform mutation allows the search to explore the space uniformly at smaller values of the generation and locally as the generation increases, increasing the chances of generating new numbers close to their successors, rather than randomly selecting any number [56], [63]-[65]. The mutation is defined as follows: If $x_t^t = \{x_1, x_2, x_3, \dots, x_m\}$ is a chromosome and an element x_k is selected for mutation, then the resultant vector of the next generation is given as

$x_i^{t+1} = \{x'_1, x'_2, x'_3, \dots, x'_m\}$ whereby the mutated element of the next generation is given by:

$$x'_k = \begin{cases} x_k + \Delta(t, UB - x_k) & \text{if } \rho \text{ is } 0 \\ x_k - \Delta(t, x_k - LB) & \text{if } \rho \text{ is } 1 \end{cases} \quad (3.4)$$

where ρ is a random selected number $U(0,1)$

LB and UB are the lower and upper boundaries of the variable x_k

$$\Delta(t, y) = y(1 - r^{(1-\frac{t}{T})})^b, \quad (3.5)$$

where:

$$y = \begin{cases} (t, UB - x_k) & \text{if } \rho \text{ is } 0 \\ (t, x_k - LB) & \text{if } \rho \text{ is } 1 \end{cases} \quad (3.6)$$

Where r is a uniform random number from $[0,1]$, t is the current generation, T is the maximum generation number, while b is the system constant parameter determining the degree of dependency on the iteration number. Clearly from equation 3.5 and equation 3.6, it can be observed that $\Delta(t, y)$ always retain a value between 0 and y depending on the current generation and the value of r . If r is closer to zero, or at lower values of t , then a value closer to y is returned, while as t increases, approaching T , then a value closer to 0 is returned, therefore making the changes smaller as the current generation increases in value, thus localising the search [56], [63]-[64]:

3.2.5 Chromosome Representations

There are many advantages that support the idea of real or floating point chromosome over binary-coded chromosomes in genetic algorithm and these are discussed below [59], [66], [67], [60].

- ❖ Real value chromosome representation increases the efficiency of the genetic algorithm as there is no need of chromosome conversion
- ❖ Real value takes up less CPU time as the internal computer representation can be used directly.
- ❖ It has increased precision as there is no discretization from binary to another type of representation.
- ❖ It allows a variety of genetic operators to be used, in the sense that more than one recombination can be used in a single optimization and many different genetic operators can be used (there are several types of recombination and mutation

operators), as opposed to binary which only allows simple crossover and binary mutation to be used.

- ❖ For optimization problems with continuous variable, it is easier and more direct to use real valued representation instead of binary. This will lead to a simpler and more efficient implementation.

3.2.6 Termination

The genetic algorithm optimization gets terminated when an optimum value has been obtained or in event when the maximum number of iterations has been reached. A simple flow chart for the genetic algorithm is shown in Figure 3.6.

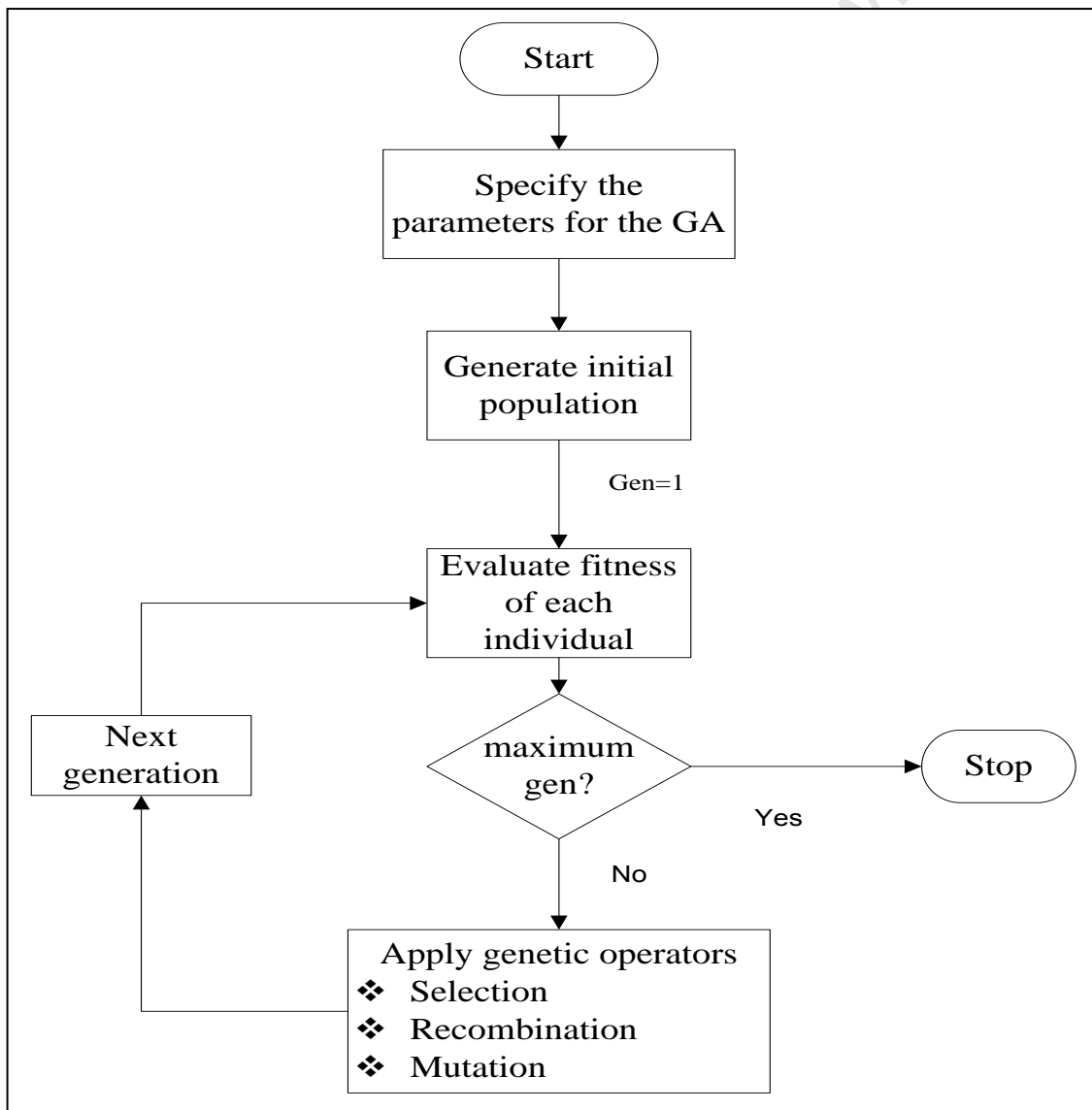


Figure 3.6: Flowchart of the Genetic Algorithm

A major setback in GA is the likelihood of premature convergence, whereby a good but not optimal solution dominates the population. This problem has been minimised in BGA due to the small additional injection of randomness to the population [15].

3.3 Breeder Genetic Algorithm (BGA)

Originally proposed and developed by Professor Muhlenbein [16], Breeder Genetic Algorithm is a breed of genetic algorithms. It is based on artificial selection similar to the one used in animal breeding, as opposed to the “*Darwinian evolution*” [16]. Artificial selection (selective breeding) refers to the intentional breeding for certain qualities or a combination of qualities (e.g. breeding a rose plant to produce large flowers or chicken to lay more eggs). This has been recently applied to cattle to produce more milk and beef. In contrast, natural selection is based on the differential reproduction of organisms with certain qualities which are attributed to the improved survival or reproductive ability (Darwinian fitness) [16]. In other words, natural selection is when nature chooses the organism with the favourable characteristics to survive (e.g. long-necked giraffes are chosen by nature, because they have the favourable characteristics of being tall which allows them to reach higher branches in higher trees.). It is a very simple, but very powerful tool, extremely versatile and a highly effective function optimizer. It allows for very few parameters to be specified by the user. BGA, similar to GA, is also based on survival of the fittest, but trial solutions in BGA are represented by vectors of real numbers as opposed to classical GAs, which are mainly binary and sometimes floating or integer representation [15], [16], [66].

This thesis employs a slightly modified type of BGA called Adaptive Breeder Genetic Algorithm (AMBA) [15]. The modification is done to preserve the diversity of the population by adding small randomness or mutation. Before a child trial solution is inserted into a population, a small vector of normally-distributed zero - mean random number is added. This helps in reducing the likelihood of premature convergence, whereby a non-optimal solution comes to dominate the population. Similar to classical GA, BGA also employs selection, recombination and mutation, but slightly differs from the ones used in GA [15], [62].

3.3.1 Selection

Breeder genetic algorithm uses a selection method called “*truncation*”. In truncation selection, a selected top T% of the fittest individuals are chosen from the current generation, and they go through recombination and mutation to form the next generation [15], [17], [61], [62]. The remaining individuals are discarded. An “*ellist*” as referred to in truncation methods, is the fittest individual in the generation and is guaranteed a place in the next generation. The remaining (T-1) % of the top individuals go through the recombination and mutation in generating the next generation. Recombination is similar to crossover in binary representation and mutation will be discussed in the subsequent sections. The process is repeated until an optimal solution is obtained [15], [16], [66].

3.3.2 Recombination

Adaptive Mutation Breeder Genetic Algorithm uses more than one recombination operator, different to GA where a single type of recombination is used. This is to allow the recombination to search the space with a particular bias, since there is no prior knowledge as to which recombination will give better results. Several recombination methods allow the selection to do the elimination [15], [16], [66]. The two methods employed in AMBA are volume and line recombination.

In volume recombination, a random vector r , equal to the parents in length, is generated and the offspring produced is modelled by the following expression:

$$z_i = r_i x_i + (1 - r_i) y_i \quad (3.5)$$

where:

z_i is a component of the child

x_i and y_i are the two respective parent components

r_i is the random vector component

In this type of recombination children are said to be located at random points in the inside of the hyper box defined by the parents. The child takes a random position in the hyper box [15], [16] as shown in Figure 3.7.

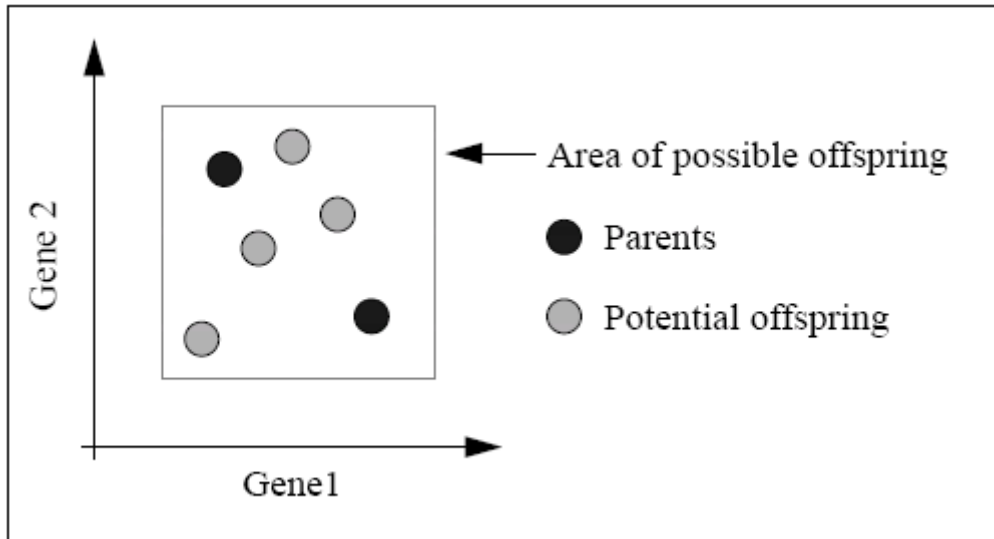


Figure 3.7: Volume recombination

In line recombination, a single random number r , between 0 and 1, is generated and the offspring produced is modelled by the following expression:

$$z_i = rx_i + (1 - r)y_i \quad (3.6)$$

Analogically a child can be said to be located randomly at a selected point on a line connecting the two parents, X and Y, as shown in Figure 3.8 [15], [16].

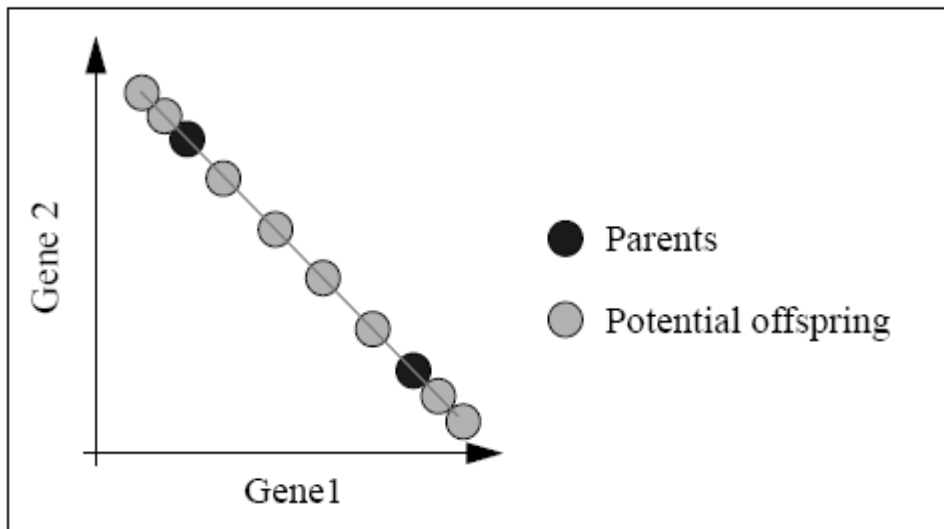


Figure 3.8: Line recombination

There are other methods for recombination that can be used. These include: uniform, extended intermediate and extended line recombination [15], [38], [52], but they are not discussed in this thesis.

3.3.3 Adaptive Mutation

As mentioned before, the major concern in GA has been the issue of premature convergence. This is minimised in BGA, by preserving the diversity of the population due to the addition of small, normally distributed zero mean random numbers to each child, before inserting it into the population. The random numbers have a certain standard deviation R [15]. Care must be taken when deciding upon the value of R , since it is critical in determining the convergence of the optimization. If the value of R is too small, the solution might result in premature convergence to local optima, while a high value of R might impair the search and reduce its ability to converge optimally [15]. The AMBA method however proposes an adaptive approach to determining the value of R , during the course of the search. The population gets divided into two equal halves, A and B. A gets a mutation rate of double R ($2R$), while B gets a mutation rate of half R ($1/2R$). The mutation rate, R gets adjusted depending on the performance of each half population (A or B). If A gives better and fitter individuals, the mutation rate is increased by a certain percentage (10% in this case); similarly if B produces better and fitter individuals, then the mutation rate gets reduced by a similar percentage.

3.4 Population Based Incremental Learning (PBIL)

Population Based Incremental Learning has long been preferred by many researchers over genetic algorithm due to its simplicity, less computation time, capacity required and in most cases performs better than the GA [6], [67]. PBIL was initially proposed and developed by Shumeet Baluja [16], [17] [67]. It is a combination of certain aspects of GA and competitive learning in Artificial Neural Networks. It extends the features of the evolutionary Genetic Algorithm (EGA) through the re-examination of the performance of the GA in terms of competitive learning [14], [17], [67]. In PBIL, the crossover operator is removed by redefining the role of the population. PBIL works on probabilistic vectors, whereby probabilistic vectors control the random bit strings generated by PBIL and are used to create some other vectors through competitive learning. Through that, PBIL uses

the current probability distribution to create N individuals. The objective function is used to measure the relative strength of the individual in relation to the task it is suppose to accomplish. Depending on the performance of an individual, the probability is updated to increase the likelihood of producing solutions, corresponding to the current best individual. Mutation is used in PBIL to maintain diversity and the probability of premature convergence [14], [17].

3.4.1 Competitive Learning

Competitive learning often clusters a number of unlabelled points into distinct groups. The members are grouped according to similarities within their characteristics in relation to the study, but since no prior information is known in accordance with the number of groups or respective features of each group, the CL is allowed the freedom to determine the important features for each group and assign each member to their respective groups using the match between the relevant features [14]. Competitive learning is often studied in the context of artificial neural networks as it is easy to model in such a format [14]. Competitive learning networks are comprised of inputs and outputs. The inputs correspond to the feature vector for each point, while the output corresponds to the class in the network, in which the point has been placed.

3.4.2 Population in PBIL

Population is one of the key fundamental aspects in genetic algorithms; it gives the GA, the ability to search the solution space in parallel from multiple entrances [6], [14], [67]. But as the optimization search reaches the later stages in GA, the effectiveness of population becomes limited. To address the issue, PBIL has replaced the role of the population with the probability vector (PV), by specifying the probability of each position containing a particular value [6], [14], [67], [68]. The role of the population, including the genetic operators has been redefined in PBIL. The genetic operators include crossover or recombination, fitness functions as well as selection. The probability vector in PBIL controls the bit strings generated by the PBIL and is used to create other individuals through learning [6], [14], [67].

3.4.3 Mutation

As mentioned before, mutation plays a very important role in optimization problems by maintaining the diversity within the search and avoiding premature convergence. Two different methods can be used to perform mutation in PBIL [14], [17], [69]. The first method is to mutate the generated vectors (population) directly. The second method works by applying the mutation on the generated probability vector; this can be referred to as a small perturbation on the respective position in the probability. In this thesis, the second method is used but with a slight difference to the one used in [14], [17], such that a forgetting factor is used to relax the probability vector towards a neutral value of 0.5 [6], [63]. The effect of the above defined methods is similar to the role of mutation in a standard GA. In order for the role and relevance of the genetic operators to be understood in PBIL, it's required that their role and relevance in GA is well defined and clearly understood. An example is crossover; crossover plays an important role in the early stages of optimization, improving it towards reaching the optimal value, but the diversity within the solution comes as a result of mutation. Recombining similar chromosomes does not improve the fitness of the individual towards meeting the objectives [14]. Even though research has shown that mutation improves the algorithm performance, especially in GA, PBIL tend to benefit less from it. In fact mutation tends to slow down the convergence of the phenotype towards an extreme value [14].

3.4.4 Learning rate

Many parameters in PBIL resemble the genetic operators in GA, but there seems to be one which is not paralleled in GA. The learning rate does not have an equivalent parameter in GA. The importance of the learning rate is unparalleled, it determines how fast or slow the prototype vector is shifted towards the best individuals. The magnitude of the learning rate plays a major role and its significance cannot be undermined. A larger rate speeds up convergence, but it reduces the function space to be searched, while a smaller rate will slow down the convergence, even though it increases the exploration of a bigger search space, thereby increasing the likelihood of better optimal solutions. A learning rate that is too small is undesirable [14].

3.4.5 Termination

PBIL only stores the current best solution and the current solution being evaluated, and therefore it runs as long as the current best solution keeps being updated. Sometimes this might take a long time to reach convergence and therefore require certain conditions for the termination of the program. The program is terminated when the number of iterations reaches a specified maximum number; this is similar to the ones used in both GA and BGA.

3.5 Summary

The theory behind the evolutionary algorithm techniques are presented in this chapter. The three evolutionary algorithm techniques that were considered are standard genetic algorithm (GA), Breeder Genetic Algorithm (BGA) and Population-Based Incremental Learning. GA is based on natural selection (Darwinian evolution), BGA is based on artificial selection similar to the type of breeding used in animal breeders. PBIL combines the aspects of GA and competitive learning. The role of population is redefined in PBIL by removing the crossover/ recombination operator.

Chapter 4

Application of Evolutionary Algorithms to Power System Stabilizer Design

4.1 Introduction

After discussing the theory behind Evolutionary Algorithm techniques and their ability to solve highly non-differentiable, non-linear and non-convex problems, it is useful to investigate how their application was used in this thesis. The problem of selecting the parameters of a power system stabilizer which simultaneously stabilizes a set of plants was converted to an optimization problem which was solved by Genetic Algorithm, Breeder Genetic Algorithm and Population-Based Incremental Learning using an eigenvalue based objective function [6]. The advantage of using computational methods in this case EA methods, as has been explained in Chapter 1, is to help obtain the optimal parameters for the PSS, such that the PSS is able to stabilize the system over a wide range of operating conditions. Designing PSS using conventional methods is not easy especially in multi-machine systems, where there is more than one type of electromechanical modes, therefore the need for Evolutionary Algorithm techniques to optimize the PSS parameters, ensuring that the PSS is robust enough. This chapter presents the design operating conditions that were considered in designing the different PSSs.

4.2 Structure of the PSS

The typical PSS usually consists of a washout function, a phase compensator (lead/lag blocks) as well as the gain. The performance of the PSS is determined primarily by the phase compensator (lead/lag blocks, comprising of the time constants) and the gain, therefore when tuning the PSS, these two parameters forms the focal point of the tuning process. Usually two first order phase compensation blocks are considered, but this depends on the degree of compensation. If the degree of compensation is small (less than 30 degrees) then a single first- order block may be used

The following PSS was used in the simulations:

$$U_{pss}(s) = K \frac{sT_w}{1+sT_w} \frac{1+sT_1}{1+sT_2} \frac{1+sT_3}{1+sT_4} \Delta\omega(s) \quad (4.1)$$

As explained in Chapter 1, K is the gain of the PSS, T_1 to T_4 are lead/lag time constants, T_w is the washout time constant. T_1 and T_2 form the first lead/lag block, while T_3 and T_4 forms the second lead/lag block of the PSS. In the SMIB simulations only one lead/lag block was used, meaning that only K , T_1 and T_2 were optimized. In the Two-Area Multi-machine system, the PSS consisted of two lead/lag blocks, meaning that 5 parameters (K and T_1 up to T_4) for the PSS were optimized simultaneously per generator. $U_{PSS(s)}$ is the output signal of the PSS, while $\Delta\omega(s)$ is the input signal, which in this case is the speed deviation. T_w was fixed at 2.5 seconds for the SMIB, and 10 seconds for the multi-machine system. In the multi-machine system, all the four generators were equipped with PSSs. The PSS on generator 1 was similar to generator 2, while the PSS on generator 3 was similar to the PSS on generator 4. This was done to reduce the number of parameters to be optimized and since G1 and G2 are in the same area, similar to G3 and G4, thus reducing the optimization time. In this case a total of 10 parameters were optimized simultaneously.

4.3 Objective function and PSS tuning

The objective function is the function used to provide the measure of how individuals performed in the problem domain. In this instance, the problem domain was that the PSS should stabilize the system over a certain range of specified operating conditions by maximising the lowest damping ratio. To be more specific, the requirement used in this thesis is to maximize the minimum damping ratio of the electromechanical modes in the closed loop system. This helps in ensuring that all the closed loop eigenvalues lie on the left hand side of the complex s – plane. Furthermore, it helps improve the damping ratio of critical modes and setting time as well as ensuring some degree of relative stability and robustness of the PSS [6, 68]. All the eigenvalues were computed across all the operating conditions and stored in the vector, called *damp*. Therefore the objective function *Val* is formulated as follows:

$$Val = \max (\min (damp_p)) \quad (4.2)$$

Where $damp$ is a vector of damping ratios ζ_i , such that $i = 1,2,3,4, \dots, n$ for a certain p^{th} operating condition, where n is the total number of eigenvalues at any specific operating condition and $p = 1,2,3,4, \dots, m$,

m being the total number of operating conditions under consideration.

$\zeta_i = \frac{-\sigma_i}{\sigma_i^2 + \omega_i^2}$ is the damping ratio of the i^{th} eigenvalue

i = represents the number of eigenvalue

σ_i, ω_i are the real part and imaginary part (frequency of oscillation) of the i^{th} eigenvalue respectively. The limitations put on the controller gain and the lead lag time constants where such that:

$$K_{\min} < K < K_{\max}$$

$$T_{i\min} < T_i < T_{i\max}$$

whereby K and T_i denote the controller gain and the lead lag time constants respectively, while $K_{\max}, T_{i\max}$ denote the specified possible maximum values and $K_{\min}, T_{i\min}$ denote the possible minimum values of the values of K and T_i and are the parameters to be optimized. In this thesis the following values were used for SMIB:

$$K_{\max} = 20; T_{i\max} = 5 \text{ seconds}$$

$$K_{\min} = 0.1; T_{i\min} = 0.001 \text{ seconds,}$$

While for multi-machine, the following were used:

$$K_{\max} = 20; T_{1\max} = T_{1\max} = 1 \text{ seconds; } T_{2\max} = T_{4\max} = 0.5 \text{ seconds}$$

$$K_{\min} = 0.1; T_{i\min} = 0.001 \text{ seconds;}$$

$T_{i\min}$ was chosen to be as close to zero as possible, but not equal to zero and that is why a small value has been used. The choice of these values was done arbitrary and thus it will affect the performance of the controllers, especially if the value of T_i too small.

To apply the objective function in question, the system model is linearized first around its equilibrium points, corresponding to the various operating conditions. The eigenvalues of the system A - matrix are computed and the damping ratios are calculated. Once the damping ratios are known, the lowest value is determined. This gets fed into the objective

function and thus gets maximized through iterative methods that are used in Evolutionary Algorithms. This similar objective function was used for both the single machine to infinite bus system and the multi-machine systems.

In using the objective function defined above, a restriction was imposed on the maximum damping ratio that the local area modes can attain in the SMIB system, but not in the multi-machine system. The main reason for the restriction was that the PSS from BGA, GA and PBIL gave too much damping to the electromechanical modes at some operating conditions, thereby reducing the frequency of oscillation. High damping to the electromechanical modes at the expense of other modes may affect the performance of the PSS during large disturbances.

Designing a power system stabilizer for a single machine to infinite bus system (SMIB) is relatively simple as compared to multi-machine systems. In SMIB, the focus is to find optimal values of the PSS that will help improve the stability of local modes only. In multi-machine systems, the selection of PSS parameters and the location of the PSS in the system are very critical. There are many modes of consideration in multi-machine as has been discussed previously. PSS might improve damping at one electromechanical mode, but may have adverse effect on other modes, such as the control modes.

4.4 PSS Design based on Evolutionary Algorithms (EAs)

Having discussed how the optimization problem was converted into a mathematical model, this section presents the methods and models employed in applying the three EAs to the design. In obtaining the results for both the Single Machine to Infinite Bus system and Two-Area Multi-machine, the following steps were followed. Firstly, the optimization programs (BGA, GA and PBIL) were run to obtain the optimized PSS parameters. Secondly, using the optimized PSS parameters and the CPSS, the eigenvalues of the system were obtained and analysed to determine and compare the performance of the different PSS design methods. Lastly, the time domain simulations for the different case studies were obtained with the different PSS parameters. The performances of the PSSs were investigated under small signal and transient stability.

The flow charts in Figure 4.1 to Figure 4.3 describe the procedures followed in designing the Power System Stabilizer using the three Evolutionary Algorithm Techniques. The charts show the procedures used both in SMIB and the Two Area Multi machine system (2AMM). The variables K_i , T_{1i} , T_{2i} , T_{3i} and T_{4i} denote the PSS parameters, specifically the gain and the lead/lag time constants. The idea behind GA and BGA is similar, with the only difference being in the genetic operators used as well as selection. The different values for the parameters used in the simulation are also given in this section. The parameters (mutation rate, crossover, selection as well as population size) used in the SMIB and 2AMM are the same, except for the maximum number of generations for the GA and BGA where 120 was used in the Multi-machine system.

<p><u>GA PARAMETERS</u> Population: 100 Generation: 100 Selection: normal geometric (0.03) Arithmetic crossover [2] Non uniform mutation [4 Gmax 3]</p>	<p><u>BGA PARAMETERS</u> Population: 100 Generation: 100 Selection: Truncation(15%) Line and Volume recombination Adaptive random mutation (initial $r = 0.1$)</p>	<p><u>PBIL PARAMETERS</u> Population: 100 Length of encoded solution (15 bits) Generation: 500 Learning rate: 0.1 Forgetting factor: 0.005</p>
--	--	--

Figure 4.1: GA, BGA and PBIL parameters used in the simulations

By observing the parameters given above in Figure 4.1, it can be seen that PBIL uses few parameters (no crossover or selection in PBIL) for its optimization, thereby reducing the influence of the user as well as making it easy for non experienced optimizers. In addition, 500 generations were used in the PBIL optimization to allow for enough learning within the optimization, as PBIL works by learning from the previous best and trying to find the very best individual, in essence trying to explore the space for better solutions. Another difference is in the population, whereby in GA and BGA the initial population is selected randomly, while in PBIL the role of population is redefined using probability vectors (PV). The PV is a prototype of the high evaluation vectors for the function space being evaluated. A population size of 50 was also tested in PBIL and it was found that it yields similar results to the population size of 100. In contrast, for GA and BGA the damping ratio reduces, meaning a reduction in the performance of the GA and BGA if the population is 50. A population of 100 in PBIL was just used for

comparison purposes. The A_p vector referred to in the flow charts is the vector containing all the eigenvalues, while *lowdamp* is the lowest damping ratio.

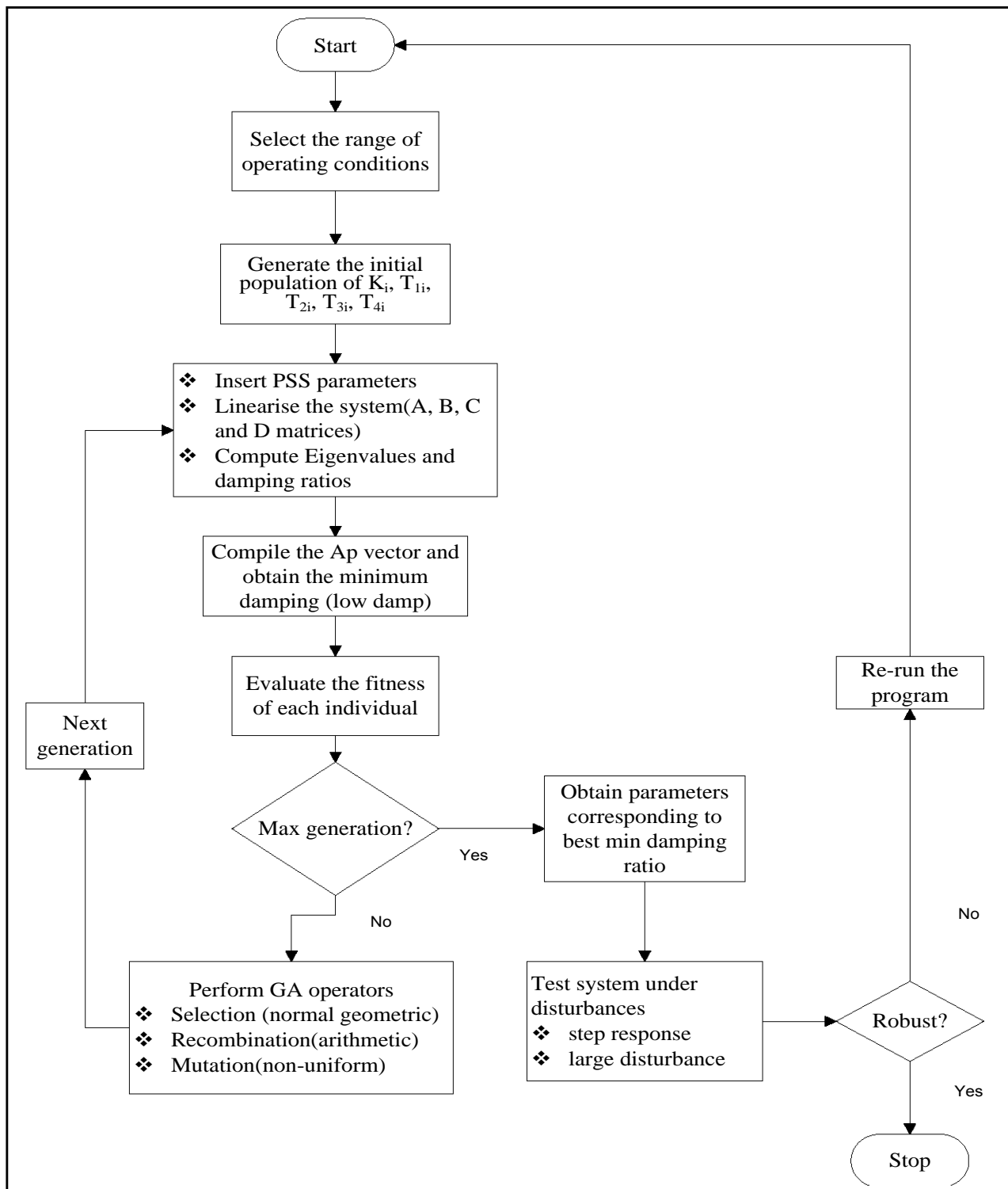


Figure 4.2: Flow chart for the PSS design using Genetic Algorithm

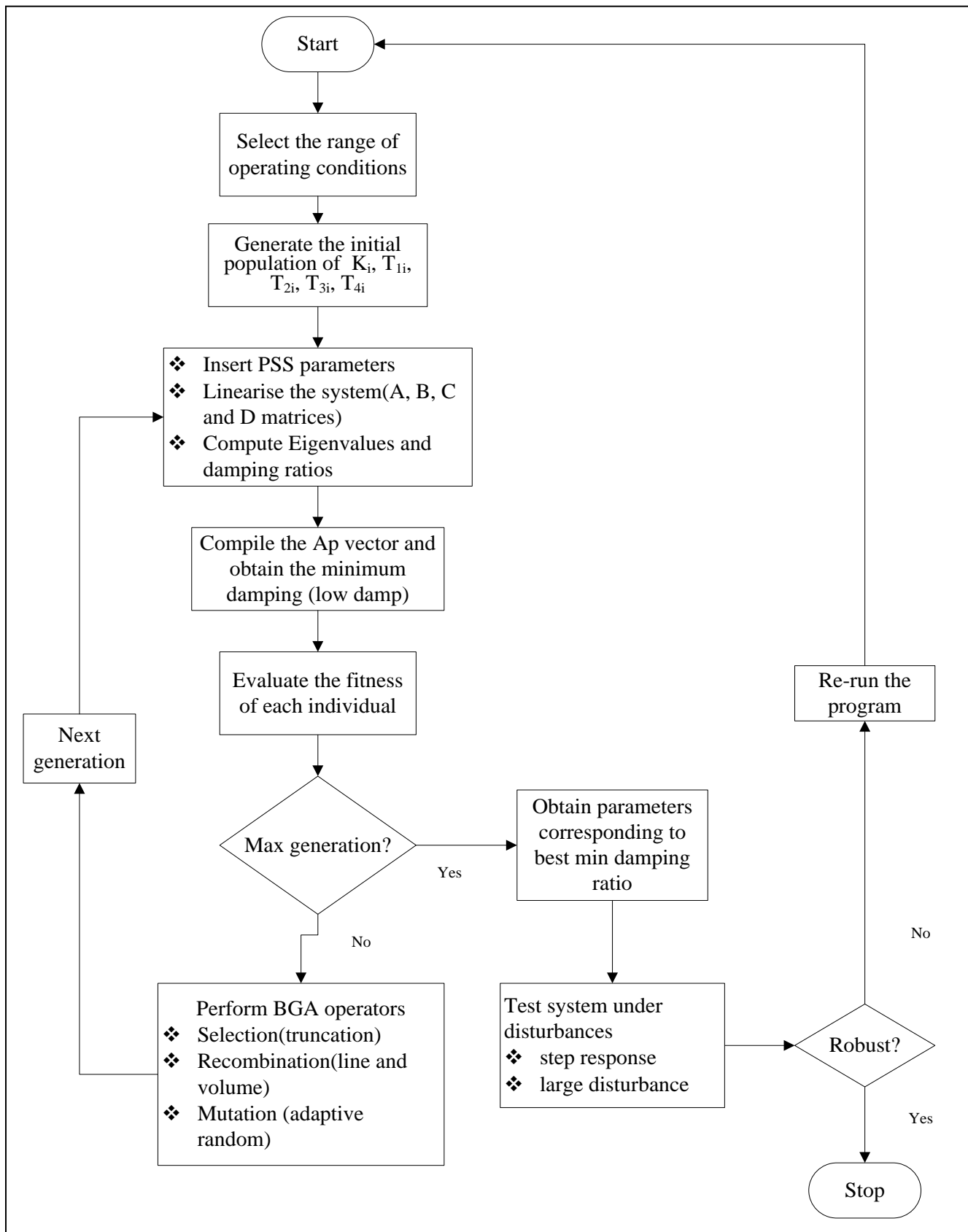


Figure 4.3: Flow chart for the PSS design using Breeder Genetic Algorithm

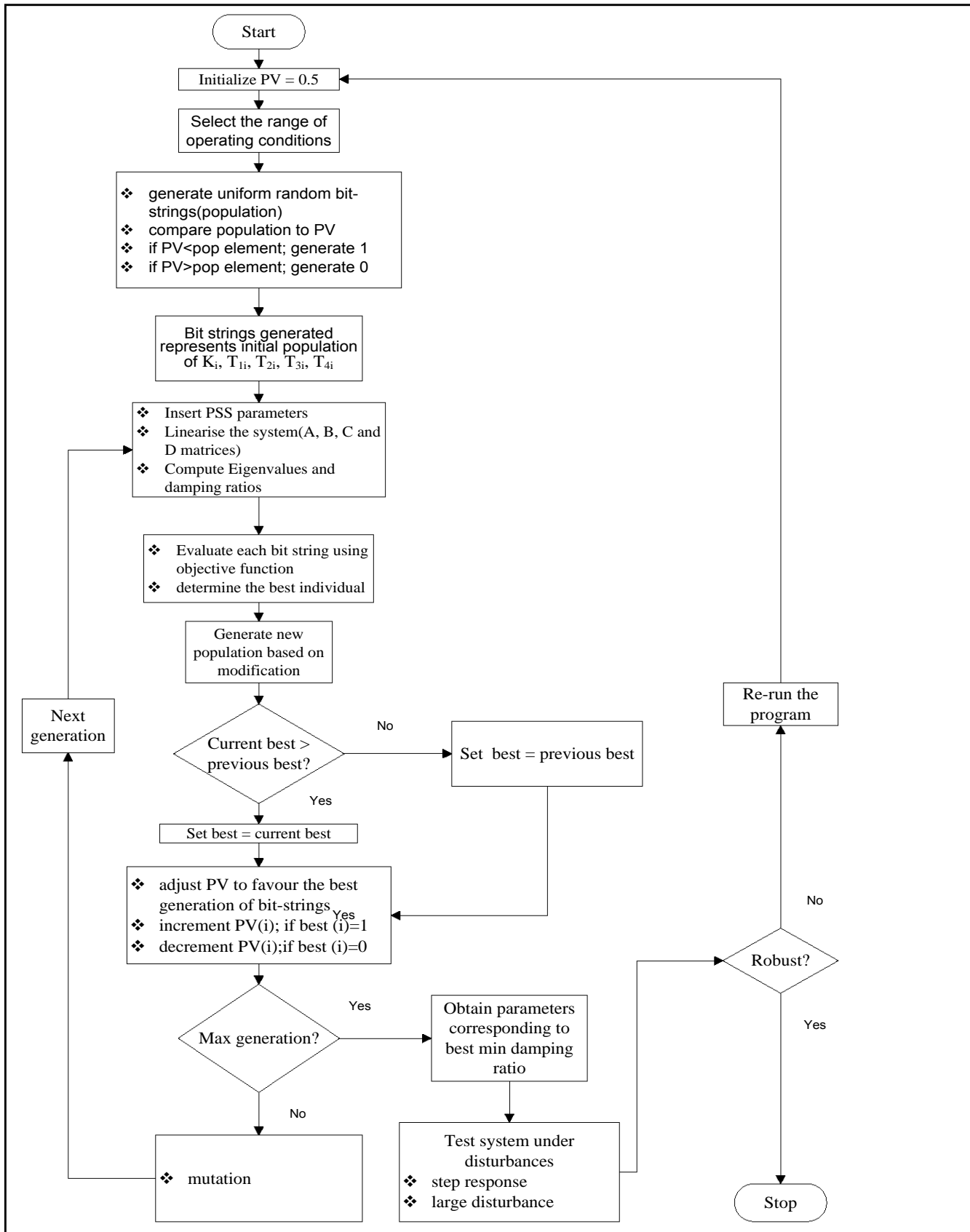


Figure 4.4: Flow chart for the PSS design using PBIL

4.5 Design Case Studies

In designing a Power System Stabilizer, selected random system operating scenarios were considered. These were obtained by varying the power output of the generators and changing the line reactance of the tie lines in the Single Machine to Infinite Bus (SMIB) case. In the multi-machine system, various operating conditions were obtained by varying the generator's output power, the loads in each area and the power flow between the two areas (Area1 and Area 2) in the system

4.5.1 Single Machine to Infinite Bus system

In this system, a single machine is connected to the infinite bus through a double transmission line. The synchronous generator is connected on Bus 1 and the lines are indicated with Line 1 and Line 2 as shown in Figure 4.5. By varying the generator output, the system was simulated from a lightly loaded system to a very highly loaded system. The generator output power was varied from 0.3pu to 0.9pu. The line reactance was also varied from 0.3pu to 1.1pu, from a weak tie line to a much stronger tie line. This was done to simulate wide varying operating scenarios in the system and design the power system stabilizer over these operating conditions.

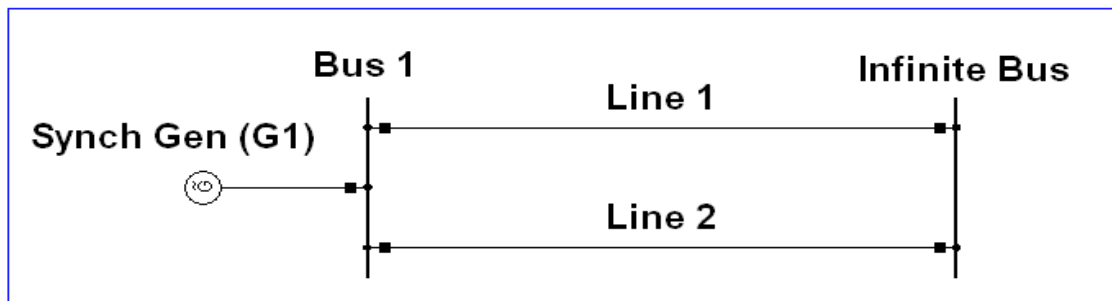


Figure 4.5: Single machine to infinite bus system

In designing the Power System Stabilizer, the following operating conditions, as shown in Table 4.1, were taken into account. They ranged from the best to the worst damping conditions. To simulate different operating conditions, the active power of the synchronous generator and the line reactance (double transmission) were varied, as has been explained before.

The nominal operating condition, as shown in Table 4.1 as Case 1, has a line reactance of 0.3 pu and the generator was supplying an active power of 0.4 pu. This Case was very well damped in the open loop (without the PSS) with a damping ratio of 15.68%. The frequency of oscillation of the system was 6.5562 rad/s.

As the line reactance and active power was increased to 0.7 pu and 0.5 pu, respectively for Case 2, the damping ratio reduced considerably to 10.80%. But the system was still stable. The frequency of oscillation reduced from 6.5562 rad/s to 5.1293 rad/s. In Case 2, the line reactance increased by more than 130% from the nominal operating condition. Cases 3 and 4 simulate the system when the line reactance is 0.7 pu, while the active power is 0.8 pu and 1.1 pu, respectively. This simulates a scenario where the active power of the generator increases by 100% and 175%, respectively from the nominal value of 0.4 pu. The open loop frequency of oscillation for the electromechanical modes for Cases 3 and 4 are 5.2072 rad/s and 5.2785 rad/s with damping ratios of 8.45% and 5.47%, respectively. The open loop damping ratio for the electromechanical modes was reducing as the system became heavily loaded.

In Cases 5, 6 and 7, indicated in Table 4.1, the line reactance increased to 1.1 pu an increase of 175% from the nominal value, while the active power increased to 0.5 pu, 0.8 pu and 1.1 pu, respectively. This meant an increase of 25%, 100% and 175% from the nominal value. The frequencies of oscillation were 4.3271 rad/s, 4.3069 rad/s and 4.1865 rad/s for Cases 5, 6 and 7, respectively. The damping ratios were 8.0%, 5.27% and 1.9%, respectively. In all the simulated operating conditions, the system was stable, but the damping ratio was very low, and as the power and line reactance increase the system may experience different scenarios, resulting in instability in some cases, hence the need for a power system stabilizer.

Table 4.1: Open Loop operating conditions used in the PSS design

Cases	Active Power Pe (pu)	Reactive Power Qe (pu)	Line reactance Xe (pu)	Eigenvalues	Damping ratio (%)
1	0.4	0.4128	0.3	-1.0408 ± 6.5562i	15.68
2	0.5	0.2184	0.7	-0.5571 ± 5.1293i	10.80
3	0.8	0.2933	0.7	-0.4414 ± 5.2072i	8.45
4	1.1	0.4070	0.7	-0.2894 ± 5.2785i	5.47
5	0.5	0.1839	1.1	-0.3472 ± 4.3271i	8.0
6	0.8	0.3079	1.1	-0.2275 ± 4.3069i	5.27
7	1.1	0.5101	1.1	-0.0797 ± 4.1865i	1.9
8	0.9	0.3372	0.9	-0.2704±4.7212i	5.72
9	1.3	0.9049	1.3	0.0846±3.1305i	-2.70

Table 4.1 show the various operating conditions that were used in the design process. The table shows the generator's active power, generator's reactive power, line reactance and the open loop frequency and damping ratio (in percentages) for the electromechanical modes. In order to check for the robustness of the designed PSS, two extra cases were used (Case 8 and Case 9). Under the two Cases, the line reactance and the active power were both 0.9 pu for Case 8, while for Case 9 it was 1.3pu. For case 8, the frequency of oscillation was 4.7212 rad/s and the damping ratio was 5.72%. While for case 9, the frequency of oscillation was 3.1305 rad/s, and a damping ratio of -2.70%. In fact for case 9, the local area mode is unstable due to the negative damping.

4.5.2 Two Area Multi-machine System

The system shown in Figure 4.6 consists of two areas, each with identical generating units [1]. All the generators were equipped with similar Automatic Voltage Regulators as well as similar turbine governors. The parameters for the generators, AVR's and the turbine governor are given in Appendix C. All generating stations have the same ratings. The loads in the two areas are different from each other. The parameters of the system are given in Appendix C. Note that in this study, three operating conditions were used to design the evolutionary algorithm based PSSs. In particular the nominal operating

condition is different from the one used in [1]. At the nominal operating condition, 150MW is transferred from Area 1 to Area 2 via the two tie lines.

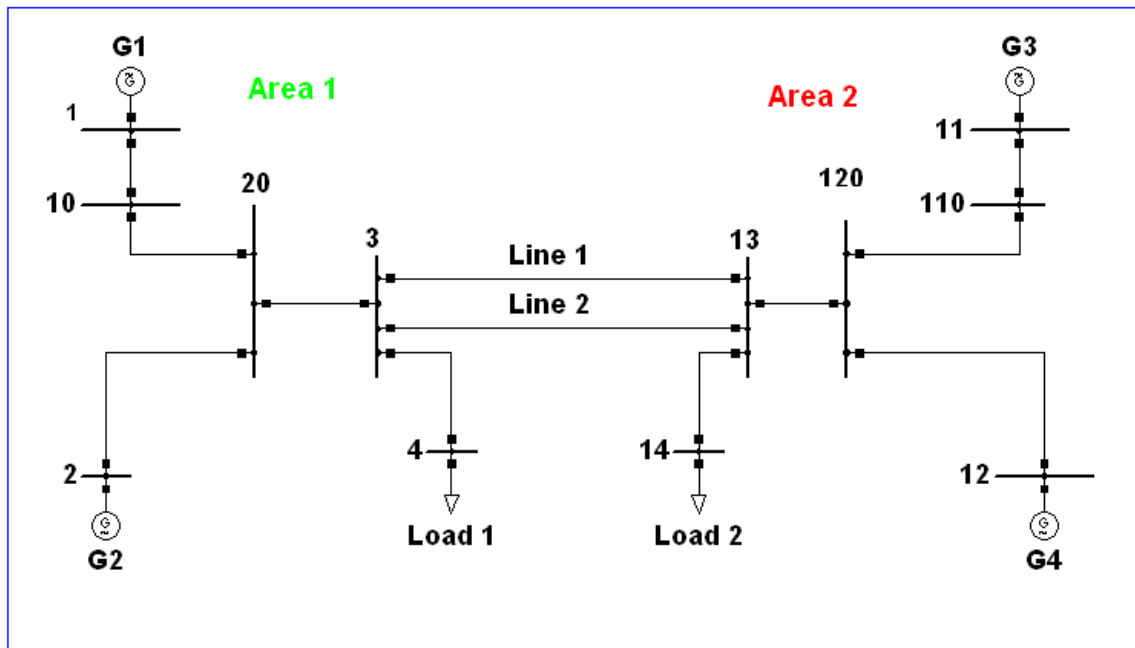


Figure 4.6: Two Area multi-machine system line diagram

Case 1: In this condition, the load on bus 4 was 1137MW, while the load on bus 14 was 1367MW. This reduces the amount of power flowing from Area 1 to Area 2 through the two lines to 150MW, with each line carrying half of that. The active power and reactive power supplied by the generators is shown in Table 4.2. This Vase was used as the nominal operating condition as the open loop electromechanical modes were relatively marginally stable and therefore the CPSS was designed around this operating condition.

Table 4.2: Case 1 generator's Output Values

Generator	Active power (pu)	Reactive power (pu)
G1	7.1303	1.014
G2	6.000	1.3258
G3	6.235	0.4502
G4	6.235	0.4090

Case 2: In this Case study, the loads on bus 4 and bus 14 were 967MW and 1767 MW respectively. Both tie lines between buses 3 and 13 were in operation, each carrying approximately 200 MW, totalling 405.45 MW from Area 1 to Area 2. The system was generating 2800 MW active power, with each generator generating the active power and reactive power as shown in Table 4.3:

Table 4.3: Case 2 generator Output Values

Generator	Active power (pu)	Reactive power (pu)
G1	7.0937	1.3371
G2	7.000	2.2045
G3	7.000	1.3060
G4	7.000	2.1841

Case 3: Under this condition, area 1 was exporting approximately 500MW to Area 2 through the two tie lines; the loads on bus 4 and bus 14 were 876 MW and 1876 MW respectively. The generators were supplying the amount of active power as shown in Table 4.4.

Table 4.4: Case 3 generators Output Values

Generator	Active Power (pu)	Reactive Power (pu)
G1	8.2615	1.9256
G2	6.00	2.7426
G3	8.00	1.9456
G4	6.00	2.9825

In order to test for the robustness of the PSSs, two extra operating conditions (Case 4 and Case 5) were considered for the time domain simulations, but were not included in the evolutionary algorithm based PSSs design. For Case 4, the generators were supplying the same amount of active as Case 2 above. The power flow between Area 1 and Area 2 was also similar to Case 2 above, but Line 2 was removed, so only a single line was in operation in Case 4. Case 5 simulated a system with the generator's output power similar to case 3, with approximately 500MW flowing between Area 1 and Area 2, but with Line 2 removed, power was only flowing through a single transmission line. Table 4.5 shows the open loop electromechanical modes of the system. As expected, the system has inter-

area oscillatory modes due to the flow of power between the two areas which causes the two areas to oscillate against each other. Two local area modes were also observed, one in each area and these are referred to as local area mode 1 and mode 2 in Table 4.5. As can be seen from Table 4.3, the inter-area modes have very low damping ratio (0.0062) in case 1, whereas these modes are unstable in Case 2 and 3. This is because these two cases 2, and 3, simulate scenarios where there is more power flowing through the two tie lines. The damping ratio for Case 2 and Case 3 are -0.0082 and -0.0143, respectively. The frequency of oscillation for the inter-area modes ranges from 0.752Hz for case 3 to 0.79Hz for case 1. The two local area modes have a relatively low damping ratio, but still enough for the modes to be classified stable and in a good state. The damping ratio of the two local area modes ranges from 0.0629 to 0.0922 across all the three operating conditions. At the nominal operating condition, the inter-area mode is marginally stable, with a damping ratio of 0.0062, while the local area modes have a damping ratio of 0.0872 and 0.0922 respectively. The electromechanical modes for Case 4 and Case 5 are presented in Table 4.6. The inter-area modes for Cases 4 and Case 5 are all unstable with damping ratios of -0.0095 and -0.0147, respectively. The two local area modes are poorly damped across both operating conditions.

Table 4.5: Open loop poles for the selected design operating conditions

Case	Inter-area mode	Local area mode 1	Local area mode 2
1	-0.03 ± 4.96i (0.0062)	-0.63 ± 7.25i (0.0872)	-0.68 ± 7.36i (0.0922)
2	0.04 ± 4.82i (-0.0082)	-0.51 ± 7.24i (0.0705)	-0.52 ± 7.36i (0.0706)
3	0.07 ± 4.73i (-0.0143)	-0.46 ± 7.24i (0.0629)	-0.53 ± 7.24i (0.0727)

Table 4.6: Open loop electromechanical modes for Case 4 and Case 5

Case	Inter-area	Local are mode 1	Local area mode 2
4	0.04±3.74i (-0.0095)	-0.54±7.21i (0.0743)	-0.50±7.25i (0.0686)
5	0.05±3.42i (-0.0147)	-0.38±7.22i (0.0526)	-0.45±7.33i (0.0617)

4.6 Summary

The procedure used is designing the evolutionary algorithm based PSSs were defined in this chapter, the different parameters are presented. Also included was the objective function used in all the three optimization techniques. The objective function was defined such that the tuned PSS maximizes the lowest damping ratio in the system. This was applied over a wide range of operating conditions. The operating conditions used for the PSSs design were defined and the open loop eigenvalues and damping ratios were presented. In most operating conditions, especially for the Two-Area Multi-machine, the inter-area mode is unstable, except for the nominal operating condition where it was marginally stable with a damping ratio of 0.0062.

University of Cape Town

Chapter 5

Simulation Results for the Single Machine Infinite Bus System (SMIB)

5.1 Introduction

This chapter presents the simulation results for the single machine to infinite bus system. It covers the eigenvalues analysis for the optimized PSSs as well as the conventional PSS, and the time domain simulations for Cases one to seven. The time domain simulations include the responses of the system to a small disturbance for Cases one to seven as well as the responses of the system to a large disturbance for Cases one to five. The comparison is done between the system equipped with CPSS as well as the optimized PSSs.

5.2 Fitness Values and PSS parameters

The CPSS was designed at the nominal operating condition using the phase compensation method. The phase lag in the system was first obtained, which was found to be 20° , thus the reason why only a single block was used in the SMIB PSS instead of two. After obtaining the phase lag, a PSS with a phase lead was designed by varying the PSS time constants T_1 and T_2 to give a phase lead of approximately 18° , thus giving the system a slight phase lag of 2° . Once the phase lag is improved, then the damping needed to be improved as well by varying the gain K . Different values were tried using try and error method. Similar procedure was used in multi-machine system as well, taking into account the different electromechanical modes that exist in a multi-machine system. The idea used in CPSS design is similar to the one used in [18].

Figures, 5.1, 5.2 and 5.3 show the fitness values of the different optimization methods. Remembering that the objective function used was to maximize the lowest damping ratio and put a restriction on the highest damped electromechanical mode not to be more than

50% across all the operating conditions. The GA optimization converged to a value of 0.2774 corresponding to the electromechanical damping ratio of Case 5. The BGA and PBIL optimization converged to a value of 0.2849 and 0.2854, respectively. Considering the restriction that was imposed on the highest damping ratio of the electromechanical modes, the BGA-PSS and PBIL reached that value, corresponding to operating Case 4, while the GA converged to a slightly lower value. Also, considering the results obtained and presented in Appendix C, whereby the limiting value was increased to 0.7, it can be deduced that the BGA and PBIL almost converged to the value of 0.7, with BGA providing a value of 0.6847, while the PBIL reached a maximum damping 0.6788. The GA provided a slightly lower value of 0.6169. Clearly the objective function used in the simulation influenced the results slightly, as it could be argued that a different objective function might have yielded different results.

The observation made from Figures 5.1 to Figure 5.3 indicates that the BGA and PBIL methods perform slightly better than the GA. This could be as a result of premature converging on the part of the GA as it might have reached a local point instead of a global one. The BGA and GA optimization were run over a 100 generations in which they converge within 20 generations or less. The PBIL converges around 200 generations and that is why the maximum number of generations considered was 500. There is a likely hood of premature convergence within the GA and BGA optimization, as they converged within few generations (approximately 15). This can be investigated further with scenarios where the global optimal solution is known. For Figure 5.3, the chattering behaviour comes up because the algorithm is still searching for the best solution and thus exploring all the possibilities.

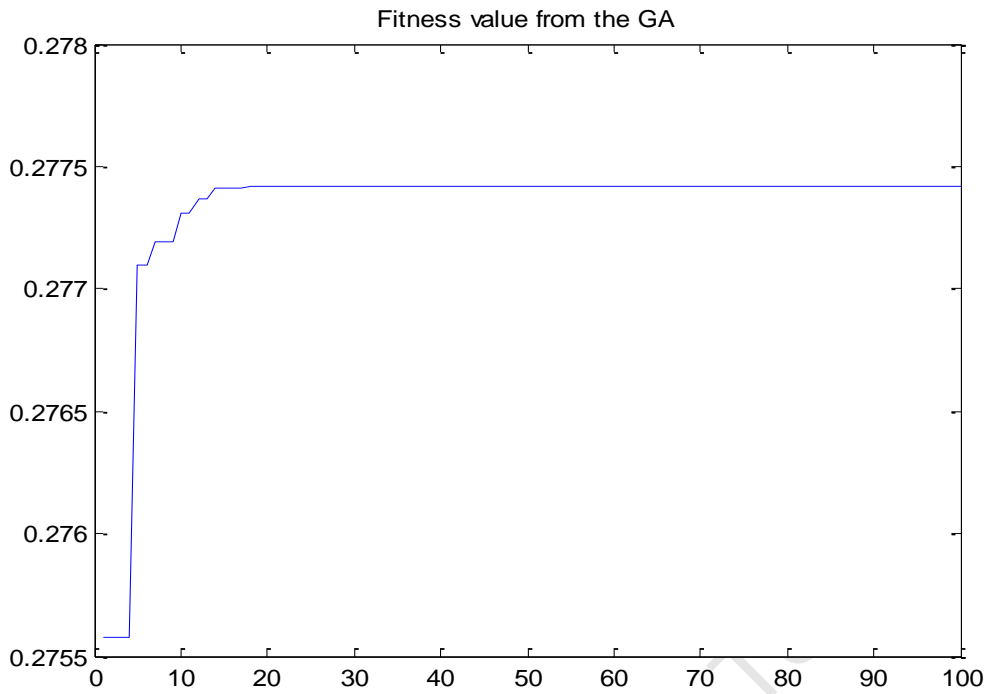


Figure 5.1: Fitness value from GA objective function

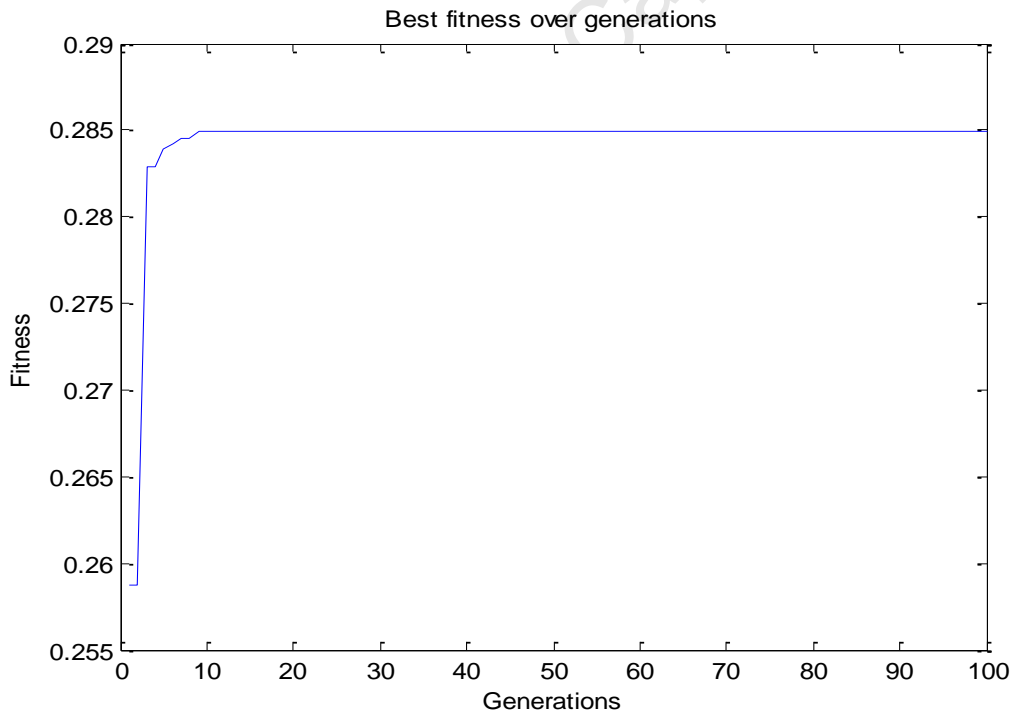


Figure 5.2: Fitness value from the BGA objective function

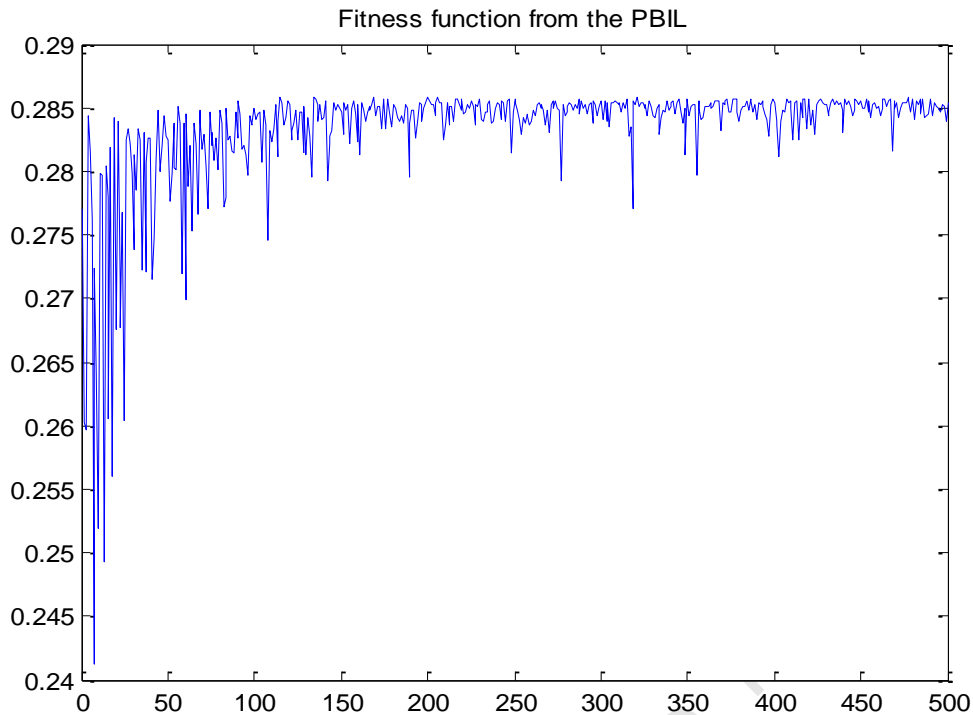


Figure 5.3: Fitness value from the PBIL objective function

The following Power System stabilizer parameters were obtained from the optimization programs. Also shown in Table 5.1 are the CPSS parameters used in the simulation.

Table 5.1: Power System Stabilizer parameters for different optimization programs

	K	T1	T2
CPSS	9.7928	1.1686	0.2846
BGA-PSS	17.5508	4.1075	1.7684
GA-PSS	13.7358	3.5811	1.2654
PBIL	18.7976	4.5313	2.0753

5.3 Small Signal Stability

The results shown in this section are for the small signal stability analysis of the SMIB system. The first section deals with the eigenvalue analysis of the system equipped with the different PSSs. The second section outlines the performance of the system with CPSS

and optimized PSSs using time domain simulations. The time domain shows response of the system to a small disturbance (a 10% step response on the generator).

5.3.1 Eigenvalue Analysis

Table 5.2 shows the electromechanical modes of the closed loop and the open loop system and the respective damping ratio in brackets. Case 1, which is the nominal operating condition shows that PSSs designed based on evolutionary algorithms gave very similar performances, with BGA having a slight higher damping ratio of 35.59% to 35.21% for GA and 35.54% for PBIL. This means that the damping ratio provided by the BGA is 0.05% higher than PBIL and 0.38% higher than that of the GA. This difference is practically negligible. The CPSS performs very well at the operating condition with a damping ratio of 40.79%, which is higher than the damping ratios of evolutionary algorithm based PSSs. This was expected since the CPSS was designed around this operating condition. Case 2 shows that the damping of the electromechanical modes has dropped slightly from the nominal Case with the BGA-PSS giving a damping ratio of 32.54%, GA-PSS giving a damping ratio of 31.90%, PBIL-PSS with 32.55% and CPSS with a damping ratio of 31.04%. The PSSs seem to perform very well as the generator output power increases from 0.8pu (Case 3) to 1.1pu (Case 4). The damping of the BGA-PSS is 42.17% and 50%, respectively, whereas the GA-PSS provided a damping ratio of 41.28% and 48.85%, respectively. The PBIL-PSS provides a damping ratio of 42.14% and 49.94%. The CPSS gave a damping ratio of 40.06% and 44.93%. This is in agreement with the expected performances of the CPSS, which was suppose to perform very well around the nominal operating condition and degrades as the system loading changes. Case 4 seems to be very well damped when using all the different PSSs. The BGA-PSS gives a damping ratio of 28.49% for Case 5, 36.84% for Case 6 and 43.22% for Case 7. This is slightly higher than the damping ratio of the GA-PSS which has damping ratios of 27.74%, 35.74%, 41.72%, respectively. The PBIL-PSS gives damping ratios of 28.54%, 36.87% and 43.24% for Cases 5, 6, and 7, respectively. These damping ratios are slightly higher than that of the BGA-PSS. The CPSS give the lowest damping ratios of 23.48%, 27.36% and 27.10%, respectively.

Case 8 and Case 9 shown in Table 5.2 were not included in the designing of the PSSs, but were just used to check for the robustness of the PSS. The damping ratios provided by the

BGA-PSS for Cases 8 and 9 are 41.55% and 47.45% respectively. GA-PSS provide damping ratios of 40.48% and 44.25%, respectively. The PBIL-PSS provides a damping of 41.54% and 47.73%, respectively. The CPSS provides a damping of 33.59% and 17.38%. The damping ratio provided by the BGA-PSS is 1.07% and 3.22% higher than that provided by the GA-PSS for the two operating conditions, respectively. The damping ratio provided by the GA-PSS for Cases 8 and 9 is 6.89% and 26.87% higher than that of the CPSS. The damping ratio for the open loop system for Case 8 and 9 is 5.72% and -2.70% respectively. Actually the open loop system under Case 9 was unstable, but after introducing the different PSSs, the system became stable.

Table 5.2 also shows the frequency of oscillations under different PSSs differs, especially comparing the frequency of oscillation with Evolutionary Algorithm PSSs and the CPSS. The general trend observed in the frequency of oscillation for the electromechanical modes is that the optimized PSSs increase the frequency of oscillation, especially for Cases 1 to 4, whereas the optimized PSSs reduces the frequency of oscillation for Cases 5 to 9. The increase in frequency of oscillation suggests that the PSSs also slightly add to the synchronizing torque in addition to the damping torque that it improves. On the other hand the, CPSS slightly reduces the synchronising torque, thus the reduction in frequency of oscillation. However this slight reduction in synchronising torque is acceptable, as it does not really affect the electromechanical mode's stability, thus its sufficient enough to prevent the system from going into aperiodic instability.

Table 5.2: Electromechanical modes of the system with different PSSs Designs

Cases	BGA-PSS	GA-PSS	PBIL-PSS	CPSS	No PSS
1	$-2.7719 \pm 7.2784i$ (0.3559)	$-2.7069 \pm 7.1949i$ (0.3521)	$-2.7748 \pm 7.2987i$ (0.3554)	$-2.9002 \pm 6.4914i$ (0.4079)	$-1.0408 \pm 6.5562i$ (0.1568)
2	$-1.8022 \pm 5.2367i$ (0.3254)	$-1.7466 \pm 5.1886i$ (0.3190)	$-1.8079 \pm 5.2524i$ (0.3255)	$-1.5307 \pm 4.6879i$ (0.3104)	$-0.5571 \pm 5.1293i$ (0.1080)
3	$-2.4681 \pm 5.3068i$ (0.4217)	$-2.3724 \pm 5.2350i$ (0.4128)	$-2.4776 \pm 5.3316i$ (0.4214)	$-1.8932 \pm 4.3303i$ (0.4006)	$-0.4414 \pm 5.2072i$ (0.0845)
4	$-3.0630 \pm 0.3053i$ (0.5000)	$-2.9208 \pm 5.2172i$ (0.4885)	$-3.0774 \pm 5.3388i$ (0.4994)	$-1.9876 \pm 3.9516i$ (0.4493)	$-0.2894 \pm 5.2785i$ (0.0547)
5	$-1.2782 \pm 4.2996i$ (0.2849)	$-1.2305 \pm 4.2616i$ (0.2774)	$-1.2843 \pm 4.3133i$ (0.2854)	$-0.9529 \pm 3.9443i$ (0.2348)	$-0.3472 \pm 4.3271i$ (0.0800)
6	$-1.6586 \pm 4.1855i$ (0.3684)	$-1.5804 \pm 4.1298i$ (0.3574)	$-1.6688 \pm 4.2071i$ (0.3687)	$-1.0444 \pm 3.6719i$ (0.2736)	$-0.2275 \pm 4.3069i$ (0.0527)
7	$-1.8727 \pm 3.9077i$ (0.4322)	$-1.7633 \pm 3.8405i$ (0.4172)	$-1.8880 \pm 3.9366i$ (0.4324)	$-0.9546 \pm 3.3911i$ (0.2710)	$-0.0797 \pm 4.1865i$ (0.0190)
8	$-2.1222 \pm 4.6454i$ (0.4155)	$-2.0268 \pm 4.5784i$ (0.4048)	$-2.1332 \pm 4.6708i$ (0.4154)	$-1.3865 \pm 3.8881i$ (0.3359)	$-0.2704 \pm 4.7212i$ (0.0572)
9	$-1.3768 \pm 2.5540i$ (0.4745)	$-1.2304 \pm 2.4938i$ (0.4425)	$-1.4062 \pm 2.5891i$ (0.4773)	$-0.4460 \pm 2.5267i$ (0.1738)	$0.0846 \pm 3.1305i$ (-0.0270)

5.3.2 Time Domain Simulation

The time domain simulations of the system were performed to evaluate and test the designs of the different PSSs under small disturbance. In the following simulations results, the system is subjected to a small change in the voltage reference of the synchronous machine (see Figure 4.1). A 10% step change in voltage reference was applied and the system's active power and speed deviation responses at different operating conditions are obtained as shown in Figures 5.4 to 5.21.

For the nominal operating condition (Case 1), shown in Figure 5.4 and Figure 5.5, it can be seen that the responses of the system when equipped with all the PSSs is well damped. The PSSs are able to stabilize the system very well, with CPSS, the response has a slightly higher overshoot as compared to the rest of the PSSs, but settles in about 2

seconds, while the evolutionary algorithm based PSSs settle in about 2.7 seconds. This shows that the systems actually performs slightly better with the CPSS as compared to the other PSSs in terms of their settling time, but tend to have a slightly higher overshoot as compared to other PSSs in the speed response. For the active power response, the CPSS performs better in terms of overshoots and undershoots as shown in Figure 5.5. The performance of the CPSS is good as expected around the nominal operating condition since it was designed around that.

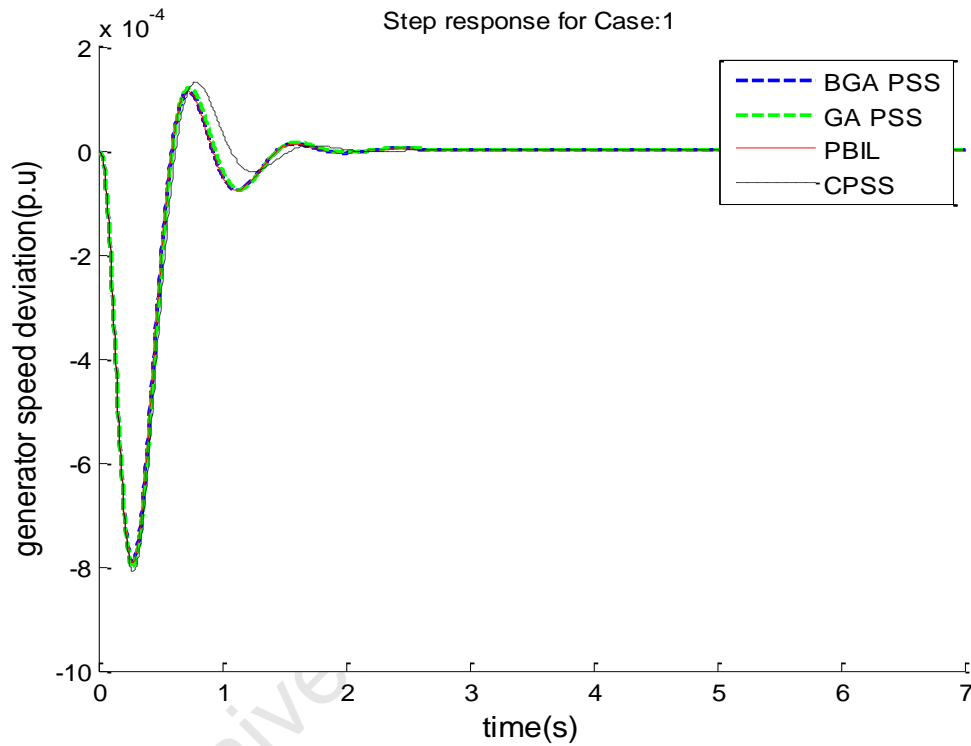


Figure 5.4: System response (speed) for Case 1

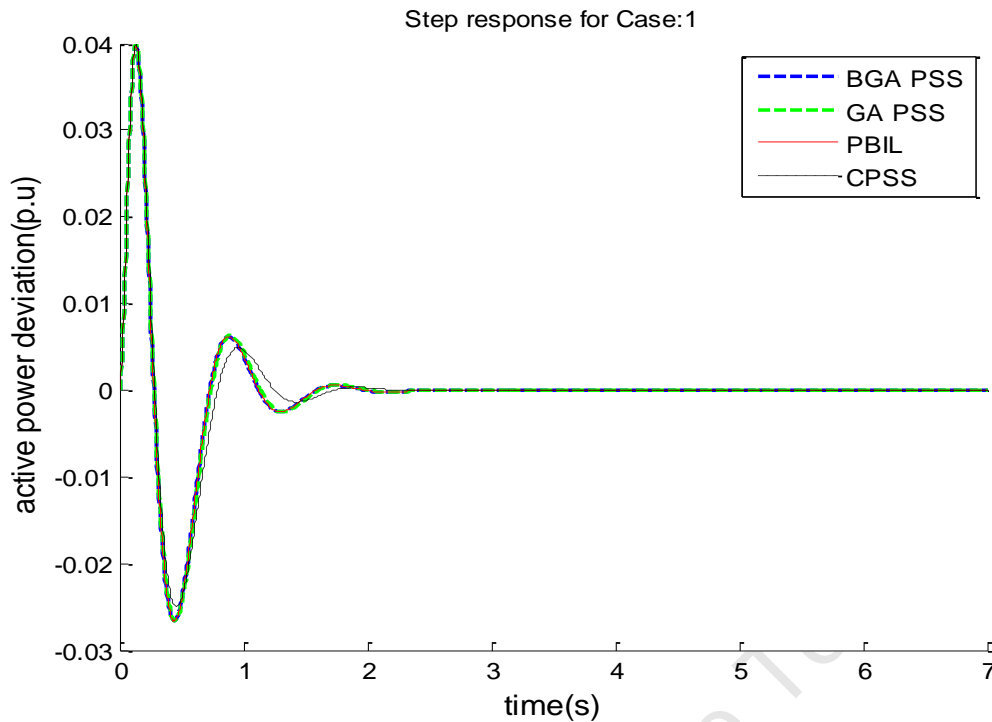


Figure 5.5: System response (active power) for Case 1

Figure 5.6 and Figure 5.7 show the generator speed and active power responses for Case 2. The system remains stable under all the PSSs including the CPSS. The CPSS has the highest overshoot, while the PBIL has the lowest overshoot. The settling time with the CPSS is around 3.5 seconds as compared to about 2.5 for GA-PSS, BGA-PSS and PBIL-PSS. Figure 5.7 shows the active power response of the generator to a step response in voltage reference, where under all PSS, the system is well damped, but tends to experience higher overshoot and higher undershoot when equipped with CPSS, approximately 0.007pu for CPSS and 0.005pu for evolutionary based PSSs. The system with GA-PSS has a slightly high overshoot and high undershoots as compared to the BGA-PSSs and PBIL. PBIL has the lowest undershoots.

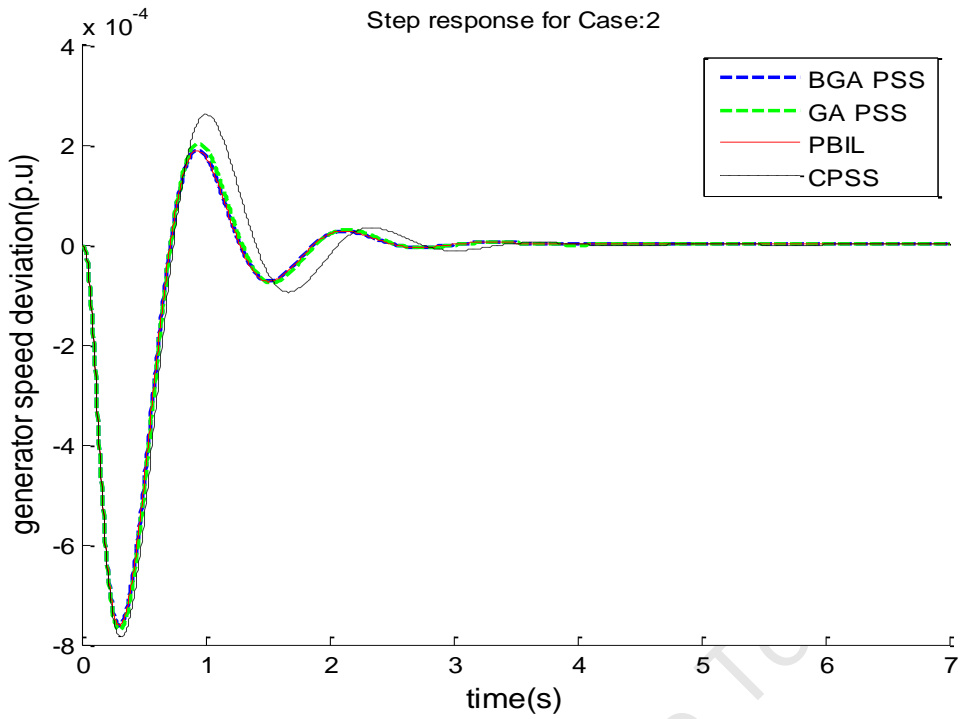


Figure 5.6: System response (speed) for Case 2

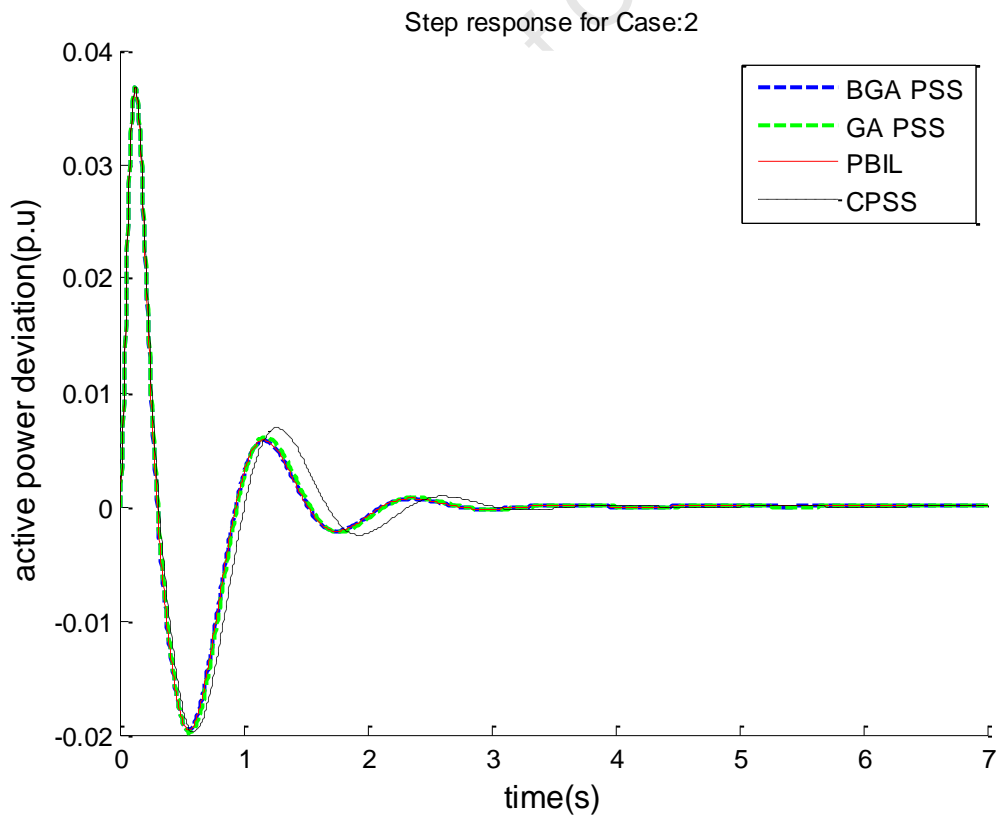


Figure 5.7: System response (active power) for Case 2

Figure 5.8 and Figure 5.9 show the active power and speed deviation responses of Case 3. It can be observed that the performance of the CPSS is deteriorating. In Figure 5.8 which shows the generator speed deviations, the system equipped with a CPSS has an overshoot of more than 3.5×10^{-4} pu with the settling time of about 3 seconds. It can be seen that the GA-PSS gives a slightly high overshoot of 2.1×10^{-4} pu as compared to 2.0×10^{-4} pu for the BGA-PSS and PBIL PSS. The settling time for the system with BGA-PSS, GA-PSS and PBIL-PSS is approximately the same, around 2 seconds.

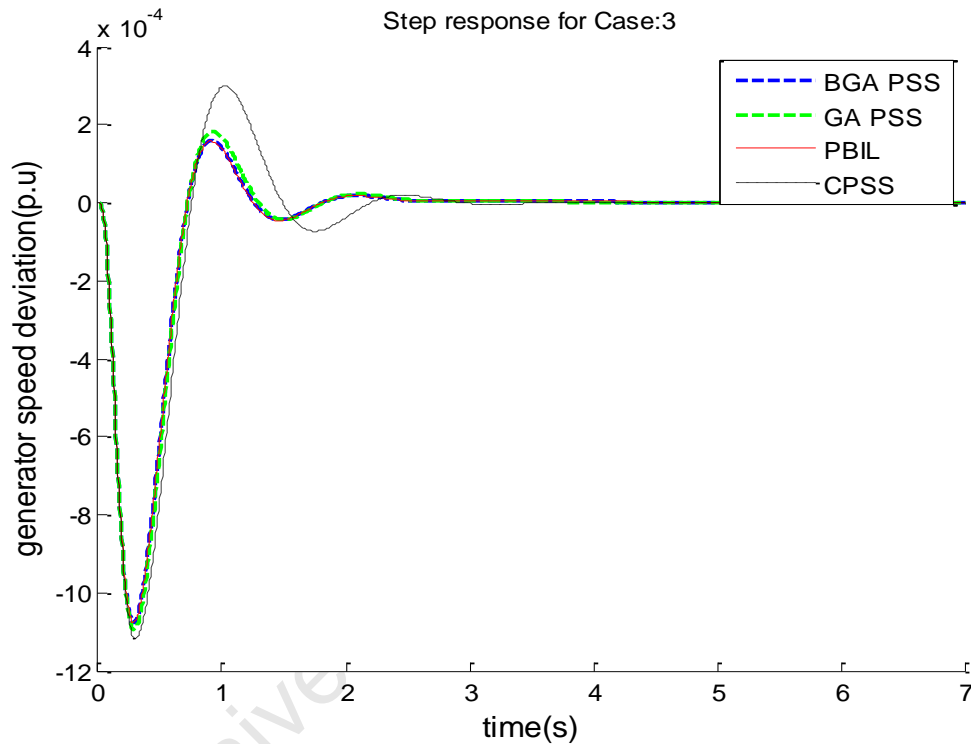


Figure 5.8: System response (speed) for Case 3

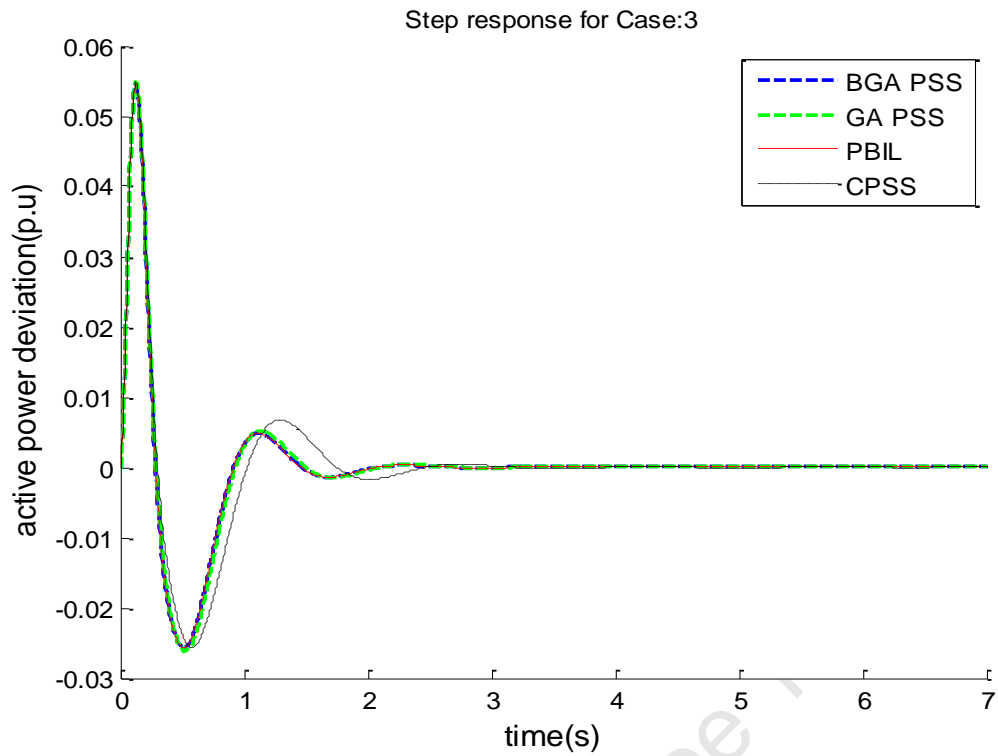


Figure 5.9: System response (active power) for Case 3

The active power and speed deviation of Case 4 as shown in Figure 5.10 and Figure 5.11 shows a similar trend to the ones observed in Cases 2 to 3, where the system equipped with CPSS has higher overshoots and higher undershoots as well as a longer settling time of about 3 seconds. As for the GA, the system experiences a second swing of roughly 2.0×10^{-4} pu, but the settling time is now less than 2 seconds.

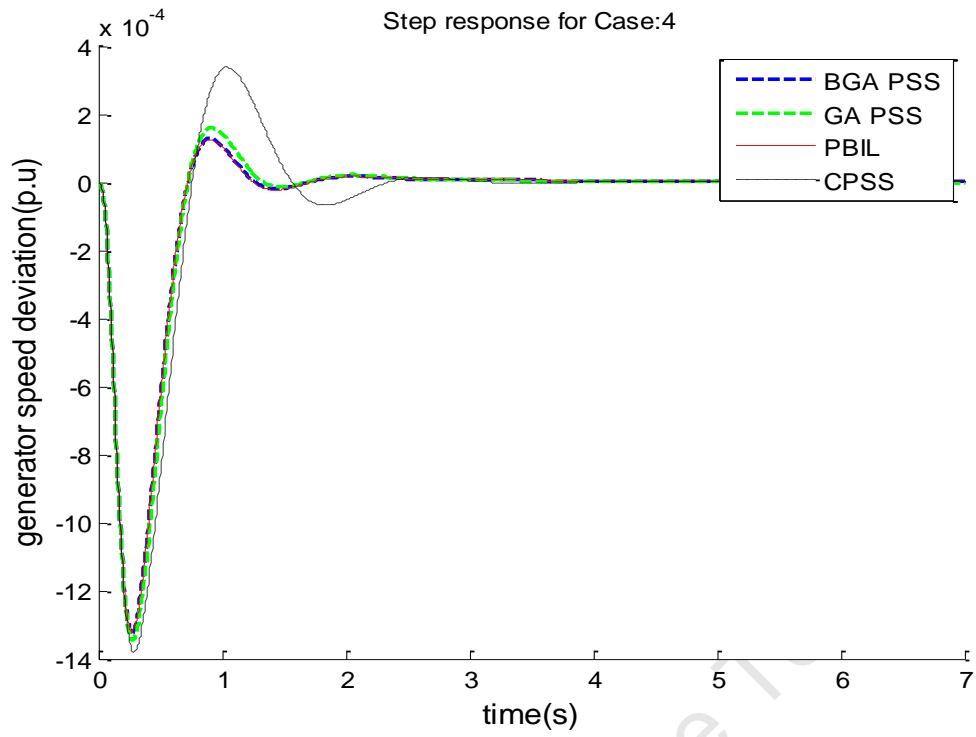


Figure 5.10: System response (speed) for Case 4

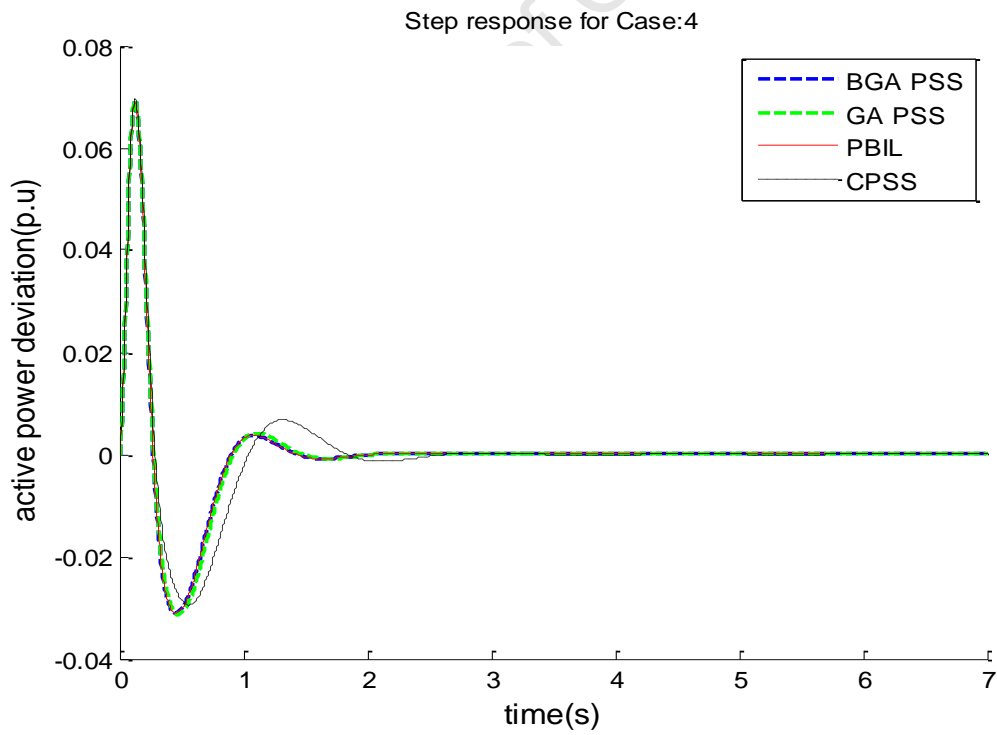


Figure 5.11: System response (active power) for Case 4

The active power and speed deviation response of Case 5 as shown in Figure 5.12 and Figure 5.13 show a similar trend to the ones observed in the previous Cases. In this Case the system takes a bit longer to settle under all the PSSs as compared to Case 4. This is consistent with the results in Table 5.2 which show that the lowest damping ratio for all the operating conditions considered occurs in Case 5. When the system is equipped with the GA-PSS, it takes roughly 4 seconds to settle, similar to the system equipped with BGA-PSS and PBIL. Figure 5.13 shows the active power deviation of the generator and it can be observed that the systems oscillations have increased, with the settling time, of the system with CPSS, more than 5 seconds.

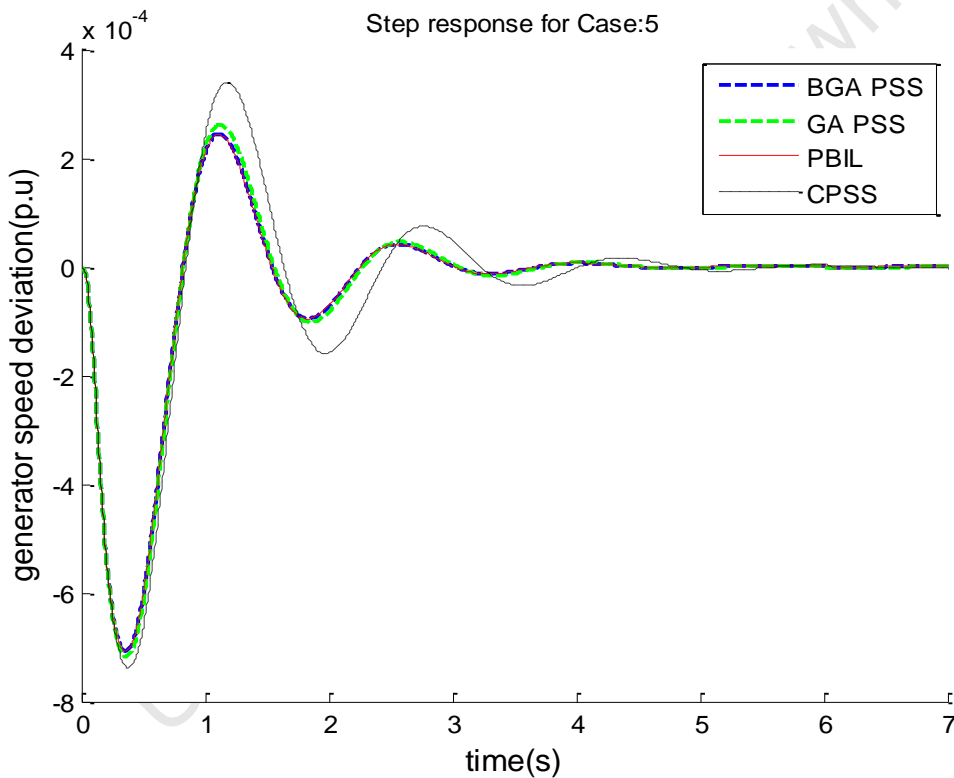


Figure 5.12: System response for Case 5

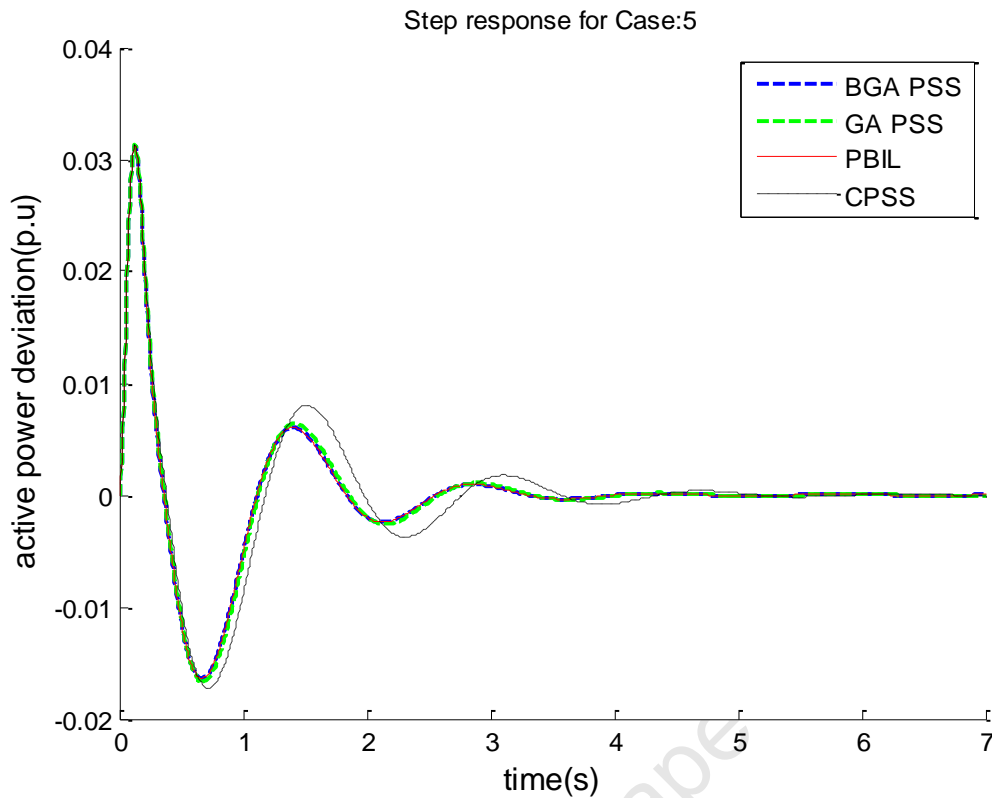


Figure 5.13: System response (active power) for Case 5

The active power and speed deviation responses of the system are shown in Figure 5.14 and Figure 5.15 for Case 6. It can be observed that the performance of the CPSS worsens especially with maximum overshoot in Figure 5.14 which is above 4.0×10^{-4} pu. It can also be observed that the system with GA-PSS experiences a slightly higher overshoot and undershoot compared to the BGA-PSS and PBIL. This suggests that GA-PSS experiences slightly higher oscillations than the BGA and PBIL.

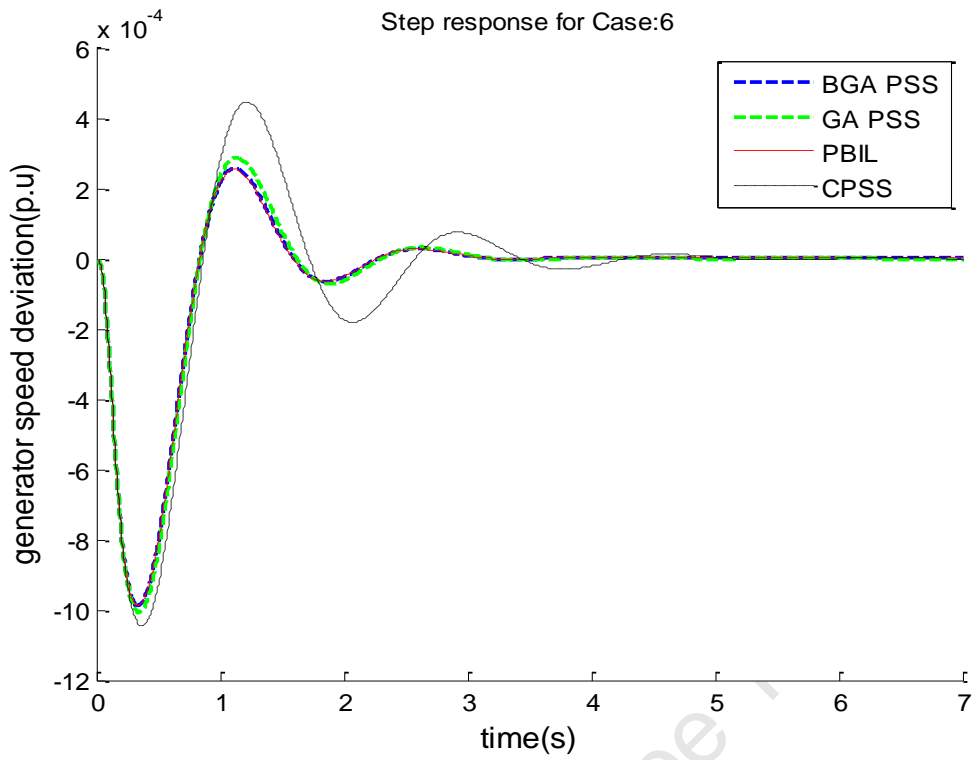


Figure 5.14: System response (speed) for Case 6

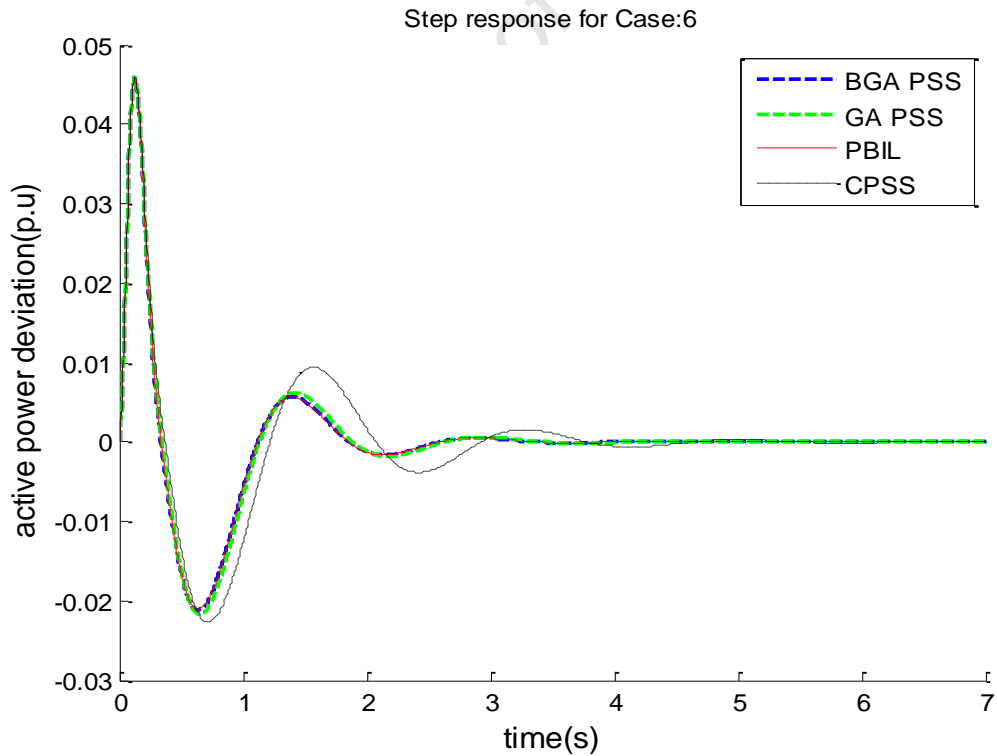


Figure 5.15: System response (active power) for Case 6

The responses in Figure 5.16 and Figure 5.17 for Case 7 show that the response of the CPSS is getting worse with a maximum overshoot in Figure 5.16 of approximately 6.0×10^{-4} pu and a settling time of more than 5 seconds. The overshoot of the system equipped with GA-PSS is also slightly higher than that of BGA-PSS and PBIL which is around 3.0×10^{-4} pu. However GA-PSS, BGA-PSS and PBIL have the same settling time of around 3 seconds. As expected the performance of the CPSS worsen as the operating conditions moves away from the nominal operating condition.

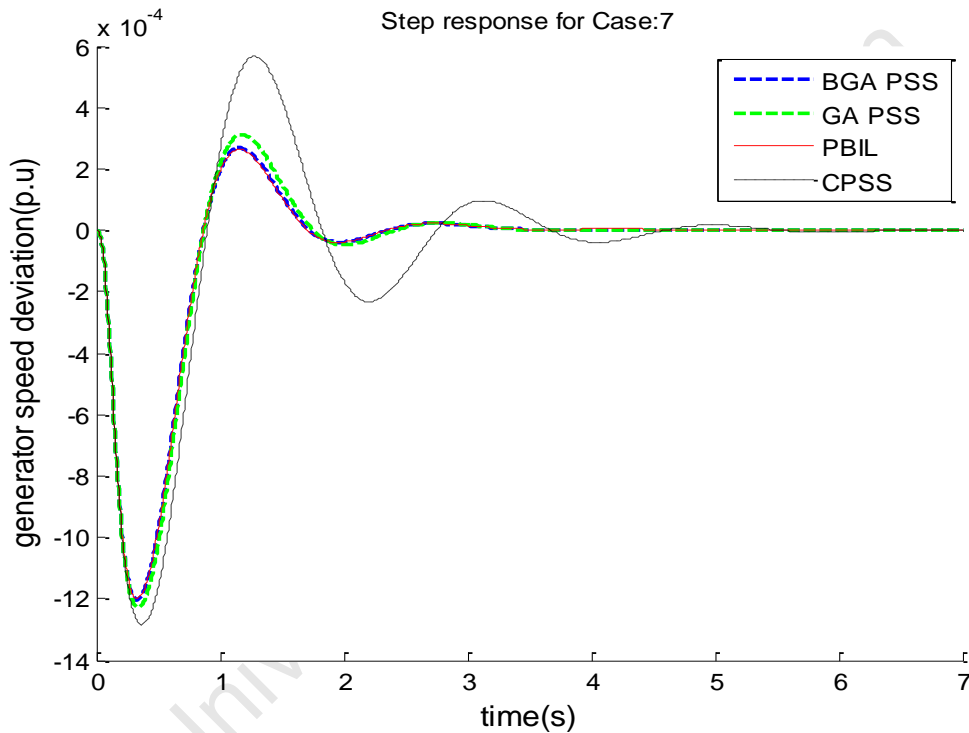


Figure 5.16: System response (speed) for Case 7

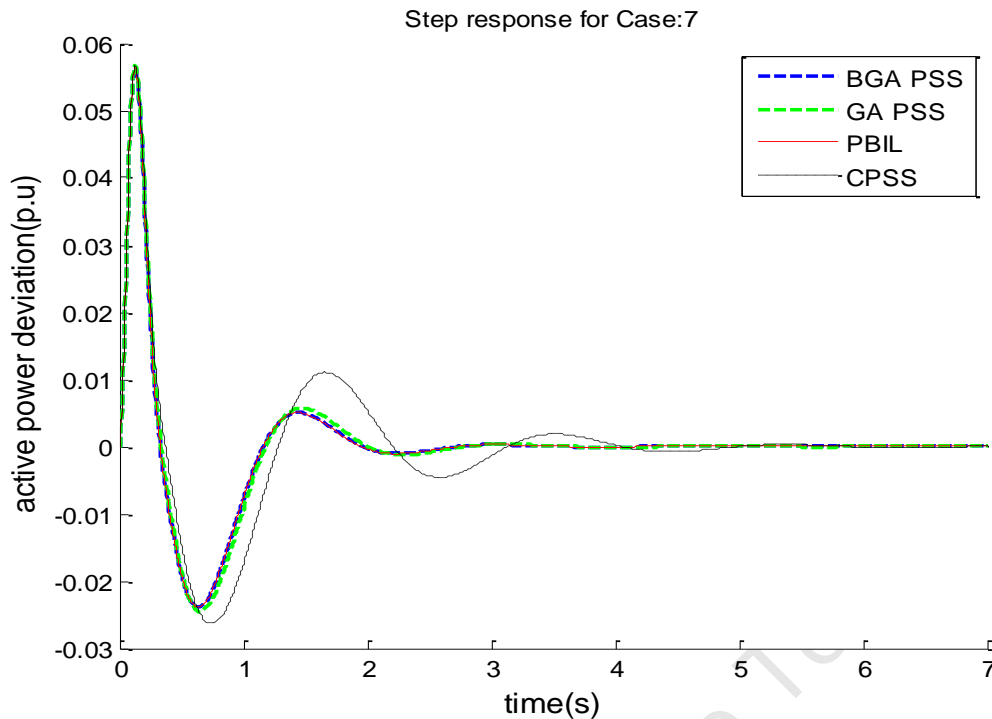


Figure 5.17: System response (active power) for Case 7

5.3.3 PSS Robustness Evaluation

As has been mentioned before, Cases 8 and 9 were not included in the evolutionary algorithm based PSSs design, but analysed to check for the robustness of the designed PSSs.

The responses of Case 8 are shown in Figure 5.18 and Figure 5.19. It can be seen from Figure 5.18 and Figure 5.19 that the system equipped with CPSS experiences higher oscillations. The maximum overshoot is over 4×10^{-4} pu. The GA-PSS gives the second highest overshoot, whereas the overshoots of the system with BGA-PSS and PBIL-PSS are relatively close.

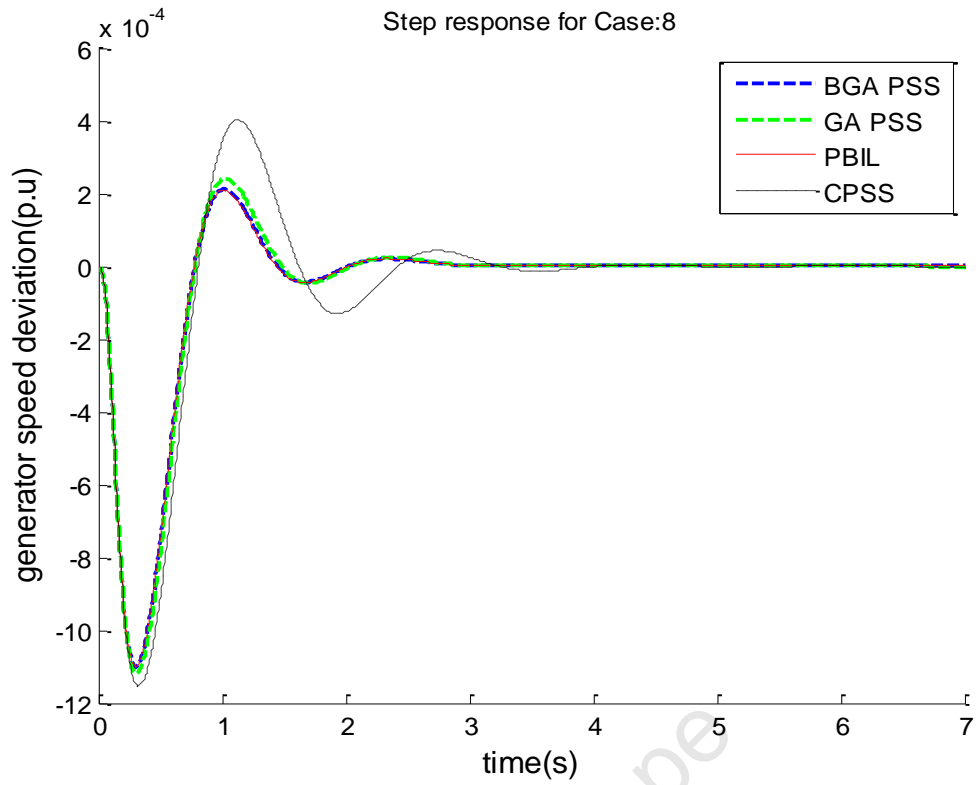


Figure 5.18: System response (speed) for Case 8

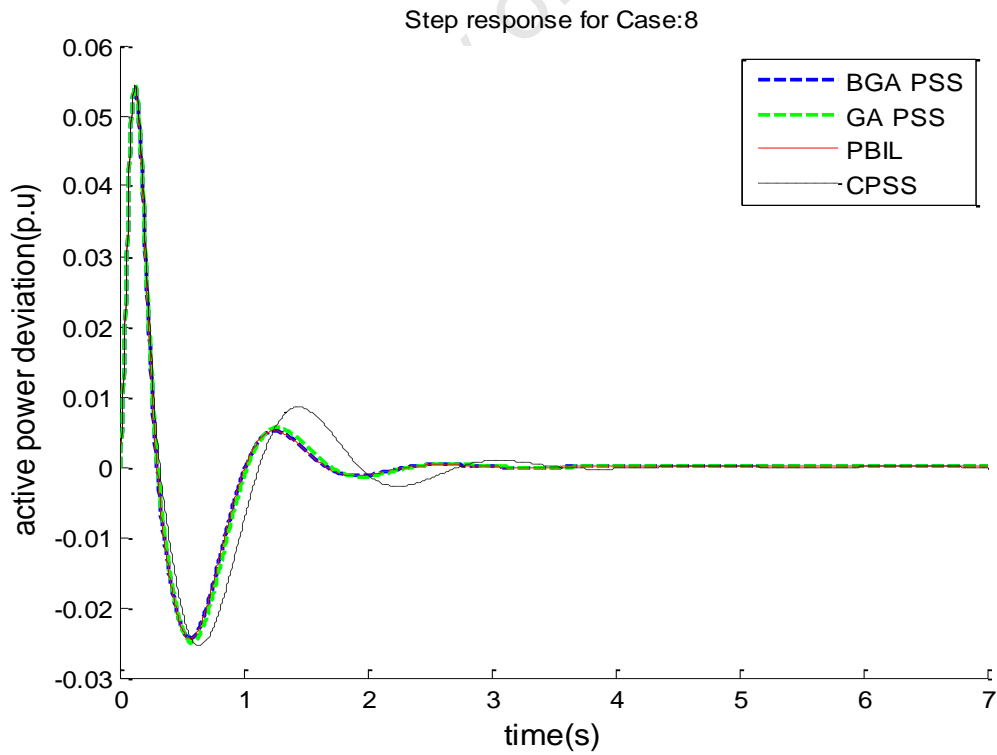


Figure 5.19: System response (active power) for Case 8

It can be seen in Figure 5.20 and Figure 5.21, the performance of the CPSS gets worse. Compared to Case 8, the CPSS responses have further deteriorated. Not only that the overshoot and undershoot become very large, but the oscillations have also increased. The settling time of the system with CPSS in Case 9 is more than 7 seconds. This clearly shows that the performance of the CPSS deteriorates as the system operating condition changes away from the nominal operating condition. GA-PSS also gives a relatively high overshoot as compared to the BGA-PSS and PBIL. The settling time of the system with GA-PSS is around 4 seconds while for the system with BGA and PBIL is around 2.5 seconds.

Clearly the system with CPSS is deteriorating both in settling time as well as in the system oscillations. This explains the need to design the PSS over a wide range of operating conditions as compared to designing it over a single condition. It can be observed to that designing the PSS with GA provides good damping and the system is well damped across all operating conditions, but at the same time the level of performance also slightly decreases under some operating conditions and in this Case it was when the system was heavily loaded.

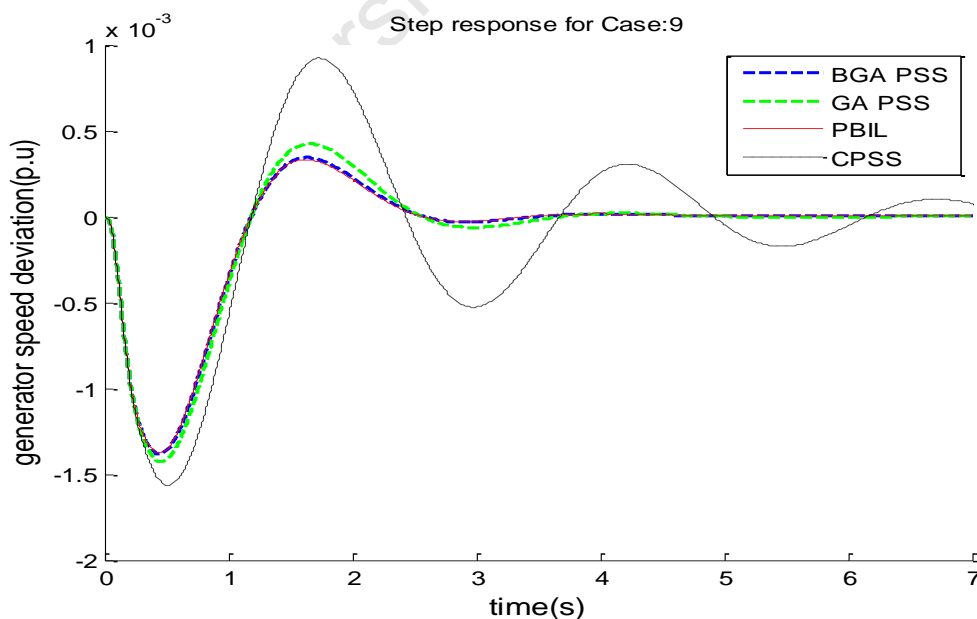


Figure 5.20: System response (speed) for Case 9

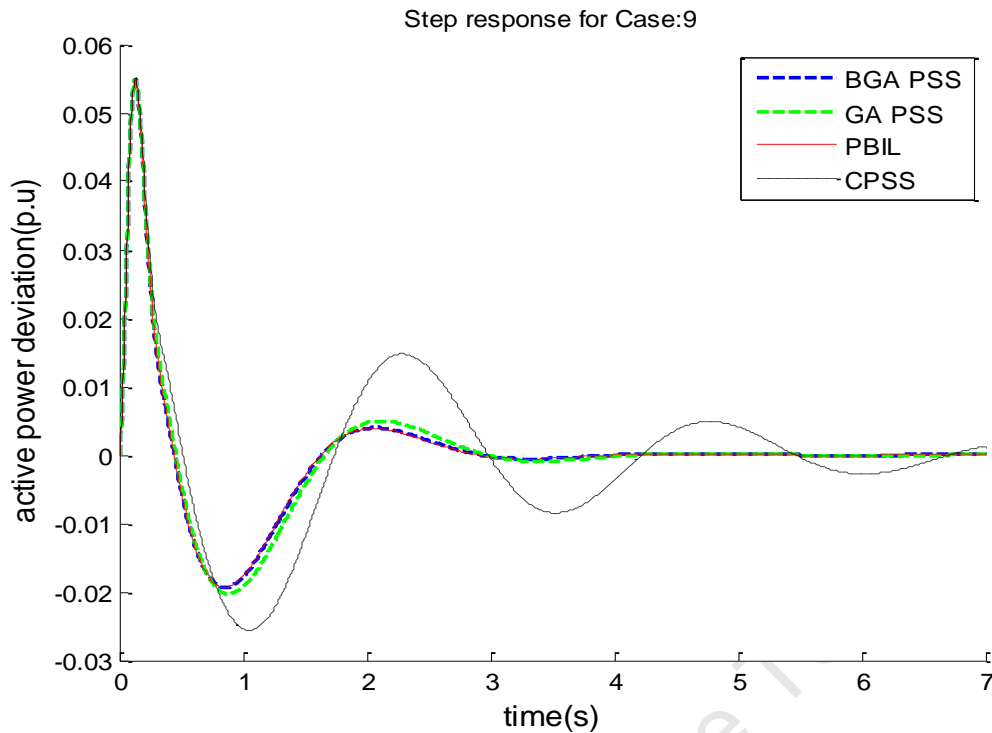


Figure 5.21: System response (active power) for Case 9

5.4 Transient Stability

Transient stability simulation was also performed to evaluate the performance of the system under large disturbances. In the following simulations, we consider a three phase fault applied closer to Bus 1 on line 2 (Figure 4.1). The fault was applied at 0.1 seconds and lasted for 0.2 seconds and cleared by disconnecting the line. The fault applied was used to test for extreme cases that the system may be subjected to; in general the fault should be between three to five cycles. This fault was only applied over Case 1 to Case 5. Case 6 to Case 9 were not considered under the transient simulation due to the power angle being very high (at least 59°) after line disconnection and also due to the limitation of the software which does not allow for the clearance of the fault without removing the transmission line. The post fault power angle for Case 6 was 69.41° and 59.51° for Case 8. The angles for Cases 7 and 9 were more than 90° after the line disconnection. The system could no longer sustain a line removal without reaching instability in Cases six to nine.

5.4.1 Case 1: nominal operating condition

Using Case 1 (nominal operating condition), the responses of the voltage terminal, real power, speed, rotor angle and field voltage after the three phase short circuit fault with line disconnection are shown in Figure 5.22 to Figure 5.26. All the responses, except for the rotor angle show that the system performs better when equipped with the CPSS as compared to the evolutionary algorithm based PSSs. From Figure 5.22, the voltage on Bus 1 drops almost to zero during the fault, but recovers in time after the fault was cleared. Figure 5.23 shows the active power response of the generator to a step change in voltage reference, it shows that the system has lower overshoot with CPSS as compared to the evolutionary algorithm based PSSs, but with a slightly longer settling time of about 3.5s as compared to evolutionary algorithm based PSSs with settling time of about 3s. Figure 5.24 and Figure 5.25 show the generator speed and rotor angle response to the three phase fault. The speed response shows a close performance between the CPSS and evolutionary algorithm based PSS, but the rotor angle shows a better performance of the evolutionary algorithms as compared to the CPSS. This could be attributed to the fact that the damping ratio for the high frequency oscillatory modes in Table B.1 (Appendix B) is slightly low damped with CPSS as compared to other PSS. Figure 5.25 shows that the initial rotor angle was 14° before the fault was applied, but it settled to a value of above 18° after the fault was cleared. This is because the fault was cleared by removing the line. The post fault condition of the system is less stable than the pre-fault condition. Figure 5.26 for the field voltage shows that after 1 second there is a slightly better performance from the CPSS, with undershoot being smaller than the other PSSs. All other evolutionary algorithms (GA-PSS, BGA-PSS and PBIL) show a similar performance around this operating condition. Overall the CPSS has a good performance around this operating condition as expected.

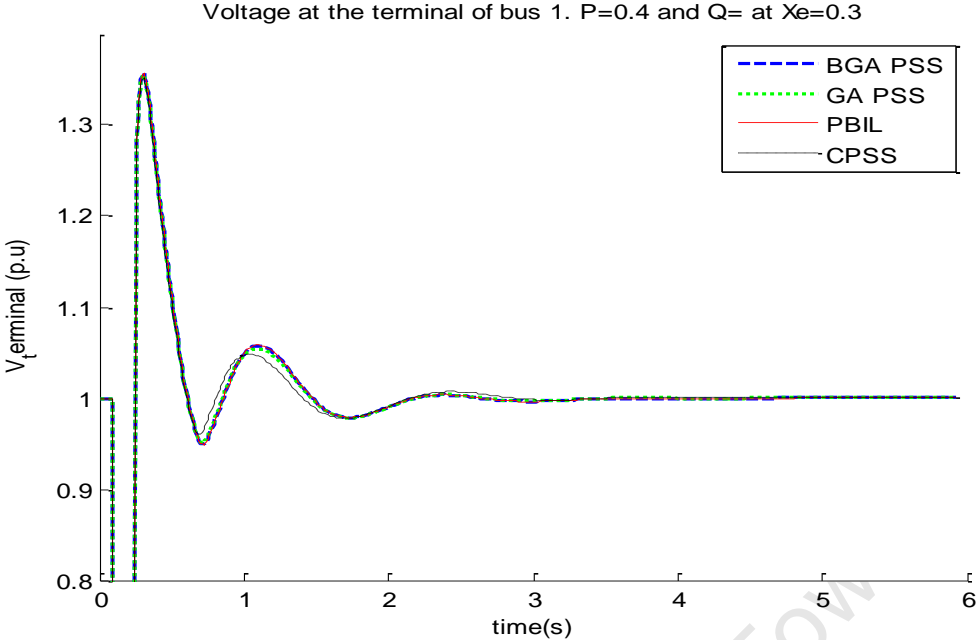


Figure 5.22: Voltage terminal response of Case 1 under three phase fault

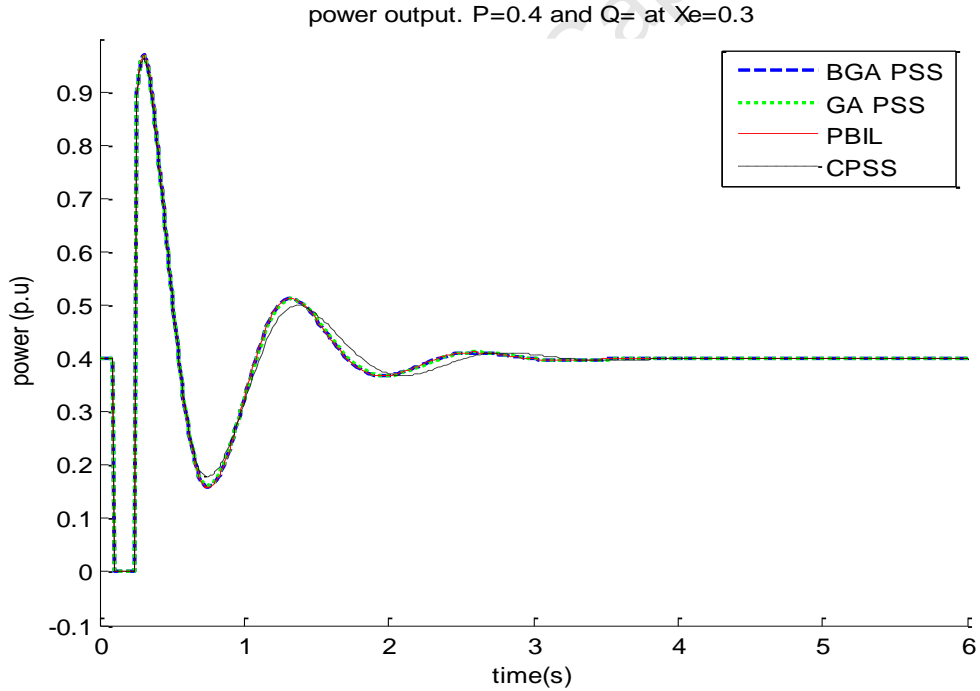


Figure 5.23: Power response of Case 1 under three phase fault

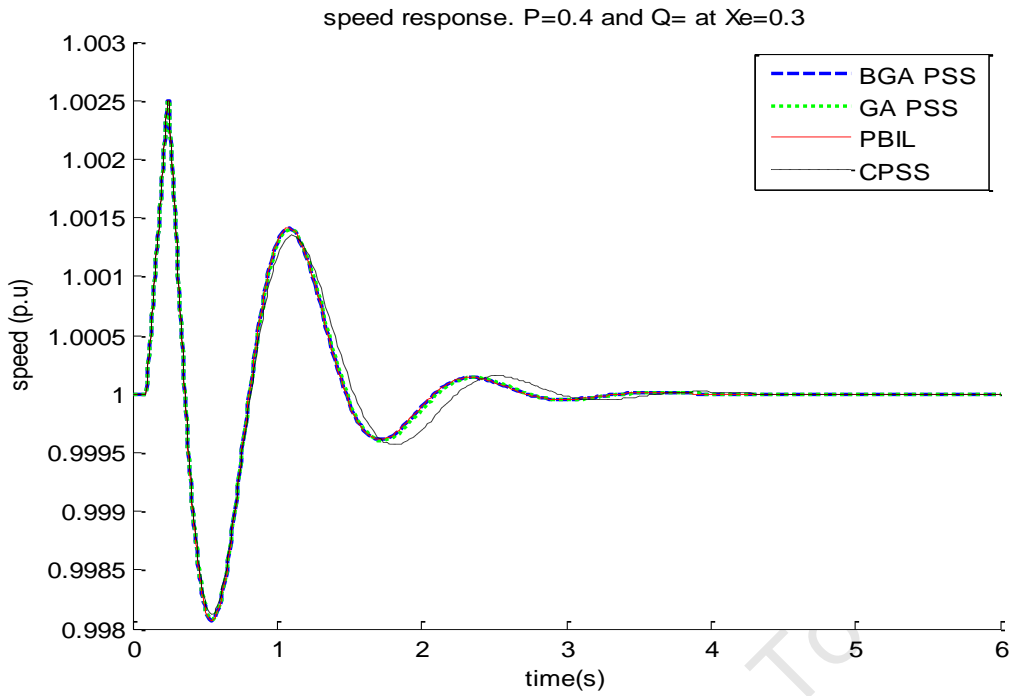


Figure 5.24: Speed response of the generator under three phase fault

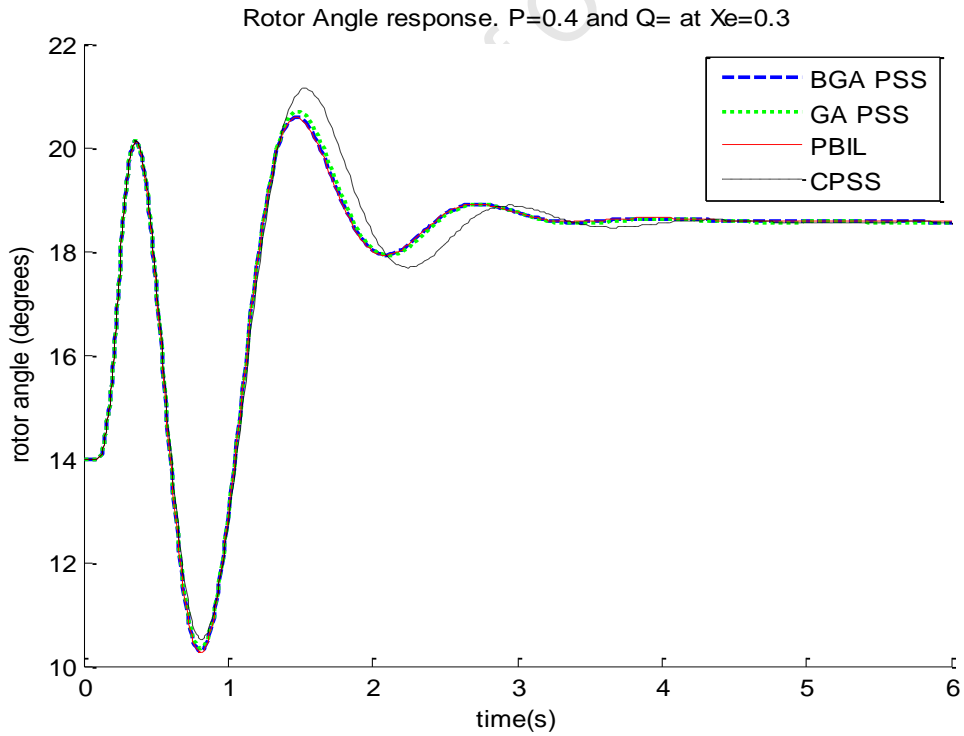


Figure 5.25: Rotor angle response of the system under three phase fault

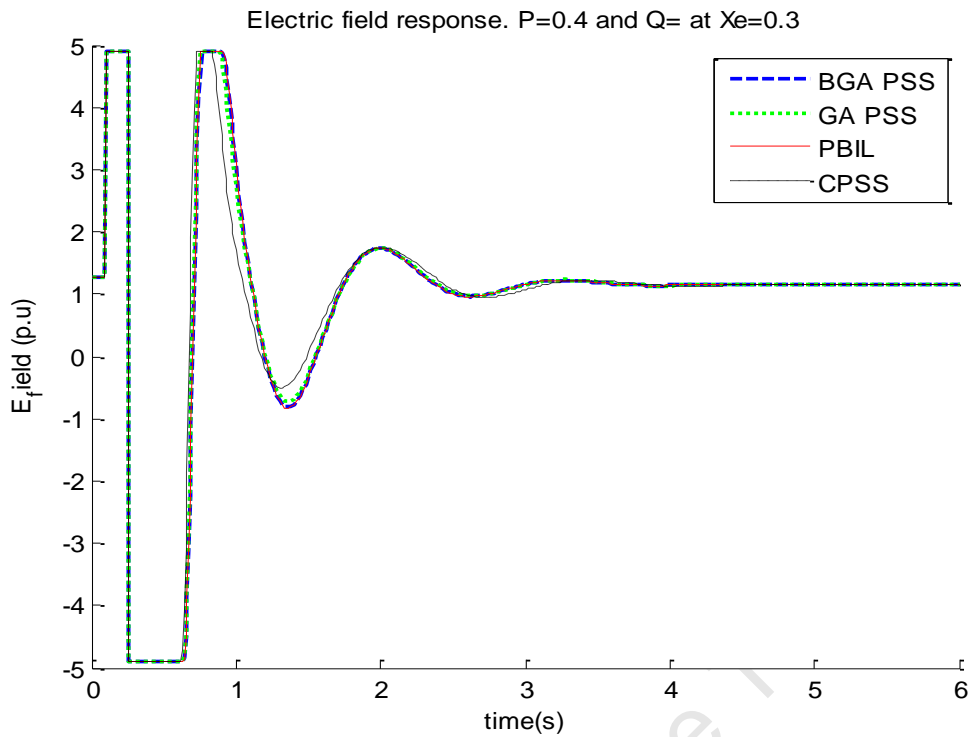


Figure 5.26: Electric field voltage response of the system under a three phase fault of Case 1

5.4.2 Case 2: System condition, $P_e=0.5$ pu; $Q_e=0.2184$ pu; $X_e=0.3$ pu

The voltage terminal, real power, speed, rotor angle and electric field voltage are shown in Figure 5.27 up to Figure 5.31. The system performance with all the PSSs is relatively the same. The active power response of the generator as depicted in Figure 5.28 shows a similar trend to the observations made in Case 1, where the difference in performance of all different PSS is minimal. Figure 5.29 and Figure 5.30 show the generator speed and rotor angle response respectively, the system with CPSS exhibits a lower overshoot as compared to the evolutionary algorithm based PSSs, but the settling time of the system with CPSS is slightly longer than the other PSSs. It can be observed from Figure 5.30, that before the fault the angle was roughly 25° , but after the line was cleared it settled at around 36° . The difference is due to the line disconnection. Figure 5.31 shows the systems electric field response during and after a fault. The performance of the system in this scenario is much the same.

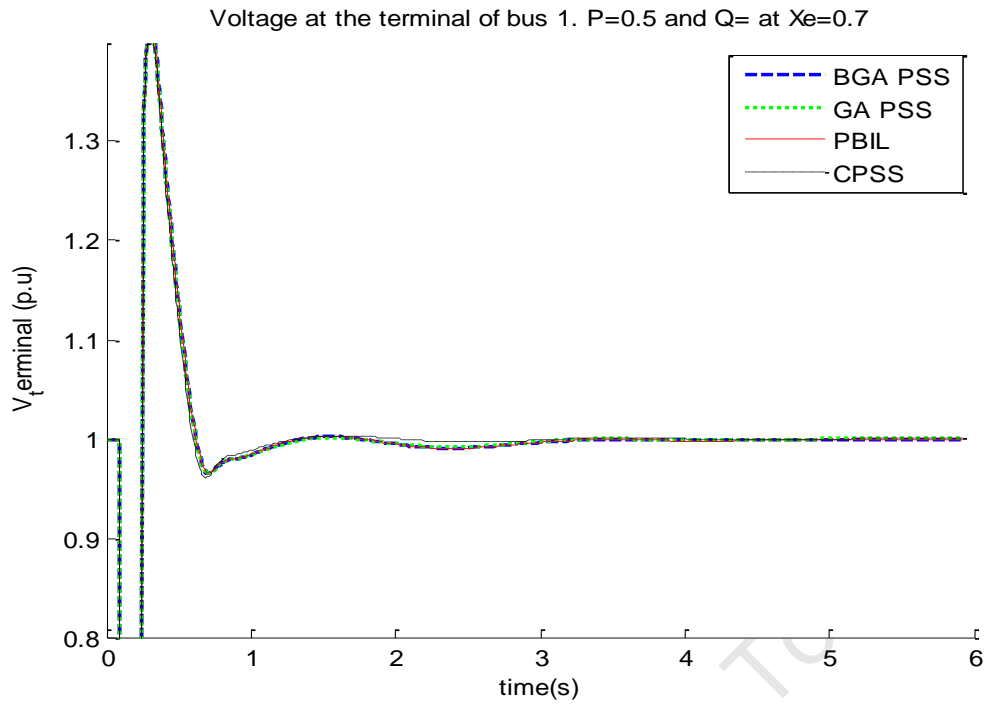


Figure 5.27: Voltage terminal response of the system under three phase fault of Case 2

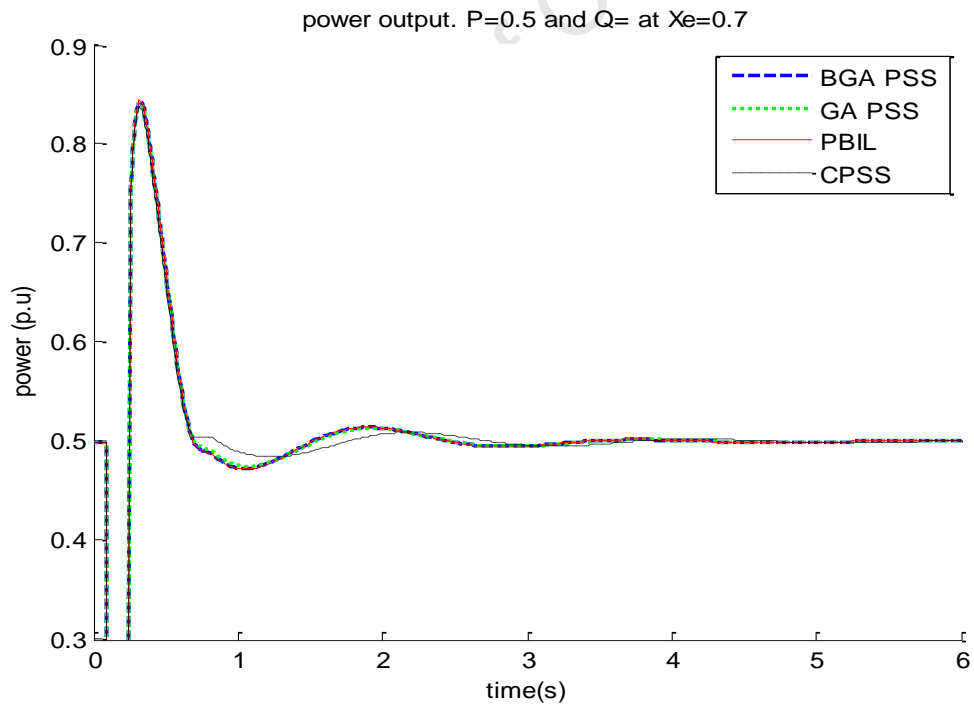


Figure 5.28: Power output response of the system under three phase fault of Case 2

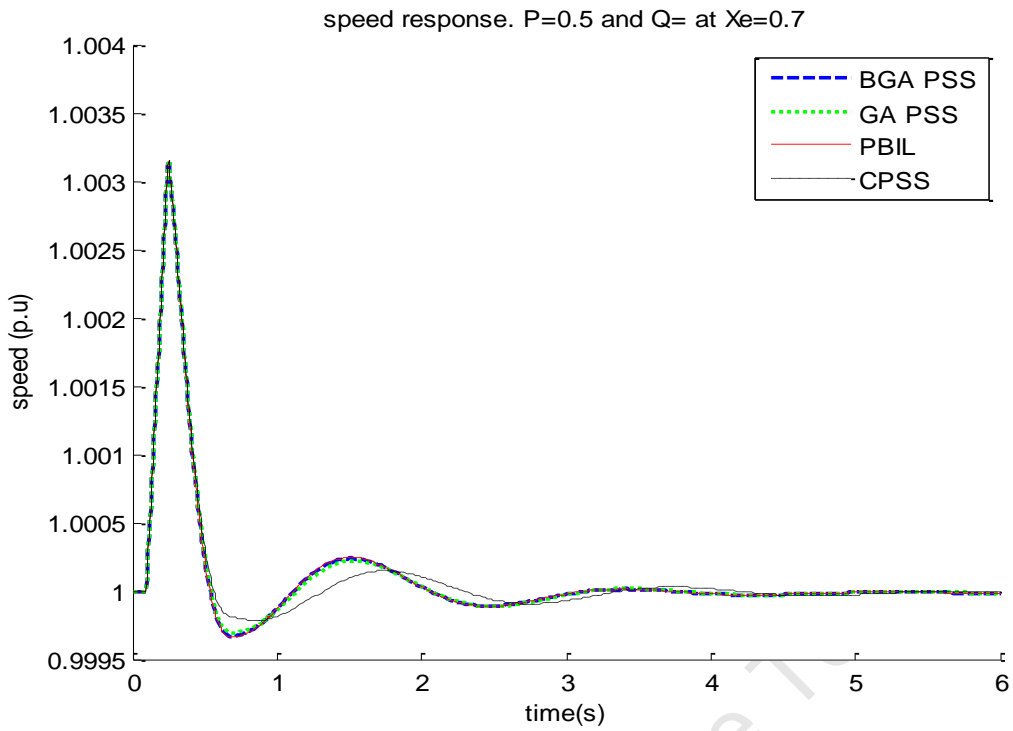


Figure 5.29: Speed response of the generator under three phase fault of Case 2

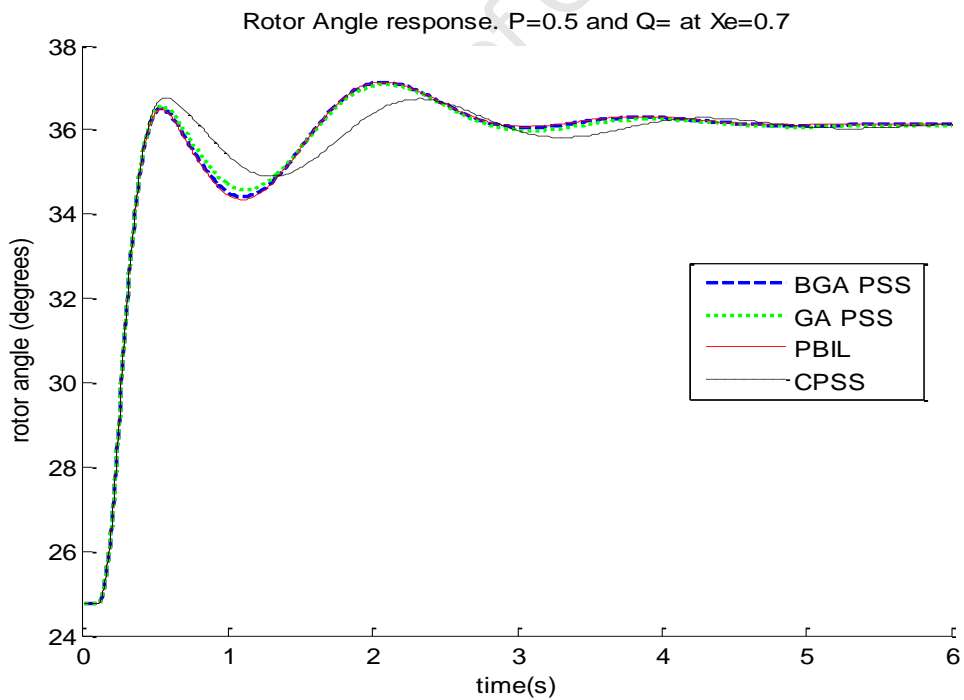


Figure 5.30: Rotor angle response of the system under three phase fault of Case 2

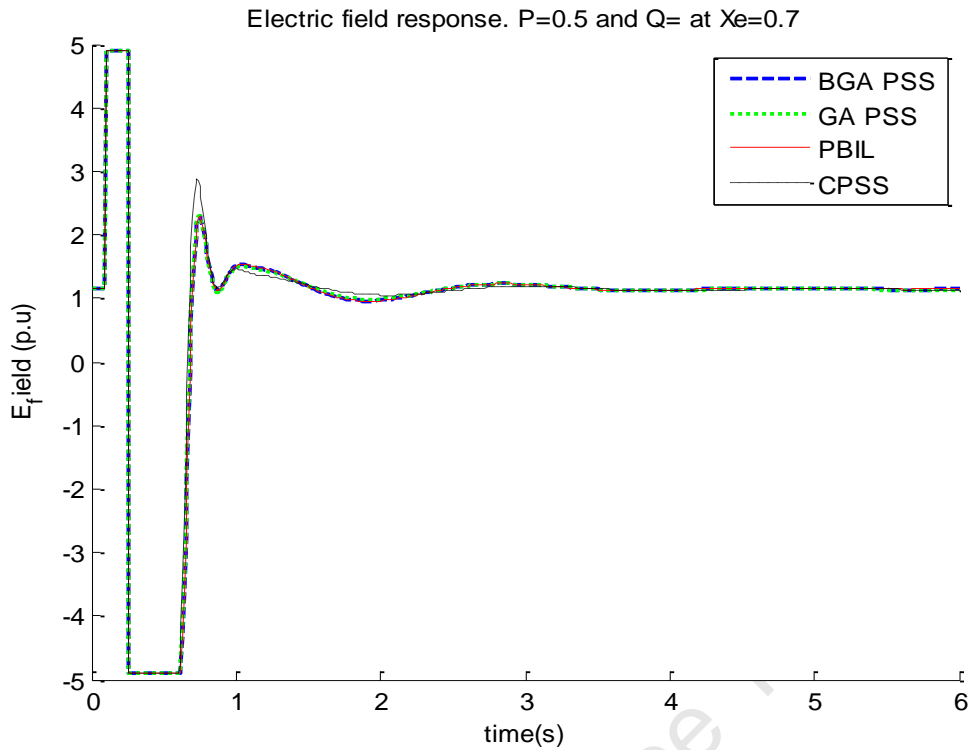


Figure 5.31: Electric field voltage response of the system under three phase fault of Case 2

5.4.3 Case 3: System condition, $P_e=0.8\text{pu}$; $Q_e=0.2933\text{pu}$; $X_e=0.7\text{pu}$

The voltage terminal response for case 3 is shown in Figure 5.32. It can be seen from Figure 5.32 that the system equipped with CPSS has more oscillations as compared to the EA based PSSs. From the generator's active power response in Figure 5.33, the CPSS performance has deteriorated as compared to the two previous cases. It takes more than 4 seconds for the CPSS to settle down, whereas the evolutionary algorithm based PSSs take roughly 2 seconds to settle down. The speed and rotor angle responses of the generator shown Figure 5.34 and Figure 5.35 show that the system actually takes longer to settle when equipped with CPSS as compared to the system with evolutionary algorithm based PSSs. The electric field voltage response shown in Figure 5.36 also shows a similar trend whereby the CPSS performance deteriorates as compared to the BGA, GA and PBIL.

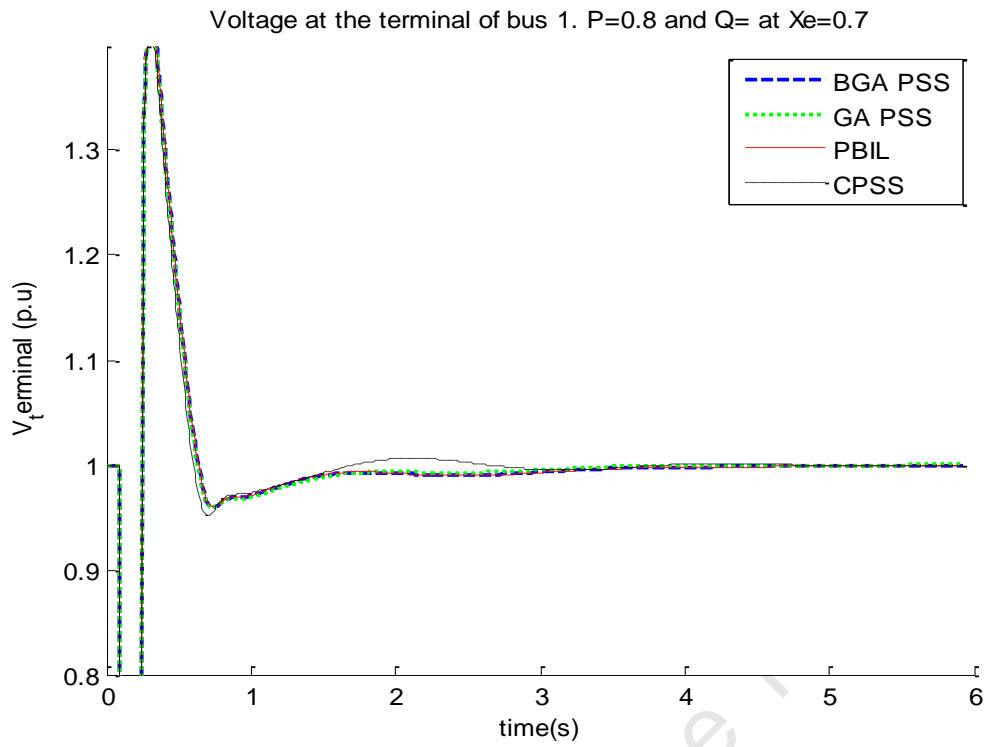


Figure 5.32: Voltage terminal response of the system under three phase fault of Case 3

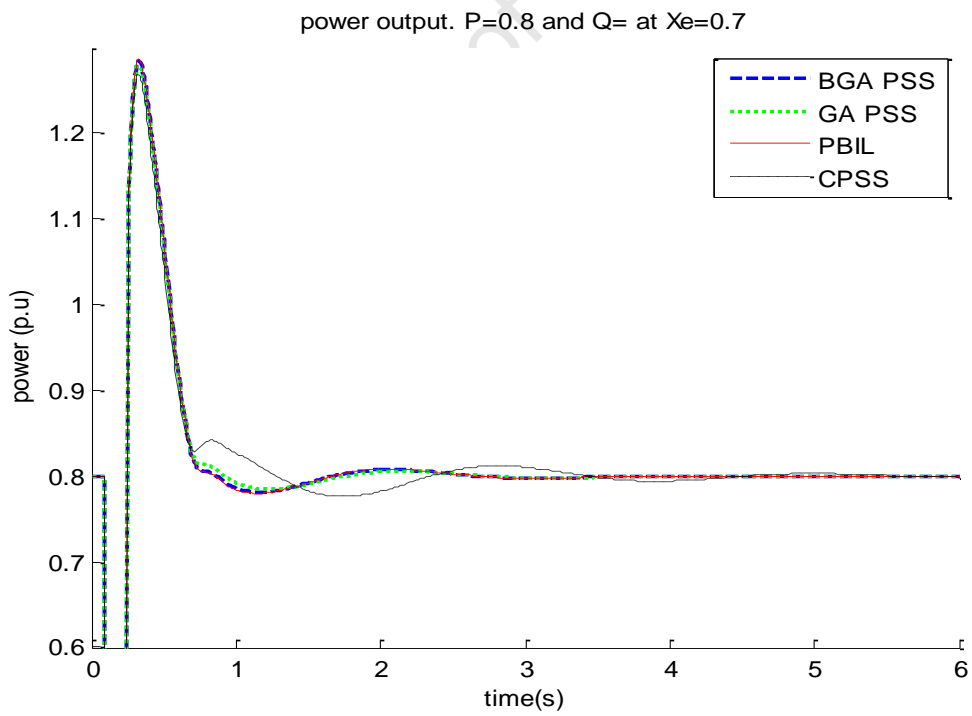


Figure 5.33: Active Power response of the generator under three phase fault of Case 3

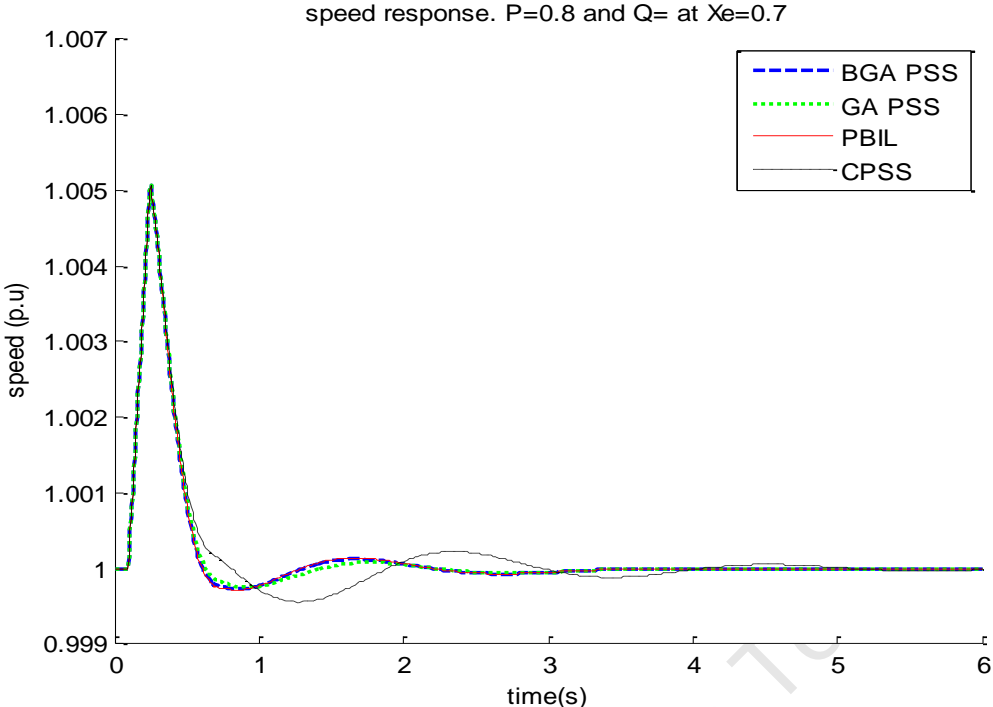


Figure 5.34: Generator speed response under three phase fault of Case 3

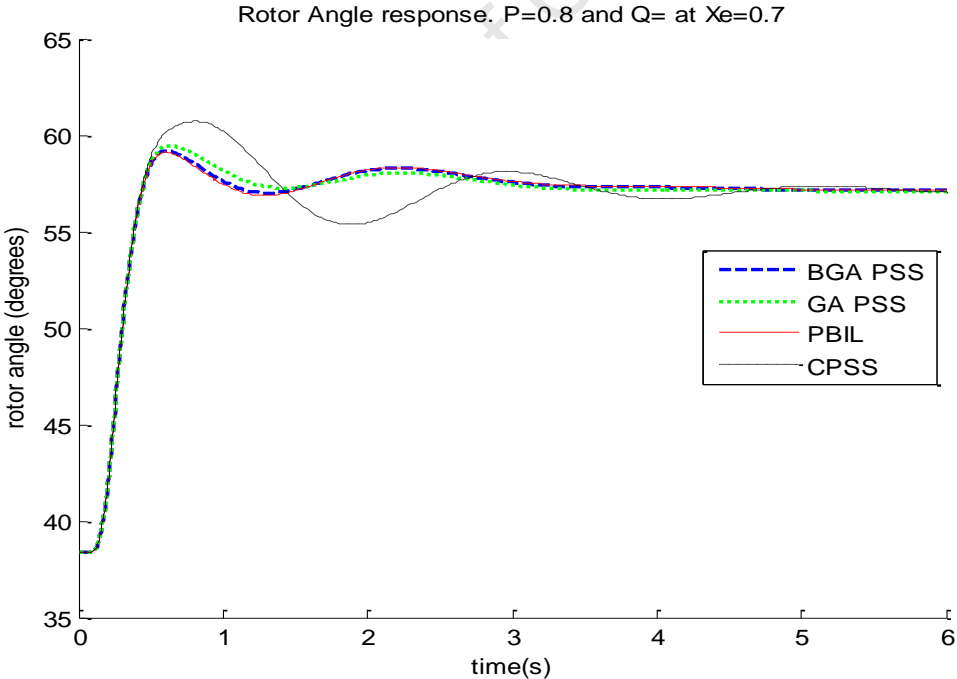


Figure 5.35: Rotor angle response of the system under three phase fault for Case 3

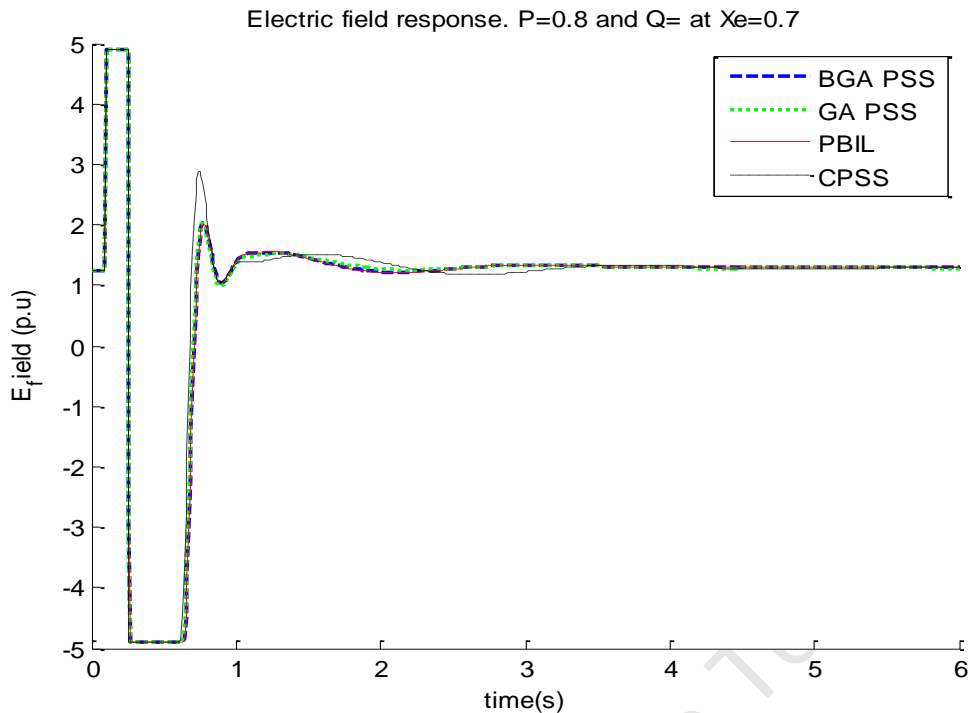


Figure 5.36: Electric field voltage response of the system under three phase fault of Case 3

5.4.4 Case 4: System condition, $P_e=1.1pu$; $Q_e=0.4070pu$; $X_e=0.7pu$

The system is stable with all the PSSs in case 4, however the CPSS produces more oscillations as compared to the evolutionary algorithm based PSSs. Figure 5.37 shows the response of the terminal voltage to the fault with all the PSSs included. The voltage response with CPSS shows that the system does not settle even after 5 seconds. The system with GA-PSS also has slightly higher oscillations compared to BGA-PSS and PBIL-PSS. The active power of Figure 5.38 also shows a similar trend where the CPSS does not settle after 6 seconds, at the same time, the oscillations are reducing in amplitude. Figure 5.39 shows the generator speed response, the system with CPSS still shows a similar trend to the voltage and power above. Also, from Figure 5.40, it can be observed that the system with GA-PSS has slightly higher oscillations than the BGA-PSS and PBIL. Figure 5.40 shows the generator rotor angle response, before the fault the angle was just above 50° , but after the fault, the rotor angle increased to above 81° . Clearly it can be seen that the system is heavily loaded, looking at the rotor angle. But the performance is still similar to the voltage, power and speed. Figure 5.41 shows the electric field voltage response of the system with the different PSSs.

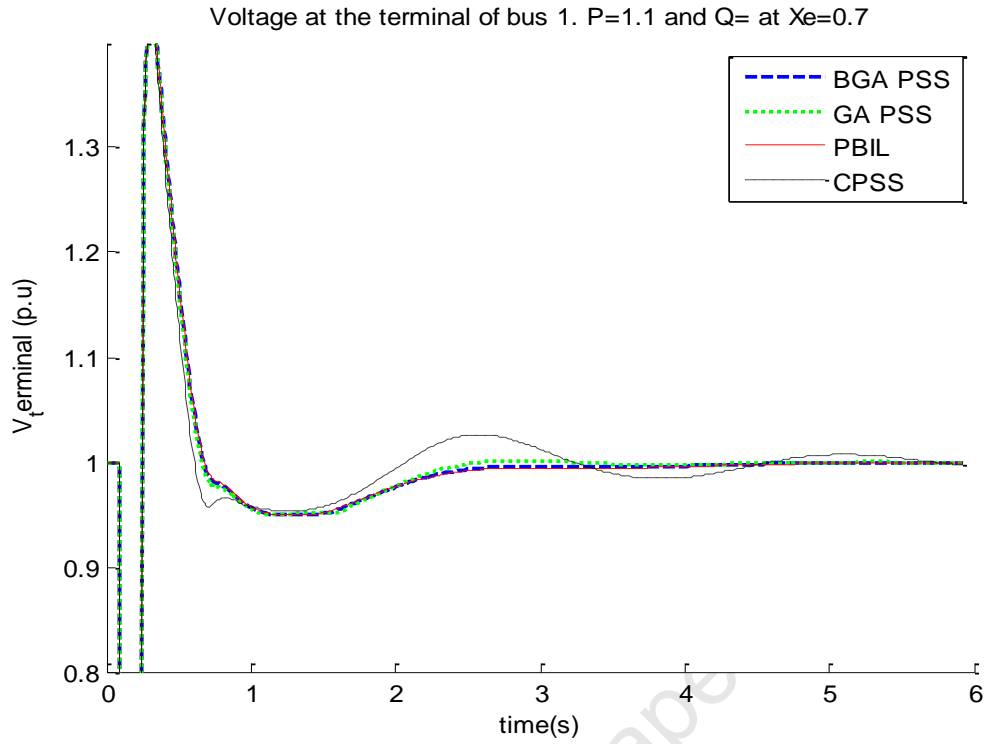


Figure 5.37: Voltage terminal response of the system to a three phase fault of Case 4

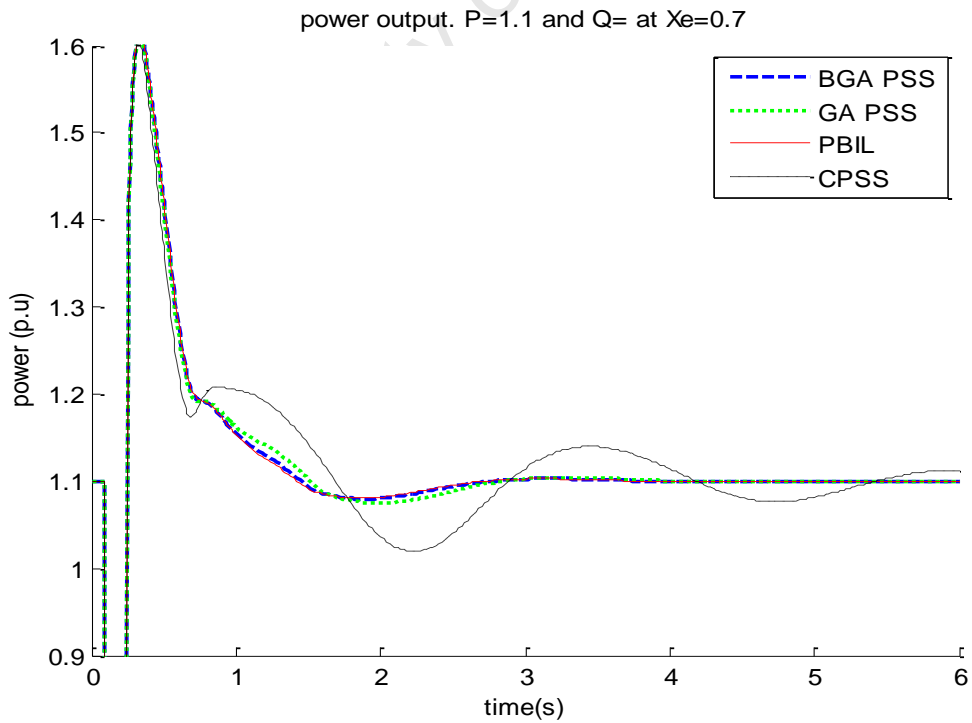


Figure 5.38: Active power response of the generator to a three phase fault at Case 4

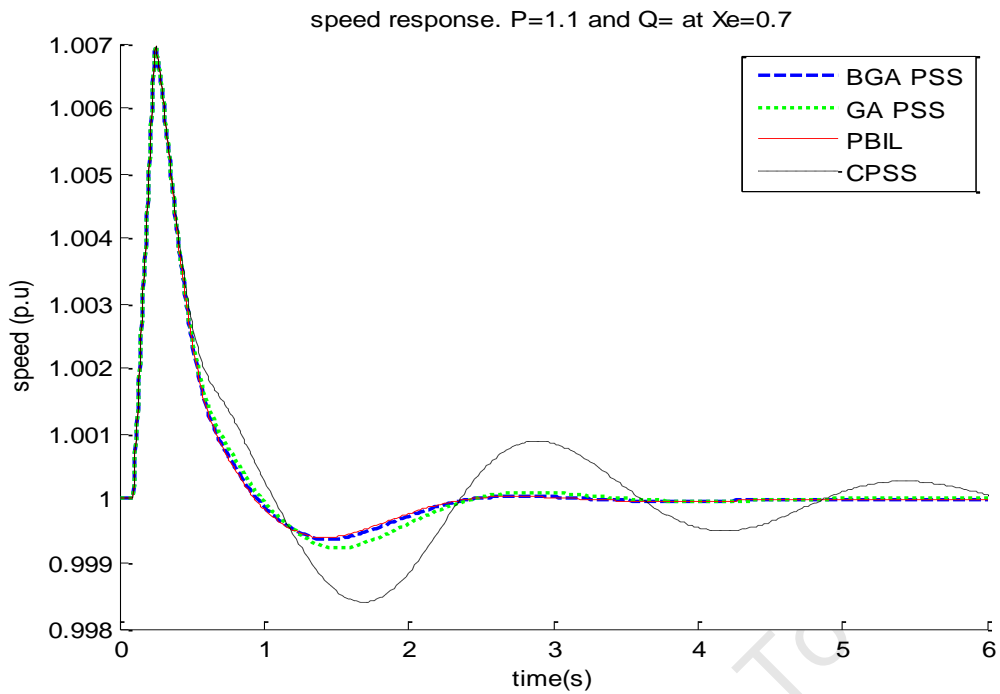


Figure 5.39: Generator speed response under three phase fault of Case 4

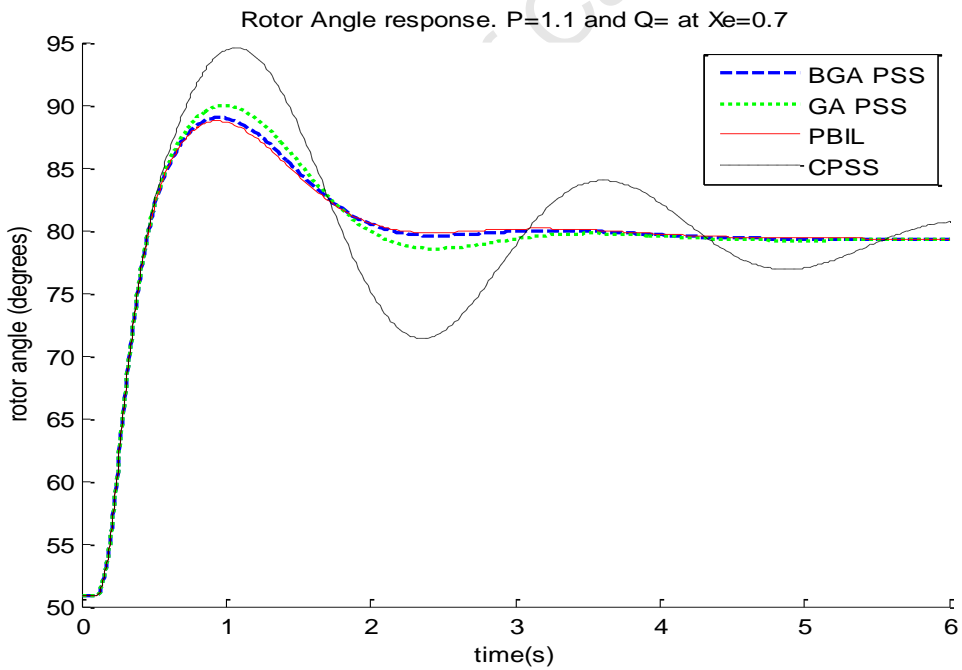


Figure 5.40: Rotor angle response of the generator under three phase fault at Case 4

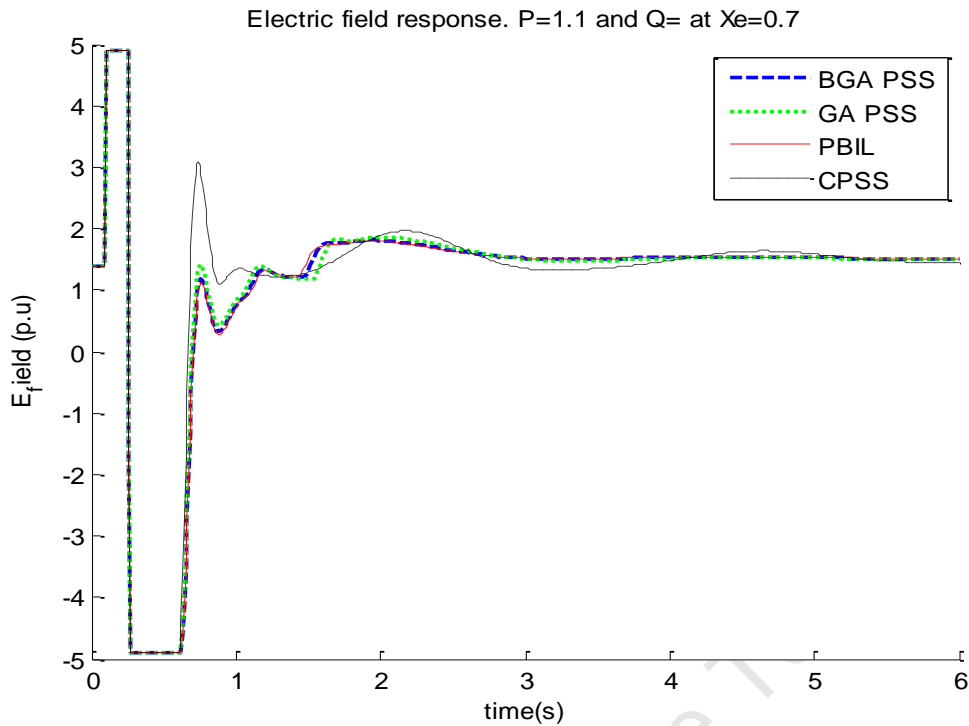


Figure 5.41: Electric field voltage response of the generator under three phase fault at Case 4

5.4.5 Case 5: System condition, $P_e=0.5pu$; $Q_e=1839pu$; $X_e=1.1pu$

In case 5, the system is stable after the fault was cleared. Figure 5.42 which show the terminal voltage response, shows that the CPSS performance is clearly deteriorating while the other PSSs still maintains a good level of performance. Figure 5.43 shows generator active power response to a three phase fault. Clearly from the Figure, the CPSS is not performing well at all. Figure 5.44 shows the generator speed response, while Figure 3.45 shows the rotor angle response of the system. The rotor angle was above 31° before the fault and after the fault was cleared it increased to approximately 50° . The change in rotor angle is brought up by the increase in line reactance due to the removal of the transmission line to clear the fault. Figure 5.46 shows the electric field voltage response of the system to the three phase fault. The system in case 5 is slightly more stable than case 4.

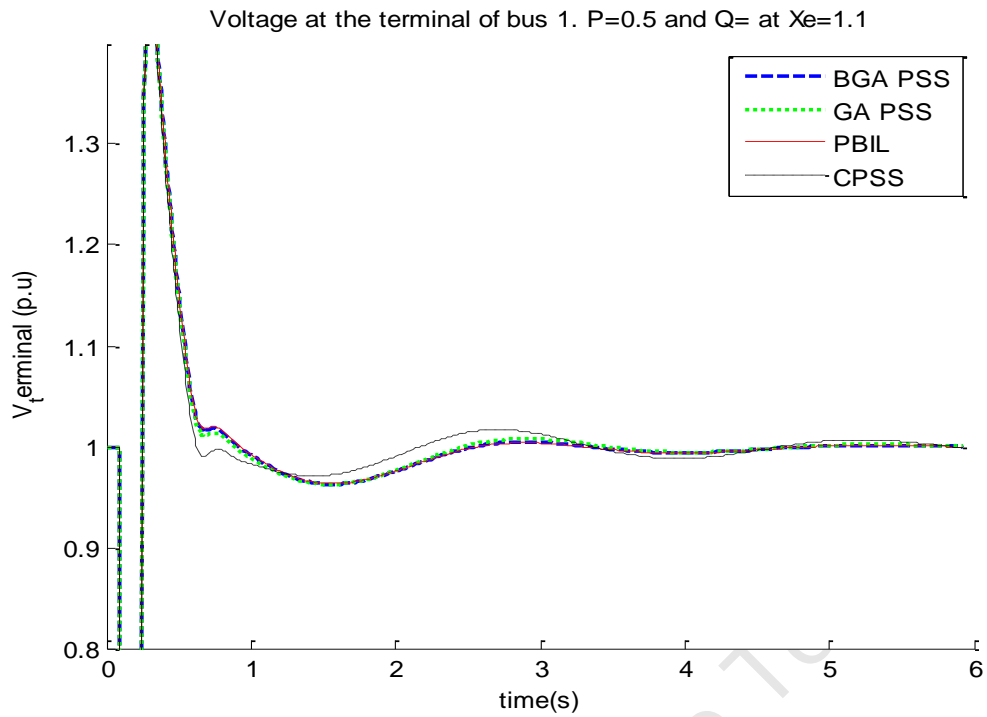


Figure 5.42: Voltage terminal response under three phase fault at Case 5

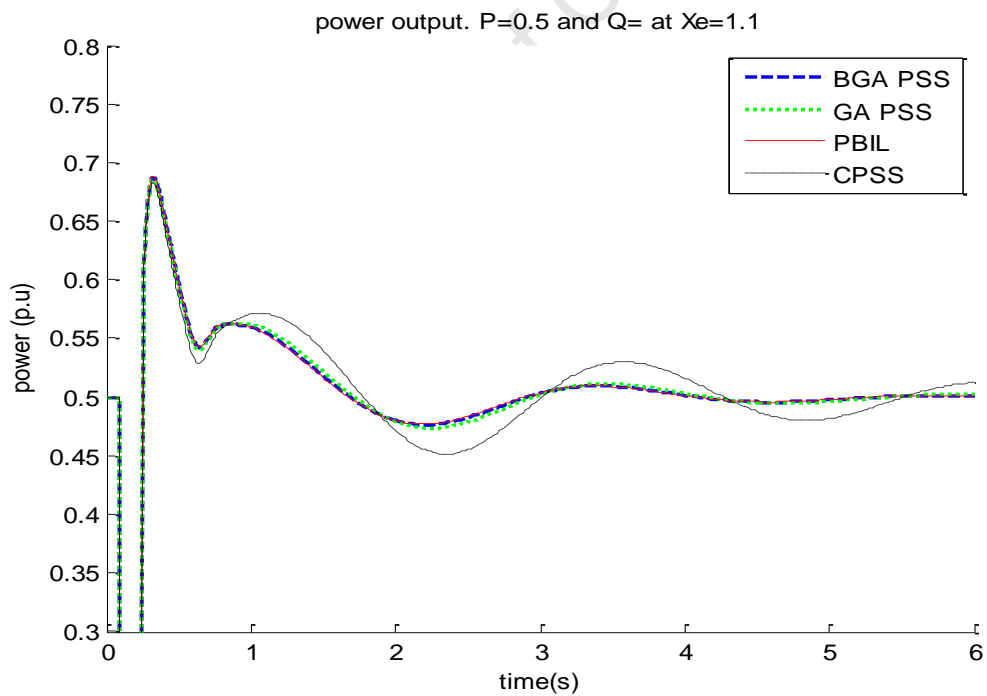


Figure 5.43: Active power response of the generator under three phase fault at Case 5

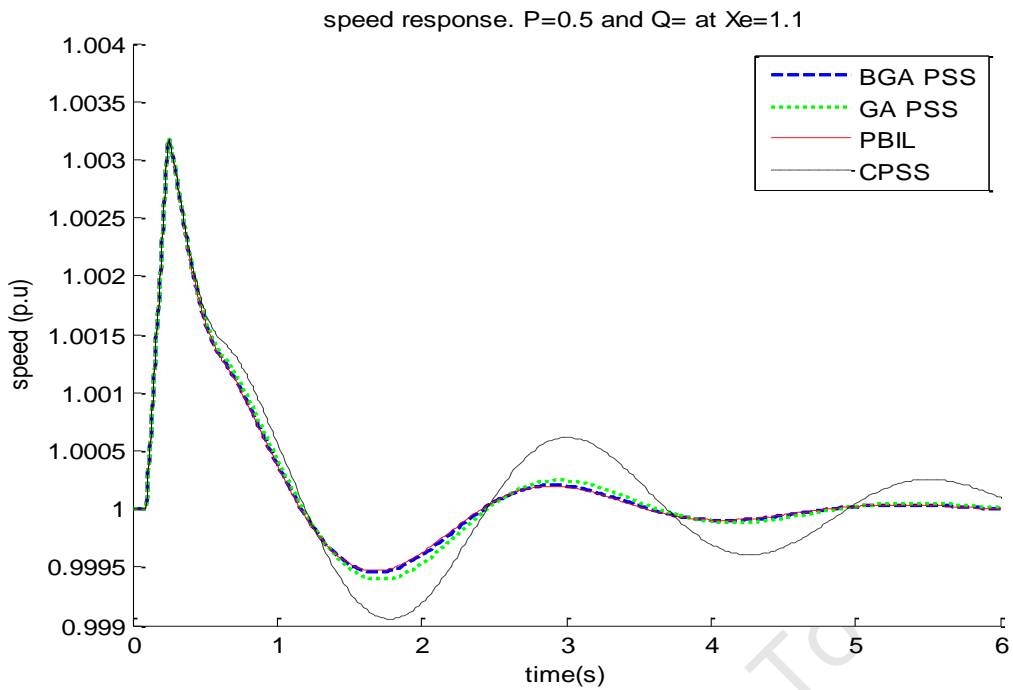


Figure 5.44: Generator speed response under three phase fault at Case 5

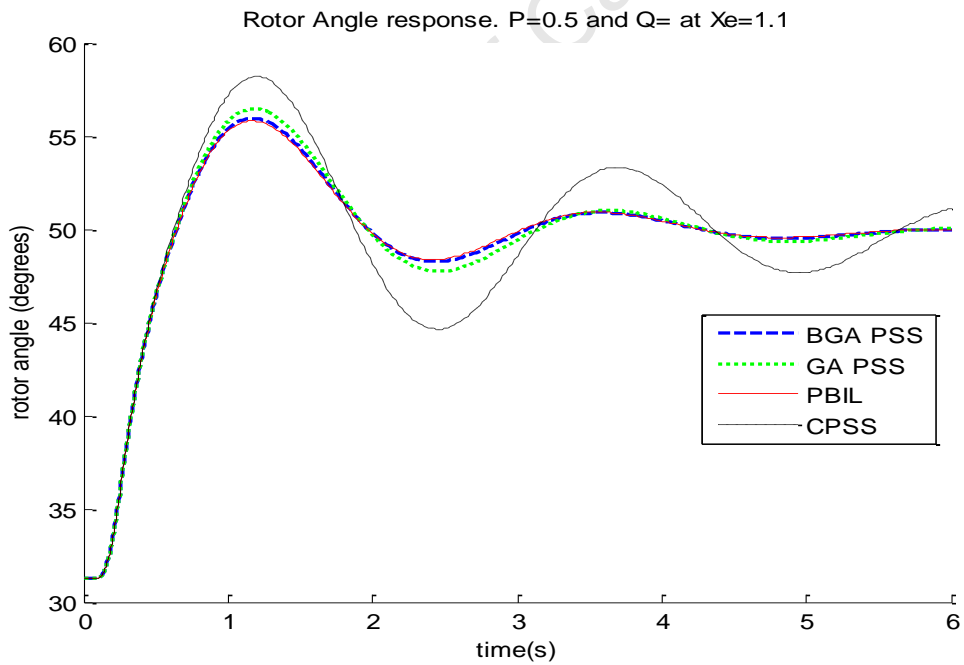


Figure 5.45: Rotor angle response of the generator under three phase fault at Case 5

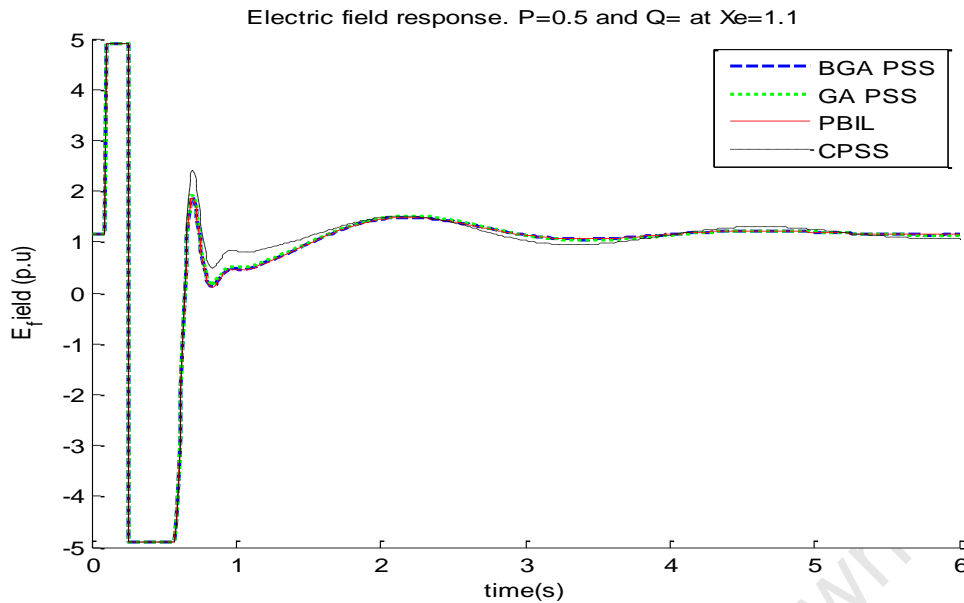


Figure 5.46: Electric field voltage response of the system under three phase fault at Case 5

5.5 Summary

The CPSS and evolutionary algorithm based PSSs were designed for an SMIB system and it was found that the CPSS performs very well at the nominal operating condition, but the performance deteriorates as the system's loading increased. It was found that the evolutionary based PSSs perform very well across all operating conditions. The analysis was done using eigenvalue analysis by comparing the damping ratios for the systems equipped with CPSS and evolutionary based PSSs. It was found that the BGA-PSS and PBIL-PSS perform closely and slightly better than the GA-PSS. The robustness of the PSSs was tested on operating conditions that were not included in the PSS design process. Included in this chapter was also the time domain simulations comprising the response of the system to a 10% step change in Voltage reference of the generator and the three phase fault on bus 1. In all simulations considered, the systems equipped with evolutionary based PSSs perform better than the CPSS, except at the nominal operating condition where the CPSS performs better.

Chapter 6

Simulation Results for the Multi-machine system

6.1 Introduction

The results shown in this section are for the Two Area Multi-machine System. The first section deals with fitness values obtained from the optimization and presents the PSS parameters obtained. The second section deals with the small signal stability analysis. This includes eigenvalue analysis of the system equipped with different PSSs, comparing the damping ratios provided by the PSSs as well as the response of the system to a small disturbance. The third and last section deals with the transient stability of the system. This was evaluated using a three phase fault. In obtaining the results for the Multi-machine system, three design operating conditions were considered, from a light loaded system (Case 1) to a heavy loaded system (Case 3). In designing the EA-PSSs, no constraints were imposed on the maximum damping ratio of the electromechanical modes, unlike in the SMIB case. The PSSs were placed on all four machines, but the PSSs in area 1 were same, similar to the PSSs in area 2 are the same. For comparison purposes, the conventional PSS has also been designed and included. The performances of the PSS under small disturbances and large disturbances are also included in section 6.3 and section 6.4, respectively.

6.2 Fitness Values and PSS parameters

Figure 6.1 to Figure 6.3 show the fitness value (minimum damping ratio) of the system when the GA, BGA and PBIL are used for the optimization. The objective function used is similar to the one used in the SMIB as discussed in Chapter 4, but with no restriction on the possible maximum damping ratio that the electromechanical modes can attain. The final value obtained from the GA optimization is 0.1867. The minimum fitness value from the BGA was 0.205, while the PBIL has a final value of below 0.2095. The GA and BGA were run for 120 generations, while the PBIL was run for 500 generations. The reason for using 500 generations in PBIL is that PBIL starts to settle around 300

generations and therefore there is a need to simulate it for longer period. Clearly the BGA and GA settle just before 100 generations so no need of simulating for longer period.

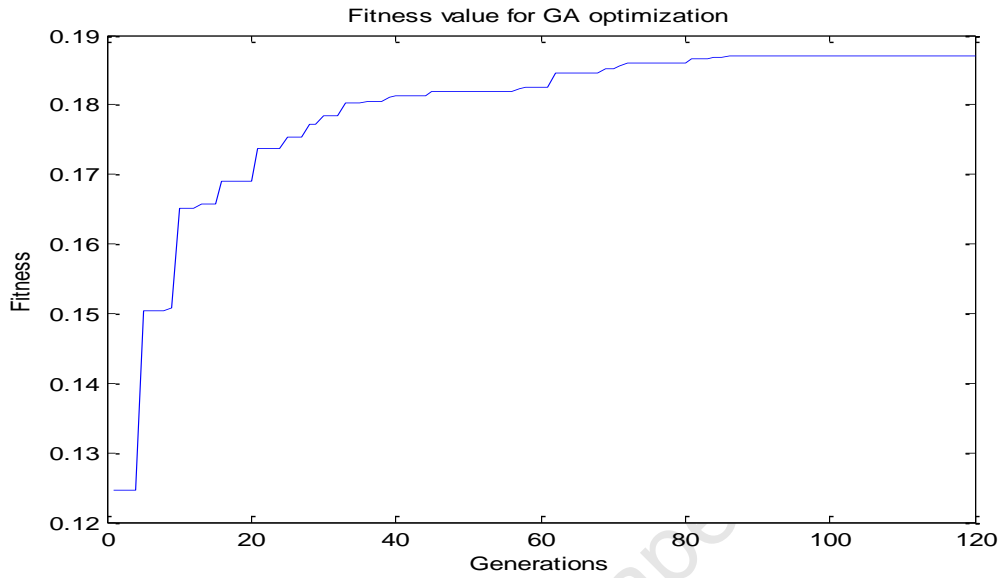


Figure 6.1: Fitness value curve from the GA optimization

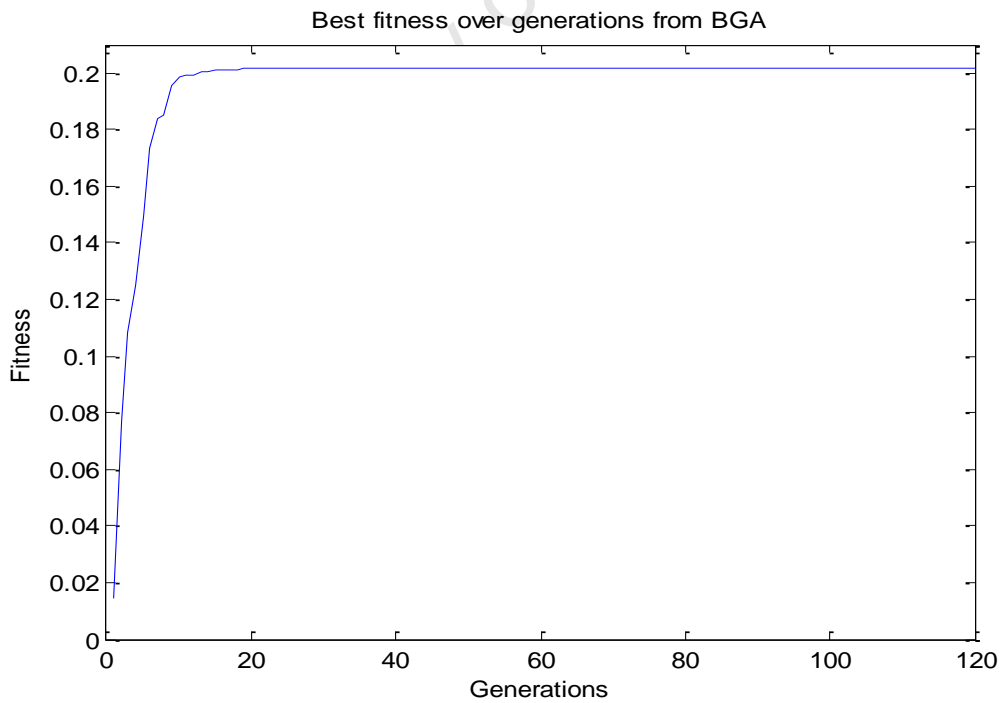


Figure 6.2: Fitness value curve from the BGA optimization

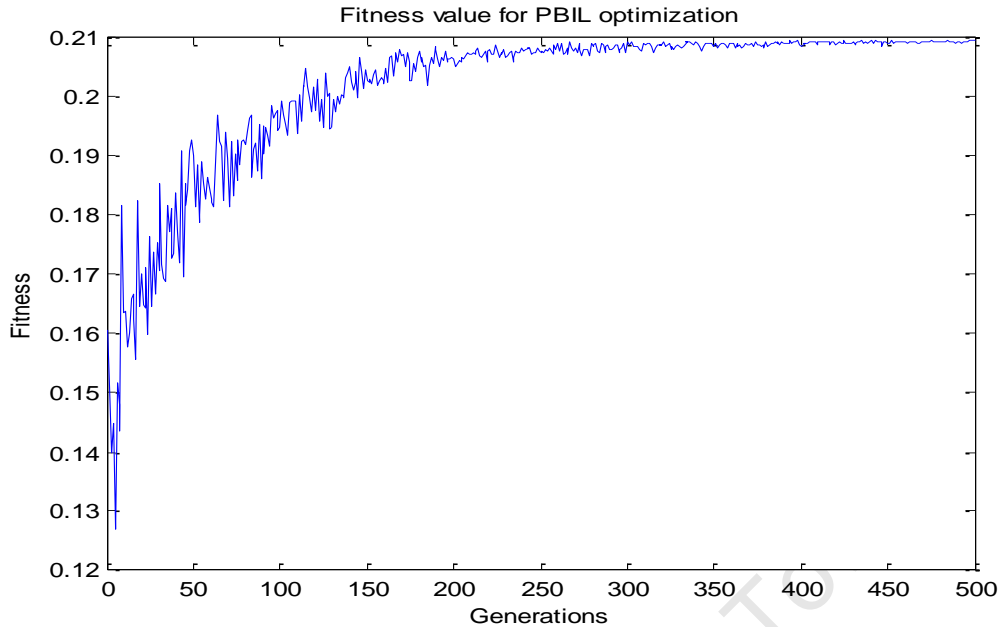


Figure 6.3: Fitness value curve from the PBIL optimization

The PSS parameters obtained from the optimization methods are given in Table 6.1 to Table 6.3, while the CPSS parameters are given in Table 6.4. Only 10 parameters were optimized for the four generators. This means that the PSS parameters for generators 1 and 2 in Area 1 are the same, while the parameters for generators 3 and 4 in Area 2 are also the same. This was applied across all the optimization methods as well as the CPSS. The washout time constant used in the Multi-machine system is 10seconds.

Table 6.1: PSS parameters for the BGA-PSS

Generator	K	T1	T2	T3	T4
1 and 2	17.3996	0.1177	0.0186	0.1295	0.0153
3 and 4	18.4294	0.0615	0.0265	0.0575	0.0223

Table 6.2: PSS parameters for the GA-PSS

Generator	K	T1	T2	T3	T4
1 and 2	18.0863	0.2280	0.0118	0.0492	0.0135
3 and 4	16.6289	0.1287	0.0825	0.0504	0.0101

Table 6.3: PSS parameters for the PBIL-PSS

Generator	K	T1	T2	T3	T4
1 and 2	18.3655	0.1168	0.0188	0.1253	0.0135
3 and 4	19.9860	0.0632	0.0114	0.0218	0.0065

Table 6.4: PSS parameters for the CPSS

Generator	K	T1	T2	T3	T4
1 and 2	9.87712	0.3070	0.0149	0.0504	0.0132
3 and 4	13.685	0.1262	0.0854	0.0620	0.0102

6.3 Small Signal Stability

The results shown in this section are for the small signal stability analysis of the Two-Area Multi-machine system. The first section deals with the eigenvalue analysis of the system equipped with the different PSSs. The second section outlines the performance of the system with CPSS and optimized PSSs using time domain simulations. The time domain simulation is response of the system to a small disturbance applied on the reference voltage of generator 2 (G2).

6.3.1 Eigenvalue Analysis

Table 6.5 shows the inter-area modes for the system with and without the PSSs. It can be seen that without PSSs, the inter-area modes were stable for Case 1, which is the nominal operating condition, but marginally stable with a damping ratio of 0.0062. In contrast, the inter-area modes for Cases 2 and 3 were unstable with damping ratios, -0.0082 and -0.0142, respectively. With the PSS, the inter-area modes are very well damped as compared to the open-loop system. In Table 6.5, it can be seen that the CPSS performs adequately and the inter-area modes are well damped. The damping ratios provided by the CPSS under the three Cases 1, 2 and 3, are 0.1777, 0.1623 and 0.1506 respectively. This means that the damping ratio provided by the CPSS is higher at the nominal operating condition as compared to Case 2 and 3. The BGA-PSS provides a damping ratio of 0.2338, 0.2181 and 0.2056 for Cases 1, 2, and 3, respectively. On the other hand, the PBIL-PSS provides a damping ratio of 0.2380 for Case 1, 0.2218 for Case 2 and 0.2095 for Case 3. Among the evolutionary algorithm based PSSs, the GA-PSS provides

the lowest damping ratios of 0.2152 for Case 1, 0.1985 for Case 2 and 0.1867 for Case 3. Clearly the PBIL-PSS provides the highest damping across all the operating conditions, slightly higher than the BGA-PSS. The frequency of oscillation reduced slightly from the open loop system to the closed loop system across all the operating conditions.

Table 6.5: Inter-area modes for Two-Area Multi-machine system and the respective damping ratios

Case	BGA-PSS	GA-PSS	PBIL-PSS	CPSS	No-PSS
1	$-1.10 \pm 4.55i$ (0.2338)	$-1.02 \pm 4.63i$ (0.2152)	$-1.13 \pm 4.61i$ (0.2380)	$-0.82 \pm 4.52i$ (0.1777)	$-0.03 \pm 4.96i$ (0.0062)
2	$-0.99 \pm 4.44i$ (0.2181)	$-0.92 \pm 4.53i$ (0.1985)	$-1.02 \pm 4.49i$ (0.2218)	$-0.73 \pm 4.41i$ (0.1623)	$0.04 \pm 4.82i$ (-0.0082)
3	$-0.92 \pm 4.37i$ (0.2056)	$-0.85 \pm 4.46i$ (0.1867)	$-0.95 \pm 4.42i$ (0.2095)	$-0.66 \pm 4.34i$ (0.1506)	$0.07 \pm 4.73i$ (-0.0143)

Table 6.6 shows the local modes for Area 1 and the corresponding damping ratios in brackets. It can be observed from the open-loop system that the local modes were stable but poorly damped for all the three operating conditions. The damping ratios are 0.0872, 0.0705 and 0.0629 for Cases 1, 2 and 3 respectively. After the introduction of the CPSS, the damping ratio increased to 0.3687 for Case 1, 0.3474 for Case 2 and 0.3291 for Case 3. This is a remarkable improvement from the open loop system. As for the optimized PSSs, the BGA-PSS provides a damping ratio of 0.4035 for Case 1, 0.3843 for Case 2, while for Case 3, the damping is 0.3660. The GA-PSS provides a damping ratio of 0.3797 for Case 1, 0.3638 for Case 2, while Case 3 gets a damping of 0.3491. The PBIL-PSS provides a damping ratio of 0.4297 for Case 1, 0.3685 for Case 2, while for Case 3 the damping ratio is 0.3517. For this local area mode, the BGA-PSS provides the highest damping of 0.4297, better than both the GA-PSS and PBIL-PSS at 0.3797 and 0.3863 respectively. The frequency of oscillation reduced slightly for the closed loop system; this is due to an increase in damping ratios for these modes.

Table 6.6: Local Area mode 1

Case	BGA-PSS	GA-PSS	PBIL-PSS	CPSS	No-PSS
1	-2.42 + 5.48i (0.4035)	-2.23± 5.43i (0.3797)	-2.35± 5.62i (0.3863)	-2.08± 5.25i (0.3687)	-0.63± 7.25i (0.0872)
2	-2.31 ± 5.55i (0.3843)	-2.15± 5.50i (0.3638)	-2.25± 5.69i (0.3685)	-1.98± 5.34i (0.3474)	-0.51± 7.24i (0.0705)
3	-2.21 ± 5.61i (0.3660)	-2.08± 5.57i (0.3491)	-2.16± 5.74i (0.3517)	-1.89± 5.42i (0.3291)	-0.46± 7.24i (0.0629)

Table 6.7 provides the local mode for Area 2 well as the damping ratio under the open loop system and the closed loop system. Again, the open loop modes are stable, with a damping ratio of 0.0922 for nominal operating condition (Case 1), 0.0706 for Case 2 and 0.0727 Case 3. However, the system damping improved significantly with the introduction of the PSSs. The CPSS provides a damping ratio of 0.6831 for Case 1, 0.6209 for Case 2 and 0.5724 for Case 3. For this mode, the BGA-PSS provides a damping ratio of 0.7502 for Case 1, 0.6977 for Case 2 and 0.6531 for Case 3. The PBIL-PSS provides the highest damping for this mode with a damping ratio of 0.7766 for Case 1, 0.7265 for Case 2 and 0.6821 for Case 3. The GA-PSS provides a slightly lower damping ratio for this mode under all the Case studies, with Case 1 having a damping ratio of 0.7453; Case 2 has a damping ratio of 0.6939 while Case 3 has a damping ratio of 0.6515. The frequency of oscillation for this mode reduced slightly from the open loop system. This is expected as the damping ratio for the local area has increased under the close loop system. In most cases the frequency of oscillation of electromechanical modes reduced as the damping ratio increases.

Table 6.7: Local Area mode 2

Case	BGA-PSS	GA-PSS	PBIL-PSS	CPSS	No-PSS
1	-6.13 ± 5.41i (0.7502)	-5.54± 4.95i (0.7453)	-6.49± 5.26i (0.7766)	-5.25± 5.62i (0.6831)	-0.68± 7.36i (0.0922)
2	-5.64 ± 5.79i (0.6977)	-5.14± 5.34i (0.6939)	-6.00± 5.68i (0.7265)	-4.77± 6.02i (0.6209)	-0.52± 7.36i (0.0706)
3	-5.24 ± 6.08i (0.6531)	-4.84± 5.63i (0.6518)	-5.60± 6.00i (0.6821)	-4.39± 6.29i (0.5724)	-0.53± 7.24i (0.0727)

Figure 6.4 shows the spread of the eigenvalues for the system equipped with the different PSSs. It can be observed from Figure 6.4, that the eigenvalues with the damping provided by the CPSS is lower than that provided by the other PSS. However, GA-PSS provides less damping as compared to BGA-PSS and PBIL-PSS. The damping provided by these two PSSs is almost similar.

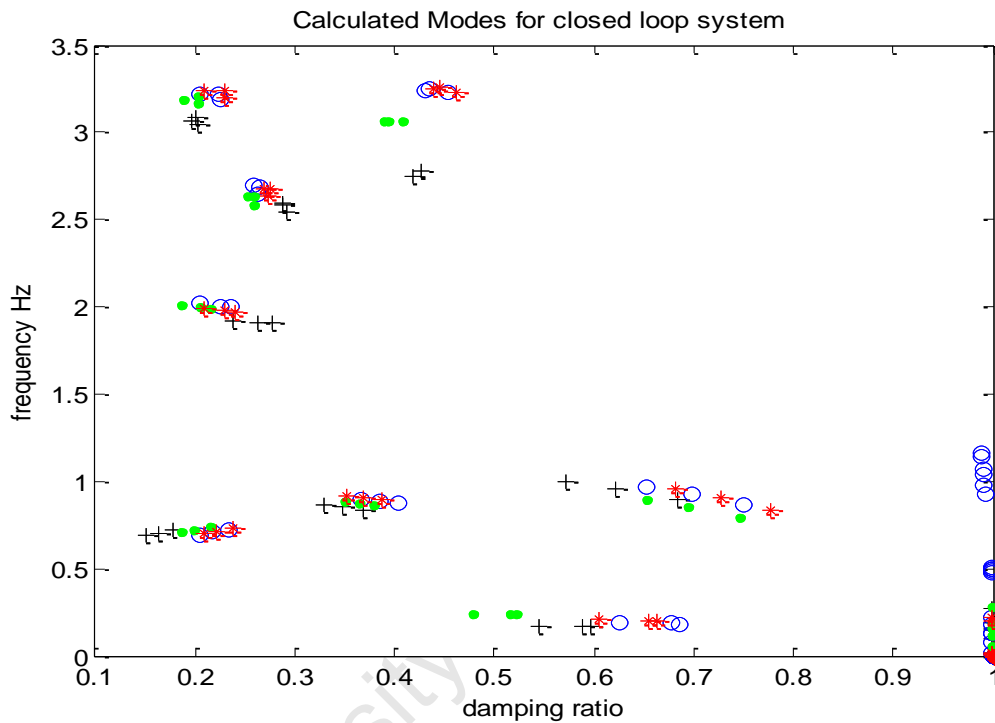


Figure 6.4: Spread of the eigenvalues across all three operating conditions

+ CPSS; . GA-PSS; o BGA-PSS; * PBIL-PSS

Tables 6.8 to 6.10 present the closed loop electromechanical modes for Cases 4 and 5. As explained in Chapter 4, Cases 4 and 5 tests for the robustness of the PSSs and thus were not included in the design. Table 6-8 which shows the inter-area modes, shows that the closed loop inter-area modes are all stable. The BGA-PSS give a damping ratio of 0.26064 for Case 4 and 0.2029 for Case 5. The PBIL-PSS gives a damping ratio of 0.2075 for Case 4 and 0.2019 for Case 5. The GA-PSS gives the lowest damping ratio among the evolutionary based PSSs with 0.1781 for Case 4 and 0.1687 for Case 5. The damping ratio of the CPSS is 0.1504 and 0.1490 for Cases 4 and 5 respectively.

Table 6.8: Inter-area modes for the closed loop system

Case	BGA-PSS	GA-PSS	PBIL-PSS	CPSS
4	-0.74±3.53i (0.2064)	-0.67±3.68i (0.1781)	-0.76±3.58i (0.2075)	-0.53±3.50i (0.1504)
5	-0.67±3.25i (0.2029)	-0.58±3.41i (0.1687)	-0.68±3.31i (0.2019)	-0.48±0.0321i (0.1490)

Table 6.9 shows a similar trend as observed in Table 6.8, where all the closed local area 1 modes are stable. The BGA-PSS gives a damping ratio of 0.3650 and 0.3364 for Cases 4 and 5, respectively. PBIL-PSS provides damping ratios of 0.3505 for Case 4 and 0.3241 for Case 5. The GA-PSS gives a damping ratio of 0.3473 for Case 4 and 0.3239 for Case 5, whereas the CPSS gives a damping ratio of 0.3273 for Case 4 and 0.2981 for Case 5.

Table 6.9: Local area mode 1

Case	BGA-PSS	GA-PSS	PBIL-PSS	CPSS
4	-2.19±5.58i (0.3650)	-2.06±5.55i (0.3473)	-2.14±0.0572i (0.3503)	-1.87±5.40i (0.3273)
5	-2.03±5.69i (0.3364)	-1.94±5.66i (0.3239)	-1.99± 5.81i (0.3241)	-1.73±5.53i (0.2981)

Table 6.10 shows the closed loop local area 2 modes, with their respective damping ratios in brackets. Similar trends observed in Tables 6.8 and 6.9 can be seen in Table 6.10, whereby the evolutionary algorithm based PSSs perform better than the CPSS across all the operating conditions. BGA-PSS and PBIL-PSS give slightly more damping than the GA-PSS.

Table 6.10: Local area mode 2

Case	BGA-PSS	GA-PSS	PBIL-PSS	CPSS
4	-5.25±6.02i (0.6570)	-4.85±5.58i (0.6555)	-5.60±5.94i (0.6859)	-4.39±6.22i (0.5769)
5	-4.98±6.42i (0.6128)	-4.65±5.98i (0.6139)	-5.33±6.37i (0.6417)	-4.14±6.63i (0.5303)

Clearly observing from all the three electromechanical modes, (Tables 6.5 to 6.10), the system equipped with Evolutionary Algorithm PSSs provides a higher damping across all the operating conditions than the CPSS, since they were designed using all three operating conditions. Also it can be observed that the BGA-PSS and PBIL-PSS provide the highest damping for all the oscillatory modes as compared to the GA-PSS.

6.3.2 Time domain Simulations

For the following simulation results, a 10% step response is applied on the reference voltage of generator 2 in Area 1. The responses of active power for all the generators are discussed in this section. Generator 1 and 2 are equipped with a similar PSS, while generators 3 and 4 are also the same.

Figure 6.5 to Figure 6.7 show the active power deviation response of the system to the step change in reference voltage of generator 2 for Cases 1, 3 and 3, respectively. The system looks very well damped across all three operating conditions. For Case 1, the system equipped with CPSS settles around 6 seconds. Also the amplitudes for the oscillations are slightly higher with the 1st swing of up to 0.14pu. The BGA-PSS, GA-PSS and PBIL-PSS all have a close settling time of approximately 3.5 seconds. Also it can be observed from Figure 6.6 that for Case 2, the system's response with the CPSS has a longer settling time of around 6.5 seconds, as compared 3 seconds for the other PSSs. Figure 6.7 shows the system responses for Case 3. This Figure shows the same trend as Case 1 and Case 2, whereby the system equipped with CPSS has slightly longer settling time as compared to the BGA-PSS, GA-PSS and PBIL-PSS.

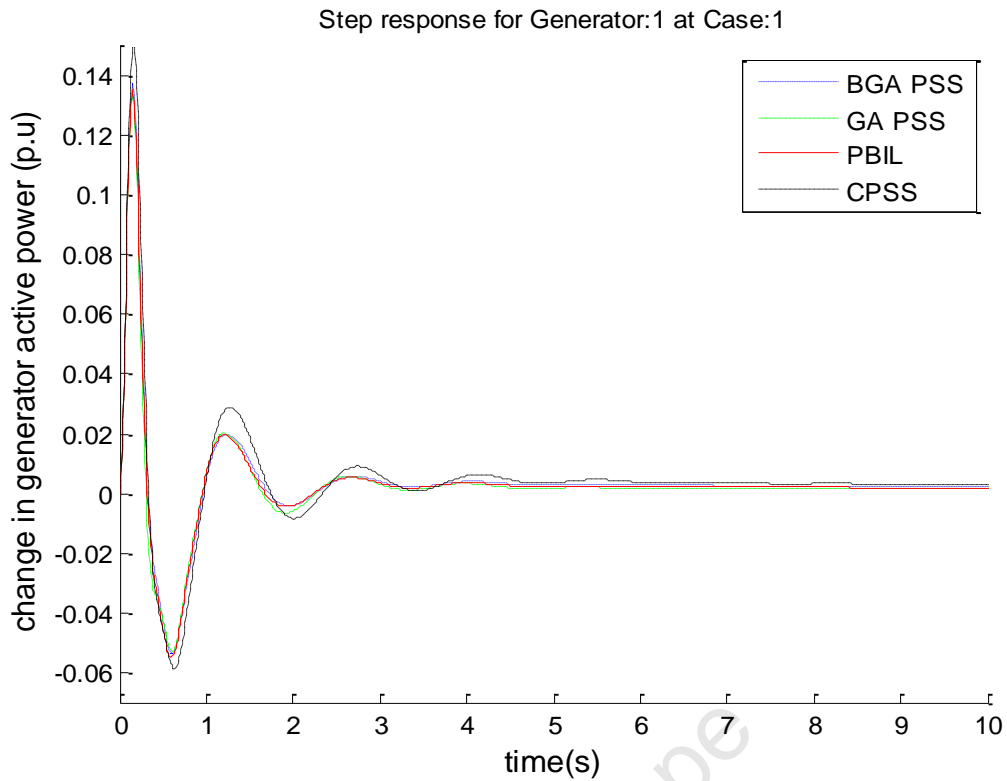


Figure 6.5: Case 1: Step response of G1 under the 10% step change in V_{ref} of G2

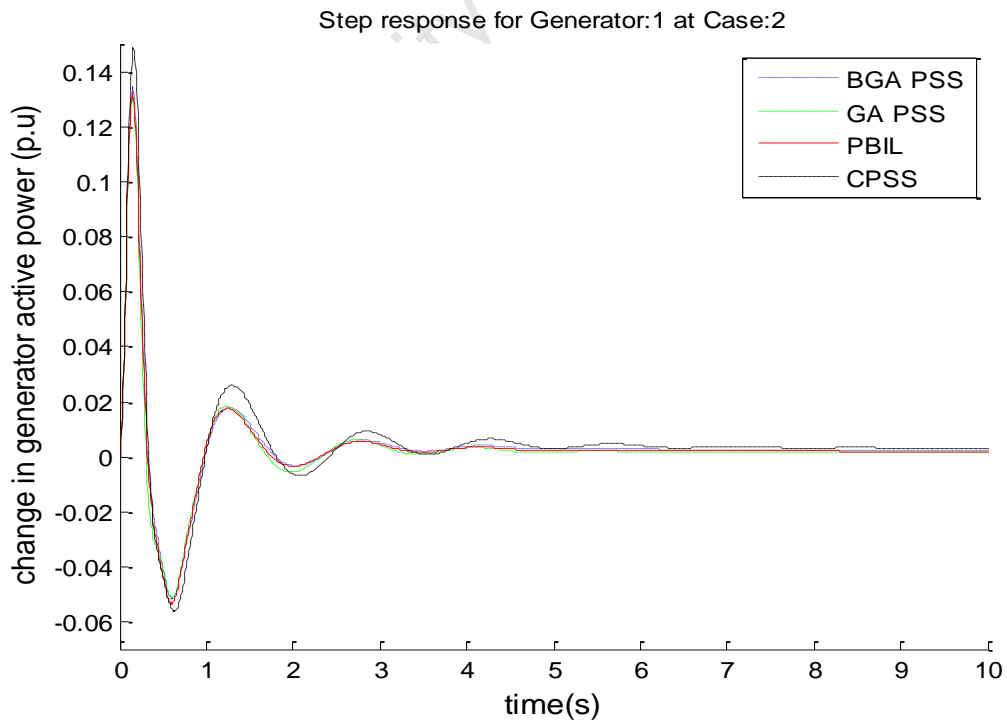


Figure 6.6: Case 2: Step response of G2 to the 10% step change in V_{ref} of G2

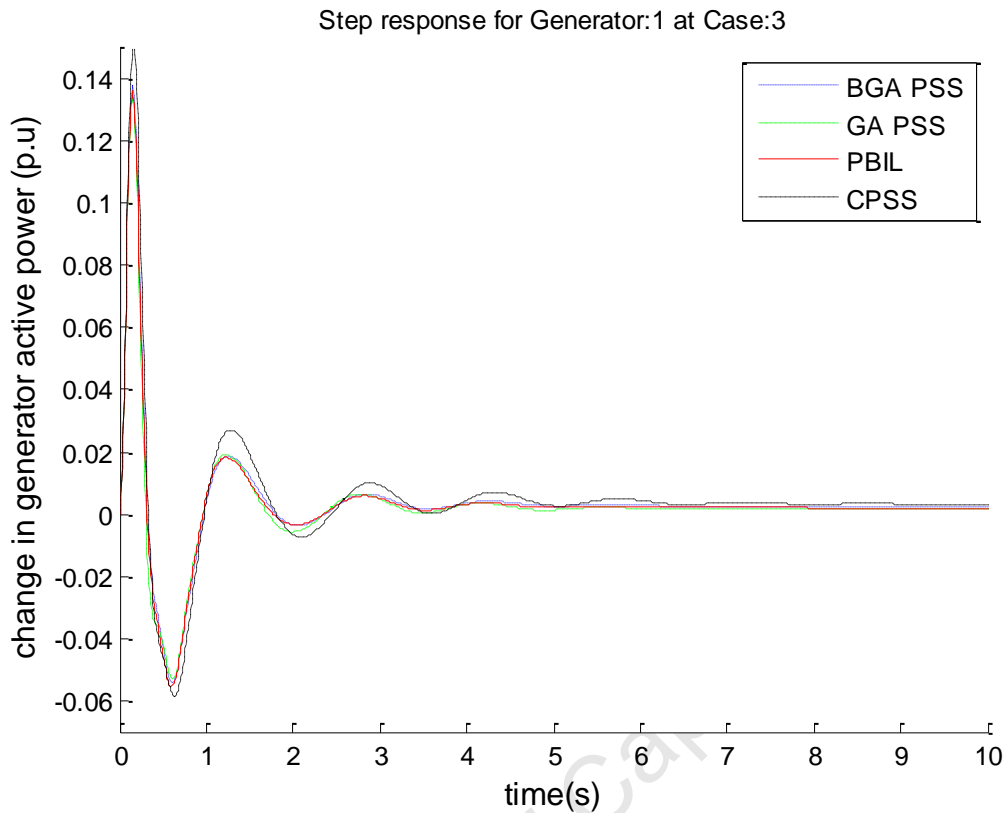


Figure 6.7: Case 3: Step response of G2 to the 10% step change in V_{ref} of G2

The step responses of generator 2 to the 10% step change in reference voltage of generator 2 are shown in Figure 6.8 to Figure 6.10. Clearly the response of generator 2 is similar to generator 1. This is due to the fact that these two generators are in the same area and they are equipped with the same PSS. The PSS on generator 1 is the same as the PSS on generator 2. As in the previous cases, the settling time for the CPSS is close to 6 seconds, while the settling times for the system equipped with EA based PSSs are 3.5 seconds. The BGA-PSS performs slightly better due to the slightly higher damping of the local modes in Area 1 as shown in Table 6.5.

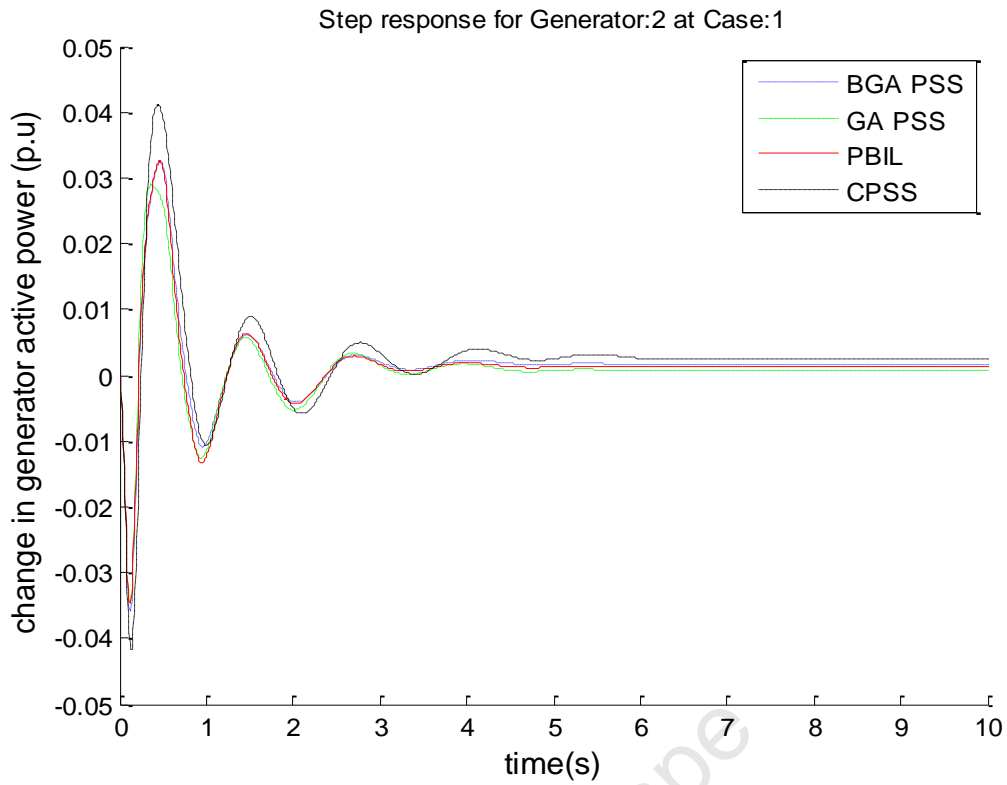


Figure 6.8: Case 1: Step response of G2 under the 10% step change in V_{ref} of G2

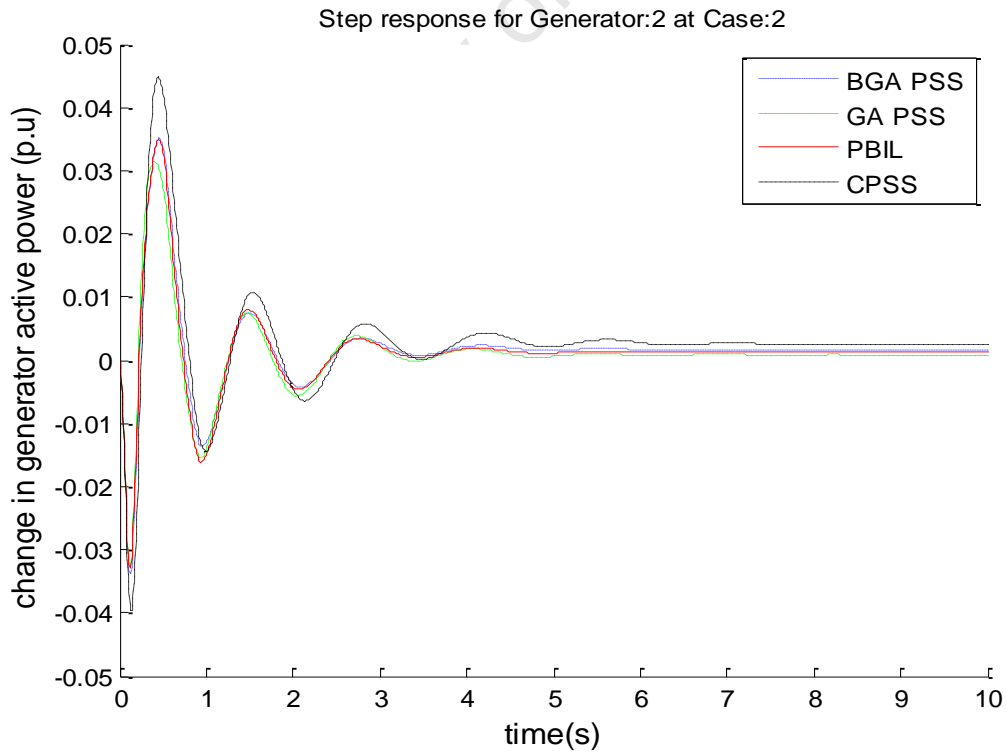


Figure 6.9: Case 2: Step response of G2 under the 10% step change in V_{ref} of G2

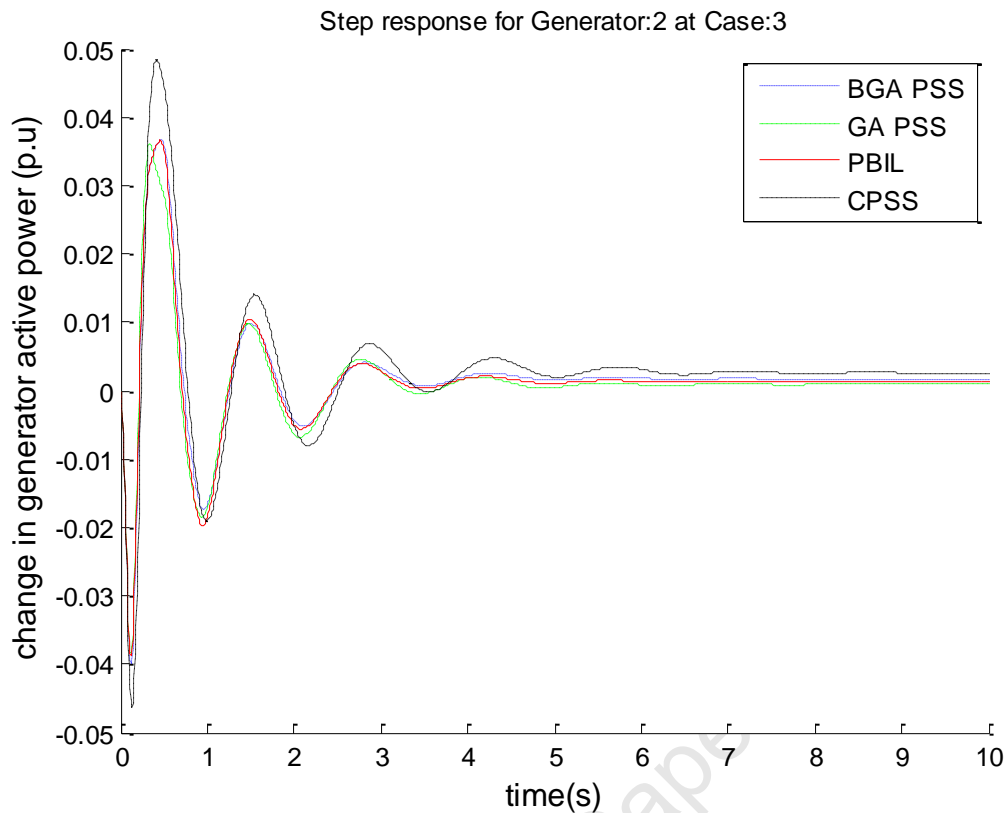


Figure 6.10: Case 3: Step response of G2 under the 10% step change in V_{ref} of G2

The responses of generator 3 to the step change in voltage reference of generator 2 are shown in Figure 6.11 to Figure 6.13. For the Case shown in Figure 6.11, the CPSS has a settling time of about 7 seconds. The first swing of the CPSS is just above 0.03pu and the system settles at a slightly higher value than the pre- disturbance value. The BGA-PSS, GA-PSS and the PBIL-PSS have a similar settling time. The first swing of the system equipped with EA based PSSs is slightly above 0.025pu. The trend is the same for Case 2 and Case 3. The settling time of the system equipped with CPSS is around 6 seconds, while for the BGA-PSS, GA-PSS and PBIL-PSS is slightly 4 seconds. From the time responses of Figure 6.11 to 6.13, it can be clearly seen that the optimized PSSs performs very well for generator 3 across all the operating conditions.

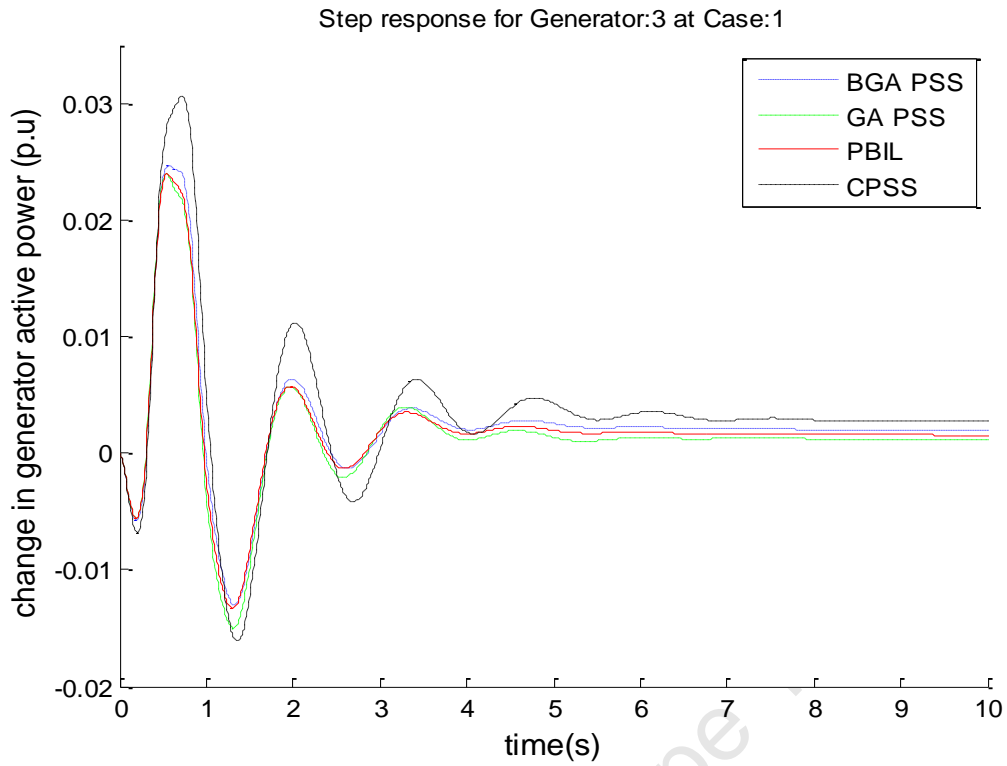


Figure 6.11: Case 1: Step response of G3 under the 10% step change in V_{ref} of G2

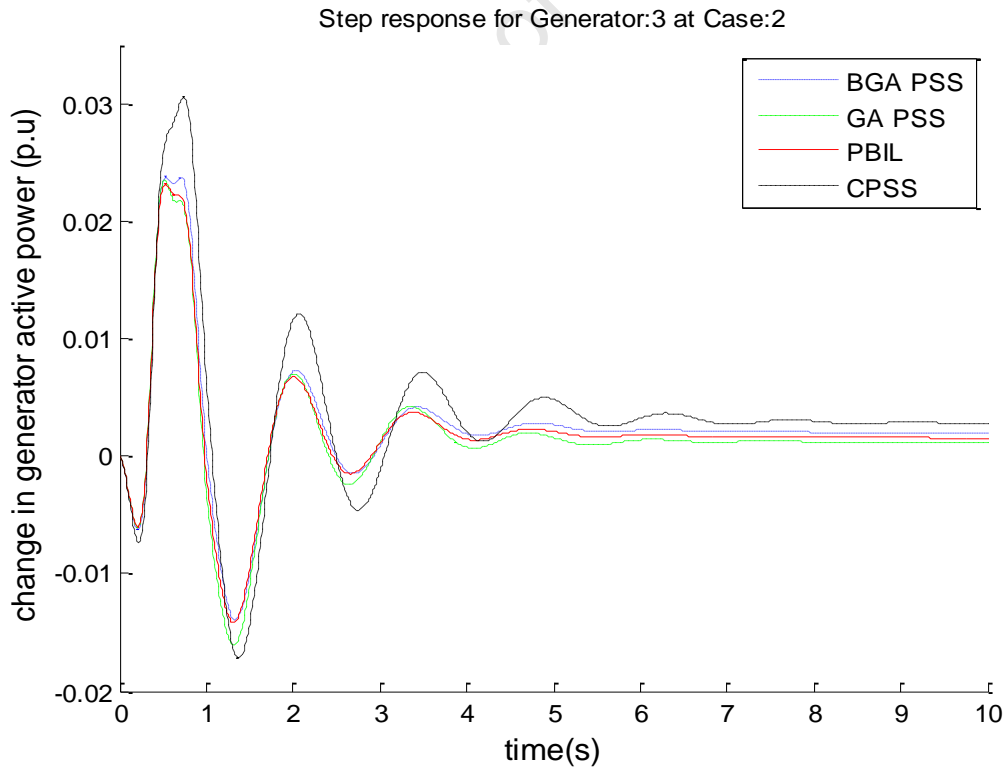


Figure 6.12: Case 2: Step response of G3 under the 10% step change in V_{ref} of G2

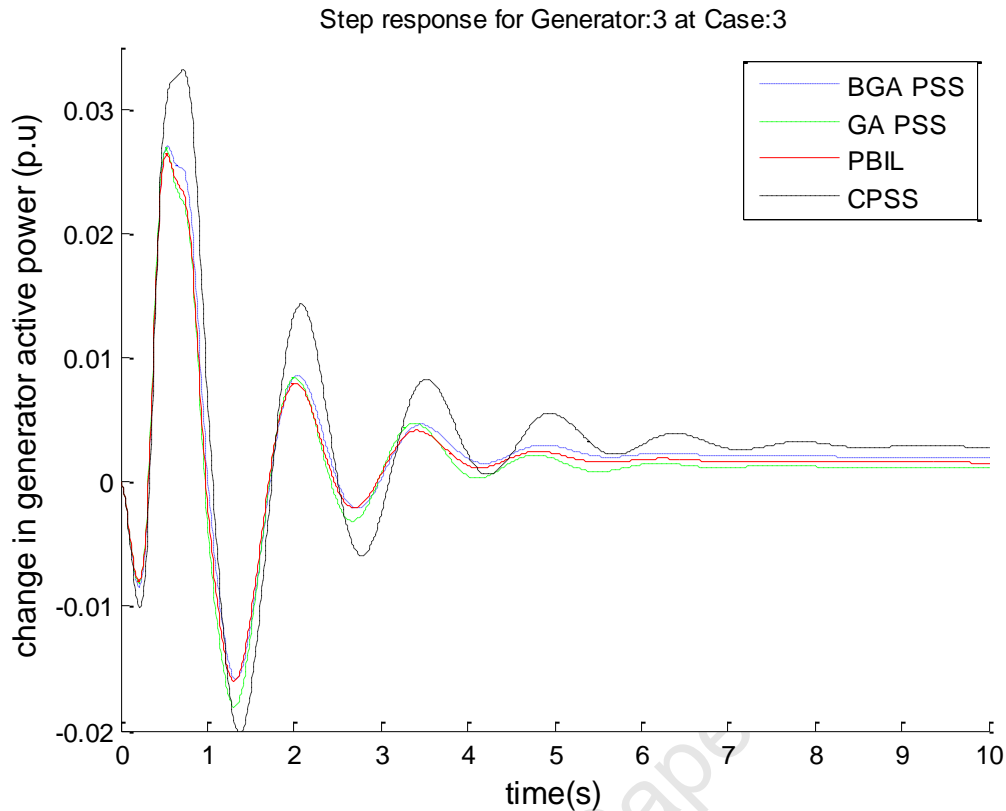


Figure 6.13: Case 3: Step response of G3 under the 10% step change in V_{ref} of G2

The step responses of generator 4 to the step change in reference voltage of generator 2 are shown in Figure 6.14 to Figure 6.16. The responses of generator 4 are similar to the responses of generator 3, as they are in the same area and they are equipped with a similar PSS. The CPSS has a settling close to 7 seconds for Case 1, around 7.5 seconds for Case 2 and 8 seconds for Case 3. The BGA-PSS and PBIL-PSS settle around 4 seconds for Case 1 and Case 2, while the settling time for Case 3 is slightly longer, around 5 seconds. The GA-PSS settles around 5 seconds for Case 1, 5.5 seconds for Case 2 and around 6.5 seconds for Case 3. This shows that the BGA-PSS and PBIL-PSS perform better than the GA-PSS. Two extra cases were included to observe and test the robustness of the PSSs. These two operating conditions were not included in the design of the EA-PSSs.

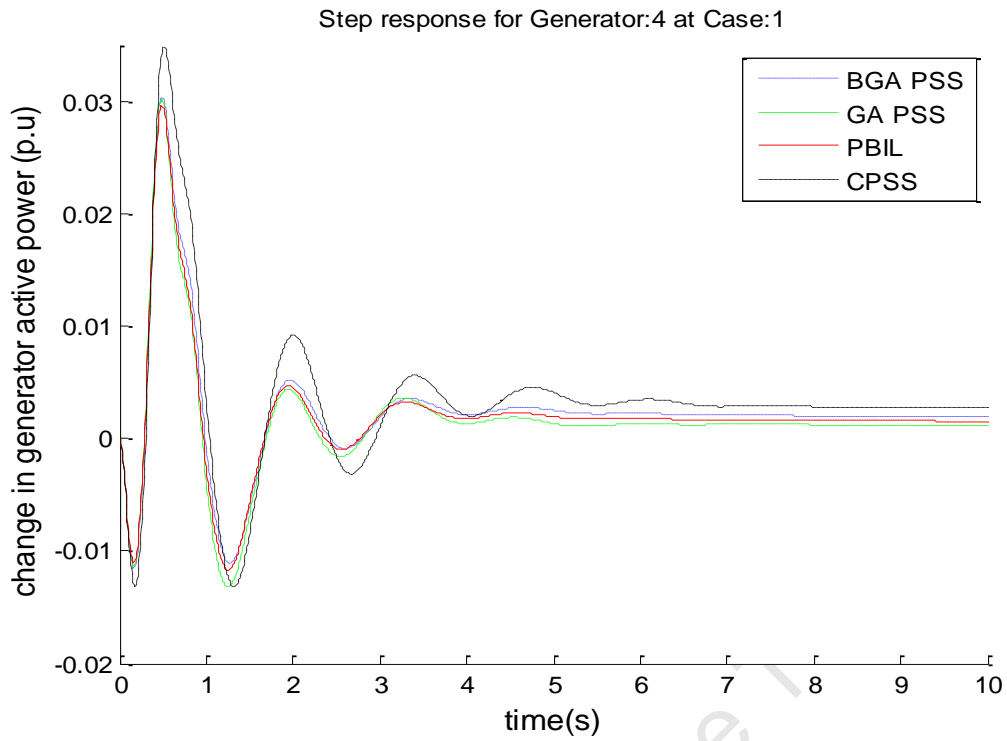


Figure 6.14: Case 1: Step response of G4 under the 10% step change in Vref of G2

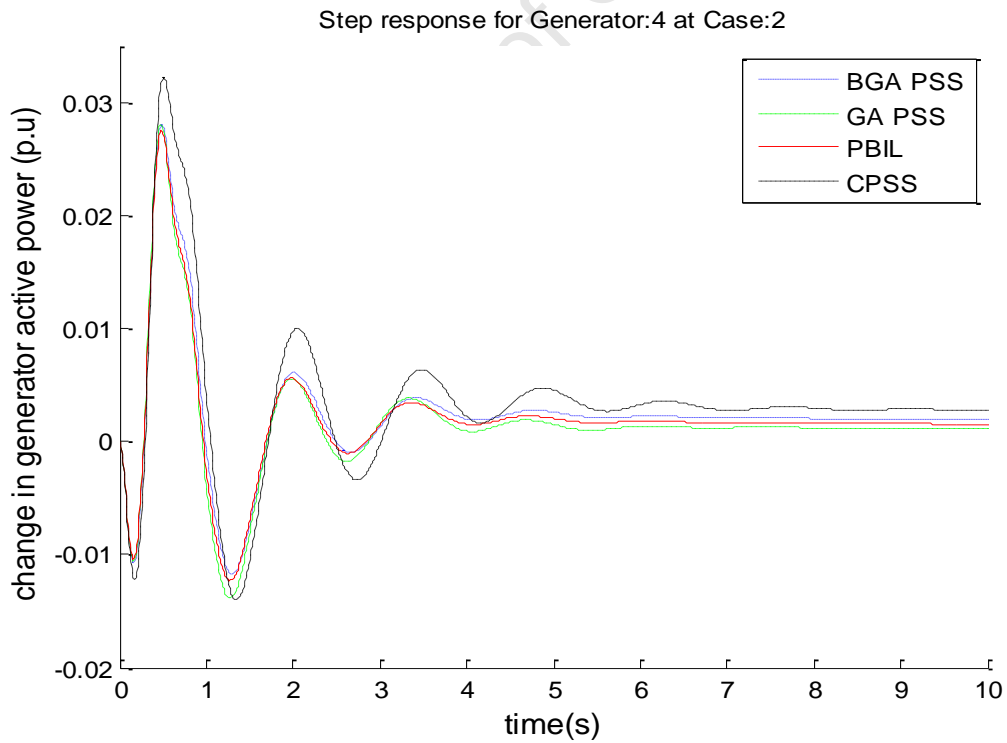


Figure 6.15: Case 2: Step response of G4 under the 10% step change in Vref of G2

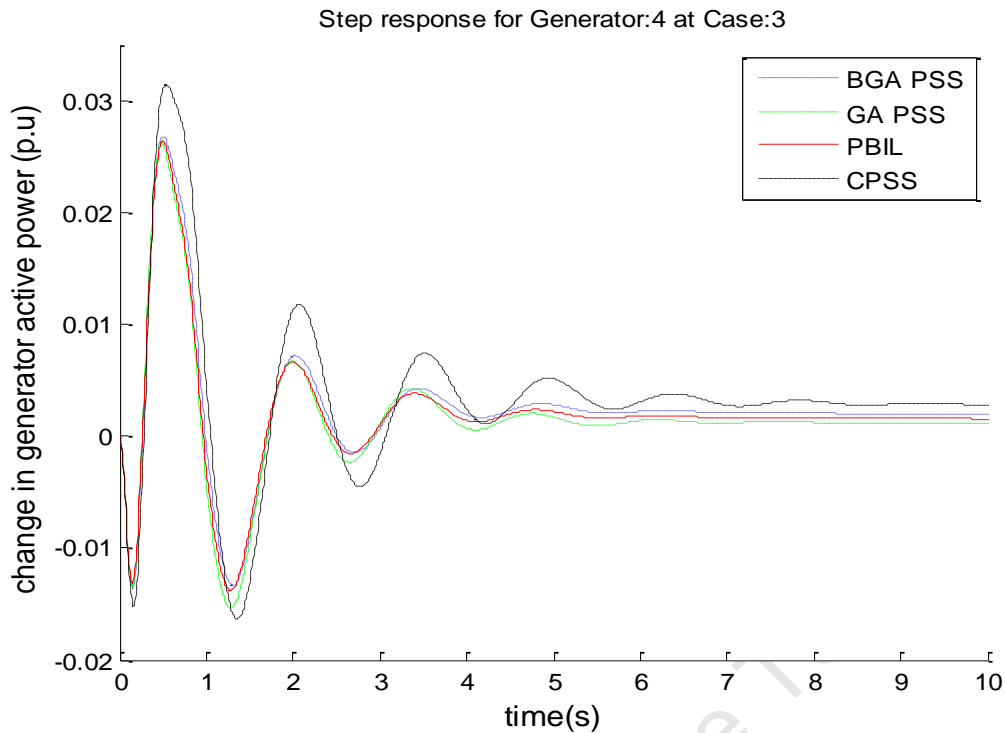


Figure 6.16: Case 3: Step response of G4 under the 10% step change in V_{ref} of G2

6.3.3 PSS Robustness

This section presents the active power deviation of the system in Cases 4 and 5. The two cases are being used to test the designed PSS for robustness and they were not included in the evolutionary algorithm based PSSs design.

Case 4

Figure 6.17 to Figure 6.20 show the responses of the four generators (G1 to G4) after the 10% step response on V_{ref} for generator 2. The responses show that the system is stable with all the PSSs designs. The responses of generator 1 and 2 (Figure 6.17 and Figure 6.18) are similar, the CPSS settles around 6 seconds, while the evolutionary algorithm PSSs settle in 5 seconds, but the GA-PSS has slightly higher oscillations as compared to BGA-PSS and PBIL-PSS. Figure 6.19 and Figure 6.20 show the responses for generator 3 and 4. The CPSS has bigger undershoots and overshoots as well as a longer settling time of 9 seconds as compared to the evolutionary algorithm based PSS with a settling time of 5 seconds, except the GA-PSS that has a settling time of about 7 seconds. Among the evolutionary algorithm based PSSs, the GA-PSS has higher undershoots and overshoots as compared to BGA-PSS and PBIL-PSS.

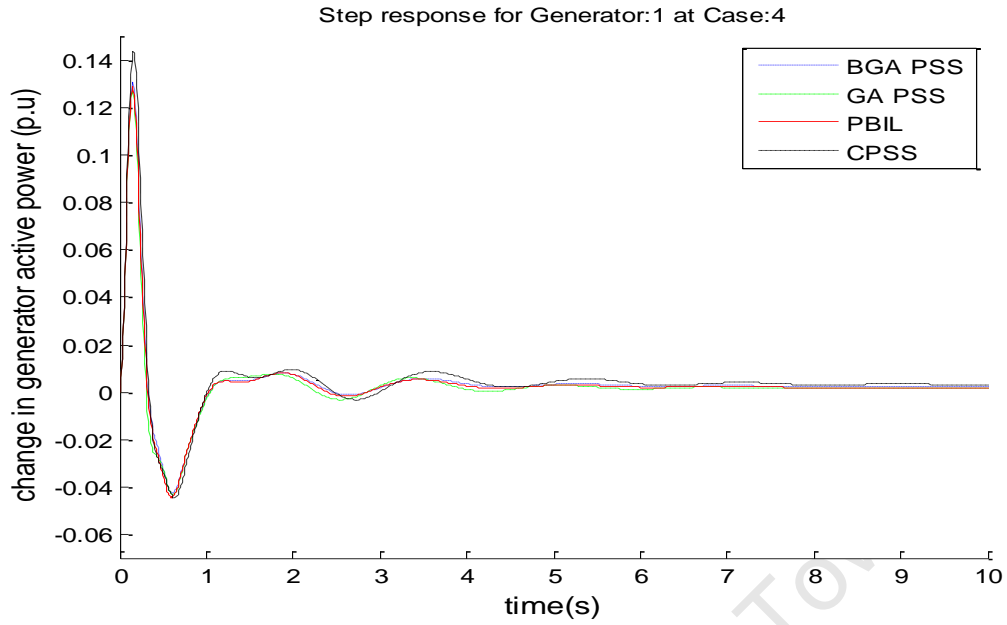


Figure 6.17: Case 4: Step response of G1 under the 10% step change in V_{ref} of G2

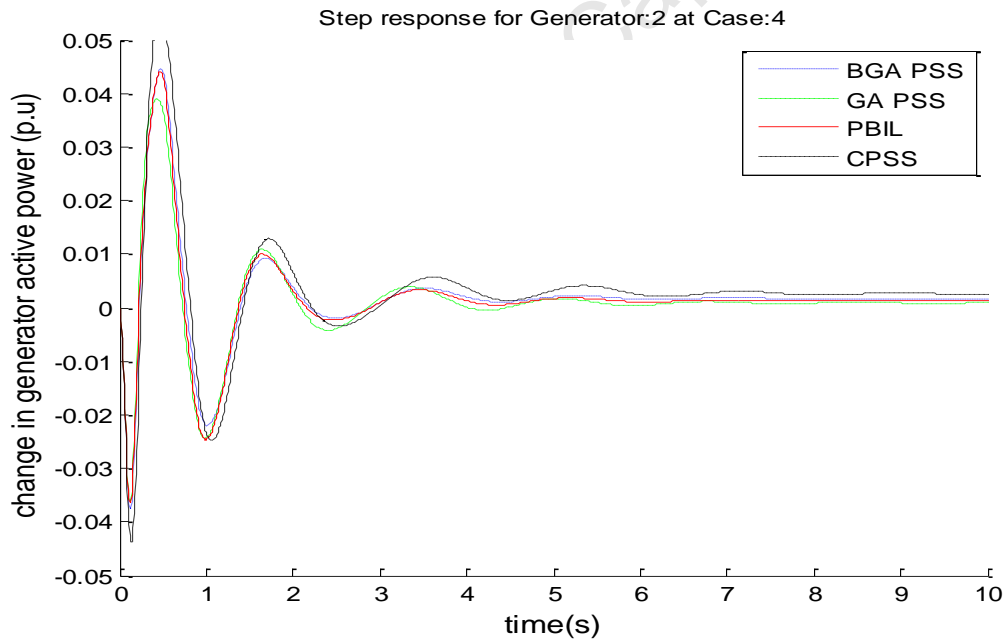


Figure 6.18: Case 4: Step response of G2 under the 10% step change in V_{ref} of G2

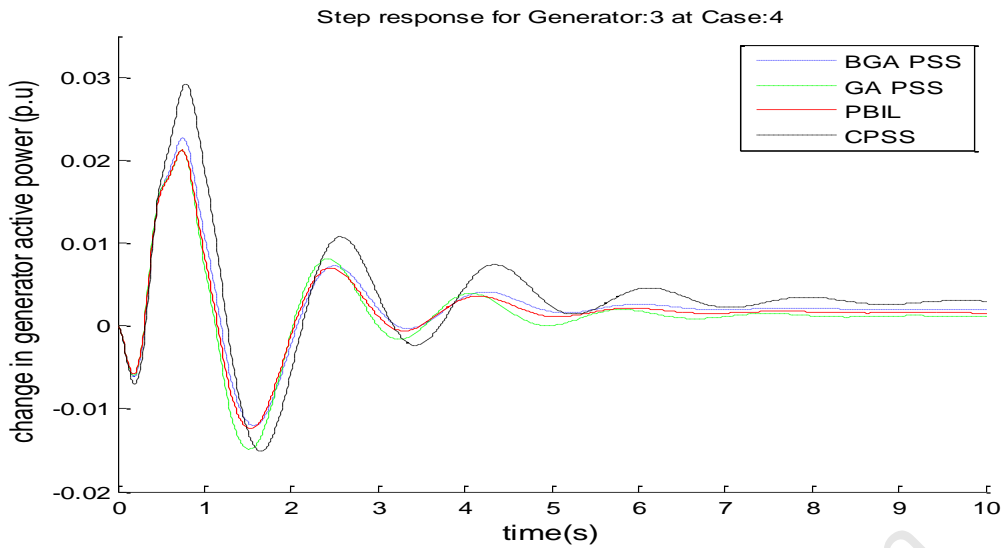


Figure 6.19: Case 4: Step response of G3 under the 10% step change in V_{ref} of G2

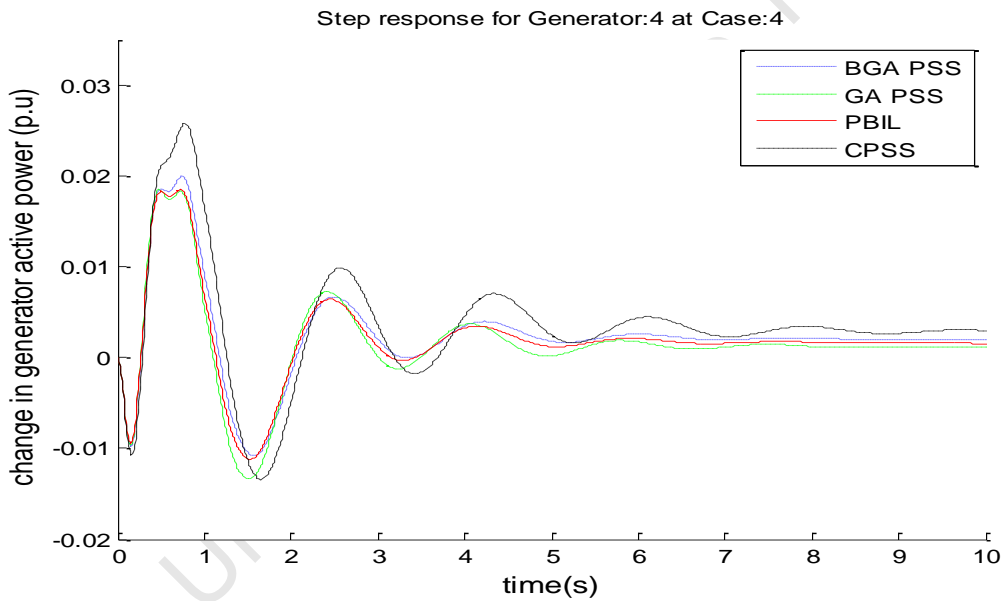


Figure 6.20: Case 4: Step response of G4 under the 10% step change in V_{ref} of G2

Case 5

Figure 6.21 to Figure 6.24 show the responses of generator 1 to generator 4 under Case 5. The responses of Figures 6.21 to 6.24 shows a similar trend to the ones observed in Case 4, where the CPSS takes longer time to settle as compared to the evolutionary algorithm based PSSs. Also, among the evolutionary algorithm based PSSs, the GA-PSS takes longer time to settle and has bigger undershoots and overshoots as compared to the BGA-PSS and PBIL-PSS.

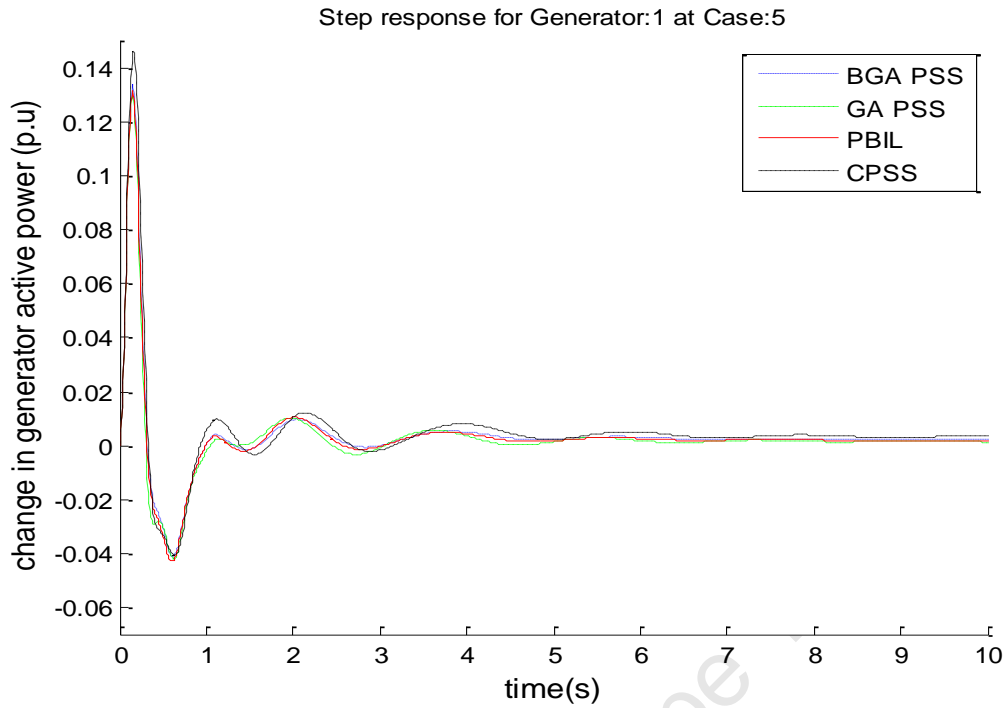


Figure 6.21: Case 5: Step response of G1 under the 10% step change in Vref of G2

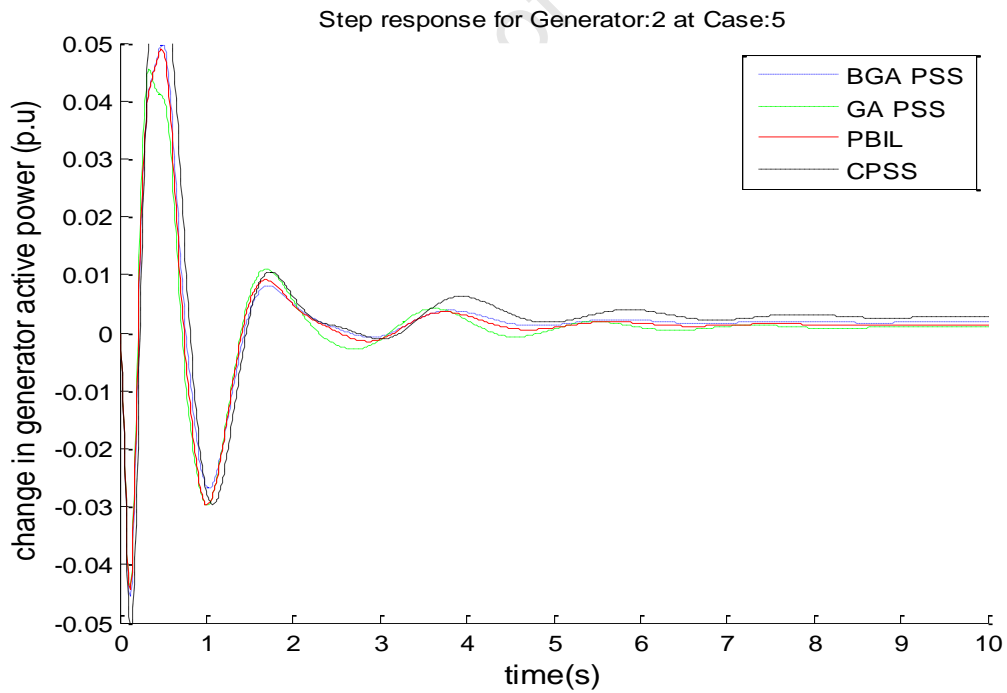


Figure 6.22: Case 5: Step response of G2 under the 10% step change in Vref of G2

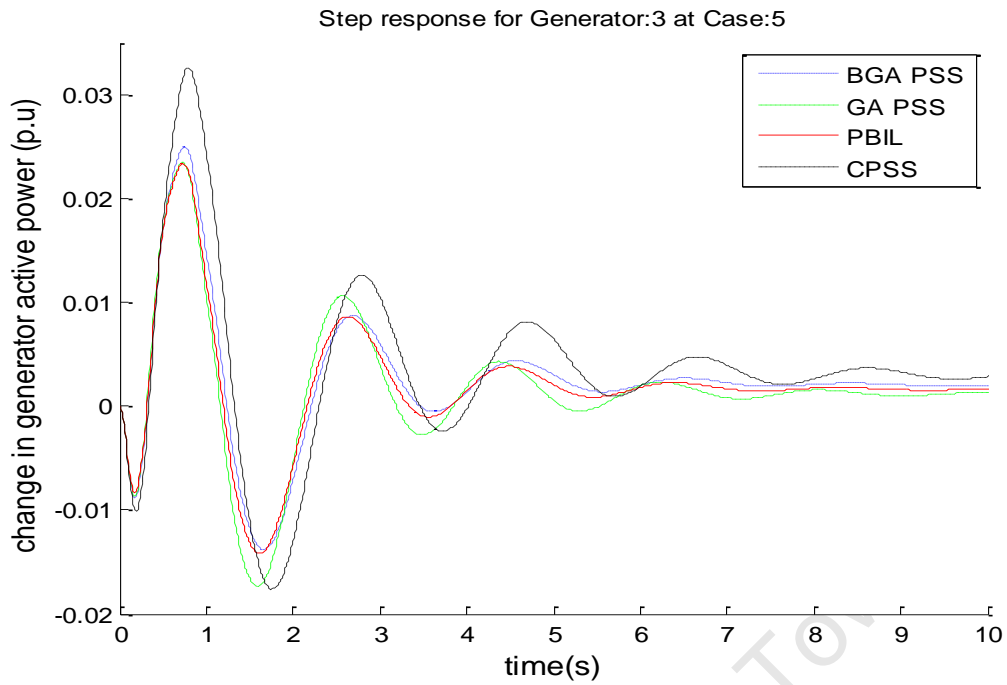


Figure 6.23: Case 5: Step response of G3 under the 10% step change in Vref of G2

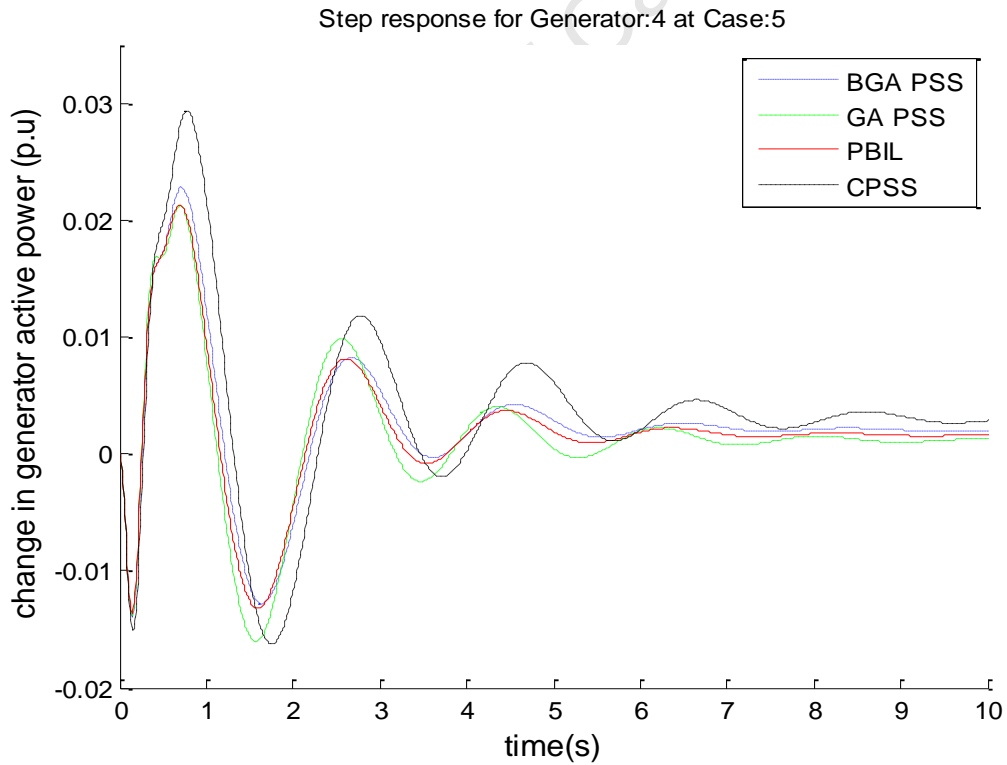


Figure 6.24: Case 5: Step response of G4 under the 10% step change in Vref of G2

Overall, the BGA-PSS, GA-PSS and PBIL-PSS perform better than the CPSS as was expected, further outlining the importance of PSS parameter optimization across all operating condition. Also the BGA-PSS and the PBIL-PSS perform slightly better than the GA-PSS across all scenarios, especially for Case 5, while the PBIL-PSS performs slightly better than the BGA-PSS. The same observation done on the three electromechanical modes considered in the eigenvalue analysis. Furthermore, the system is stable in the closed loop as compared to the open loop where the damping ratio for the inter-area for Case 1 and Case 2 was negative except for the Case 3. The CPSS was designed using conventional methods, but as observed in the time domain, it shows that designing using conventional methods is not an easy task especially in Multi-machine systems, where more than one CPSS needs to be designed.

6.4 Transient Stability

Large disturbance was applied to the system in a form of a fault at bus 3 and this was cleared by removing the transmission line between bus 3 and bus 13. This was done to evaluate the robustness of the designed PSSs. After the fault was cleared, the system settles to a different operating condition with only one tie line transmitting power from Area 1 to area 2 for Case 1 to Case 3, respectively. The fault was applied for 0.2 seconds at 0.5 seconds and cleared at 0.7 seconds. The responses are for generator 2 in area 1, since it is close to the fault and likely to be adversely affected by the fault as compared to the generators in Area 2.

6.4.1 Case 1: Nominal operating condition

Figure 6.25 to Figure 6.28 show the bus 3 voltage, active power output, speed, as well as the Electric field voltage of generator 2, respectively for Case 1. Under this Case the Voltage at bus 3 and the Electric field voltage with the different PSSs settle more or less at the same values. This is expected as the CPSS was designed around this operating condition, even though it does not have a better settling time than the other three PSS. This is to illustrate that designing a Conventional PSS for a Multi-machine system is a bit complex as compared to designing a CPSS for a Single Machine to Infinite Bus system (SMIB), where it was shown that the CPSS performed better than the optimized PSS. The system is still stable under all the Power System Stabilizers. Another observation can be

made from Figure 6.27 for the speed response where the PBIL-PSS and the BGA-PSS perform slightly better than the GA-PSS.

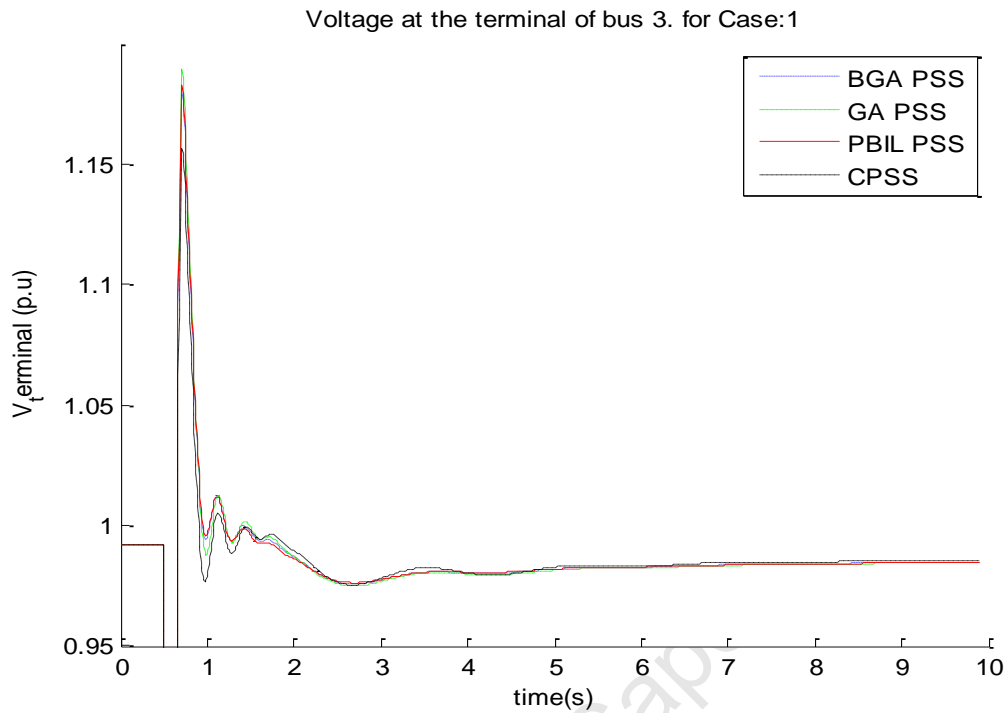


Figure 6.25: Voltage on Bus 3 following a three phase fault on bus 3 for Case 1

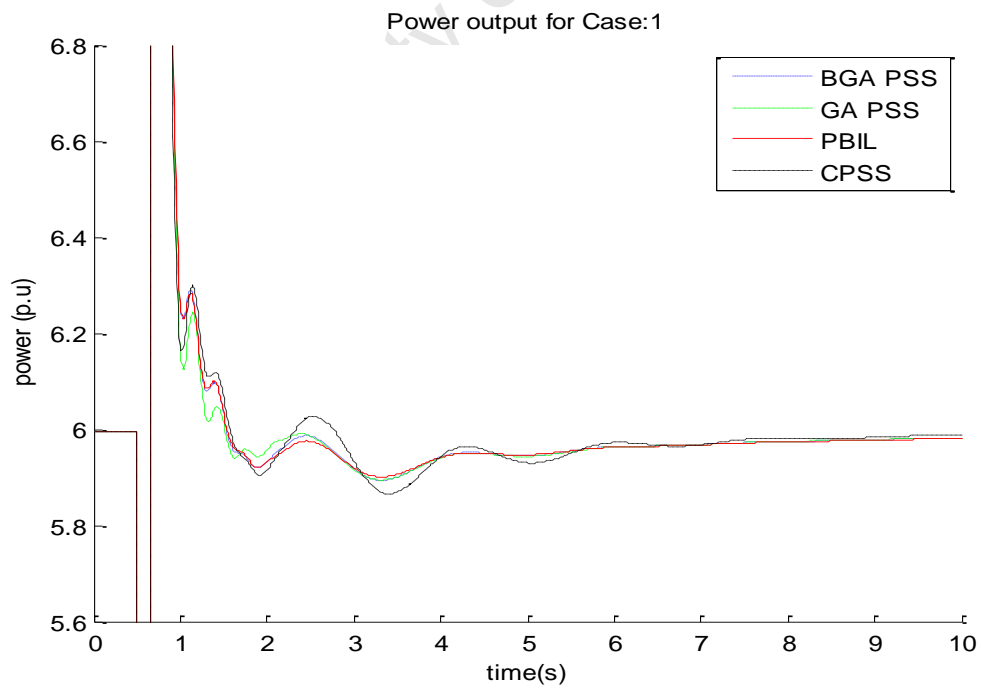


Figure 6.26: Active power response of generator 2 to a three phase fault on bus 1 for Case 1

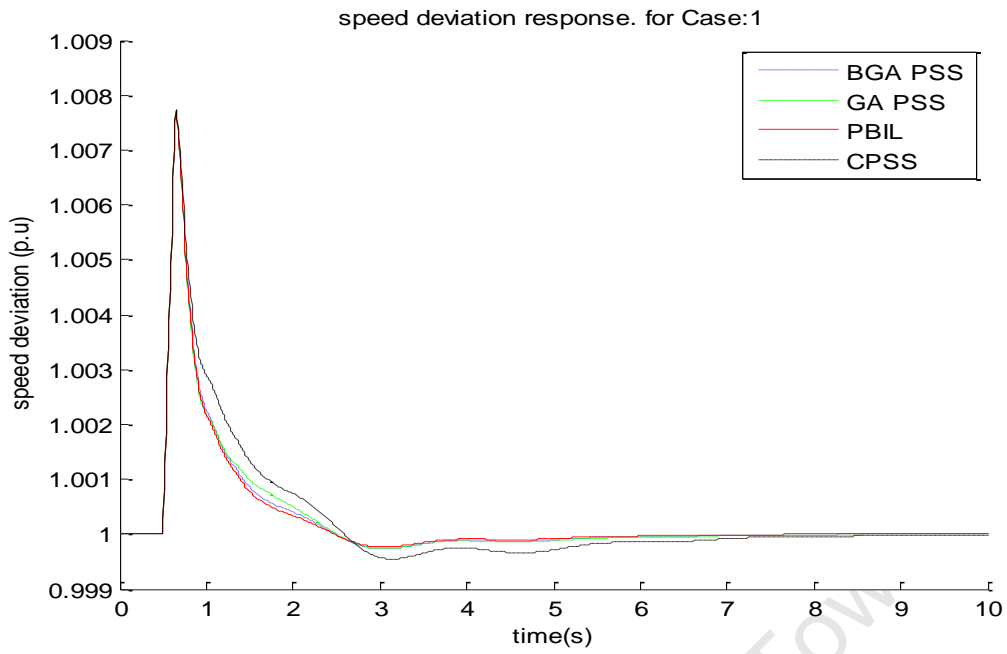


Figure 6.27: Speed response for generator 2 after the 3 phase fault on bus 3 for Case 1

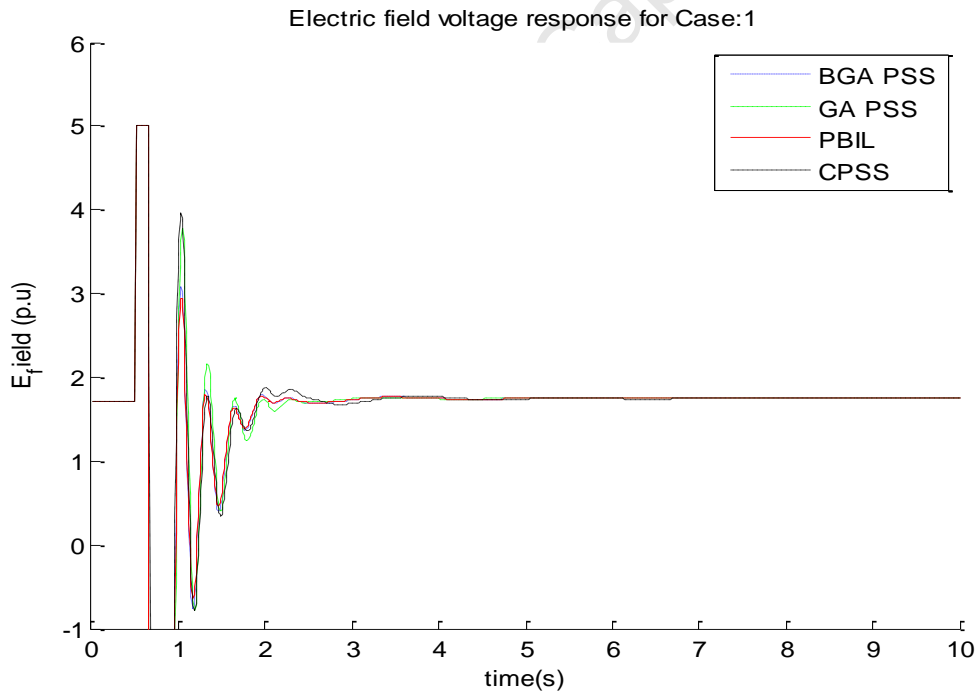


Figure 6.28: Electric field voltage of generator 2 following a 3 phase fault on Bus 3 for Case 1

6.4.2 Case 2: Middle loading operating condition

Figure 6.29 to Figure 6.32 show the active power, speed and electric field voltage of generator 2 respectively, after the 3 phase fault on bus 3. For the active power shown in Figure 6.30, the system equipped with CPSS takes around 7 seconds to settle down; while for the BGA-PSS, GA-PSS and PBIL-PSS, the settling time is less than 3 seconds. The speed and electric field voltage have the same trend as compared to the active power response, where the EA-PSSs perform better than the CPSS. The PSSs stabilize the system very well, but the high gains introduce some oscillations straight after the fault, especially in the voltage of Figure 6.29 and the Electric field voltage in Figure 6.32. These oscillations are not desirable and needs to be considered when designing PSS.

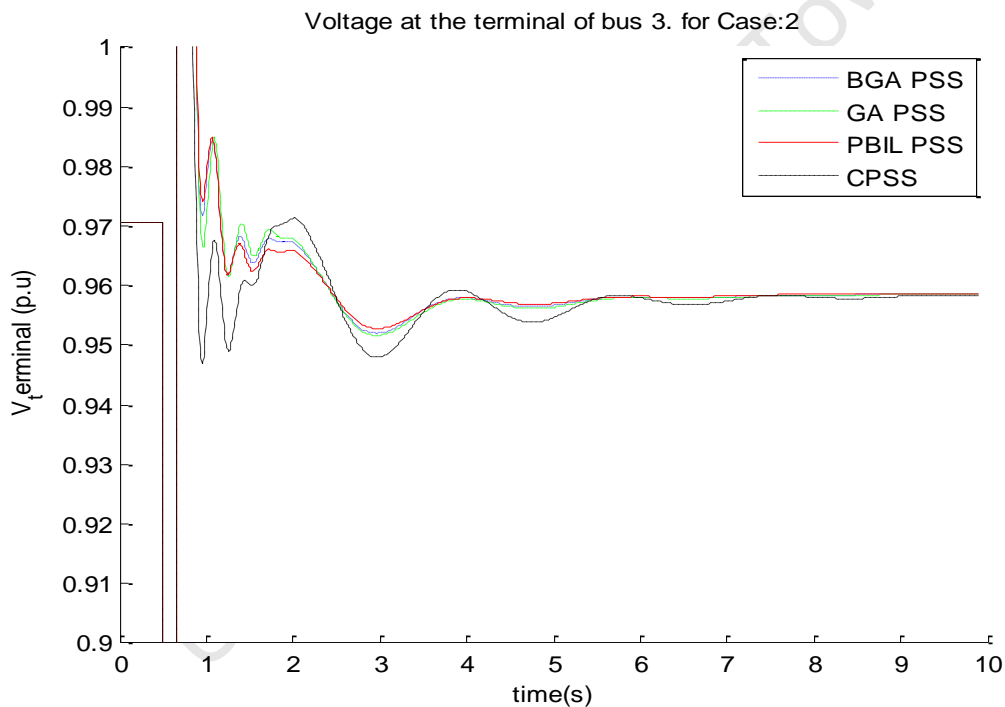


Figure 6.29: Voltage on Bus 3 following a three phase fault on Bus 3 for Case 2

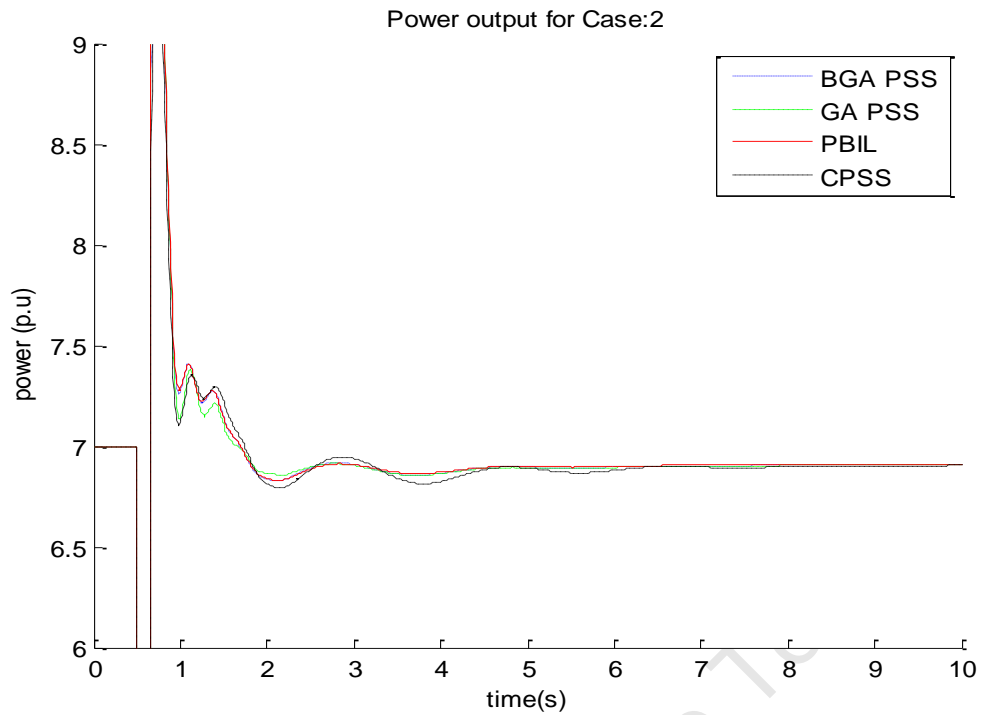


Figure 6.30: Active power response of generator 2 to a three phase fault at bus 3 for Case 2

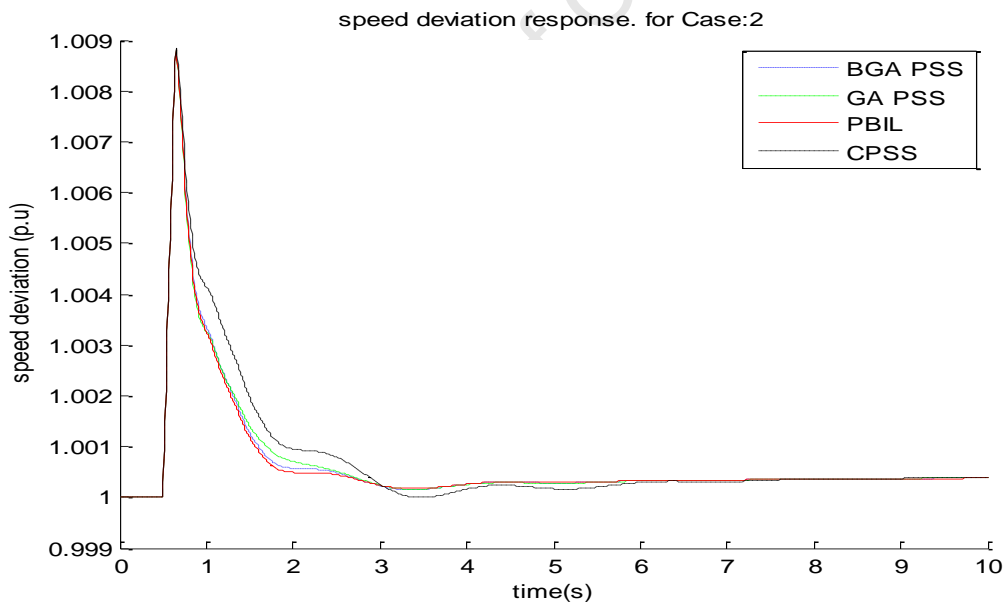


Figure 6.31: Speed response of generator 2 to a three phase fault at bus 3 for Case 2

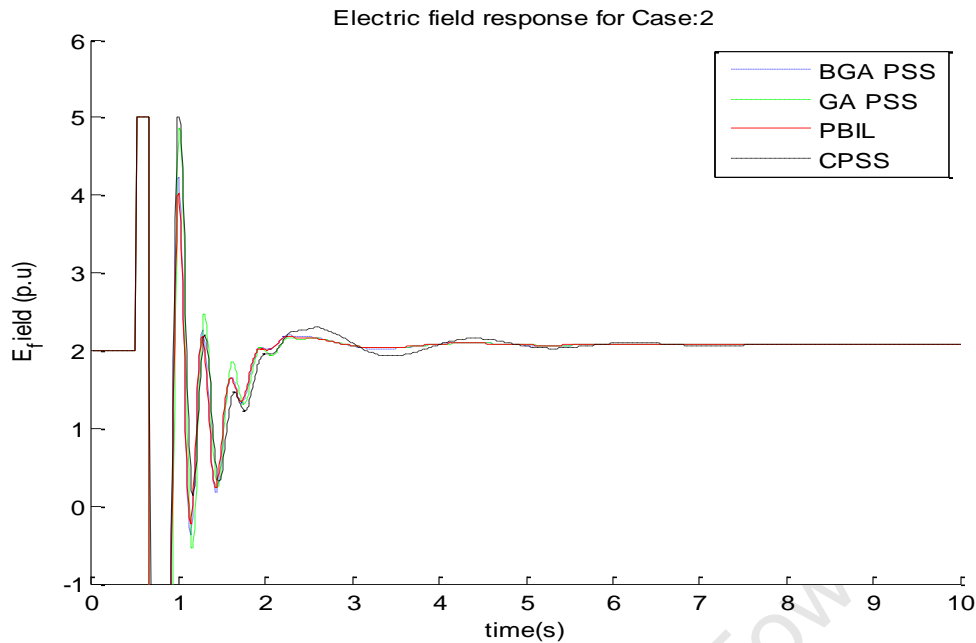


Figure 6.32: Electric field voltage response of generator 2 to a 3 phase fault on Bus 3 for Case 2

6.4.3 Case 3: Heavy loading operating condition

Figure 6.33 to Figure 6.36, show the active power, speed and electric field for generator 2, respectively under Case 1, it can be seen that the PSS settles at slightly different values, but the system remains stable after the fault was cleared. Clearly from Figure 6.33 which shows the voltage on Bus 3, where the fault was applied; the system with CPSS has many oscillations, which persist even after 8 seconds. For the system equipped with BGA-PSS, GA-PSS and PBIL-PSS, the voltage on Bus 3 settles at around 3 seconds, but the system with PBIL-PSS performs slightly better than the BGA-PSS and GA-PSS. For the active power output shown in Figure 6.34, the system with the CPSS take around 6.5 seconds to settle down, while the BGA-PSS, GA-PSS and PBIL-PSS takes around 3.5 seconds to settle down. Even though the system is stable with CPSS, the performance in terms of settling time is not as good as those of evolutionary algorithm based PSSs. The same trend applies in Figure 6.35 where the speed response is shown, the CPSS system has very high oscillations as compared to the BGA-PSS, GA-PSS and PBIL-PSS. In the electric field response of Figure 6.36, the system equipped with CPSS settles within 6 seconds, while the EA based PSSs settles within 3 seconds.

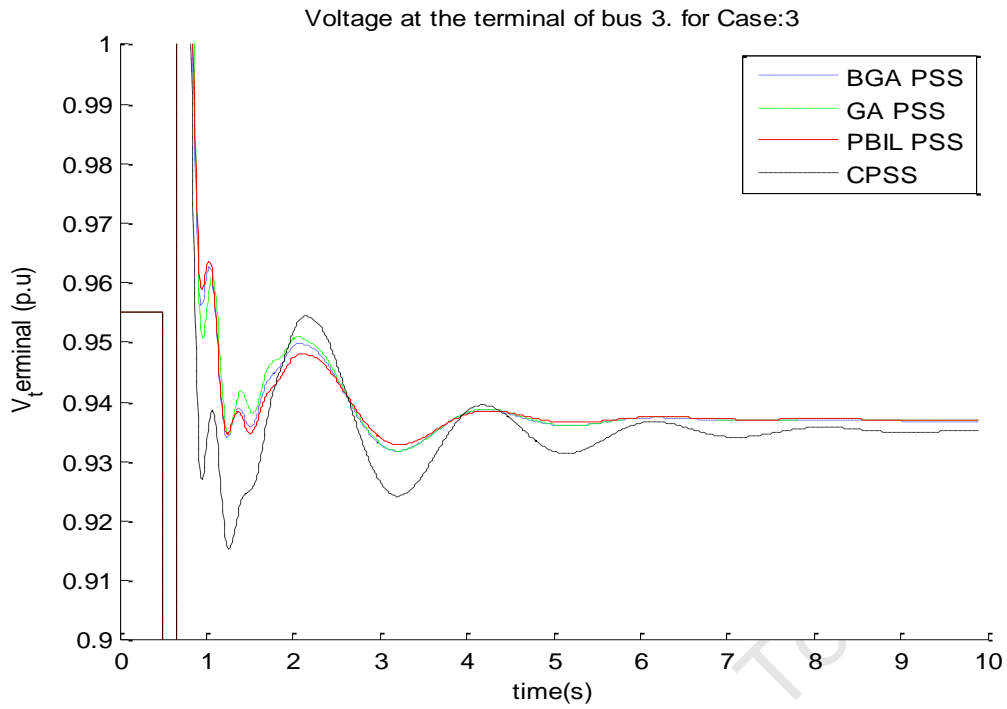


Figure 6.33: Voltage on Bus 3 following a 3 phase fault on bus 3 for Case 3

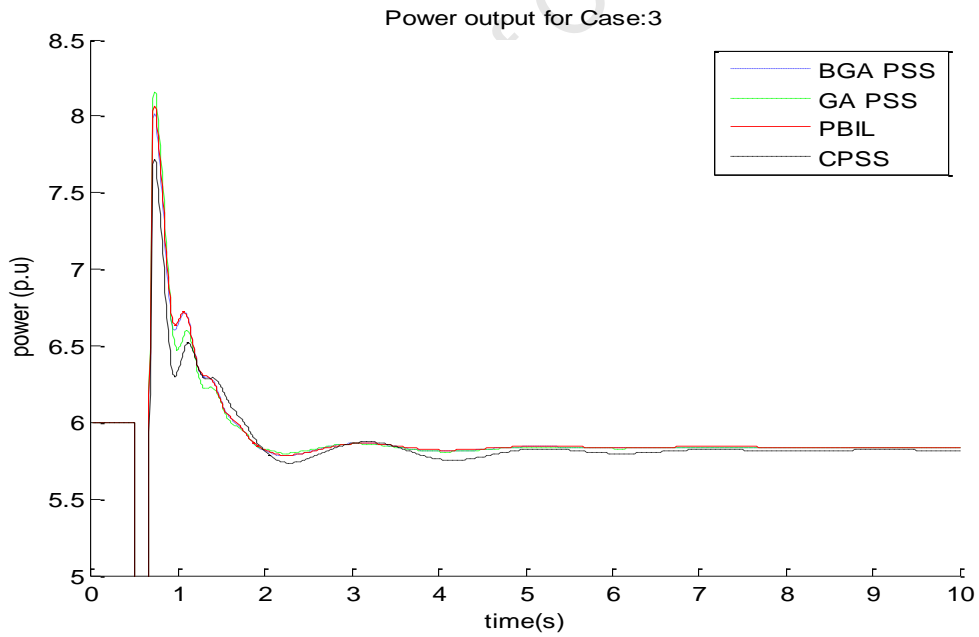


Figure 6.34: Active power response of generator 2 to the 3 phase fault on bus 3 for Case 3

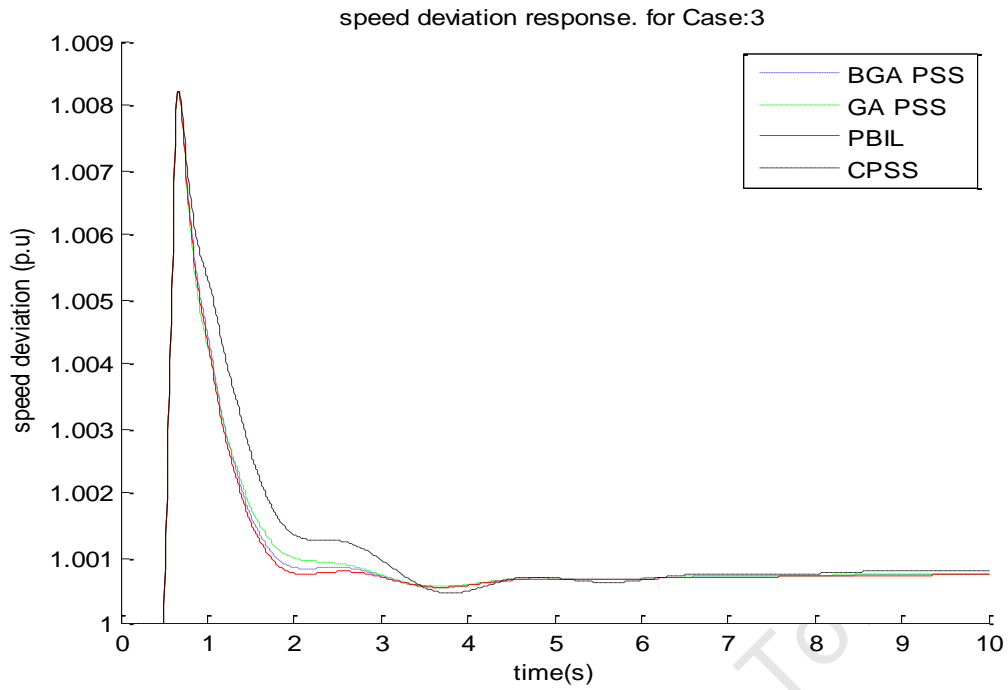


Figure 6.35: Speed response of generator 2 to a 3 phase fault on Bus 3 for Case 3

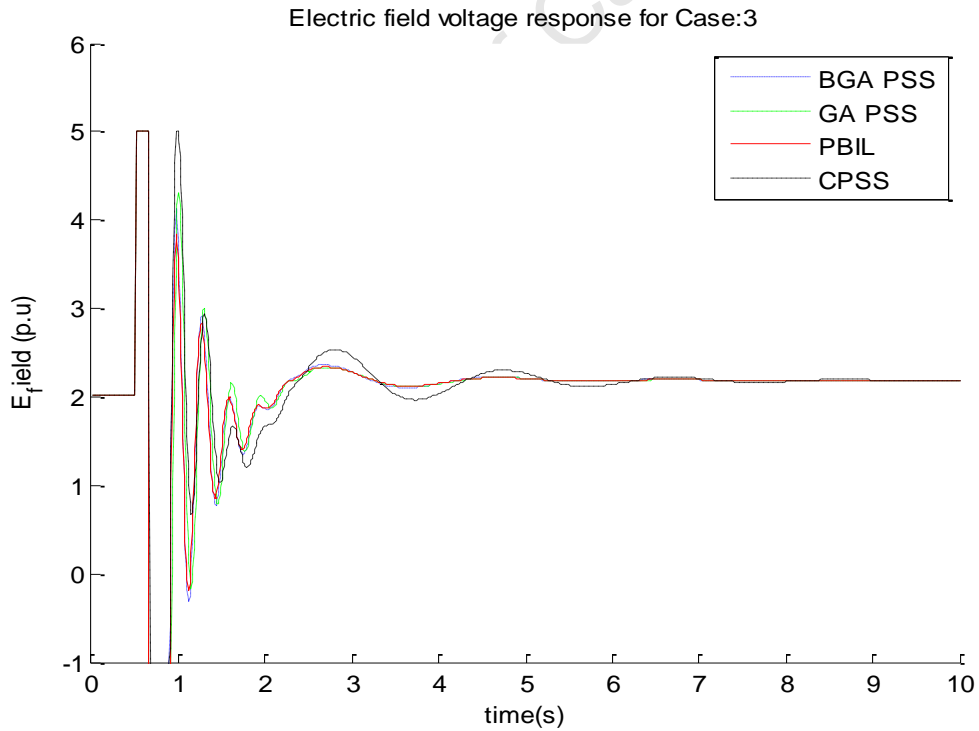


Figure 6.36: Electric field voltage response of generator 2 to a three phase fault on Bus 3 for Case 3

6.5 Summary

Even though the Eigenvalue analysis showed that the BGA-PSS and PBIL-PSS performed slightly better than the GA-PSS, little can be distinguished in the time domain simulations. This adds further to the idea that it is important to include the transient stability criteria (like properly tuning the gain so that it is not too high to negatively affect the voltage response of the system) within the design of the Power System Stabilizer so as to improve the system responses for both small signals as well as under transients (especially voltage). High gains of the PSS may affect the amplitude of the oscillations as has been observed in the three Case studies, evident more in the electric field voltage response, where the signal tend to reach the limits of ± 5 pu.

University of Cape Town

Chapter 7

Real Time Implementation of Power System Stabilizers

7.1 Introduction

This chapter summarises the work that was done at the Department of Electrical and Computer Engineering at the University of Calgary. This is an implementation of the real time simulation for the system with PSSs designed using Evolutionary Algorithms. It gives a description of the system that was available in the Laboratory; the procedures in implementing the PSS as well as the results obtained when the real time system was equipped with three different PSSs. The PSSs that were implemented were CPSS, BGA-PSS and PBIL-PSS. The last section presents the design simulation results obtained from the software used. This chapter also compares the performances of the PSSs in the simulations as well as on the real time system.

7.2 The Experimental System Description

The system consists of a DC motor and a synchronous generator set. A Combination of π section units of inductance and capacitor are used to simulate transmission lines. Each unit represents a 50 km length of actual transmission line. There are 12 units available to form different lengths of transmission lines, depending on the length of the transmission line desired.

The DC machine acts as the turbine with rated parameters 220 V DC, 30 A, 1800 RPM, 7.5 hp, excitation 40/20/10 V DC. The synchronous micro-alternator is working as the generating unit with the rated parameters 220/127 V AC, 7.9 A, 3 kVA (chosen as power base for per unit system), 3 phase, 60 Hz, and a power factor of 0.8 lagging. An electrical device called the Time Constant Regulator (TCR) is used to set the effective field time constant of the micro-alternator to simulate the time constant of a large generator. With TCR, the effective field time constant of the micro-alternator can be set as large as 10 seconds. But usually a value between 2 to 5 is used.

Two different types of Transmission line model are available in the lab. There is a 500KV, 600km single transmission line, formed by connecting all the 12 units in series. The second can be formed by connecting 6π units in series to form up to a 500KV, 300 km transmission line. It is also important to note that the system and the transmission line are running at around 250V, the voltage on the utility. This set can be altered to form a double transmission line especially in a case of faults testing, whereby a fault is applied in the middle of one of the transmission line.

The generator is also equipped with a conventional AVR to control the terminal voltage of the generating unit. A PC with a DAQ card AT-MIO-16E-2 from National Instruments and real time workshop software environment from Matlab or any other software can be used to produce V_{pss} control signal.

A variety of disturbances can be applied to the system. A switch in the excitation field circuit of the DC motor can be used to accomplish step change of input torque of the generator. Similarly, step change of terminal voltage of the generator can be realized by a switch on Printed Circuit Board (PCB) of AVR. In addition, different types of faults can be applied to simulate large disturbances by a logic controller. Different operating conditions can be simulated by adjusting the active and power factor of the generator, this is achieved by adjusting the armature or field current of the DC motor and terminal voltage of the generator respectively. The block diagram representation of the system is shown in Figure 7.1 below.

7.3 Power System Stabilizer Implementation

The PSS that was designed consists of two lead/lag circuits. This was designed with two different EA techniques, but for the analogue CPSS the transfer function is given by the following transfer function:

$$-9.6 * \frac{2.5s}{1+2.5s} \frac{1+0.1s}{1+0.08s} \frac{1+0.1s}{1+0.08s} \Delta P_e(s) \quad (7.3)$$

The analogue PSS needed to be converted to its equivalent digital PSS and this was done in the Matlab environment. Simulink was used to read the analogue input through the DAQ card AT-MIO-16E-2 and similarly to output the feedback signal from the PSS. The lead/lag elements for the PSS were discretized using zero hold technique with a sampling rate of 0.05 seconds. The schematic diagram from the Simulink environment is shown below in Figure 7.2.

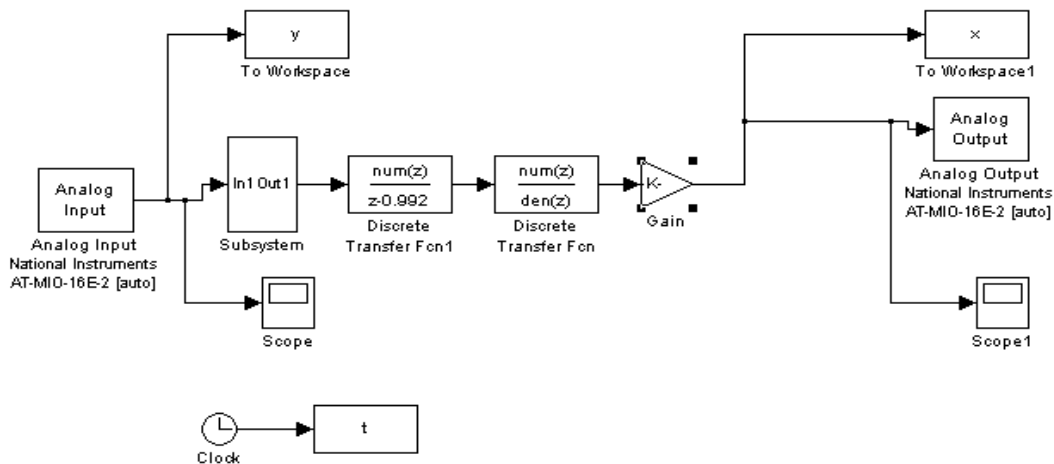


Figure 7.2: Simulink implementation model

An analogue CPSS was also attempted, but was found not to be functioning properly and therefore the results presented in this thesis are only for the digital controllers. Also due to the time constraints, all three evolutionary based PSSs could not be designed.

7.4 Real Time Simulation Results

The results from the real time simulations are presented in this section. To give the results presented in this section, the system was subjected to a single phase to ground fault applied in the middle of the transmission line (see Figure 7.1) for a period of 100ms. After the fault was applied, the circuit breakers opened and closed almost instantly (reclosure). The experimental results for seven operating conditions are presented in Figures 7.3 to Figure 7.8. The results show that the system was adequately damped when equipped with the PBIL and BGA PSS. The performance is poor for the CPSS as well as for the open loop system.

The performance of the BGA and PBIL PSS are very close even though the PBIL outperforms the BGA slightly in most operating conditions, except for the operating conditions shown in Figures 7.5. The simulations results shown in Figure 7.5 show that the system takes roughly 5 to 6 seconds to settle down when equipped with PBIL and BGA PSS. The CPSS and open loop takes relatively longer to settle down. The amplitude of the oscillations is higher for the open loop system as compared to the closed loop system, owing to the performance of the PSS. Figure 7.4 and 7.6 show a similar trend with the open loop system having higher oscillations as compared to the controlled system and at the same time, the open loop system takes longer to settle down as compared to the closed loop system. For the operating condition shown in Figure 7.6, the open loop system takes approximately 4 seconds together with the system controlled by the CPSS. But the open loop has higher oscillations as compared to the system with the CPSS. When the system is equipped with the PBIL and BGA PSS, it takes approximately 4 seconds to settle down and the only oscillations that exist are the 1st, 2nd and 3rd swing oscillations. This shows a remarkable improvement in the system damping as well as the system response when equipped with a PSS designed around such operating conditions. Figure 7.7 and Figure 7.8 shows the PBIL performing slightly better than the BGA PSS, especially considering the amplitude of the oscillations. But the settling time are relatively close, approximately 3 seconds. The system equipped with the CPSS settles faster than the open loop system (Figure 7.8), taking approximately 4 seconds as compared to the open loop which takes close to 6 seconds. At the same time, the open loop system has higher oscillations as compared to the system with CPSS.

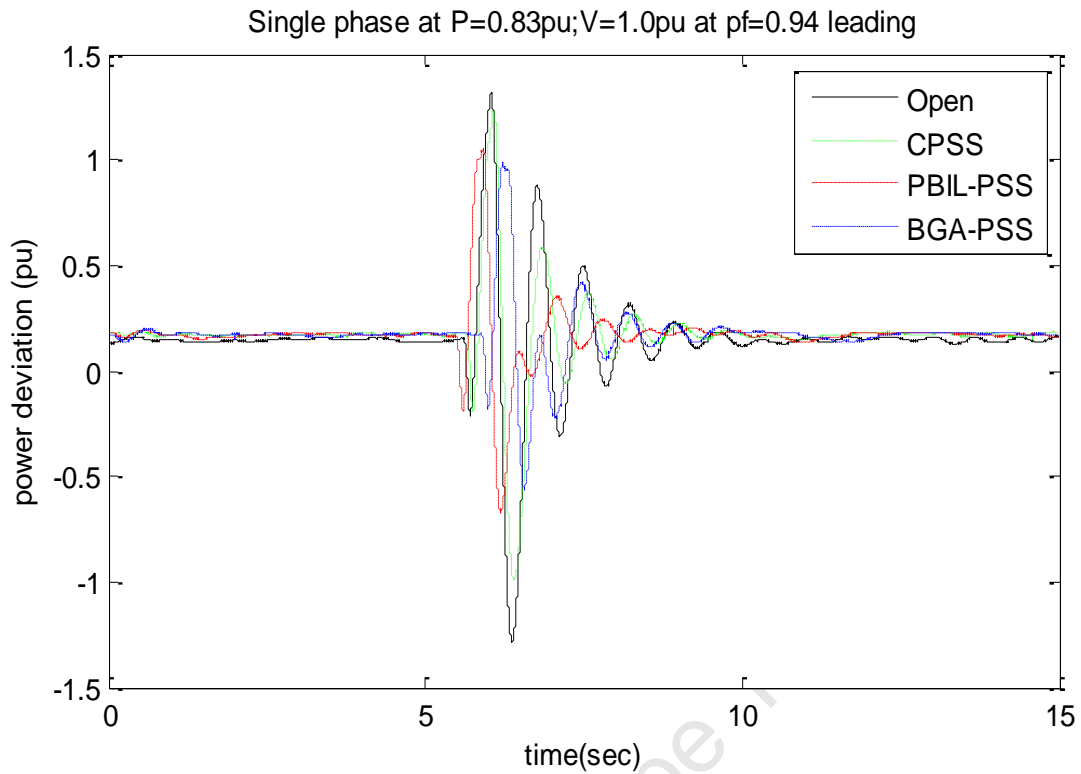


Figure 7.3: System response to a single phase fault at P=0.83pu; V=1.0pu at 0.94 leading power factor

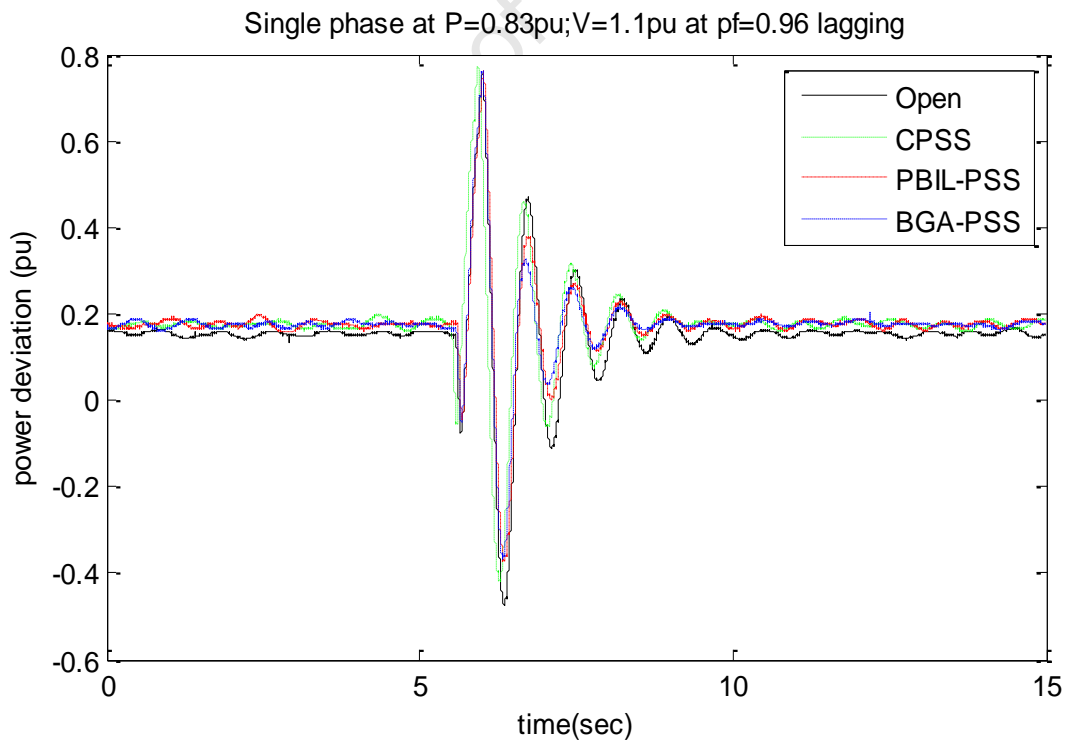


Figure 7.4: System response to a single phase fault at P=0.83pu; V=1.1pu at 0.96 lagging power factor

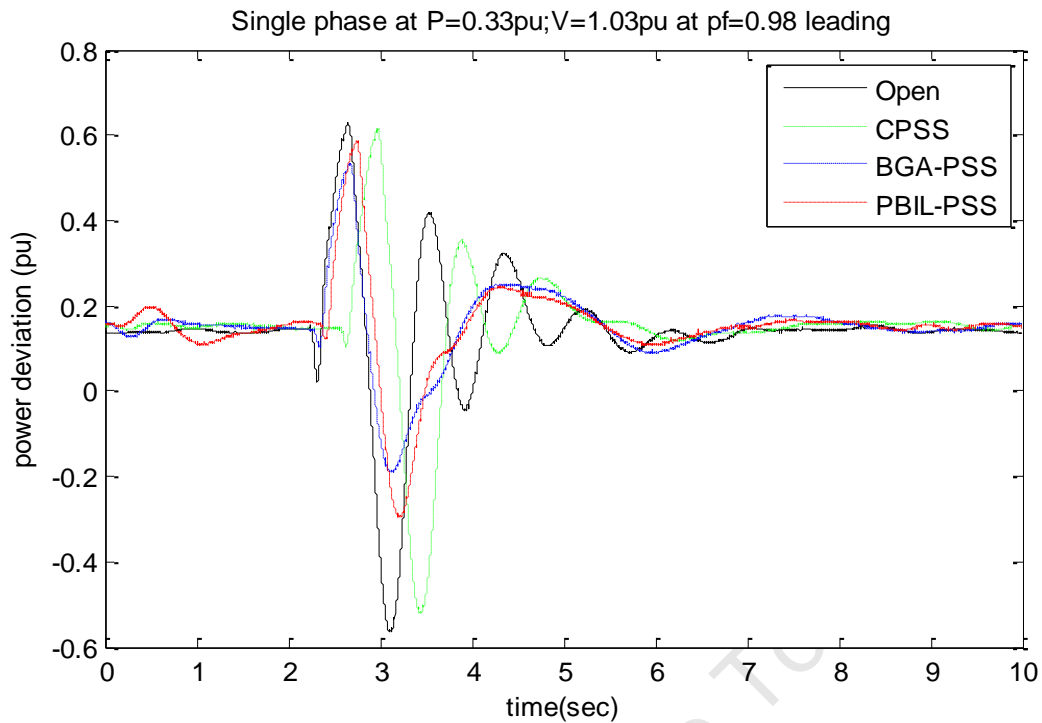


Figure 7.5: System response to a single phase fault at $P=0.33\text{pu}$; $V=1.03\text{pu}$ at 0.98 leading power factor

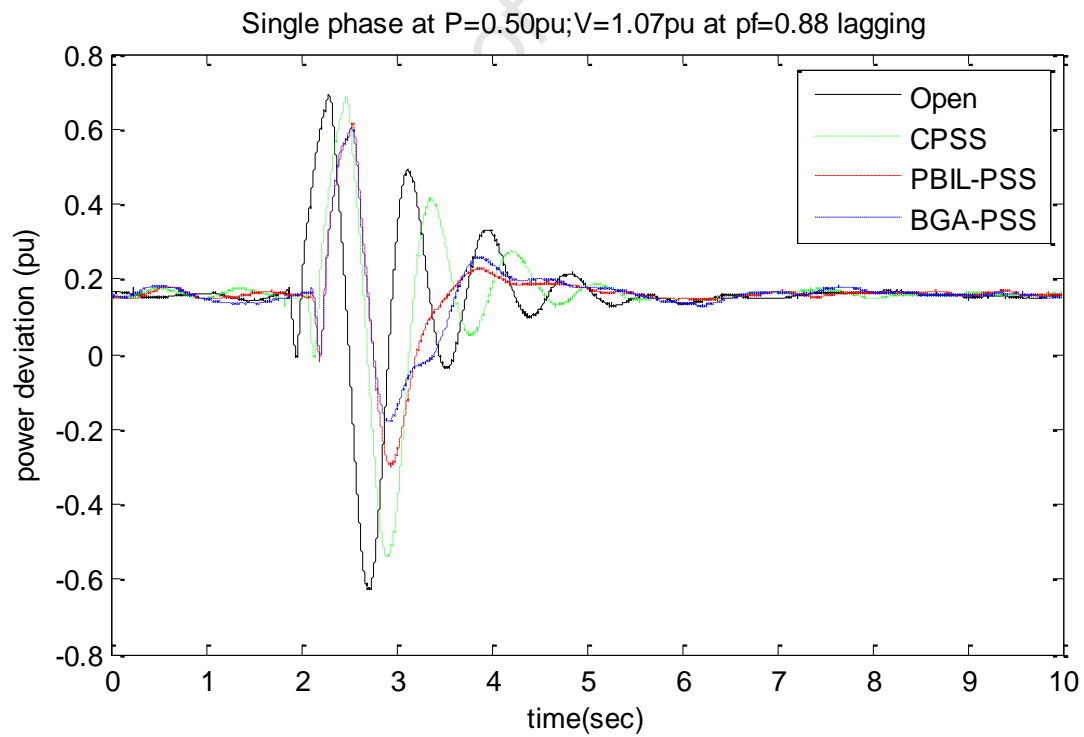


Figure 7.6: System response to a single phase fault at $P=0.50\text{pu}$; $V=1.07\text{pu}$ at 0.88 lagging power factor

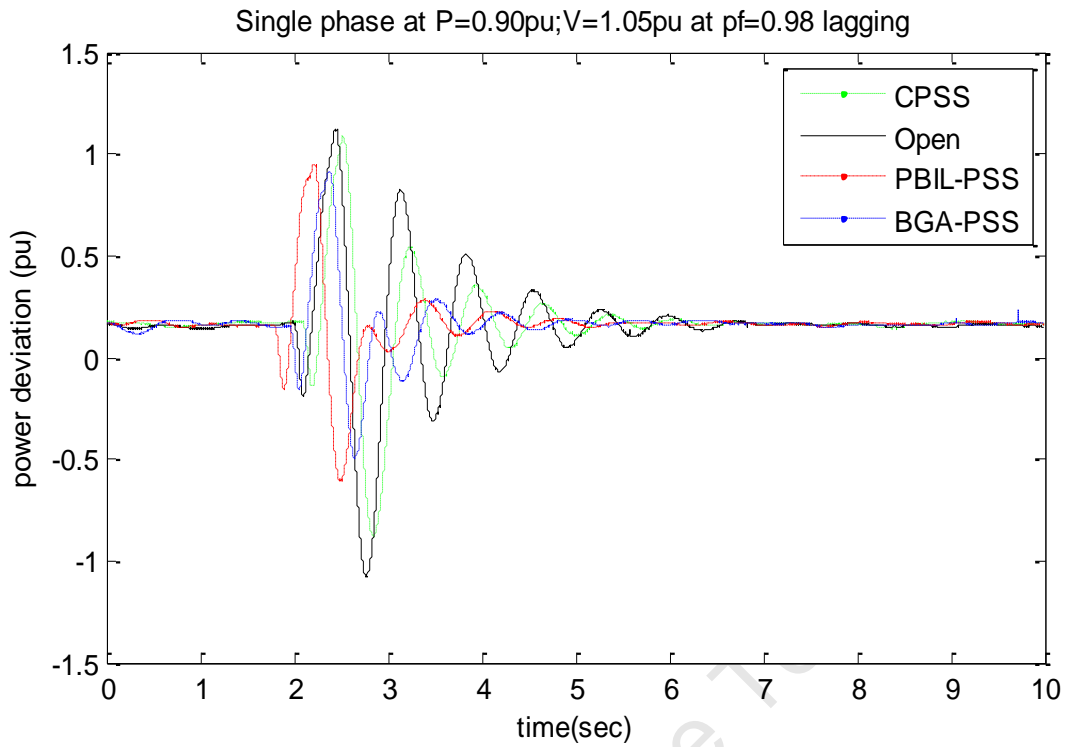


Figure 7.7: System response to a single phase fault at P=0.90pu; V=1.05pu at 0.98 lagging power factor

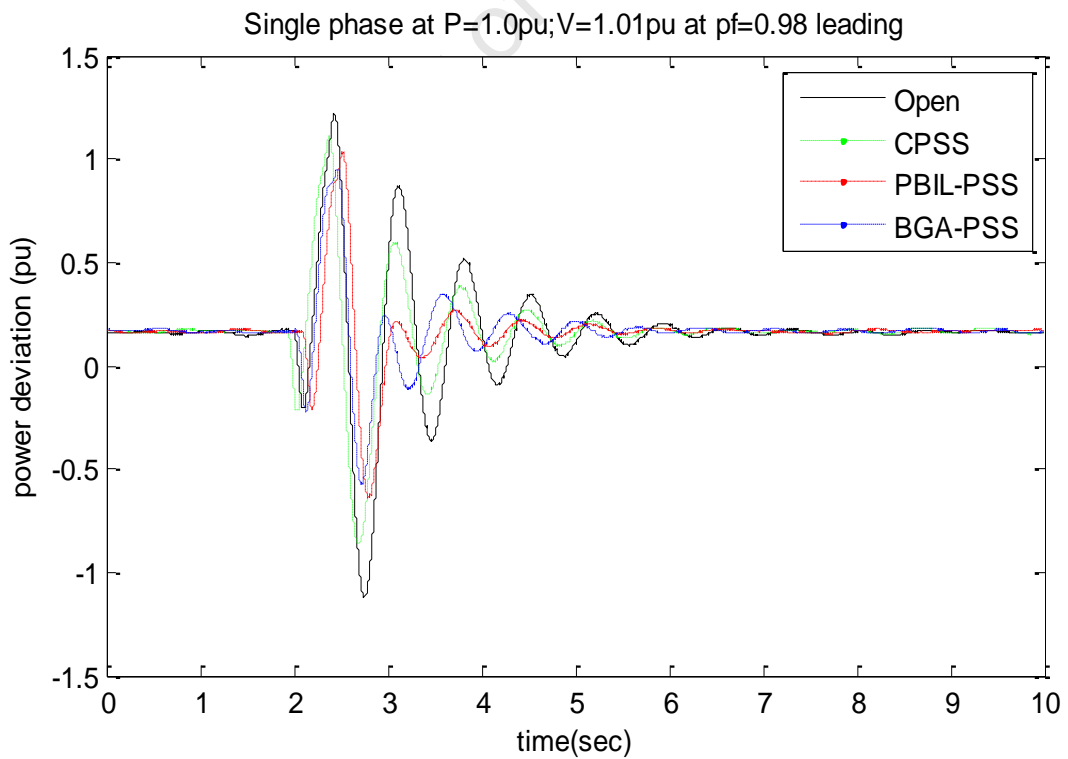


Figure 7.8: System response to a single phase fault at P=1.0pu; V=1.01pu at 0.98 leading power factor

A power system stabilizer was designed using two different evolutionary algorithm techniques implemented and tested on a physical system in the laboratory. The experimental results of the two PSSs are compared with that of the system equipped with CPSS. As expected, the BGA PSS and the PBIL PSS are suppose performance better than the CPSS and open loop respectively, while the CPSS is expected to perform better than the open loop system, since there is no controller in the open loop system. In most of the operating conditions presented above, the BGA and PBIL are performing much better than the CPSS. It can also be concluded that the system equipped with a PSS designed using PBIL and BGA techniques, performs very closely. The system parameters are presented in Appendix A.

7.5 Simulations results for the real time system

In order to compare the results of the real time system to a simulated system, the results presented in this section show the response of the simulated system to a small disturbance in reference voltage as well as to a single phase to ground. The graphs shown in Figure 7.20 to 7.26 shows the simulations step responses of the system that was implemented at the University of Calgary. The generator was subjected to a 10% change in reference voltage and the generator's active power deviation is shown in the Figures. The results are similar to the operating conditions considered in the real time simulations. The different operating conditions were simulated by varying the generator active power as well as the terminal voltage on Bus 1, where the alternator was connected. The objective function used was similar to the one used for the results presented in Chapter 5, whereby the aim was to maximize the lowest damping ratio in the system. This was designed based only on the small signal stability of the system, even though the transient is also considered in this section to test for the robustness of the designed PSS. As has been mentioned before in section 7.4, only the BGA-PSS, PBIL-PSS and CPSS were considered and the simulated system is not exactly the same as one observed in the laboratory. There are therefore expected differences between the simulation results and the real time simulation results. The following differences were observed in the modelling of the two systems:

- ❖ There was a transformer modelled in the simulations (see Figure A.1, Appendix C) while there is no transformer in the system implemented in the laboratory (see

Figure 7.1), thus increasing the reactance in the simulated system. This is because based on the information obtained; the alternator operates at 220V, while the transmission lines are rated at 500KV. But it was out in the laboratory that the transmission line was also operating at 220V.

- ❖ The lines parameters were calculated based on 500KV while the experimental system was at 220V. 500KV was used in simulations because that is the information that was obtained before visiting the laboratory.
- ❖ There is a dc motor acting as a speed governor in the experimental system, while in the simulation results, there was no governor included
- ❖ Also the PSS used in the simulations is continuous, while with the experimental is digital equivalent of it.
- ❖ The experimental system is based on the rating of the alternator which is 3KVA, while the simulation was based on the base of 100MVA. The software used only

The simulation results were obtained before visiting the laboratory and they are based on the information that we obtained before hand. Time could not allow for the redesign of the PSSs when we got to the laboratory. In light of these differences the results presented could be improved by taking into account all the discrepancies discussed above.

7.5.1 Step responses

Figure 7.9 to Figure 7.14 show the response of the simulated system to a 10% change in the reference voltage of generator. The active power deviation of the generator is plotted at various operating conditions, from a light loaded system to a heavily loaded system. Figure 7.9 shows that the BGA-PSS and PBIL-PSS perform reasonably well except that the under shoot is a little bit higher than the CPSS. The under shoot of the BGA-PSS is roughly -0.037pu while for the PBIL- is slightly above -0.03pu. The CPSS has a slightly smaller undershoot of approximately 0.025pu. However the settling time of the system equipped with BGA-PSS and PBIL-PSS is slightly better than the CPSS, at around seven seconds, while for the CPSS the settling time is roughly 10 seconds.

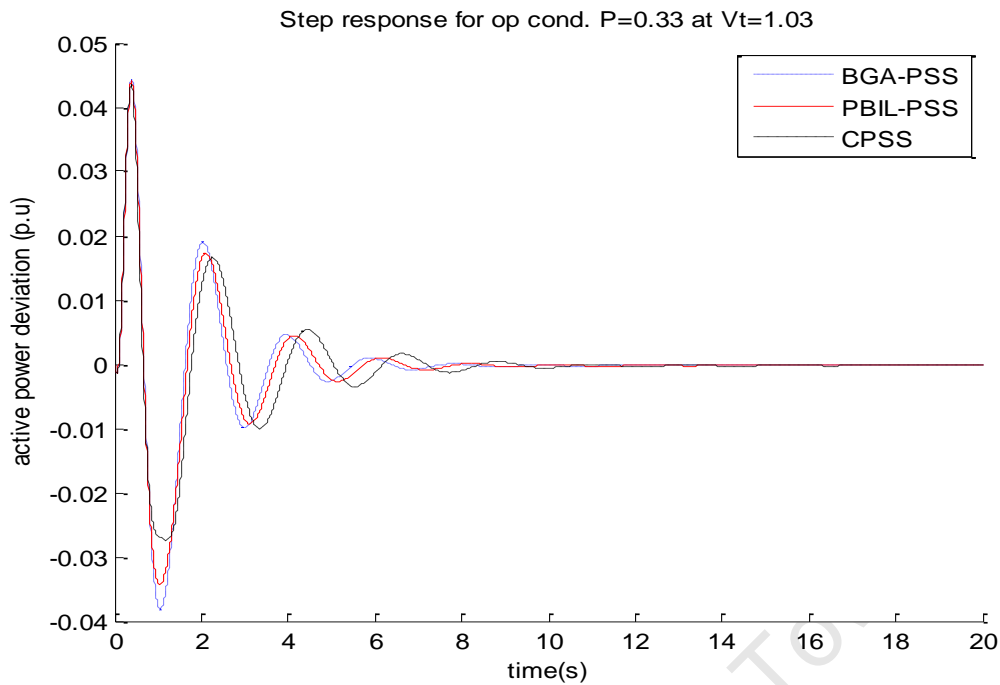


Figure 7.9: Step response of the system to a 10% change in reference voltage at P=0.33 and Vt=1.03

Figure 7.10 shows the generator's active power deviation when the generator was supplying 0.5 per unit of active power while the voltage terminal was 1.07 per unit. Similar to the results observed in the previous operating condition, the BGA and PBIL has slightly bigger undershoot as compared to the CPSS. The system equipped with BGA-PSS has an undershoot of approximately -0.038, the PBIL-PSS has an undershoot of -0.033 while the CPSS has an undershoot of -0.028. In addition the settling time is also similar to the one observed in the previous operating condition, but the system under this operating condition settles a bit earlier than the previous condition. The settling time of the system equipped with BGA and PBIL settles within 6 seconds, while the CPSS settles around 9 seconds.

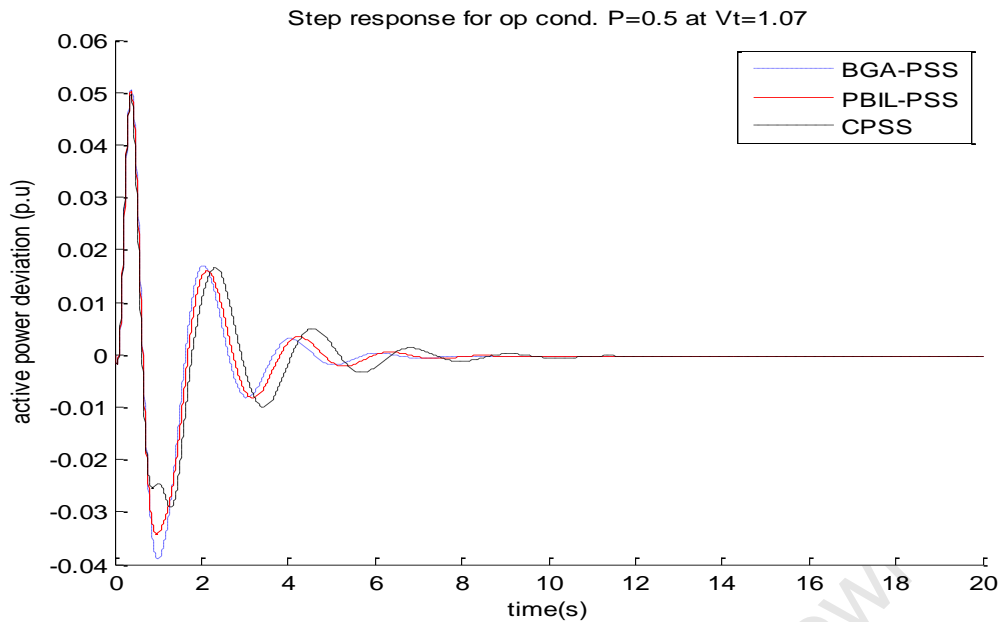


Figure 7.10: Step response of the system to a 10% change in reference voltage at P=0.5 and Vt=1.07

Figure 7.11 shows the active power deviation of the generator at the operating condition when the generator was supplying active power of 0.83 per unit and voltage terminal of 1.0 per unit. As opposed to the two previous operating conditions where the BGA and PBIL- PSS equipped system had bigger undershoot, here the CPSS has a slightly bigger overshoot. The system equipped with BGA-PSS and PBIL-PSS settles a little faster around 6 seconds while the CPSS system settles a little later at around 9 to 10 seconds, the advantage of optimizing the PSS can be clearly observed in the settling time of the system equipped with BGA-PSS and PBIL-PSS.

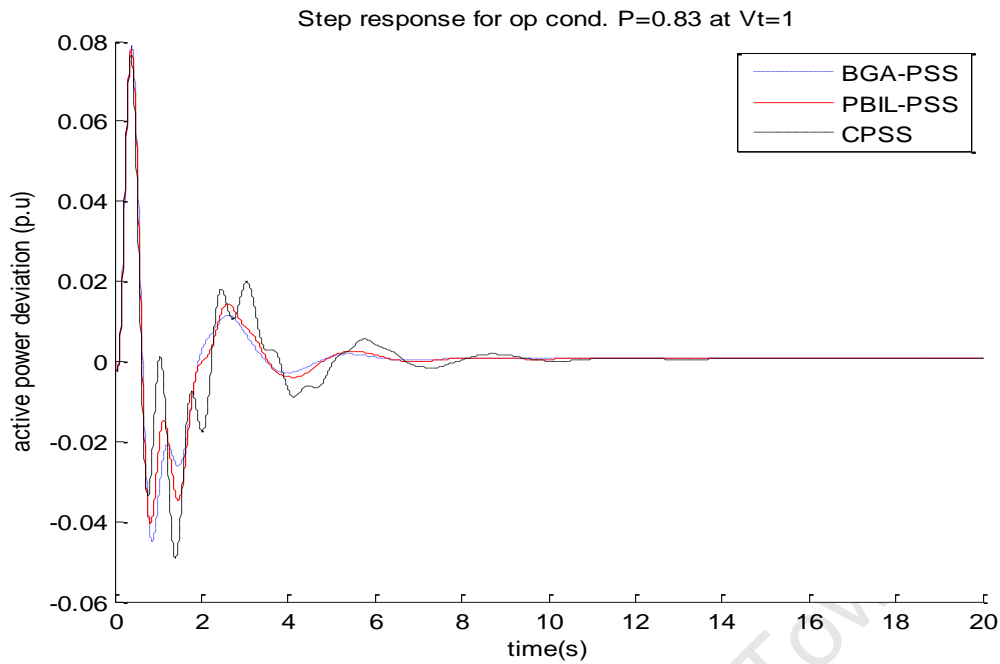


Figure 7.11: Step response of the system to a 10% change in reference voltage at $P=0.83$ and $V_t=1.0$

Figure 7.12 shows the active power deviation of the generator when the generator was supplying active power of 0.83 per unit while the terminal voltage was 1.1 per unit. Similar to the same trend in the previous operating condition, the BGA-PSS and PBIL-PSS settles around 5 seconds while the CPSS settles at around 8 seconds.

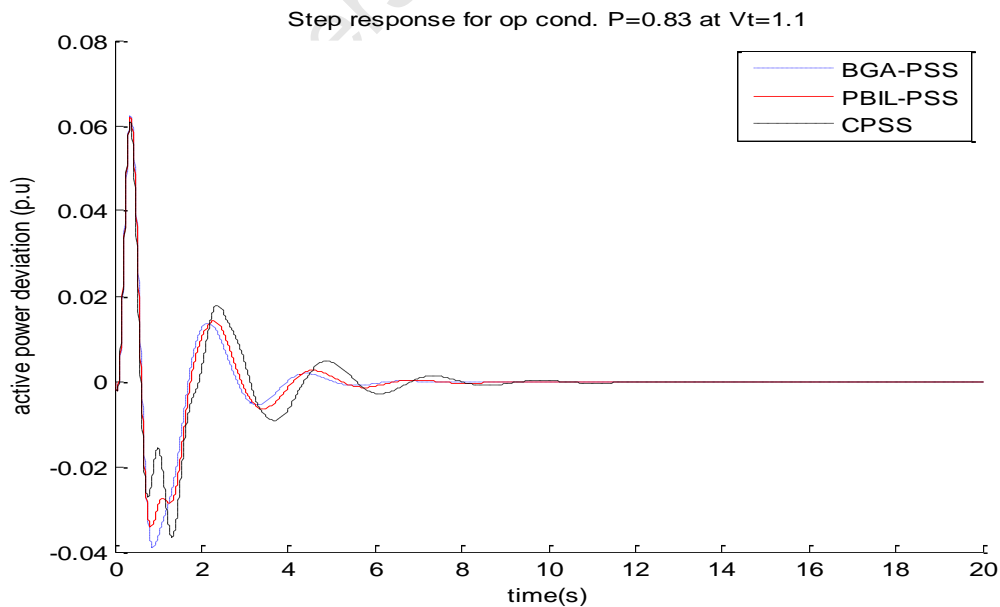


Figure 7.12: Step response of the system to a 10% change in reference voltage at $P=0.83$ and $V_t=1.1$

Figure 7.13 shows the active power response of the generator to a step in reference voltage. At this operating condition, the generator was supplying active power of 0.9 per unit while the active power was 1.05 per unit. The settling time of the system equipped with BGA-PSS and PBIL is around 5 seconds while the CPSS is around 8 to 9 seconds. Clearly the BGA-PSS and PBIL-PSS perform better than the CPSS, emphasizing the need and the benefits of optimizing PSS parameters.

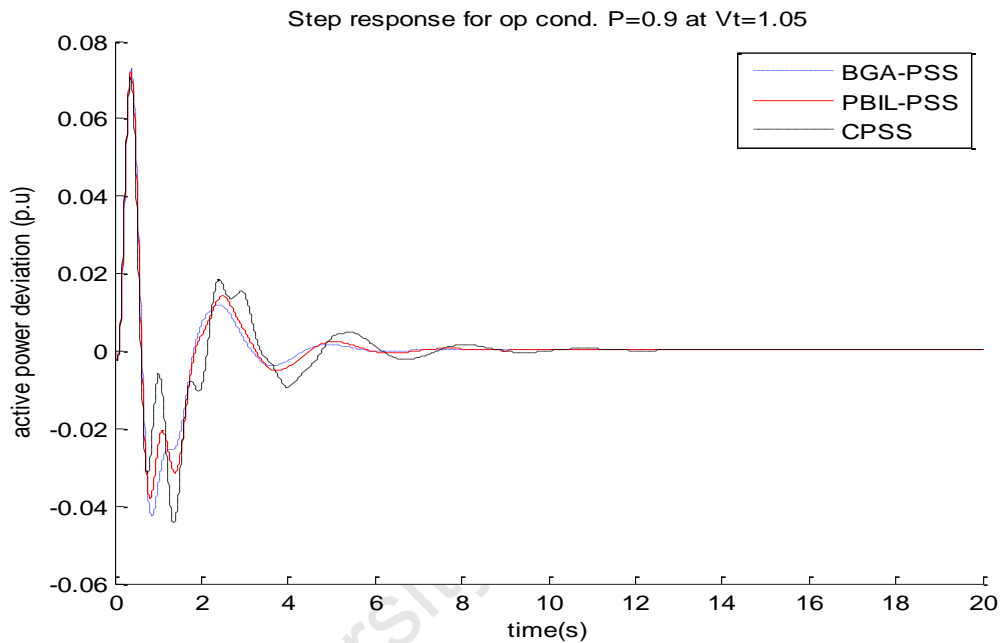


Figure 7.13: Step response of the system to a 10% change in reference voltage at $P=0.9$ and $V_t=1.05$

The last operating condition considered was when the generator was supplying active power of 1.0 per unit while the terminal voltage was 1.01 per unit. The response shows the same trend observed in previous operating conditions, where the BGA-PSS and PBIL-PSS settle faster than the system equipped with CPSS. The BGA and PBIL perform very closely around all the operating conditions. This has been the observation in all the simulations presented in this thesis. The next section presents the single phase fault response of the system.

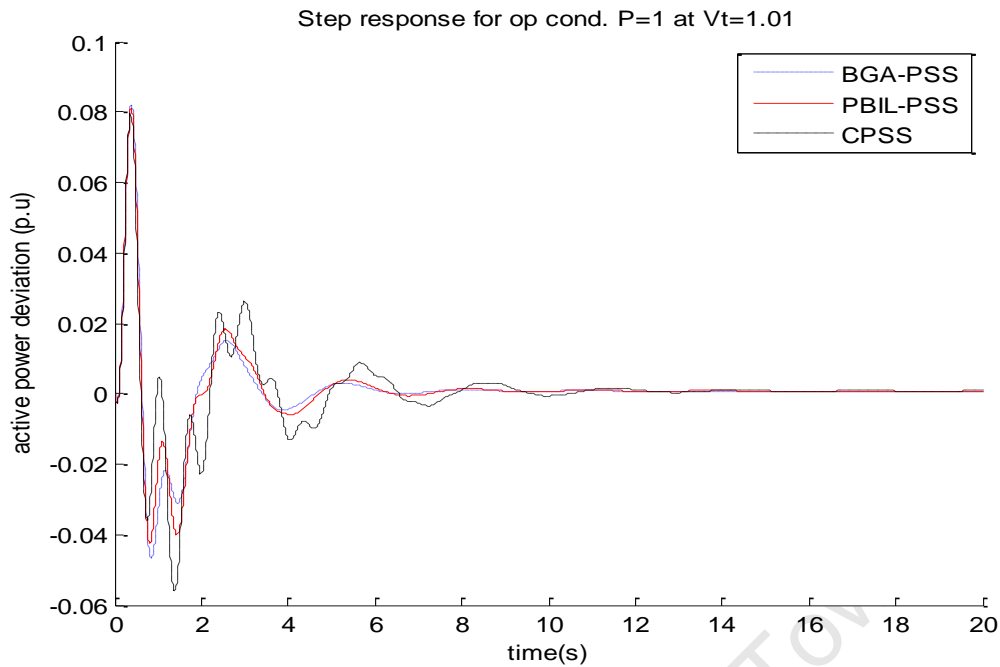


Figure 7.14: Step response of the system to a 10% change in reference voltage at P=1.0 and Vt=1.01

7.5.2 Large disturbance

After the step response of the simulated system, it is imperative to test how the different PSS perform under transient disturbances. In this section, the response of the system to a single phase to ground fault is observed. The single phase is used to compare how the simulated system fares against the real time system. The fault was applied at Bus 2 (see Figure A-1 in Appendix A) and cleared by disconnecting the line from the system. This is the same approach that was used in running the real time system. The fault was applied for 0.2 seconds.

Figure 7.15 and Figure 7.16 show the voltage of Bus 2 (see Figure A-1 in Appendix A) and the active power response of the generator respectively at the operating condition when the generator was supplying 0.33 per unit active power and terminal voltage of 1.03 per unit. Both the active power and voltage show that the BGA and PBIL-PSS perform better than the CPSS. The settling time of the system equipped with BGA and PBIL PSSs is around 6 seconds for the voltage while the power is roughly 4 seconds. The CPSS has a settling time of 9 seconds for the voltage while the active power is around 7 seconds. Comparing with the real time system shown in Figure 7.5 for the same operating

condition, the real time system settles a little faster than the simulated system time, whereby the settling time of the real time system is approximately 2.5 seconds for the PBIL-PSS and BGA-PSS while for the simulated system it is around 3.5 to 4 seconds. Also under this Case the BGA-PSS performs slightly better than the PBIL-PSS.

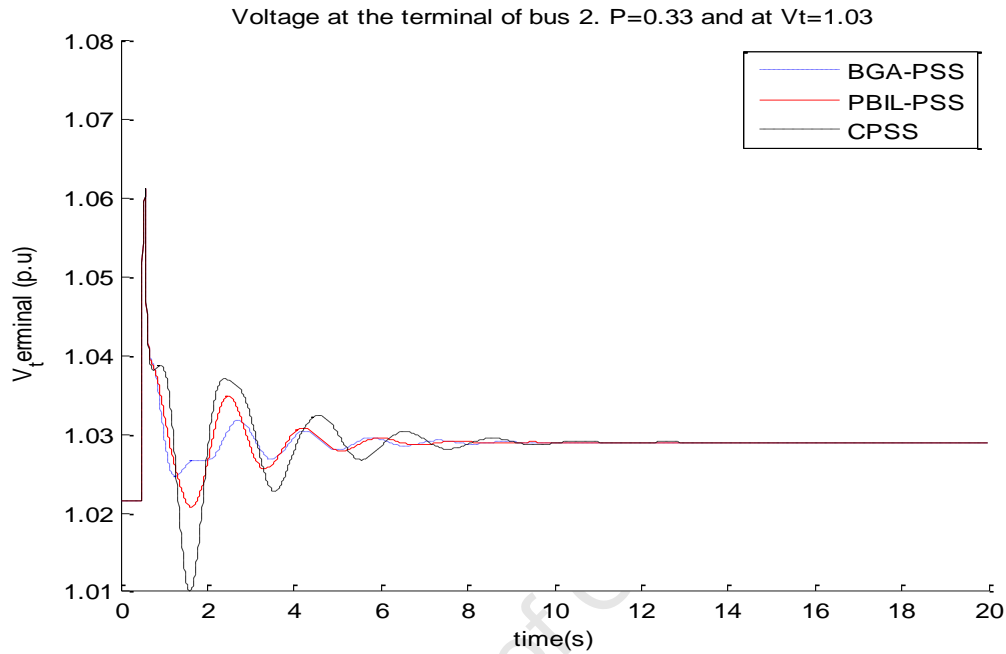


Figure 7.15: Bus 2 voltage response to a single phase fault on Bus 2 at P=0.33 and Vt=1.03

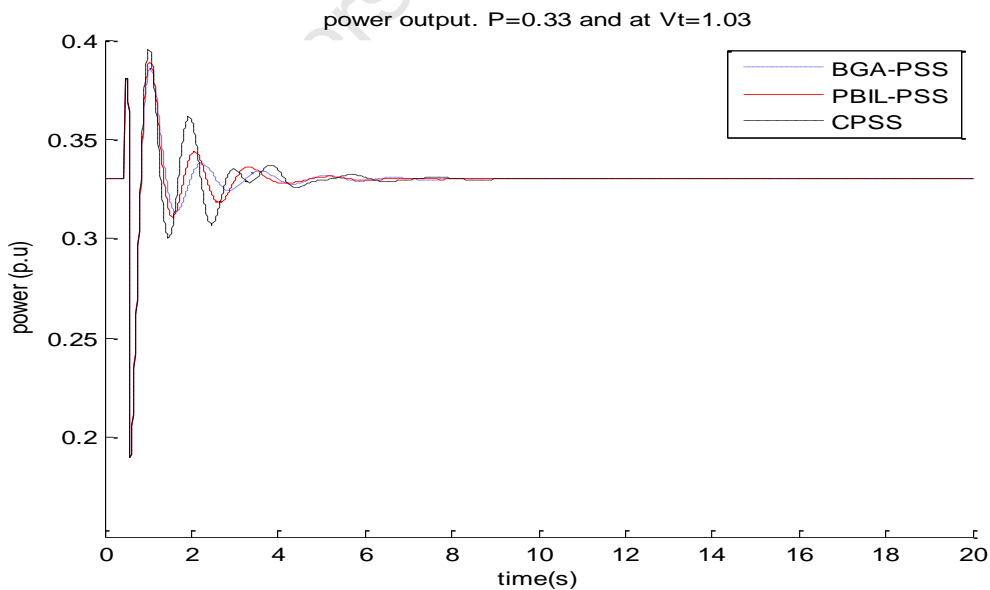


Figure 7.16: Generator active power response to a single phase fault on Bus 2 at P=0.33 and Vt=1.03

Figure 7.17 to Figure 7.18 present the terminal voltage and active power response respectively of the simulated system to a single phase to ground. At this operating condition, the generator was supplying active power of 0.5 per unit while the terminal voltage was 1.07 per unit. The same trend applies where the BGA-PSS was performing slightly better than the PBIL-PSS. The real time system of Figure 7.6 shows that the system equipped with BGA-PSS and PBIL-PSS settle around 2 to 2.5 seconds, while the simulated system settle close to 4 seconds.

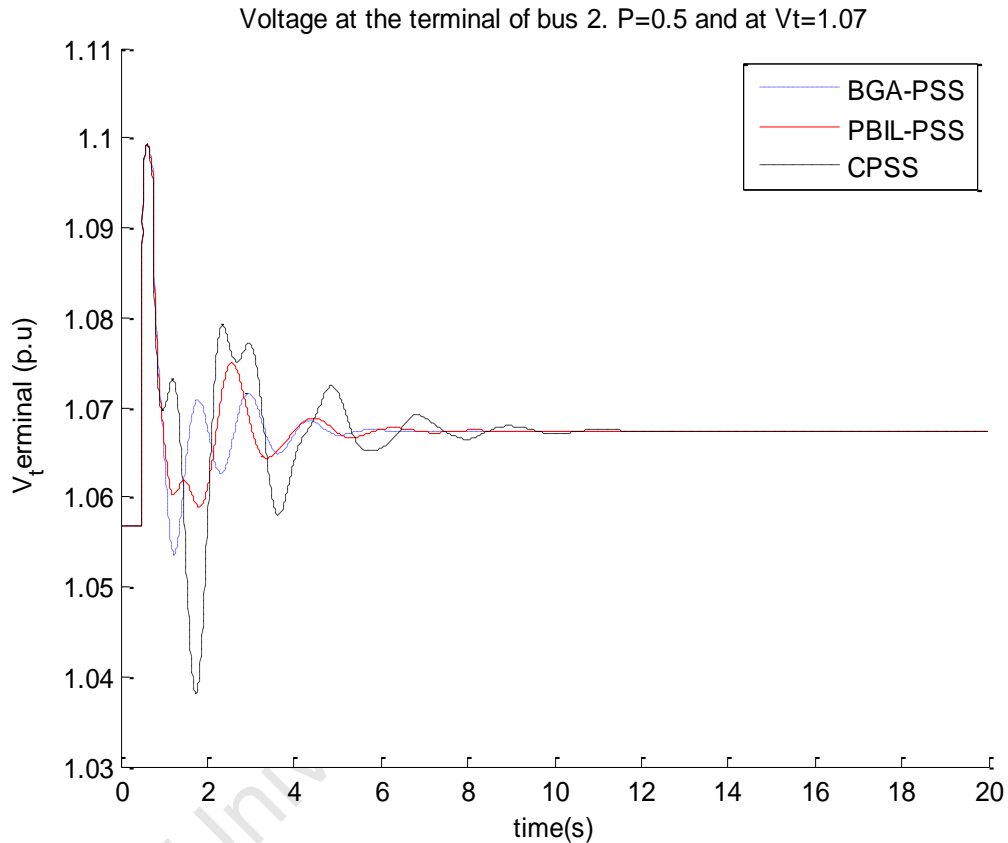


Figure 7.17: Bus 2 voltage response to a single phase fault on Bus 2 at P=0.5 and $V_t=1.07$

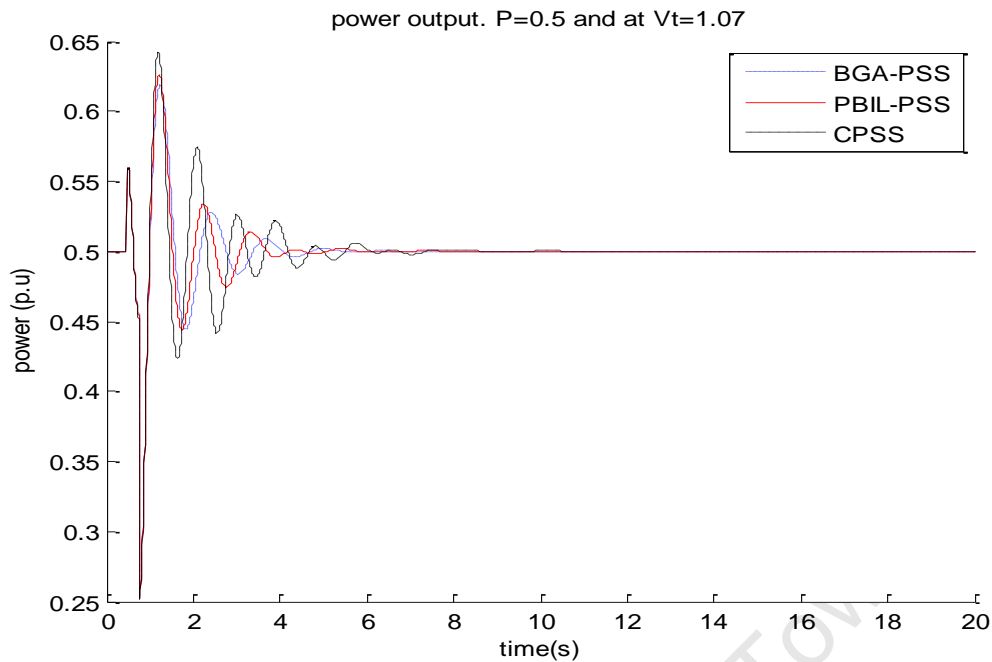


Figure 7.18: Generator active power response to a single phase fault on Bus 2 at $P=0.5$ and $V_t=1.07$

Figure 7.19 to Figure 7.20 show the voltage and active power response of the simulated system to a single phase to ground fault. The loading under this Case has increased and therefore the system takes much longer to settle. System equipped with BGA-PSS and PBIL-PSS settle at around 9 seconds for the voltage while the active power is around 10 seconds, the CPSS does not even settle after 20 seconds. Comparing the results to the real time of Figure 7.3, the trend is similar even though the real time system settles within 5 seconds as compared to the simulated system which settles roughly around 10 seconds. There is such a big difference in the simulated and real time system. This could be attributed to the differences in the systems used, as the simulated system is slightly different from the real time system that was available in the lab.

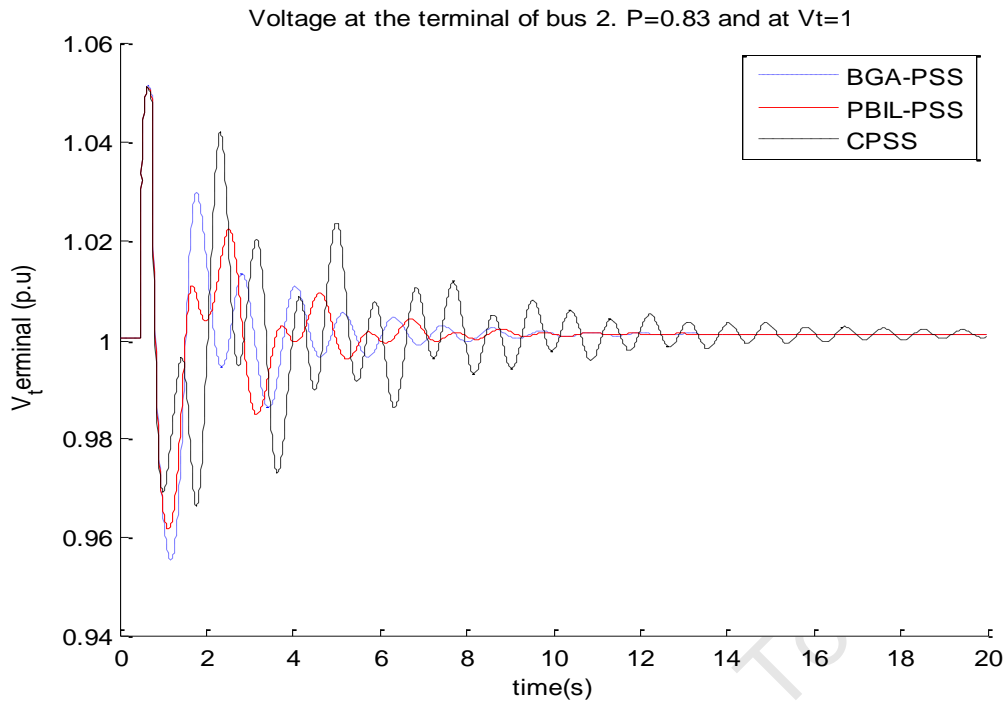


Figure 7.19: Bus 2 voltage response to a single phase fault on Bus 2 at $P=0.83$ and $V_t=1.0$

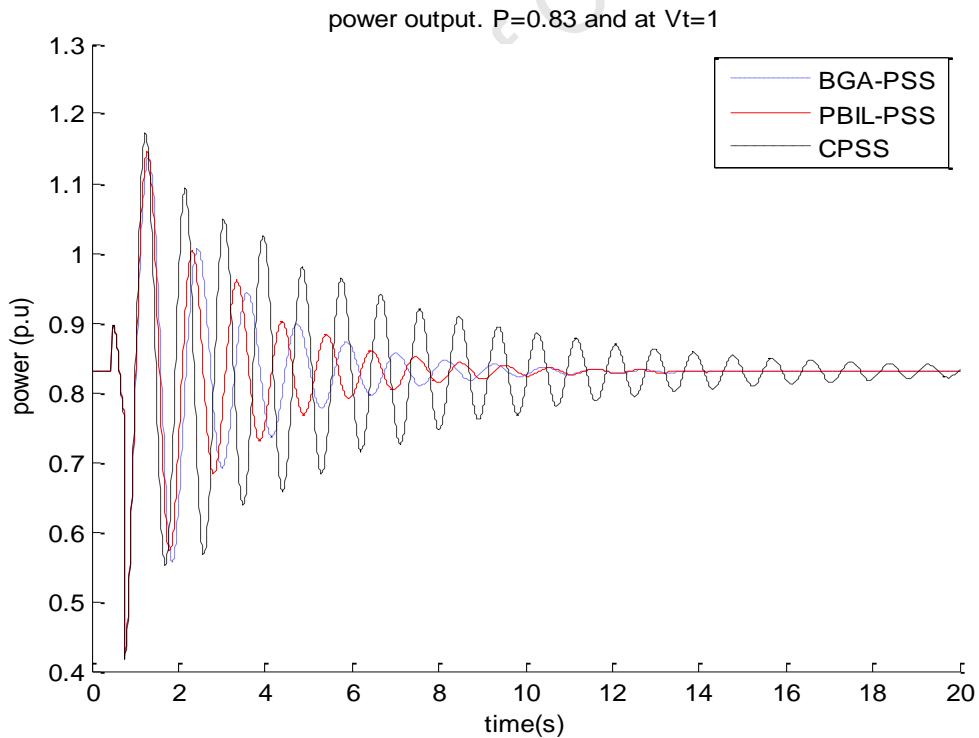


Figure 7.20: Generator active power response to a single phase fault on Bus 2 at $P=0.83$ and $V_t=1.0$

Figure 7.21 to Figure 7.22 show the voltage and active power repose of the system when the generator was supplying 0.9 per unit of active power and 1.05 per unit terminal voltage. The terminal voltage of Figure 7.21 shows that the system equipped with BGA-PSS and PBIL-PSS settles around 8 seconds while the CPSS settles close to 20 seconds. Comparing the results obtained at this operating condition with Figure 7.7 where the real time result is shown, it shows the same trend observed above where the real time system performs better than the simulated system. The settling time of the real time system is around 4 to 5 seconds.

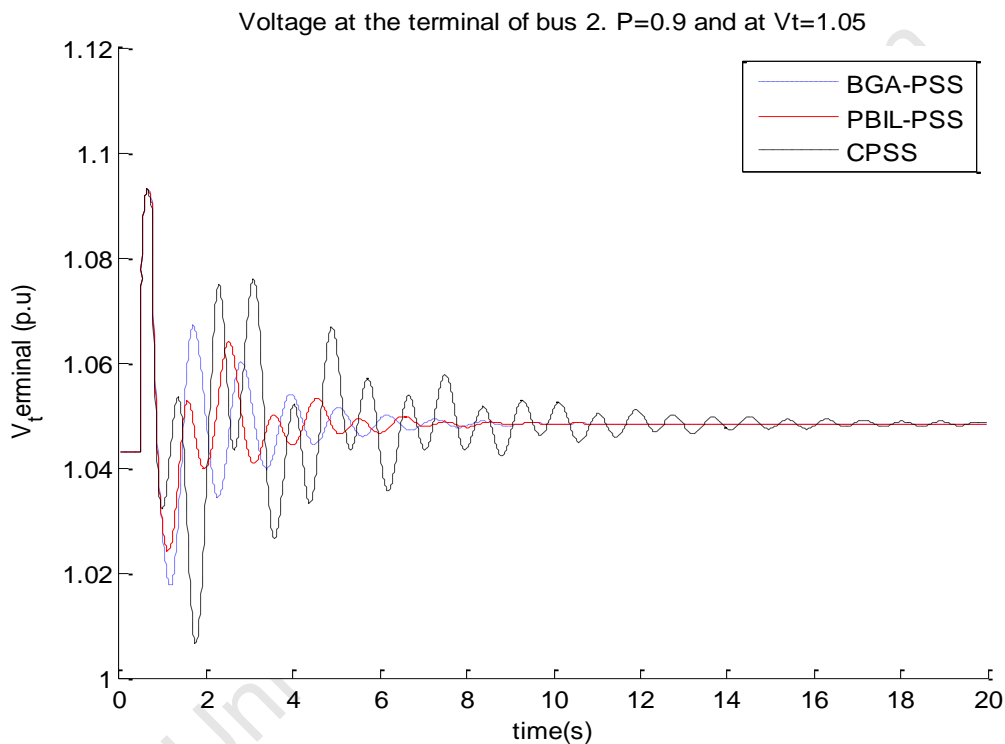


Figure 7.21: Bus 2 voltage response to a single phase fault on Bus 2 at $P=0.9$ and $V_t=1.05$

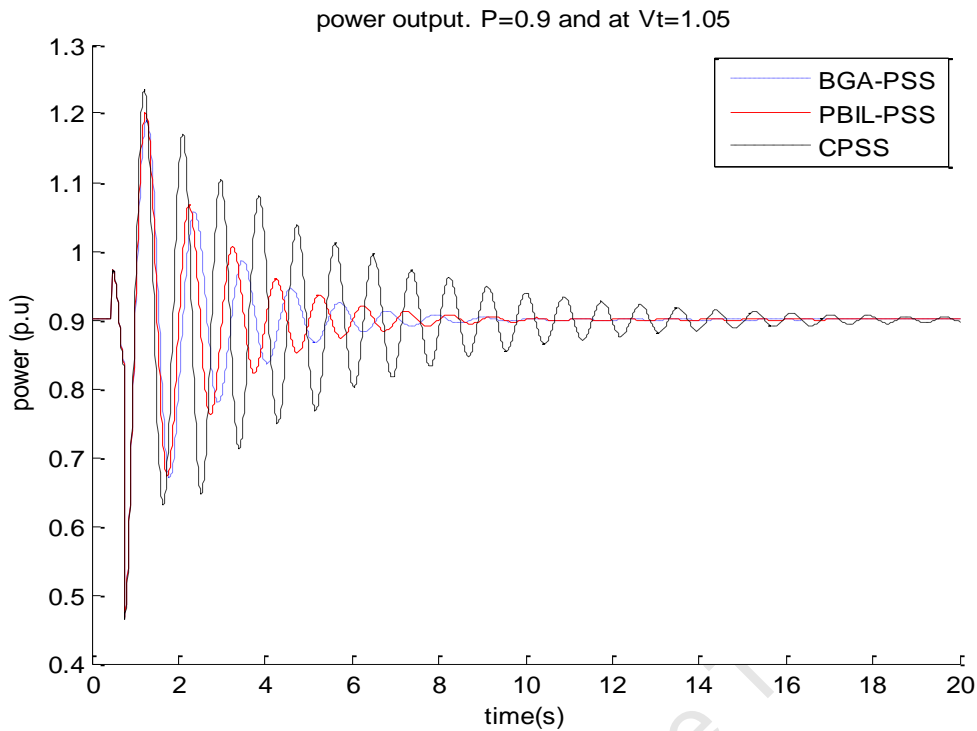


Figure 7.22: generator active power response to a single phase fault on Bus 2 at $P=0.9$ and $V_t=1.05$

Figure 7.23 to Figure 7.24 show the response of the terminal voltage as well as the active power of the generator to a single phase to ground. Under this operating condition, the generator was supplying 0.83 per unit of active power at terminal voltage of 1.1 per unit. The voltage response of Figure 7.23 shows that the system equipped with BGA-PSS and PBIL-PSS settle around 5 seconds, while the system equipped with CPSS settles around 12 seconds. The active power in Figure 7.24 shows the same trend in the voltage but the settling time of the BGA-PSS and PBIL-PSS is slightly longer, close to 6 seconds. Comparing the simulation results to the real time results of Figure 7.4, it shows that the real time system settles within 4 seconds, while the simulated system settles around 7 seconds.

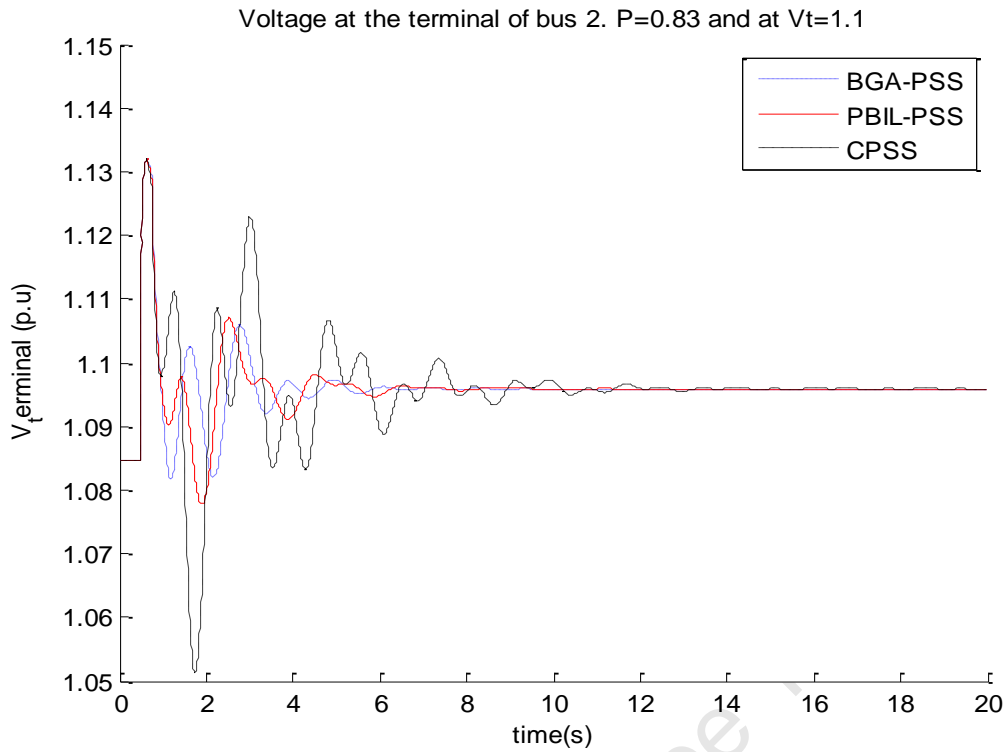


Figure 7.23: Bus 2 voltage response to a single phase fault on Bus 2 at $P=0.83$ and $V_t=1.1$

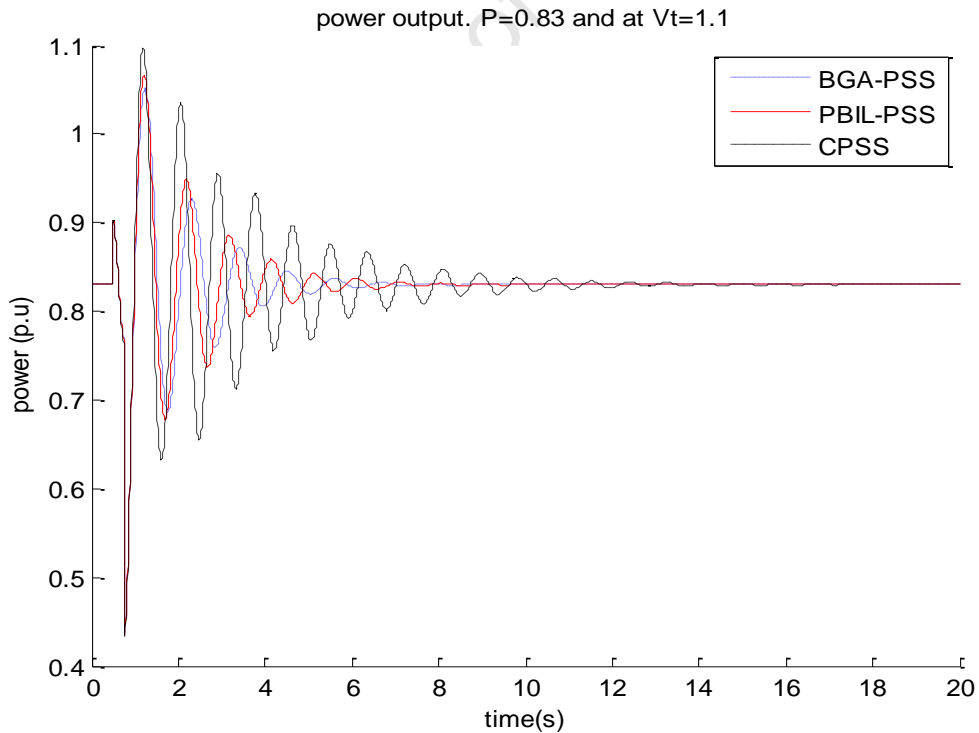


Figure 7.24: Generator active power response to a single phase fault on Bus 2 at $P=0.83$ and $V_t=1.1$

7.6 Summary

The results presented in this chapter show a similar trend in the performances of the PSSs when implemented on the real time system as well as the simulated system. The observations made show that the real time system with PSSs settle faster than the simulated system across all the operating conditions considered. In addition the evolutionary algorithm PSSs perform very well, better than the CPSS across all the operating conditions within the two systems. The difference in the real time and simulated systems could be due to different aspects, one being the slight differences in the systems used, as the software capability could not allow the exact system that was available in the lab to be simulated. The information supplied was not adequate and some assumptions needed to be made as discussed earlier. Improvements can be made in the results obtained above, especially if an exact system can be designed and simulated before testing the PSSs on line. Overall the results obtained further emphasize the need for the optimal tuning of the PSS parameters as compared to the conventional methods that only perform well around the lightly loaded conditions, but not so well as the loading of the system increases. In some instances the system may become unstable.

Chapter 8

Conclusions and Recommendations

This thesis addressed the issue of damping of the electromechanical oscillations in Power systems using Power System Stabilizers. The focus was on the optimal tuning of the PSS parameters, using Evolutionary Algorithm (EA) Techniques. Three EA techniques were considered, namely the standard Genetic Algorithm (GA), Breeder Genetic Algorithm (BGA) and Population Based Incremental Learning (PBIL).

The objective function used was to maximise the lowest damping across all the operating conditions considered in the design. This objective function worked well in both the SMIB and multi-machine system, but for the SMIB a restriction was imposed on the maximum damping ratio that the electromechanical modes can attain (a value of 0.5 was used in the simulations, while a system with a maximum damping of 0.7 is shown in Appendix C). This was done to prevent the electromechanical damping ratio increasing too high and thus reducing the damping ratio of other oscillatory modes which may negatively affect the system response to transients. A method of designing an effective PSS using all three EAs was developed in this thesis.

The simulations showed that GA is able to optimally tune the PSS parameters as the PSS was able to stabilise the system across all operating conditions. The PSS designed using GA worked well in both small disturbances and large disturbances. In terms of convergence, it was also found that the GA converged within 20 generations in the Single machine to infinity bus system (SMIB) and around 83 generations for the Multi-machine system and that is why the maximum number of generations was set at 100 and 120 for the SMIB and Two Area Multi-machine, respectively. This could be due to premature convergence as has been discussed in literature. Premature convergence can only be confirmed if the global optimal solution is known, but since the global optimal solution is not known in this case, we can only conclude that there is a likelihood of it. Similar to GA, BGA also converged around 15 generations for the SMIB and approximately 20

generations for the Two-Area Multi-machine. That is why the maximum number of generations was set to 100 and 120, respectively. There is also a possibility that BGA converged to a local optima, other than a global optimum and this needs to be investigated further as it does not allow the whole space to be explored and thus leaving out some possible good solutions. Even though as presented in literature, BGA tend to converge very fast and thus the likelihood of premature convergence is very low. The PBIL converged around 300 generations and that is why the maximum number of generations was set at 500. The likelihood of premature convergence is eliminated in PBIL and that's why the PBIL algorithm converges around 300 generations as compared to BGA and GA.

Based on the simulation results obtained, it can be concluded that PBIL offers the following advantages over GA and BGA.

- ❖ Population-Based Incremental Learning (PBIL) requires few parameters than BGA and GA, thereby reducing the need of optimizing the genetic operators as well, a situation which is difficult to do in BGA and GA due to the non linear interaction between the parameters. There is no crossover or selection in PBIL.
- ❖ PBIL is able to produce the same or better results than BGA and GA using a smaller population, as compared to BGA and GA which needs a bigger population to produce good results. Thus making PBIL a better optimization technique.
- ❖ PBIL requires less CPU memory as only two solutions are stored (the current best solution and the solution being evaluated) and the probability vector, while in BGA and GA, the whole population is stored.

BGA was found to be similar to GA in its operation as it used all the genetic operators required in GA, but differ in the sense that BGA used artificial selection as compared to GA which uses natural selection. It was found that BGA perform slightly better than GA. As expected, artificial selection performs better than natural selection in most optimization problems. Also BGA proposed in this thesis uses an adaptive based mutation, thereby reducing the influence of the initial value of R (the standard deviation of the random numbers for the vector or mutation rate) since it was also being optimized as the search progressed. In essence, the mutation rate is also being optimized as the

optimization progresses to lean towards the best individuals. Even with adaptive mutation, there is still a likelihood of premature converge as well in BGA, especially that the global optimal solution is not known.

Having optimized the parameters of the PSS, Chapter 5 and Chapter 6 draw the following conclusions:

- ❖ The evolutionary algorithm was able to optimally tune the PSS parameters and hence providing a very robust Power system stabilizer that was able to stabilize the system across all the operating conditions considered. In the SMIB system, the lowest damping obtained was 0.2774 for the GA, 0.2854 for the PBIL and 0.2849 for BGA. In the multi-machine system, the GA converged to a value of 0.1867; PBIL converged to a value of 0.2095 while the BGA converged to a value of 0.205.
- ❖ Optimized PSSs provide better damping than the Conventional PSS. The CPSS performs well at the nominal operating condition, but the performance deteriorates as the system changes and loading increases. This agrees with what is found in literature that the CPSS only works well at the operating condition.
- ❖ Based on the results obtained for both the SMIB and the Multi-machine system, it was observed that there is little difference between the performances of the GA-PSS, BGA-PSS, and PBIL-PSS in maximizing the damping, but at the same time it could be argued that the objective function used influenced the performances of BGA and PBIL, especially for the SMIB system where there was restriction imposed on the maximum damping to electromechanical modes. This is because the BGA and PBIL attained the possible maximum damping ratio of the electromechanical modes specified in the restriction (see Case 5 of the SMIB system, the damping ration cannot be more than 0.5) specified in objective function. Even with such little difference in the performance of the PSSs, the BGA-PSS and PBIL-PSS performs slightly better than the GA-PSS, especially for the operating conditions not included in the design process.

- ❖ The BGA-PSS and PBIL-PSS are effective in optimization as it was possible to obtain the exact possible maximum damping ratio of 0.5 for the electromechanical modes as compared to 0.4885 obtained by the GA-PSS in the SMIB case.
- ❖ The adaptive mutation used in BGA helped optimizing the mutation rate as compared to the GA mutation which was fixed.

The PSS designed using evolutionary algorithms were also tested on an experimental system. The system was setup at University of Calgary, Alberta, Canada. Only the CPSS, PBIL-PSS and BGA-PSS were implemented and tested on experimental system. The GA-PSS was not considered as the time available to do the testing was limited. The experimental results showed that the BGA-PSS and PBIL-PSS performed very closely, but better than the CPSS as expected. The results obtained and presented are based on the single phase fault applied in the middle of one of the transmission lines. The results obtained from the experimental system were compared to the simulation results and the following conclusions can be made:

- ❖ PBIL-PSS and BGA-PSS perform very closely both in the simulations and on the experimental system.
- ❖ BGA-PSS and PBIL-PSS perform better than the CPSS both in simulations and on the experimental system
- ❖ The experimental system settles faster than the simulation system for all the PSSs across most operating conditions.

The differences in the results obtained from the simulations and experimental systems could be due to the following differences in the modelling of the two systems

- ❖ There was a transformer modelled in the simulations while there is no transformer in the lab, thus increasing the reactance in the simulated system
- ❖ A model of an analogue PSS was used in the simulations as compared to the digital equivalent that was used on the experimental system
- ❖ There is a dc motor acting as a speed governor in the experimental system, while in the simulation results, there was no governor included
- ❖ The experimental system is based on the rating of the alternator which is 3KVA, while the simulation was based on the base of 100MVA. The software used only

allows for simulations with ratings in MVA and that is why 100MVA was used rather than 3 KVA.

Overall the major conclusion that can be drawn from the work carried out in this thesis is that, it is better to optimally tune the parameters of the PSS than design using conventional methods as the PSS will not perform well when the system operating conditions change. Furthermore, the performance of the BGA, GA and PBIL is based on the objective function used. Different objective functions may yield different results.

Based on the conclusions drawn from the work, the following recommendations can be made

- ❖ Further investigation needs to be done to determine which of the BGA parameters (mutation, crossover and selection) play the most important role in the optimization.
- ❖ It would also be important to investigate the possibility of premature convergence in BGA, especially in the problem where the global optimal solution is not known.
- ❖ In designing the PSSs, the optimal placement of PSS was not considered and therefore this is another area that can be investigated as it might reduce the parameters to be optimized and therefore reducing the simulation time while at the same improving the stability of the system.
- ❖ Online optimization of the PSS parameters using the EA techniques, in particular PBIL-PSS, as its is faster, effective and requires less parameters
- ❖ The exact system should be modelled and simulated if the PSSs designed is to be implemented on a real time system

References

- [1] P. Kundur, “*Power system Stability and control*”, Prentice-Hall, 1993
- [2] M. Klein, G.J Rogers, P. Kundur, “A Fundamental Study of Inter-Area Oscillations in Power Systems”, *IEEE Trans on Power Systems*, vol. 6, no. 3, pp 914-921,1991
- [3] L. Chen, “A Novel Method for Power System Stabilizer Design”, PhD Dissertation, Department of Electrical Engineering, University of Cape Town, April 2003
- [4] S. Chen, O.P Malik, “ H_{∞} optimization-based Power System Stabilizer design”, *IEE Proceedings. Generation, transmission and distribution*, vol. 142, no. 2, 1995, pp 179-184
- [5] A. Hariri, O.P Malik, “Implementation and Real Time Studies with a Self-Learning Adaptive-Network Based Fuzzy Logic PSS”, 14th PSCC, Sevilla, 2002.
- [6] K.A. Folly, “Multimachine Power System Stabilizer design based on a simplified version of genetic algorithms combined with learning”, *proceedings of the 13th International conference on Intelligent Systems Application to Power Systems*, November 2005
- [7] S. Sheetekela, KA Folly, ” Multimachine Power System Stabilizer Design Based on Evolutionary Algorithm”, *Proceeding of The 44th International Universities’ Power Engineering Conference (UPEC 2009)*,
- [8] S. Sheetekela, S. P Chowdhury, K. A Folly, “Design of Multi-Machine Power System Stabilizers using Evolutionary Algorithm” *IASTED, The Ninth European Conference on Power and Energy Systems (Euro-PES 2009)*, 7-9, September 2009
- [9] J. H Anderson, “The Control of Synchronous Machine using optimal Control Theory”, *IEEE Proceeding on Control*, vol. 59, pp 25-35, Jan, 1971

- [10] H. Yousef, M.A Simaan, "Model reference adaptive control for large scale systems with application to power systems", *IEEE Proc D, Control Theory and Application*, vol. 138, no. 4, pp 321-326, July, 1991
- [11] Y. Cao, L. Jiang, S. Cheng, D. Chen, O. P Malik, G. S Hope, "A Nonlinear variable structure stabilizer for power system stability", *IEEE Trans on Energy Conversions*, vol. 9, no. 3, pp 489-495, September 1994
- [12] W. Liu, G.K. Venayagamoorthy, D. C. Wunsch II, "Design of an adaptive neural network based power system stabilizer", *IEEE Trans on Neural Networks*, vol. 16, no. 5-6, pp 891-898, 2003
- [13] K.A. Folly, N. Yorino and H. Sasaki, "Improving the Robustness of H_{∞} - PSSs Using the Polynomial Approach", *IEEE Trans. on Power Systems*, vol. 13, no. 4, pp 1359-1364,1998.
- [14] S. Baluja, "Population Based Incremental Learning: "A method for integrating Genetic Search Based Function Optimization and Competitive Learning", Technical Report CMU_CS_49_163, June 2, 1994
- [15] J. Greene, The basic idea behind the Breeder Genetic Algorithm, Department of Electrical Engineering, University of Cape Town, 2005, unpublished
- [16] H. Mühlenbein, D. Schlierkamp-Voosen, "Predictive models for the Breeder Genetic Algorithm, I.: continuous parameter optimization, *Evolutionary Computation*", vol.1 no.1, p 25-49, spring 1993
- [17] S. Baluja, R. Caruana, "Removing the genetics from the standard Genetic Algorithm", *Proc 12th International Conference on Machine Learning*, Lake Tahoe, CA, July 1995
- [18] P.M. Anderson and A.A Fouad, "*Power System Control and Stability*", Vol. 1, The Iowa State University Press, Ames, Iowa, USA, 1997
- [19] K. R. Padiyar, "*Power System Dynamics: Stability and Control*", John Wiley, 1996.
- [20] P. W. Sauer, M. A. Pai, "*Power System Dynamics and Stability*", Prentice Hall, 1998.

- [21] M. Klein, G.J. Rogers, P. Kundur, "Analytical Investigation of Factors influencing Power System Stabilizers performance", *IEEE Trans on Energy Conversion*, vol. 7, no. 3, pp 382-390,1992
- [22] G. Rogers, "*Power System Oscillations*", Kluwel Academic Publishers, 2000
- [23] N. Mithulananthan, C.A Canizares, J Reeve, G. J Rogers, "Comparison of PSS, SVC, and STATCOM controllers for damping power system oscillations", *IEEE trans on power systems*, vol. 18, no. 2, May 2003, pp 786-792
- [24] L.J. Cai, I. Erlich, "Simultaneous Coordinated Tuning of PSS and FACTS Controller for Damping Power System Oscillation in Multi-Machine Systems", *IEEE Proceedings: Power Tech Conference*, vol. 2, 2003
- [25] P. Kundur, M. Klein, G.J. Rogers, M.S. Zywno, "Application of Power System Stabilizers for Enhancement of Overall System Stability", *IEEE Trans on Power Systems*, vol. 4, no. 2, pp 614-626, 1989
- [26] O. M. Awed-Badeeb, "Damping of Electromechanical Modes using power system stabilizer (PSS) Case: Electrical Yemeni Network", *Journal of Electrical Engineering*, vol. 57, no. 5, 2006, pp 291-295
- [27] K. Sebaa, M. Boudour, "Optimal locations and tuning of robust power system stabilizer using genetic algorithms", *International journal on Electric Energy System Research*, vol. 79, no. 2, 2009, pp 406-416
- [28] Q. Lu, Y. Z. Sun, "Non-linear stabilizing control of Multimachine systems", *IEEE Trans on Power Systems*, vol.4, no.1, pp 236-241, 1989
- [29] Q.J. Liu, Y.Z. Sun, T. L. Shen and Y.H. Song, "Adaptive non-linear co-ordinated excitation and STATCOM controller based on Hamiltonian structure for Multimachine-power- system stability enhancement", *IEE Proc, control Theory application*, vol. 150, no. 3, pp 285-294, 2003
- [30] L. Yan-Hong, LI Chun-Wen, WANG Yu-Zhen, "Decentralised Excitation control of Multi-machine Multi-load Power Systems Using Hamiltonian Function Method", *ACTA AUTOMATICA SINICA*, vol. 35, no. 7, pp 919-925, 2009
- [31] S.Y. Li-2009, S.S. Lee, Y. T. Yoon, J.K Park, "Non-linear Adaptive Decentralised Stabilization Control for Multimachine Power Systems",

- International Journal of Control, Automation and Systems*, vol.7, no. 3, pp 389-397, 2009
- [32] K. Hongesombut, Y. Mitani, K. Tsuji, "Power system stabilizer tuning in multi-machine power system based on a minimum phase control loop method and genetic algorithm", *14th Power Systems Computation Conference: PSCC, Session14*, Paper 1, pp 1-7, Sevilla, June. 2002.
- [33] A. Phiri, "Optimal Tuning of Power System Stabilizers Based on Evolution Algorithm", Bsc Thesis, Department of Electrical Engineering, UCT, 2007
- [34] M. Ataei, R. Hooshmand and M. Parastegari, "Self- Tuning Power System Stabilizer Design Based on Pole- Assignment and Pole- Shifting Techniques", *Journal of Applied Sciences*, vol. 8, no. 8, pp 1406-1415, 2008
- [35] Y.S. Chuang, S.C. Wang, C.J. Wu, "Novel Decentralised PolePlacement Design of Power System Stabilizers Using Hybrid Differential Evolution", *International Journal of Mathematics and Computers in Simulation*, vol. 1, no. 4, pp 410-418, 2007
- [36] Y. S. Chuang, C.J. Wu, S.C. Wang, P.H. Huang, "Pole Placement Design of Decentralized Output Feedback power System Stabilizers Using Hybrid Differential Evolution", *Journal of Marine Science and Technology*, vol. 15, no. 4, pp 339-350, 2007
- [37] P. Shamsollahi, "Real-Time Implementation and Experimental Studies of a Neural Adaptive Power System Stabilizer", *IEEE Trans on Energy Conversion*, vol. 14, no. 3, September 1999
- [38] D. K Chaturvedi, O.P Malik, "Experimental studies of a generalised neuron based adaptive power system stabilizer", *Soft Computing A Fusion of Foundations, Methodologies and Applications*, vol.11, no.2, 2006, pp 149- 155
- [39] H.M Soliman, A.L Elshafei, A. A Shaltout, M. F Morsi, "Robust power system stabilizer", *IEE Trans on Generation, Transmission and Distribution*, vol. 147, no. 5, pp. 23-34, 2000

- [40] K.A. Folly, "On the Prevention of Pole-zero Cancellations in H infinity Power System Controller Design: A Comparison", *SAIEE Africa Research Journal*, vol.99, no. 4, Dec. 2008
- [41] M.A. Abido, Y.L. Abdel – Magid, "Coordinated design of a PSS and an SVC-based controller to enhance power system stability", *International Journal of Electrical Power and Energy Systems*, vol 25, no. 9, 2003, pp 695-704
- [42] Y.L Abdel-Magid, M. A Abido, "Optimal Multiobjective design of robust power system stabilizers using Genetic Algorithms", *IEEE Trans on power systems*, vol. 18, no. 3, August 2003, pp 1125-1132
- [43] Y.L. Abdel-Magid, M. Bettayeb, M.M. Dawoud, "Simultaneous stabilization of power systems using genetic algorithm", *IEE Proceedings- Generation, Transmission and Distribution*, vol. 144, no. 1, January 1997, pp 39-44.
- [44] M.A. Abido, "Parameter optimization of multi-machine power system stabilizers using genetic local search", *International Journal of Electrical Power and Energy Systems*, vol.23, no.8, November 2001, pp 785-794
- [45] J.I. Corcau, E. Stoenescu, "Fuzzy Logic controller as a Power Stabilizer", *International Journal of Circuits, Systems and Signal Processing*, Vol.1, No. 3, pp 266-273, 2007
- [46] S.A. Taher, A. Shemshadi, "Design of robust fuzzy logic power system stabilizer", *International journal of Intelligence Technology (IJIT)*, vol. 2, no. 3, 2007, pp 152-159
- [47] M. A Abido, Y. L Abdel-Magid, "A Hybrid Neuro-Fuzzy Power System Stabilizer for Multimachine Power Systems", *IEEE Transactions on Power Systems*, vol. no. 4, pp 1323-1330, November, 1998
- [48] W. Liu, G. K Venayagamoorthy, C. Donald, Wunsch II, "Adaptive Neural Network Based Power System Stabilizer Design", *Proceeding of the International Conference on Neural Networks*, vol. 4, pp 2970-2975, July 2003
- [49] H. Shayeghi, A. Safari, H.A. Shayanfar, "Multimachine Power System Stabilizers Design Using PSO Algorithm", *International Journal of Electrical and Electronics Engineering*, vol. 4, no.4, pp 226-233, 2009

- [50] M.A. Abido, "Robust Design of Multimachine Power System Stabilizers Using Simulated Annealing", *IEEE Trans on Energy Conversion*, vol. 15, no. 3, 2000
- [51] Power System Toolbox Ver 2.0: Dynamic Tutorial and Functions, Cherry Tree Scientific Software, Colborne, ON, 1999
- [52] C. Houck, J. Joines, M. Kay, "A Genetic Algorithm for Function Optimization: A Matlab Implementation", NCSU-IE TR 95-09, 1995, <http://www.ie.ncsu.edu/mirage/#GAOT>
- [53] S. Gomes, Jr., N. Martins, C. Portela, "Computing Small-Signal Stability Boundaries for Large-Scale Power Systems", *IEEE Trans on Power Systems*, vol. 18, no. 2, May 2003
- [54] S. K.M. Kodsı, C.A. Cañizares, "Modelling and Simulation of IEEE 14 bus system with FACTS controllers", Technical Report 2003-3
- [55] T. Bäck, "*Evolutionary Algorithms in theory and practice*", Oxford University Press, 1996
- [56] Z. Michalewicz, "*Genetic Algorithms + Data Structures = Evolution Programs*", 3rd edition, Berlin Germany: Springer-Verlag, 1992
- [57] T. Back, U. Hammel, and H.-P. Schwefel, "Evolutionary computation: Comments on the history and current state", *IEEE Transactions on Evolutionary Computation*, vol. 1, no. 1, pp 3-17, April 1997.
- [58] A. Chipperfield, P. Fleming, H. Pohlheim, C Fonseca. Generic Algorithm Toolbox ver1.2: Users Guide, Department of Automatic Control and Systems Engineering, University of Sheffield, 1999
- [59] S. Panda, J. S. Yadav, N. P. Patidar and C. Ardil, "Evolutionary Techniques for Model Order Reduction of Large Scale Linear Systems", *International Journal of Applied Science, Engineering and Technology*, vol 5:, no. 1, 2009
- [60] S. Panda, C. Ardil, "Real-coded Genetic Algorithm for Robust Power System Stabilizer Design", *International Journal of Electrical, Computer, and Systems Engineering*, vol. 2, no. 1, pp 6-14, 2008

- [61] T. Blickle, L. Thiele, "A comparison of Selection Schemes used in Genetic Algorithms", TIK Report Nr. 11, June 1995
- [62] H.C. Chen, S.H. Chang, "Genetic Algorithms Based Optimization Design of a PID Controller for an Active Magnetic Bearing", *International Journal of Computer Science and Network Security (IJCSNS)*, vol.6 no.12, December 2006
- [63] A. Neubauer, "A theoretical Analysis of the non-uniform mutation operator for the modified genetic algorithm", *Proc of 1997 IEEE International Conference on Evolutionary Computation (ICEC'97)*, 1997, pp 93-96
- [64] Z. Michalewicz, C.Z. Janikow, J.B Krawczyk, "A modified Genetic Algorithm for optimal control problems", *Int. Journal of Computers and Mathematics with applications*, vol. 23, no. 12 , pp 83-94, 1992
- [65] X. Zhao, X.S. Gao, Z. Hu, "Evolutionary Programming Based on Non-uniform Mutation", *Int. Journal of Applied mathematics and computation*, vol. 192, no.1, pp 1-11, 2007
- [66] H. Mühlenbein, D. Schlierkamp-Voosen, "The science of breeding and its application to the breeder genetic algorithm BGA", *IEEE Trans on Evolutionary Computation*", vol. 1, no. 4, pp 335-360, 1994
- [67] S. Baluja, "An Empirical Comparison of Seven Iterative and Evolutionary Function Optimization Heuristics", Technical Report CMU CS-95-193, September 1, 1995
- [68] K.A. Folly "Small-signal stability enhancement of power systems using PBIL based power systems stabilizer", *Proceedings of the 1st International ICSC Symposium on Artificial Intelligence in Energy Systems and Power, AIESP 2006*, 7-10 February 2006, Madeira, Portugal
- [69] J. R Greene, "Simulated and Adaptive Search in Engineering Design- Experience at the University of Cape Town", *Invited key paper at world conference on Soft Computing WSC3*, Springer, Verlag, 1997

Research Publications

1. S. P. N Sheetekela, K. A. Folly, "Optimization of Power System Stabilizers using Genetic Algorithm Techniques based on Eigenvalue analysis", *18th Southern African Universities' Power Engineering Conference (SAUPEC 2009)*, January 28-29, 2009, Stellenbosch, South Africa
2. S. Sheetekela, K. Folly, "Multimachine Power System Stabilizer Design Based on Evolutionary Algorithms", *The 44th international Universities' Power Engineering Conference (UPEC 2009)*, September 1- 4, 2009, Glasgow, Scotland
3. S. Sheetekela, S. P Chowdhury , and, K. A. Folly, "Design of Multi-machine power system stabilizer using Evolutionary Algorithms", *The Ninth European Conference on Power and Energy Systems (IASTED, Euro-PES 2009)*, September 7-9, 2009, Mallorca, Spain
4. S. Sheetekela, K. Folly, and O.P Malik, "Design and Implementation of Power System Stabilizers based on Evolutionary Algorithms", *9th IEEE Africon 2009*, September 23-25, 2009, Nairobi Kenya
5. S. P. N Sheetekela, K.A Folly, A Ubisse, D. T Oyedokun, and L. C Azimoh, "Power System Stabilizer Design using Evolutionary Algorithms techniques", *19th Southern African Universities' Power Engineering Conference (SAUPEC 2009)*, January 28-29, 2010, Johannesburg, South Africa

Papers accepted, but not yet published

6. S. P Sheetekela, K. A Folly, “Application of Breeder Genetic Algorithm to Power System Stabilizer Design” *IEEE World Congress on Computational Intelligence (WCCI 2010)*, July 18-23, Barcelona, Spain

7. S. P Sheetekela, K. A Folly, “Power System Stabilizer Design: Comparison between Breeder Genetic Algorithm and Population-Based Incremental Learning” *International Joint Conference on Neural Networks (IJCNN10)*, July 18-23, Barcelona, Spain

University of Cape Town

Appendix

Appendix A: The data for the system that was used for the real time simulation at the University of Calgary is given under this section. This includes the generator data, the transmission line parameters as well as the AVR used.

Appendix B: This section gives the data for the SMIB system presented with results in Chapter 5, section 5.1. The generator parameters, transmission line data as well as the controller (AVR) are given under this section. Also presented under this section are equations that model the generator used in the simulations.

Appendix C: This section presents the results obtained when the restrictions of the damping ratio employed in the SMIB was increased to 0.7. The electromechanical modes and their damping ratio are given in this section.

Appendix D: This section presents the data used in the Multi-machine simulations of Chapter 5, section 5.2. The models used for the generators, the AVR and the speed governor are given in this section.

Appendix A

Real Time Simulations

$$X_d = 1.2; X_q = 1.2; X_D = 1.25; X_Q = 1.25; X_F = 1.27; r_d = 0.0026;$$

$$r_q = 0.0026; r_D = 0.0083; r_Q = 0.0083; r_F = 0.000747; X_{md} = 1.129;$$

$$X_{mq} = 1.129; H = 4.75$$

Automatic Voltage Regulator Transfer function

$$\frac{100}{1+s}$$

Transmission line parameters for a π section, equivalent to 50 km

$$R = 0.03175\Omega$$

$$X = 1.65 \text{ mH}$$

$$C = 8.03 \mu\text{F}$$

Physical rated parameters of synchronous micro – alternator

220/127 V AC, 7.9 A, 3 KVA, 3 phase, 60 Hz, a power factor of 0.8 lagging

Physical rated parameters of DC machine

220 V DC, 30 A, 1800 RPM, 7.5 hp, excitation 40/20/10 V

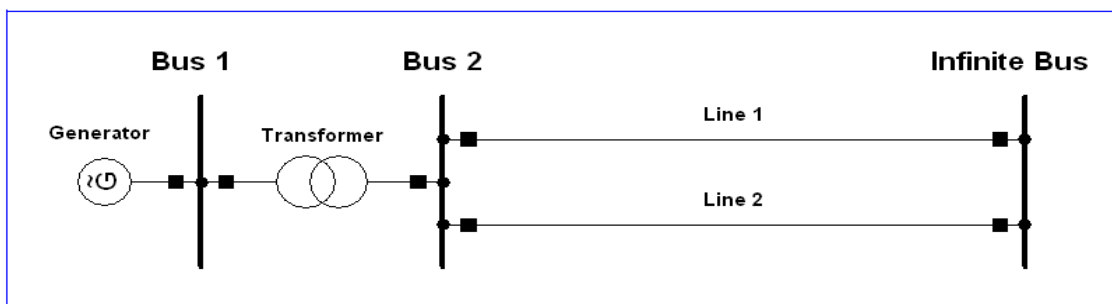


Figure A.1: Diagram for the system used in the simulations for Chapter 6

The following transient and sub transient values were used in obtaining the simulation results for the Calgary Laboratory

$$X_l = 0.071; r_a = 0.0; X_d = 1.2; X'_d = 0.1963; X''_d = 0.007487; T'_{do} = 4.5097; \\ T''_{do} = 0.06; X_q = 1.2; X'_q = 1.2; X''_q = 0.1092872; T'_{qo} = 4.5097; T''_{qo} = 0.4; \\ H = 4.75$$

The transformer data in pu:

$$R = 0.0008$$

$$X = 0.004$$

University of Cape Town

Appendix B

SMIB System

B.1 Model Equations

Simple AVR structure

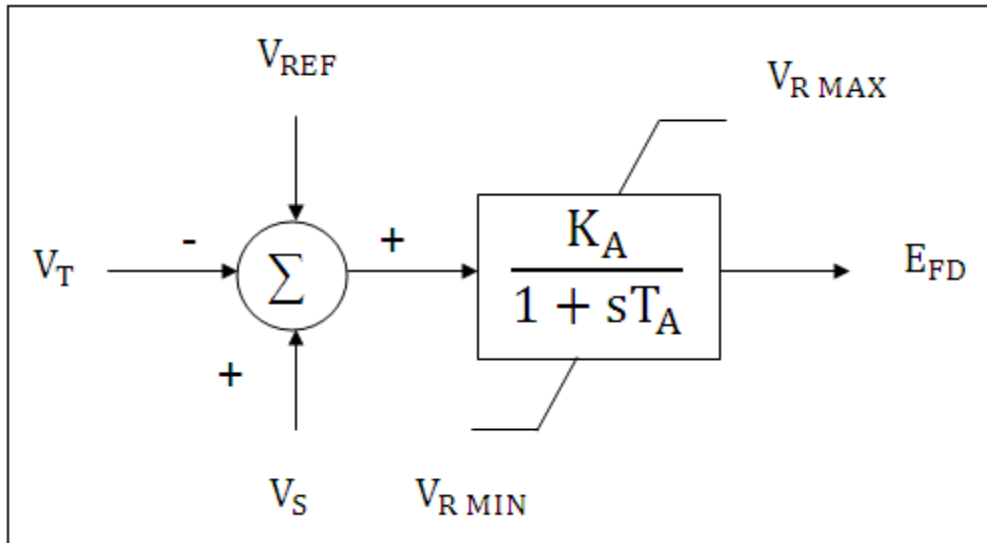


Figure B.1: AVR block diagram used in the SMIB system

Where:

T_A is the regulator time constant

K_A is the exciter gain

V_T is the terminal voltage

V_S is the PSS control signal

V_{REF} is the reference voltage

V_{RMAX} is the maximum limit of the AVR signal

V_{RMIN} is the minimum limit of the AVR signal

E_{FD} is the electric field signal

For the Single machine to infinite bus system, the following generator model was used; it's a 6th order sub-transient model.

The generator equations are:

$$\frac{d\Delta\bar{\omega}_r}{dt} = \frac{1}{2H} (\bar{T}_m - \bar{T}_e - K_D\Delta\bar{\omega}_r)$$

$$\frac{d\delta}{dt} = \omega_o\Delta\bar{\omega}_r$$

The rotor circuit equations are represented as follows:

$$\frac{d\psi_{fd}}{dt} = \frac{\omega_o R_{fd}}{L_{adu}} E_{fd} - \omega_o R_{fd} i_{fd}$$

$$\frac{d\psi_{1d}}{dt} = -\omega_o R_{1d} i_{1d}$$

$$\frac{d\psi_{1q}}{dt} = -\omega_o R_{1q} i_{1q}$$

$$\frac{d\psi_{2q}}{dt} = -\omega_o R_{2q} i_{2q}$$

The rotor currents are expressed by the following:

$$i_{fd} = \frac{1}{L_{fd}} (\psi_{fd} - \psi_{ad})$$

$$i_{1d} = \frac{1}{L_{1d}} (\psi_{1d} - \psi_{ad})$$

$$i_{1q} = \frac{1}{L_{1q}} (\psi_{1q} - \psi_{aq})$$

$$i_{2q} = \frac{1}{L_{2q}} (\psi_{2q} - \psi_{aq})$$

The electrical torque is expressed by the following:

$$T_e = \psi_{ad} i_{1q} - \psi_{aq} i_{1d}$$

B.2 SMIB System Data

The following data were used for the system generator and the AVR

Generator data

Rating: 300MVA, 24kV, 60Hz

$$X_l = 0.0742; r_a = 0.0; X_d = 1.72; X'_d = 0.45; X''_d = 0.33; T'_{do} = 6.3; T''_{do} = 0.033;$$

$$X_q = 1.68; X'_q = 0.59; X''_q = 0.33; T'_{qo} = 0.43; T''_{qo} = 0.033; H = 4.0$$

Automatic Voltage Regulator parameters

$$K_a = 200 \text{ and } T_a = 0.03$$

Transmission Line parameters

$$r = 0$$

$$b_c = 0$$

Power system stabilizer structure

The following PSS structure was used in the SMIB system; the parameters K_s , T_1 , T_2 were designed using evolutionary algorithms.

T_w of 2.5s was used

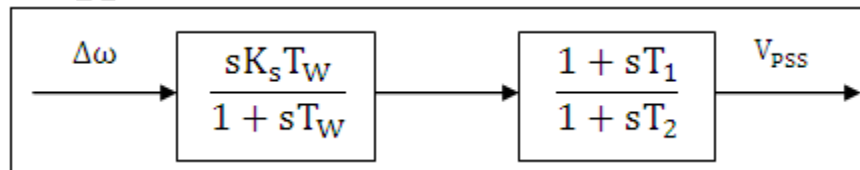


Figure B.2: Power system stabilizer structure used in the SMIB system

The line reactance was varied to simulate different operating conditions. All the reactances are in per unit, while the time constants are in seconds.

Table B.1: High frequency oscillatory modes for the SMIB system

Cases	No PSS	BGA PSS	GA PSS	PBIL	CPSS
1	-14.1037 ±16.1655i (0.6574)	-12.6574 ±14.5957i (0.6552)	-12.7180 ±14.6850i (0.6547)	-12.6578 ±14.5897i (0.6553)	-12.3501 ±14.7183i (0.6428)
2	-13.1075±20.5195i (0.5383)	-12.0455 ±19.7867i (0.5200)	-12.0921 ±19.8272i (0.5207)	-12.0443 ±19.7833i (0.5200)	-11.9439 ±19.8856i (0.5149)
3	-13.1743 ±19.9628i (0.5508)	-11.4237 ±18.7898i (0.5195)	-11.5066 ±18.8553i (0.5209)	-11.4214 ±18.7839i (0.5195)	-11.2535 -18.9822i (0.5100)
4	-13.2611±19.3529i (0.5653)	-10.8215±17.7578i (0.5204)	-10.9471 ±17.8467i (0.5229)	-10.8180 ±17.7491i (0.5204)	-10.5855 ±18.0749i (0.5054)
5	-12.7052 ±22.0331i (0.4995)	-11.8921 ±21.5320i (0.4835)	-11.9274 ±21.5598i (0.4841)	-11.8910 ±21.5295i (0.4835)	-11.8292 ±21.6039i (0.4803)
6	-12.7647 ±21.4978i (0.5105)	-11.4923 ±20.7276i (0.4849)	-11.5498 ±20.7705i (0.4860)	-11.4904 ±20.7237i (0.4849)	-11.3926 ±20.8514i (0.4795)
7	-12.8322 ±20.9938i (0.5215)	-11.1868 ±20.0097i (0.4880)	-11.2639 ±20.0642i (0.4895)	-11.1843 ±20.0046i (0.4880)	-11.0565 ±20.1830i (0.4804)
8	-12.9584 -20.6793i (0.5310)	-11.3281 ±19.6573i (0.4993)	-11.4044 ±19.7141i (0.5007)	-11.3258 ±19.6521i (0.4993)	-11.1887 ±19.8297i (0.4914)
9	-12.7236±21.4076i (0.5109)	-11.2246 ±20.5477i (0.4794)	-11.2938 ±20.5954i (0.4808)	-11.2223 ±20.5432i (0.4794)	-11.1140 ±20.6998i (0.4730)

Appendix C

SMIB System simulations

The results shown in this section are for the same SMIB system, shown under the simulation results section in Chapter 5, but these results were obtained under the objective function that maximizes the minimum damping ratio and keeping the highest electromechanical modes damping ratio less than 0.7. This was the limit in this Case. In chapter 5, the limit on the maximum was 0.5 for the damping ratio. Figure C.1 to Figure C.3 shows the fitness value of the three EA methods in maximizing the lowest damped ratio under the restriction that the maximum damping for the electromechanical modes be limited to 0.7. The GA settles at a value of 0.33, the BGA settles at a value of 0.35, while the PBIL settles at a value of 0.35 as well, meaning that the GA settles at a slightly lower value, even though the difference is insignificant. Observing Table C-1 also shows that the maximum value attained from the GA optimization is 0.6169, the BGA is 0.6847, while the PBIL attains a maximum value of 0.6788.

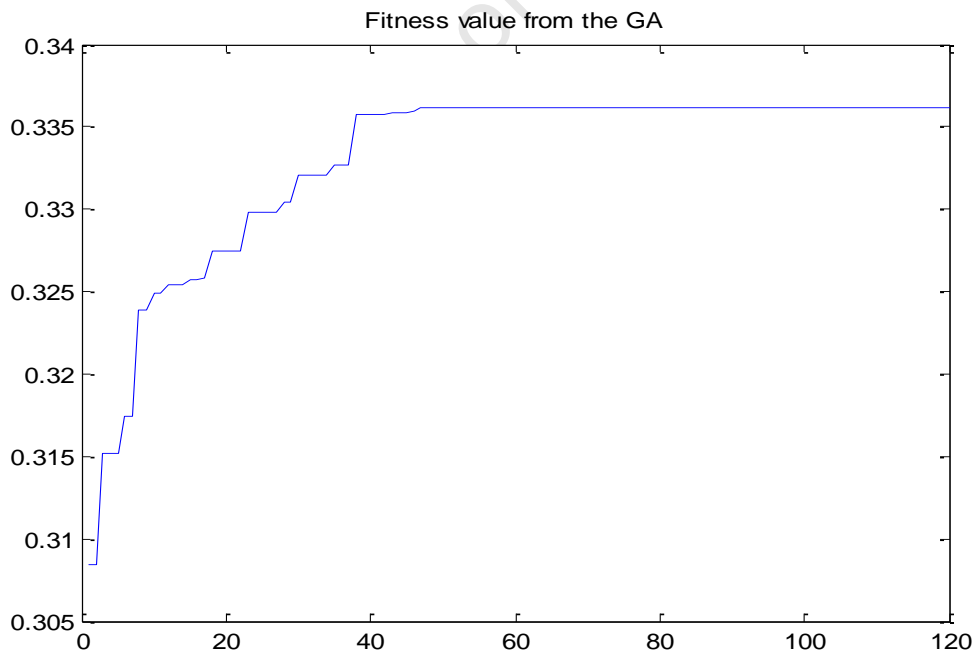


Figure C.1: Fitness value for the GA optimization

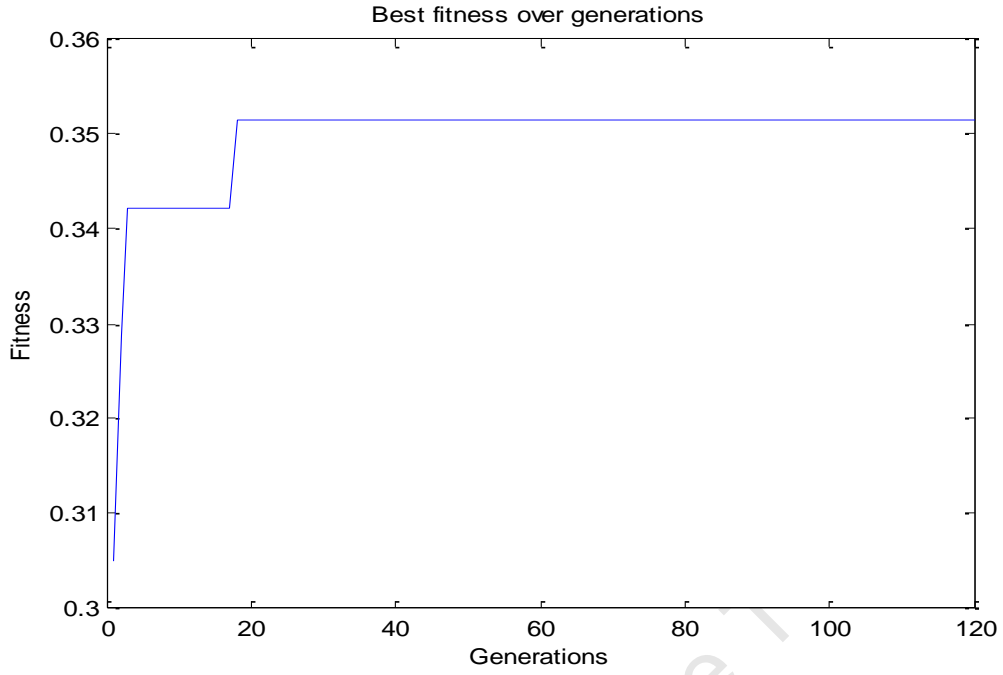


Figure C.2: Fitness value for the BGA optimization

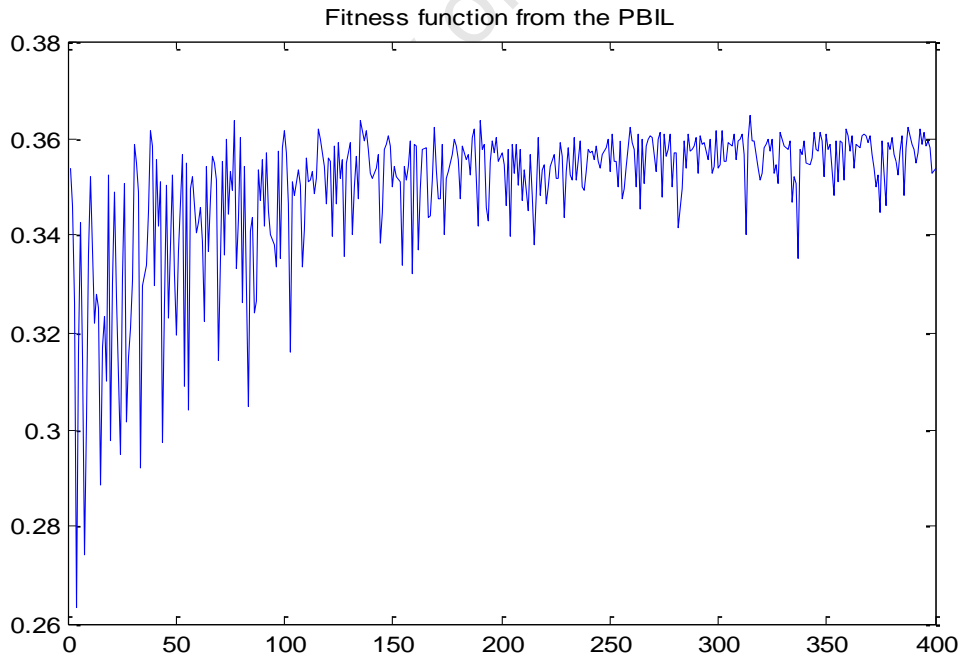


Figure C.3: Fitness value for the PBIL optimization

Table C.1: Electromechanical modes and their damping ratios

Case	BGA-PSS	GA-PSS	PBIL-PSS
1	$-4.1616 \pm 7.5065i$ (0.4849)	$-3.8933 \pm 7.7500i$ (0.4489)	$-4.1795 \pm 7.6165i$ (0.4811)
2	$-2.3297 \pm 5.1295i$ (0.4135)	$-2.2653 \pm 5.3656i$ (0.3889)	$-2.3590 \pm 5.1982i$ (0.4132)
3	$-3.3702 \pm 5.0126i$ (0.5580)	$-3.2326 \pm 5.4314i$ (0.5114)	$-3.4177 \pm 5.1254i$ (0.5548)
4	$-4.4055 \pm 4.6895i$ (0.6847)	$-4.1908 \pm 5.3469i$ (0.6169)	$-4.4775 \pm 4.8435i$ (0.6788)
5	$-1.5715 \pm 4.1869i$ (0.3514)	$-1.5697 \pm 4.3970i$ (0.3362)	$-1.6059 \pm 4.2432i$ (0.3540)
6	$-2.1090 \pm 3.8940i$ (0.4762)	$-2.1062 \pm 4.2718i$ (0.4422)	$-2.1690 \pm 3.9919i$ (0.4774)
7	$-2.4225 \pm 3.3677i$ (0.5840)	$-2.4601 \pm 3.9668i$ (0.5270)	$-2.5244 \pm 3.5197i$ (0.5828)

Table C.2: High frequency oscillatory modes for the SMIB system

Case	BGA-PSS	GA-PSS	PBIL-PSS
1	$-11.6255 \pm 13.6679i$ (0.6479)	$-11.8309 \pm 13.6577i$ (0.6547)	$-11.6000 \pm 13.5917i$ (0.6492)
2	$-11.6620 \pm 19.5302i$ (0.5127)	$-11.7221 \pm 19.5075i$ (0.5151)	$-11.6411 \pm 19.5028i$ (0.5125)
3	$-10.7259 \pm 3.626i$ (0.5044)	$-10.8330 \pm 18.3052i$ (0.5093)	$-10.6843 \pm 18.3165i$ (0.5039)
4	$-9.7404 \pm 17.2212i$ (0.4923)	$-9.8951 \pm 17.1005i$ (0.5008)	$-9.6691 \pm 17.1589i$ (0.4909)
5	$-11.6517 \pm 21.3802i$ (0.4785)	$-11.6894 \pm 21.3640i$ (0.4800)	$-11.6362 \pm 21.3618i$ (0.4784)
6	$-11.0955 \pm 20.4734i$ (0.4765)	$-11.1573 \pm 20.4418i$ (0.4791)	$-11.0690 \pm 20.4445i$ (0.4761)
7	$-10.6450 \pm 19.6687i$ (0.4760)	$-10.7282 \pm 19.6195i$ (0.4798)	$-10.6080 \pm 19.6312i$ (0.4754)

C. 1 Step responses of the system

Figure C.4 to Figure C.12 show the response of the system to a 10% step in reference voltage of the synchronous generator. The performance of the system was tested using the three EA PSS, as well as the CPSS. This was tested to further highlight the influence of the objective function on the performance of the designed PSS. Clearly it can be deduced from the figures that the performances of the different PSSs is very close.

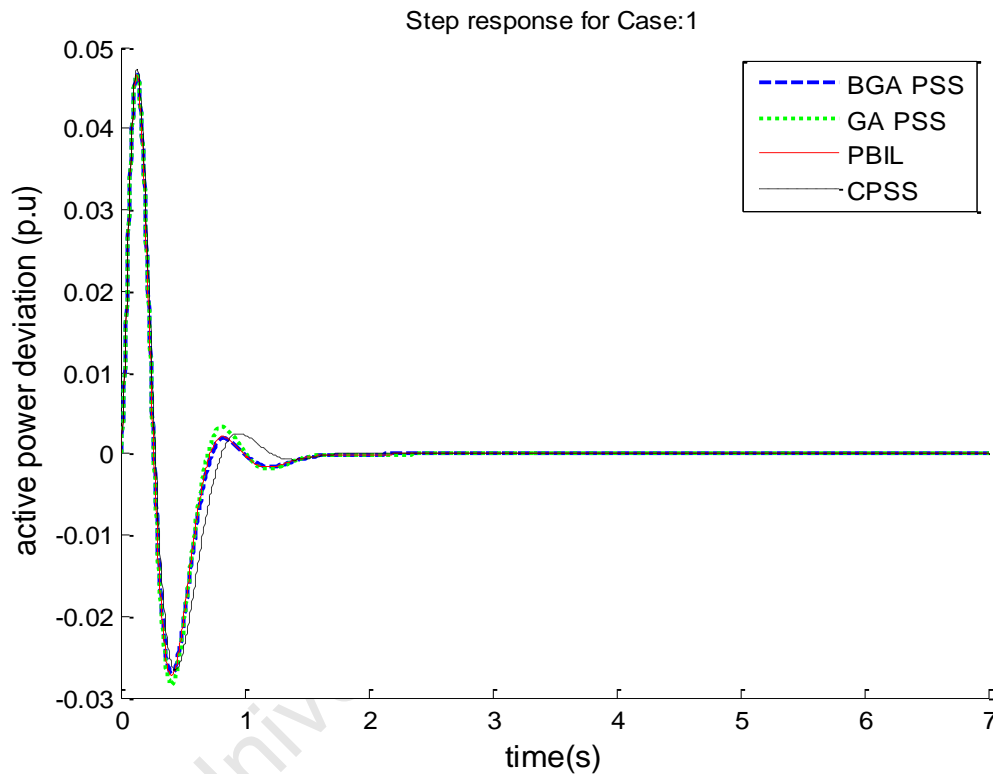


Figure C.4: Active power deviation for Case 1 under small disturbance

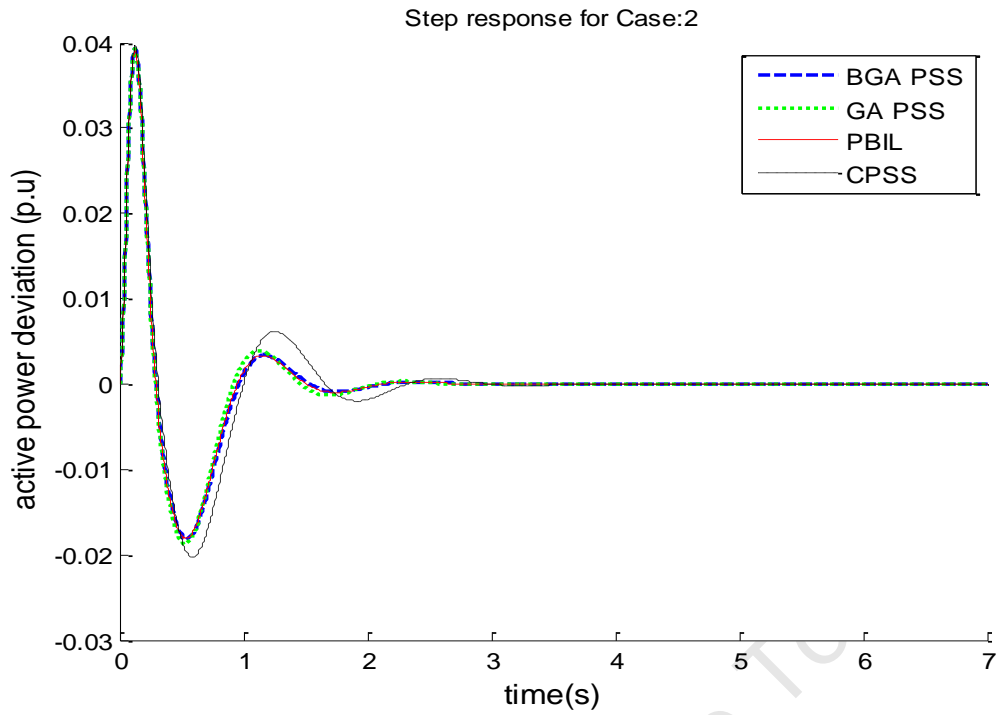


Figure C.5: Active power deviation for Case 2 under small disturbance

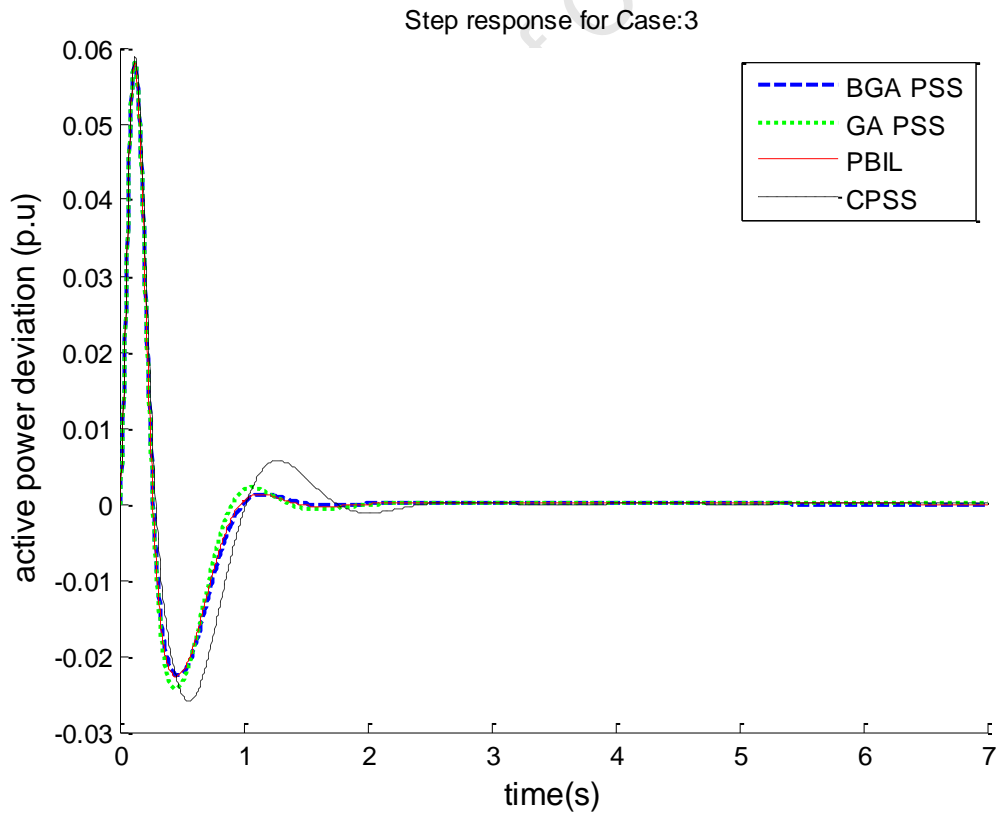


Figure C.6: Active power deviation for Case 3 under small disturbance

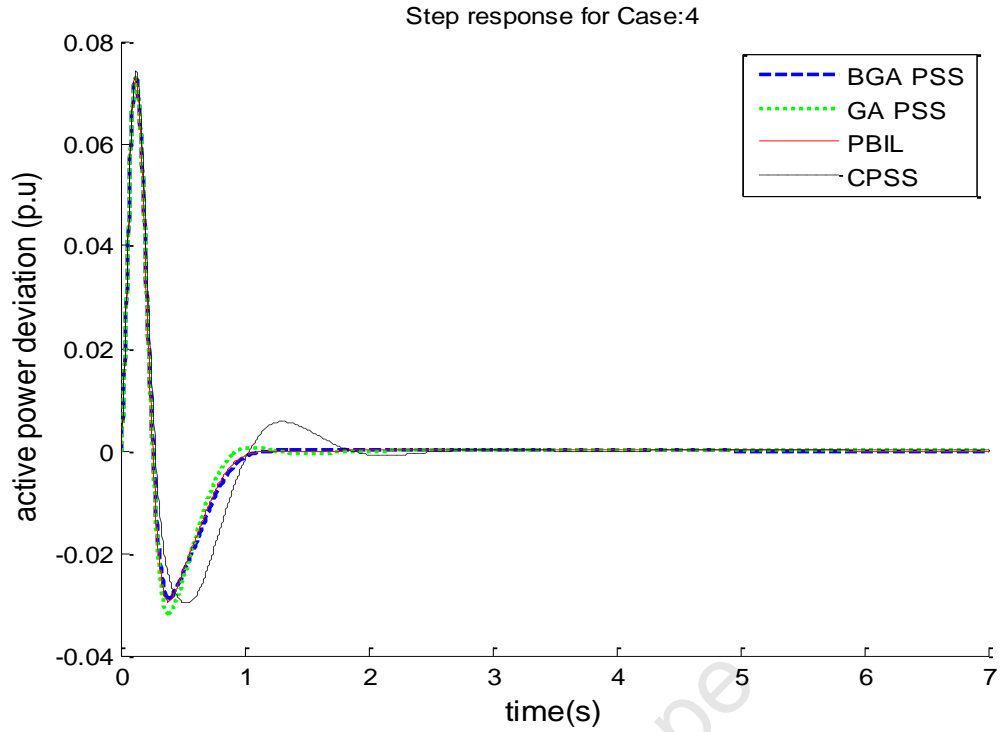


Figure C.7: Active power deviation for Case 4 under small disturbance

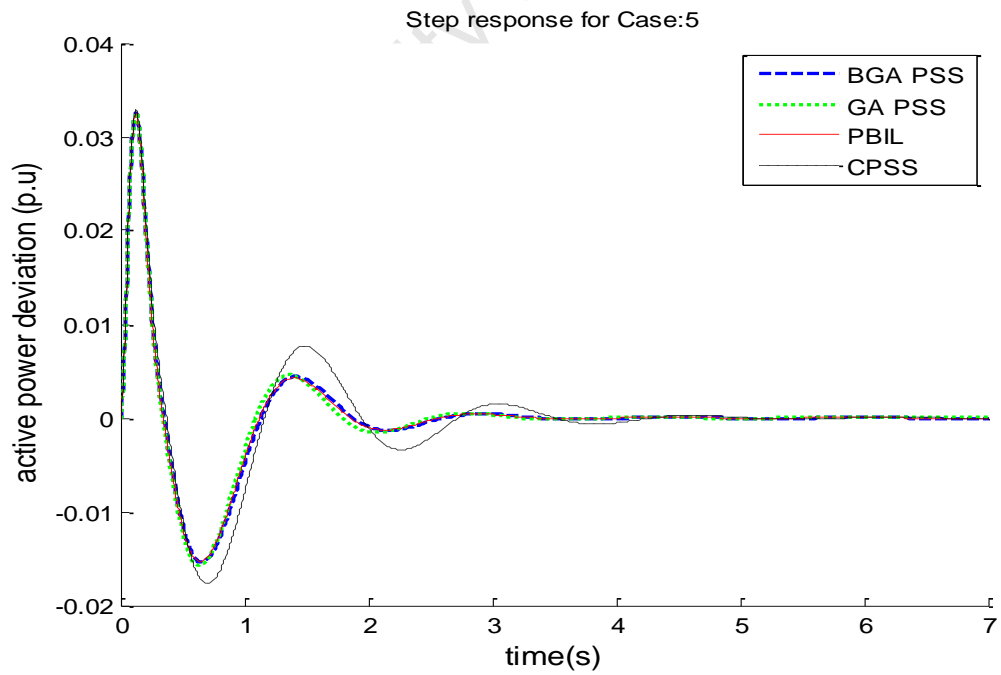


Figure C.8: Active power deviation for Case 5 under small disturbance

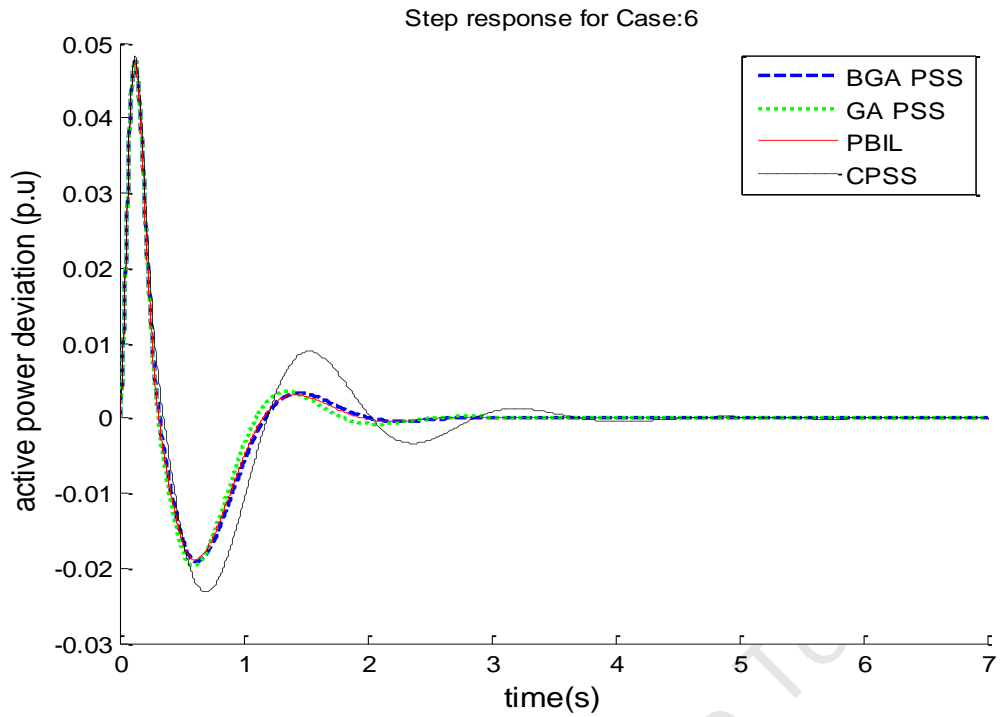


Figure C.9: Active power deviation for Case 6 under small disturbance

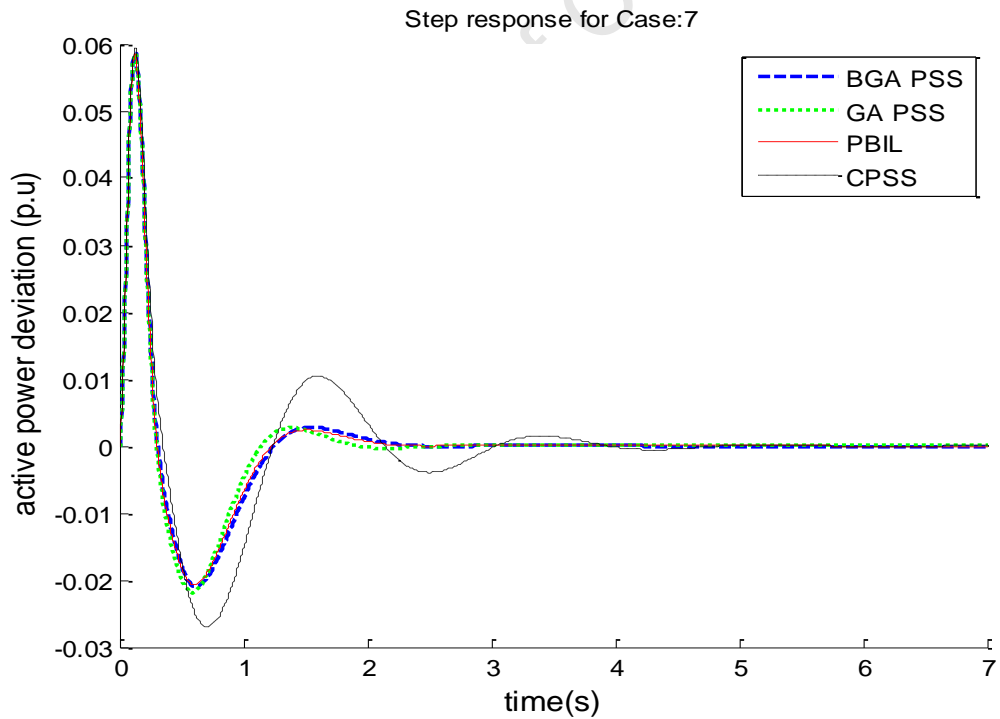


Figure C.10: Active power deviation for Case 7 under small disturbance

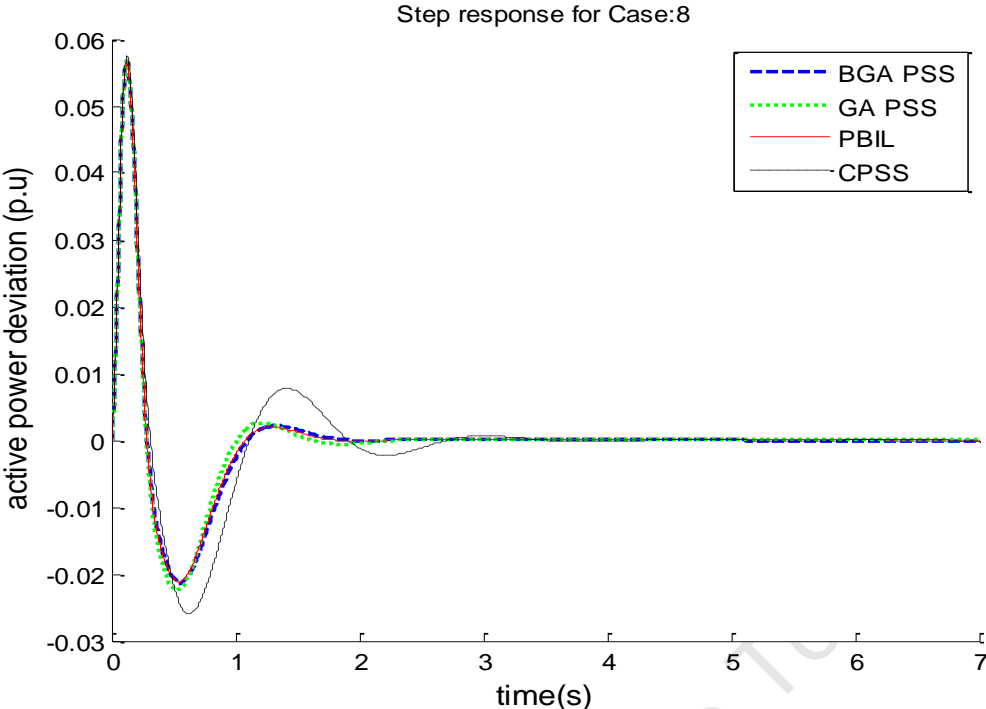


Figure C.11: Active power deviation for Case 8 under small disturbance

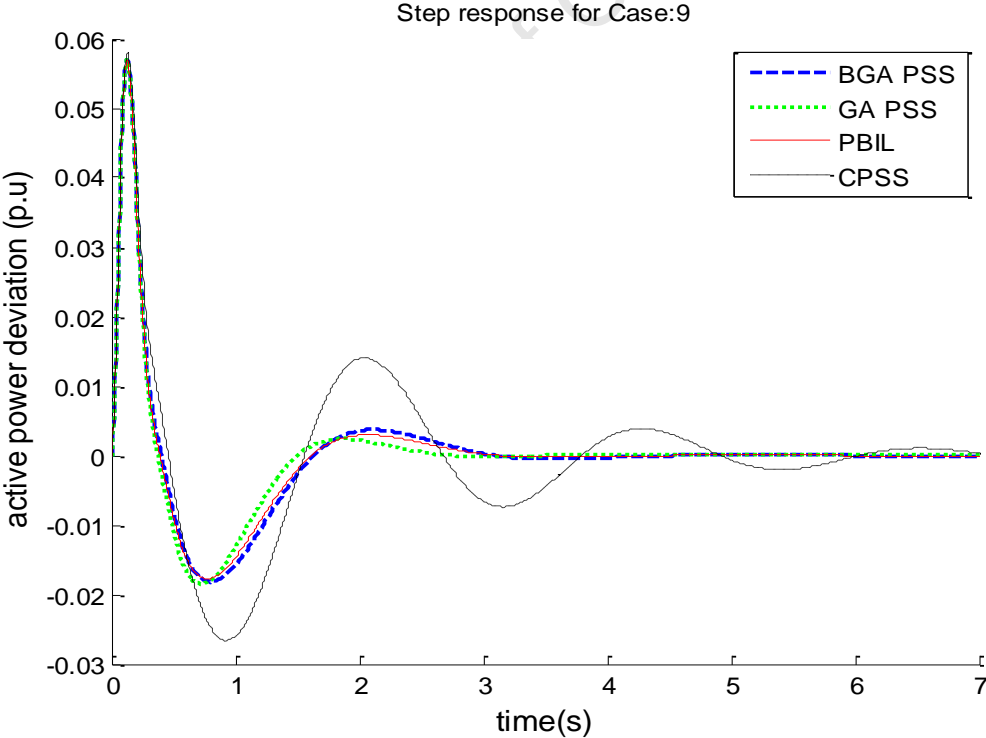


Figure C.12: Active power deviation for Case 9 under small disturbance

Appendix D

Multi- Machine System

D.1 System Model Equations

$$\frac{d\Delta\bar{\omega}_r}{dt} = \frac{1}{2H} (\bar{T}_m - \bar{T}_e - K_D\Delta\bar{\omega}_r)$$

$$\frac{d\delta}{dt} = \omega_o\Delta\bar{\omega}_r$$

The rotor circuit equations are represented as follows:

$$\frac{d\psi_{fd}}{dt} = \frac{\omega_o R_{fd}}{L_{adu}} E_{fd} - \omega_o R_{fd} i_{fd}$$

$$\frac{d\psi_{1d}}{dt} = -\omega_o R_{1d} i_{1d}$$

$$\frac{d\psi_{1q}}{dt} = -\omega_o R_{1q} i_{1q}$$

$$\frac{d\psi_{2q}}{dt} = -\omega_o R_{2q} i_{2q}$$

The rotor currents are expressed by the following:

$$i_{fd} = \frac{1}{L_{fd}} (\psi_{fd} - \psi_{ad})$$

$$i_{1d} = \frac{1}{L_{1d}} (\psi_{1d} - \psi_{ad})$$

$$i_{1q} = \frac{1}{L_{1q}} (\psi_{1q} - \psi_{aq})$$

$$i_{2q} = \frac{1}{L_{2q}} (\psi_{2q} - \psi_{aq})$$

The electrical torque is expressed by the following:

$$T_e = \psi_{ad} i_{1q} - \psi_{aq} i_{1d}$$

D.2 System Data

Generator data

All the generators used in the system are identical with the following parameters:

Rating: 900MVA, 22kV, 60Hz

$$\begin{aligned} X_l &= 0.2; & r_a &= 0.0; & X_d &= 1.8; & X'_d &= 0.3; \\ X''_d &= 0.25; & T'_{do} &= 8.0; & T''_{do} &= 0.03; & X_q &= 1.7; \\ X'_q &= 0.55; & X''_q &= 0.24; & T'_{qo} &= 0.4; & T''_{qo} &= 0.05; \\ H &= 6.5; & K_D &= 0; & A_{sat} &= 0.0654; & B_{sat} &= 0.5743; \end{aligned}$$

All the reactances are in per unit, while the time constants are in seconds

Automatic Voltage Regulator (AVR) Parameters

$$K_a = 200 \text{ and } T_a = 0.05 \quad T_r = 0.01$$

Turbine Governor block diagram and Parameters

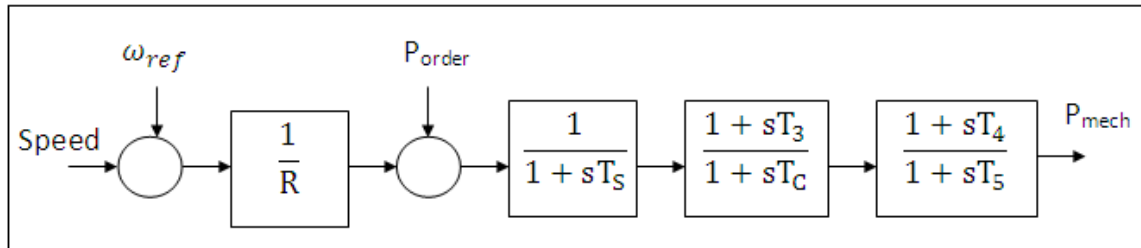


Figure D.1: Speed governor block diagram used in the simulations for multi-machine

$$\begin{aligned} \text{set point } (\omega_r) &= 1 & \text{Gain } \left(\frac{1}{R}\right) &= 25 & T_{\max} &= 1 & T_s &= 0.1 & T_c &= 0.5 \\ T_3 &= 0.0 & T_4 &= 1.25 & T_5 &= 5.0 \end{aligned}$$

Power System stabilizer Structure

The following PSS structure was used, the parameters K_s , T_1 T_2 T_3 and T_4 were designed using the evolutionary algorithms, while the washout time constant T_w of 10s was used.

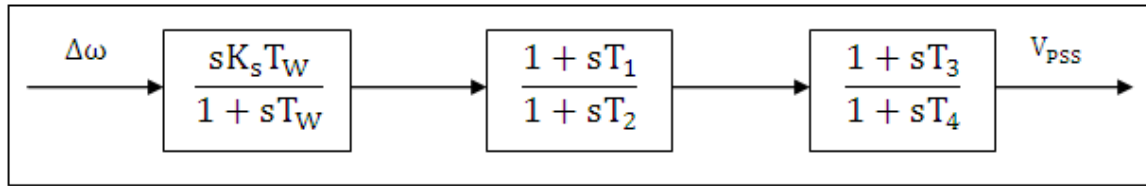


Figure D.2: Block diagram for the PSS used in the Multi-machine system

All the reactances are in per unit, while the time constants are in seconds. The generators active power output and line reactance were varied to simulate different operating conditions.

University of Cape Town